Synthesis and Supramolecular Chemistry of Trianglimine Macrocycles

by

Ana María López Periago

Submitted for the degree of **Doctor of Philosophy**

Division of Chemistry
School of Biomedical and Molecular Sciences
University of Surrey

June 2004

Abstract

This research project deals with the synthesis of a variety of macrocyclic molecules, which have been named *trianglimines* and *trianglamines*. These novel macrocycles comprise several hydrogen bonding motifs along with a lipophilic cavity, which seems to be highly suitable to bind neutral organic species, in particular pesticides.

A trianglimine is a hexaimine macrocycle of triangular shape with a ring size between 27 and 42 atoms (the style is illustrated below). This novel class of compounds are obtained *via* a [3+3]-cyclocondensation (*via* the formation of six imine bonds) between the enantiomerically pure (1*R*, 2*R*)-diaminocyclohexane and an aromatic dialdehyde. The three cyclohexane rings form the vertices of the triangle whereas the three aromatic moieties form the sides of the triangle.

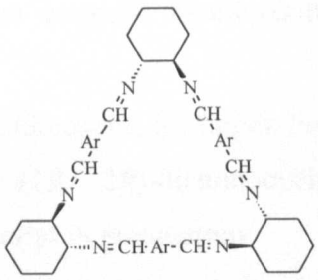

Several methods for the synthesis of aromatic dialdehydes, which are precursors to the macrocyclic trianglimines, were also developed. These methods proceeded mainly *via* the double lithium-bromide exchange reaction and double *ortho*-lithiation reaction.

The scope and limitations of the macrocyclisation reactions using various substituted aromatic dialdehydes have been investigated in detail along with the mechanism of the macrocyclisation.

In addition, the conformational properties of the novel macrocycles in solution have been studied using NMR techniques.

Simple reduction of the hexaimine macrocycles has been shown to yield trianglamines or hexaamine macrocycles.

Finally, a selection of binding studies was carried out to analyse the ability of this new class of macrocycles to act as synthetic receptors.

Diffusion NMR techniques have been shown to be useful in the qualitative determination of the binding event.

Publications

Journal Publications.

- Kuhnert, N.; Strassnig, C.; Lopez-Periago, A. "Synthesis of novel enantiomerically pure trianglimine and trianglamine macrocycles". *Tetrahedron Asym.* **2002**. *13*, 123-128.
- Kuhnert, N.; Lopez-Periago, A. "Synthesis of novel chiral non-racemic substituted trianglimines and trianglamine macrocycles". *Tetrahedron Lett.* **2002**, *43*, 3329-3332.
- Kuhnert, N.; Rossignolo G., Lopez-Periago, A. "The synthesis of trianglimines: on the scope and limitations of the [3 + 3] cyclocondensation reaction between (1*R*, 2*R*)-diaminocyclohexane and aromatic dicarboxaldehydes". *Org. Biomol. Chem.* **2003**, *1*, 1157-1171.
- Kuhnert, N.; Sauveplane, J.; Gracheva, S.; Lopez-Periago, A. "An investigation into the mechanism between (1*R*, 2*R*)-diaminocyclohexane and isophthal- and terephthalaldehyde". Manuscript in preparation.
- Kuhnert, N.; Patel, C.; Burzlaff, N.; Lopez-Periago, A. "Tuning size of macrocyclic cavities. Trianglimine macrocycles for applications in nanomachines". Manuscript in preparation.

Poster presentations.

- Winter School in Organic Reactivity- Bressanone (Italy). January 6-13th, 2001. "Synthesis and Binding Properties of Trianglimine and Trianglamine Macrocycles"
- Third International Conference on Supramolecular Science and Technology. Buenos Aires (Argentina) August 24-29th, 2002. "Synthesis and Binding Properties of Trianglamine and Trianglimine Macrocycles"
- Summer School on Green Chemistry. Venice (Italy) Aug30th-Sep7th, 2003. "On the scope and limitations of the [3 + 3] cyclocondensation reaction between (1*R*, 2*R*)-diaminocyclohexane and aromatic dicarboxaldehydes".

We are at the very beginning of time for the human race. It is not unreasonable that we grapple with problems. But there are tens of thousands of years in the future. Our responsibility is to do what we can, learn what we can, improve the solutions, and pass them on.

Richard Feynman

Acknowledgements

Over the past three years of work, there have been many people who have helped me directly or indirectly in the progress of this thesis. I would like to thank these people, as without them, this journey would never have been completed.

My gratitude to my supervisor, Dr. Nikolai Kuhnert for allowing me to work in his research group, and for encouraging me to start the fascinating adventure of trianglimines. His help, guidance and understanding during this time have been invaluable.

I also would like to thank Nikola Walker, Richard Chaundy and Judith Peter for their help with the Elemental Analysis, and mass spectra. A special thanks to Jim Bloxsidge for the exceptional NMR service and for all the help with the DOSY.

To the members of the Kuhnert group, Adam, Rob and Giulia, and to all the people in the JK lab, especially to Chris, Paul, Graham, Rob S., Hugh (thanks for proof reading!!) and Becky, for making the lab a great working atmosphere, and for introducing me into the British culture showing me the excellencies of a good pint. Cheers!

To the "Spanish crew", Noelia, Dr Manzano, Dr. Jose Javier, Alvaro, Olga, Jose and Berta, for being my surrogate family during the past three years, for all the fantastic times we spent together, and for a friendship I will never forget.

My warmest thanks to Steve, the person closest to me, for his love, constant motivation and intensive support that enabled me get through this thesis, for correcting the grammar and above all, for the incredible amount of patience he had with me for the last five months.

My eternal gratitude to my family, in particular my parents, Jose Luis and Margarita, to whom I dedicate this thesis, for the continuous support and encouragement that gave me the motivation to persevere over the past three years, for this I will never be able to thank them enough.

To Rosina and of course my grand parents.

Thanks to all

A mis padres

Abbreviations

CI-Chemical ionisation.

COSY-Correlation spectroscopy.

DCI -Desorption chemical ionisation.

DCM-Dichloromethane.

DDQ- dichlorodicyanoquinone.

DIBAL-Diisobutylaluminiunhydride.

DMAP-dimethylaminopyridine.

DMF-Dimethylformamide.

DMSO-Dimethylsulphoxide.

DOSY -Diffusion ordered Spectroscopy.

EI-Electron ionisation.

ESI- Electrospray ionisation.

EXSY-Two Dimensional Exchange spectroscopy.

FAB-fast atom bombardment.

IR-InfraRed.

LSIMS-Liquid Secondary Ion Mass Spectrometry.

MS-Mass spectrometry.

NBS-*n*-Bromosuccinimide.

NCS-*n*-Chlorosuccinimide.

NMR- Nuclear magnetic resonance.

NOE- Nuclear Overhauser Spectroscopy.

NOESY-Two Dimensional Nuclear Overhauser Spectroscopy.

R_f-Retardation factor.

SE- Steric Energy.

TEMPO-[2,2,6,6-tertramethyl-1-piperidinyloxy, free radical].

TFA- Trifluoroacetic acid.

THF-Tetrahydrofuran.

TMEDA-Tetramethylethylen diamine.

Contents

PART I

BACKGROUND

Chapter I

SUPRAMOLECULAR CHEMISTRY

1. Supramolecular chemistry. Introduction.

The interest of scientists to mimic nature has led to the development of a new kind of chemistry, inspired by biology and built on the shoulders of synthetic organic chemistry, known as *Supramolecular Chemistry*. Jean Marie Lehn, who won the Nobel Prize for his work in this area in 1987, defined it as the "chemistry beyond the molecule" or the "chemistry of molecular assemblies and of the intermolecular bond". Supramolecular chemistry therefore extends further than the area of individual molecules, to concentrate on non-covalent intermolecular interactions. These non-covalent interactions (hydrogen bonding, ion bridge, Van de Waals forces, or aromatic interactions) between molecules occur mainly in biological organisations, such as enzyme-receptor systems or the assembling of protein complexes.

In order to mimic nature, supramolecular chemists have developed systems where artificial macrocyclic receptors, or "hosts", are capable of binding strongly and selectively to a substrate, or "guest", to form "host-guest complexes" or "Supramolecular entities".

Developments in supramolecular chemistry have been driven by the increased availability of suitable macrocyclic receptors. Each time a class of macrocyclic receptors with a unique shape, distinct architecture and a set of functional groups from natural or synthetic sources, became widely available, supramolecular chemists were inspired to devise and synthesise novel sophisticated receptors and molecular devices. Early examples of this include Curtis' seminal synthesis of polyaza macrocycles,[1,2] and Pederson's crown ethers and cryptands,[3,4] cyclodextrins,[5] calix[n]arenes,[6,7,8] and curcubiturils.[9,10] Continuous discoveries of new macrocycle classes have led to rapid developments in innovative supramolecular chemistry and considerable advancements in this field.

In order for a macrocycle to make a significant impact in the field of supramolecular chemistry, it must fulfil certain requirements, mainly its ease of synthesis in sufficiently large quantities, combined with a unique molecular architecture and a particular set of functional groups that allow further elaboration into more sophisticated structures.

2. Synthesis of macrocycles.

Supramolecular chemists have developed the synthesis of hundreds of macrocycle molecules characterised by their intricate structures using elegant and somewhat simple synthetic procedures.

Pedersen defined "the macrocyclic effect"[11] as the ability of macrocycles to form more stable selective complexes than acyclic ligands. Thus, the first question to be addressed concerning the synthesis of these macrocyclic structures is, what is the driving force that permits the formation of such structures and why polymerisation does not occur.

In order to achieve the macrocyclisation, several factors must be taken into account, such as the chain length in the case of cycloalkane formation, the concentration at which the reaction is carried out, and the rigidity of the building blocks used in the ring formation (restricted flexibility can minimise the possibility of polymerisation).

Although all of these elements can be controlled in the synthesis, the macrocyclisation is not always achieved without the aid of external assistance or template, which does not always form part of the final macrocyclic product but whose participation is essential for the synthesis. Metal cations are the templates most widely used.

Taking all of these features into account, the strategies towards the synthesis of macrocycles can be divided in three main categories:

2.1. Template synthesis

2.1. High dilution synthesis

2.3. Other methods

2.1 Template synthesis.

The extensive use of template synthesis started in 1960, when Curtis[1] discovered the use of Ni(II) for the synthesis of macrocyclic complexes.

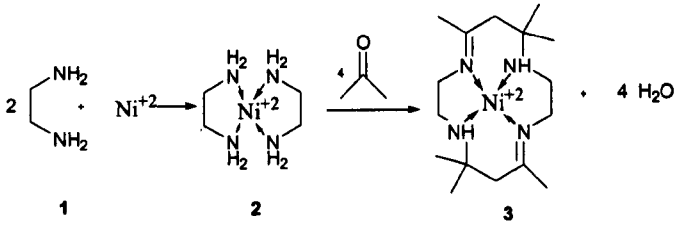

Figure 1: macrocycle formation by use of the Curtis reaction[12].

The synthetic route (Figure 1) involves the formation of an ethylenediamine-metal complex **2**, followed by the condensation of a carbonyl compound leading to the macrocyclic compound **3**.

The structure of the macrocycle obtained using this synthetic method can be easily controlled by selecting several elements of the building blocks used, such as the size,

reactivity, rigidity and geometry, as well as the structure and reactivity of the metal ion used as template.

Nelson and co-workers[13] showed an interesting example of controlled synthesis, using the synthesis of Schiff's base macrocycles as a model, illustrated in Figure 2.

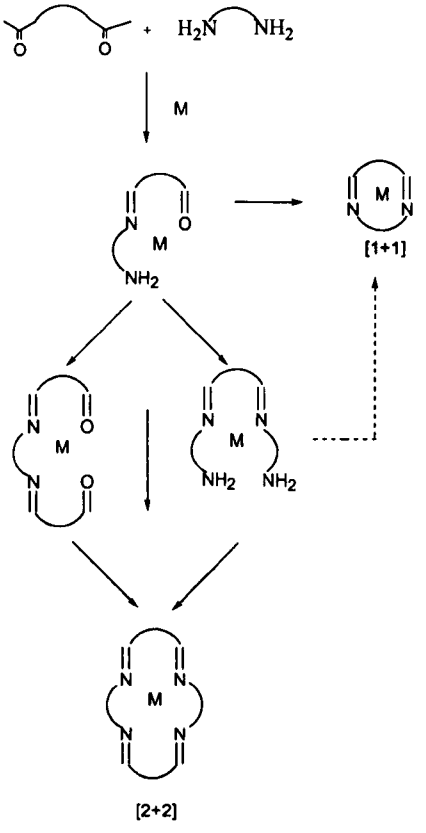

Figure 2: cyclocondensation of a diamine with a dicarbonyl compound. [12]

The cyclocondensation product between the amino and the dicarbonyl moieties depends on the nature of the building blocks as well as the template metal ion used to obtain either the [1+1] or the [2+2]-cyclocondensation products. For example, if the diamino moieties are large enough to reach the carbonyls groups, or are too rigid to adopt "chain-like" conformation, the [2+2] cyclocondensation will be favoured over the [1+1]. This situation will be also achieved if the template cation used is very bulky in relation to the cavity on the [1+1] cycle. Furthermore, the co-ordination number and geometry of the metal ion in the intermediate step has to be taken into account. Depending on the atoms taking part in the ring closure process and their orientation, one process will be favoured over the other (Figure 3).

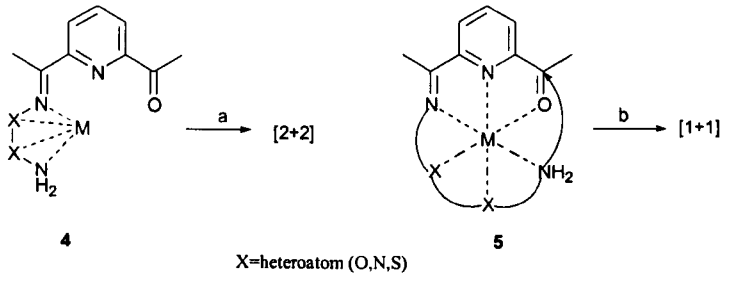

4 5

Figure 3: a)[2+2] condensation favoured by strong coordination with the NH_2 group. b) [1+1] condensation favoured by axial coordination.[12]

The example in Figure 4 shows the [1+1]-cyclocondensation reaction product **8**, where the small ion, Mg^{+2}, was used as the template.

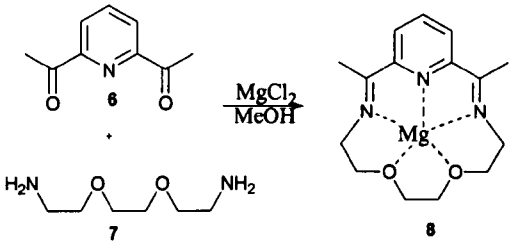

6 7 8

Figure 4: [1+1]-cyclocondensation using Mg^{2+} as templating agent.[12]

However, when the same reaction was carried out using a larger ion (Ba^{+2}) as shown in Figure 5, the [2+2]-cyclocondensation product **9** was obtained.

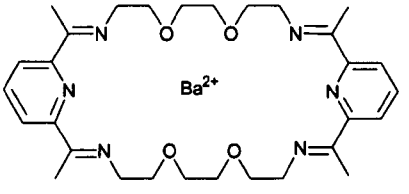

9

Figure 5: [2+2]-cyclocondensation using Ba^{2+} as templating agent.[12]

Although the size of the metal ion plays an important role in template synthesis, it is not the most significant parameter. This is the case for the relatively small ions such as Ni(II) and Cu(II), where macrocyclisation is favoured by the special co-ordination geometry that they can adopt upon complexation rather than the size of the ions. Thus, they adopt co-ordination geometries in which their bonding orbitals are orthogonal. In the case of Figure 1, Ni(II) adopts a square planar structure that stabilises the complex. This does not however, stabilise the pentagonal-planar structure preferred in macrocycles such as the ones illustrated in Figure 6.

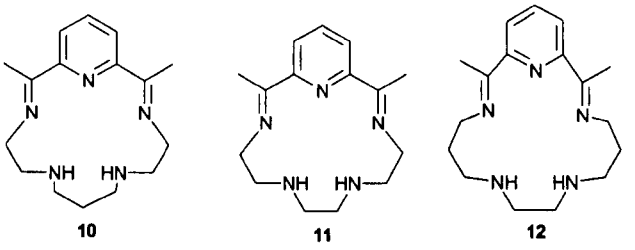

Figure 6: structures of macrocycles that are stabilised by non-transition metal ions by a pentagonal planar coordination.[12]

2.2 High dilution synthesis.

The synthesis of macrocycles involving the high dilution technique requires, as a general rule, a 1:1 molar concentration of each building block that composes the macrocycle. A plausible explanation of why high dilution favours cyclisation over intermolecular condensation or polymerisation is provided by reaction rates.[14]

In a first order reaction, which is the case for an intramolecular ring closure reaction, the rate is directly proportional to a single reactant concentration, as shown in equation 1.

$$-dA/dt=kA \qquad \textit{therefore} \qquad A=A_o e^{-kt} \quad \text{Equation 1}$$

Where: A=concentration, k=rate constant, t=time.

However, an intermolecular reaction is of second order, in which the rate is proportional to the square of the concentration, as shown in equation 2.

$$-dA/dt=kA^2 \qquad \textit{therefore} \quad 1/A - 1/A_o = kt \qquad \text{Equation 2}$$

Therefore, the higher the concentration of the reactants is the more likely it is for them to undergo polymerisation, whereas the more diluted, intramolecular condensation is more probable.

One of the best known types of macrocycles achieved using the high dilution procedure, are the cyclic polyethers or *crown ethers*. These are characterised by the number and type of donor atoms, the dimension of the cavity and the pre-organisation for most effective coordination. Crown ethers are also well known for their selectivity and binding strengths towards alkaline metal ions. One example is the dibenzo-18-crown-6 **15,** discovered by Pedersen in 1967,[4] using Williamson's ether synthesis (Figure 7).

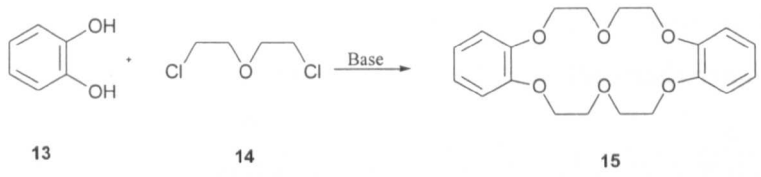

13 14 15

Figure 7: synthesis of dibenzo-18-crown-6.[15]

Examples of three-dimensional analogues of crown ethers included Lehn's cryptands **16** and cryptates **17**, whose structures are shown in Figure 8.

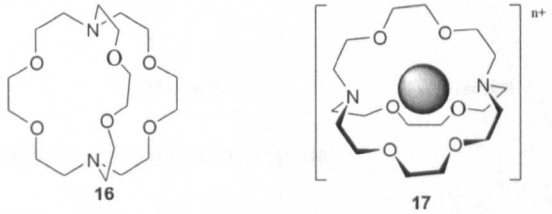

Figure 8: structures of cryptand and cryptate macrocycles.[16]

2.3 Other methods.

There are many macrocycles whose synthetic method cannot be included in the previous classification, such as porphyrins or calix[n]arenes discussed below.

2.3.1. Porphyrins.[12]

Fischer's porphyrins are macrocyclic structures comprising of four pyrrole rings **18** in a planar arrangement. They can be synthesised using different strategies such as a tetrapyrrol condensation with formic acid or condensation with formaldehyde (Figure 9).

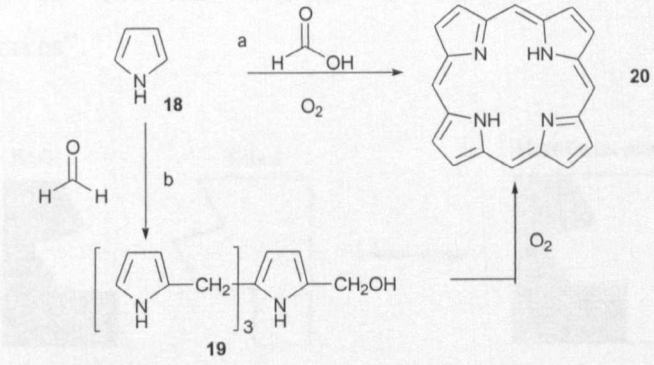

Figure 9:synthesis of porphyrin *via*: a) condensation of pyrrol and formic acid. b) condensation of unsubstituted pyrrol with formaldehyde.[12]

2.3.2. Calix[n]arenes.[6]

Calixarenes are obtained *via* condensation of phenol with formaldehyde under different conditions. They are structures with a great versatility since the number of phenyl units can be increased ([n], indicates the number of phenyl units), as well as the diversity of "R" groups that it can hold. Calixarenes are formed under high

concentration conditions. Usually calix[8]arenes are considered to be the product of kinetic control, whereas calix[4]arenes are the product of thermodynamic control.

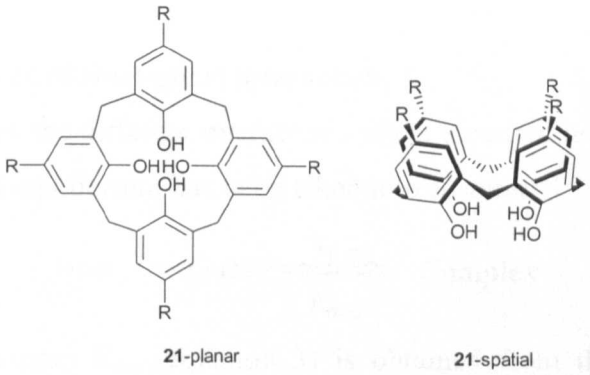

Figure 10: structure of a calix[4]arene, planar and spatial.

3. Host-guest chemistry.

One of the most significant applications of supramolecular chemistry is the molecular recognition in host-guest systems, which involves the binding of a small molecule or guest inside a large macrocycle molecule or host.

The foundation of host-guest chemistry was presented by Emil Fischer[17] with the study of receptor-substrate binding in enzymes. He introduced the term of "lock-key principle" (Figure 11) illustrating that an effective complexation can only occur when the shapes and arrangements of binding sites fit each other. Later on, host-guest systems were defined by Donald Cram (who also won the Nobel Prize in 1987 accompanied by Lehn and Pedersen), as "complexes that are composed of two or more molecules or ions held together in unique structural relationship by intermolecular forces".

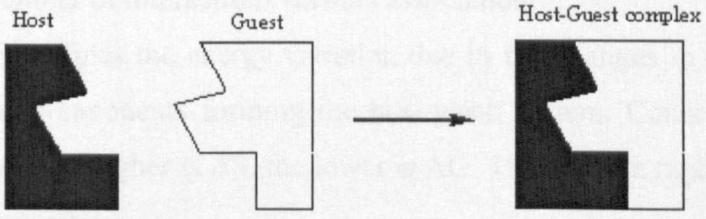

Figure 11: scheme of a host-guest complex following the "lock-key" principle.

The study of the interactions that can occur within a host-guest system is of extreme importance in the understanding of their chemical and biological behaviour.

The forces that sustain host-guest complexes are based on coexisting non-covalent interactions, thus there can be arrangements of cation-anion, or hydrogen bonding among others. This simultaneous binding is essential for a strong host-guest

interaction, because although non-covalent forces are typically weak, when they combine, a strong and specific complexation can be achieved.

3.1. Thermodynamics of Host-guest interaction.[18]

In order to study how the different interactions affect a certain host-guest system, the necessary host-guest equilibrium has to be taken into account.

$$\text{Host} + \text{Guest} \underset{k_{diss}}{\overset{k_{form}}{\rightleftharpoons}} \text{Complex}$$

The equilibrium constant K_{ass} (equation 3) is obtained from the ratio of the rate constant of complex formation (k_{form}) and dissociation (k_{diss}).

$$K_{ass}=k_{form}/k_{diss} \qquad \text{Equation 3}$$

If equilibrium constants are associated with enthalpy determinations (ΔH can be directly calculated by calorimetry), entropy and free energies can also be calculated from equation 4 and 5.

$$\Delta G=-RT\ln K \qquad \text{Equation 4}$$

$$\Delta G=\Delta H-T\Delta S \qquad \text{Equation 5}$$

If $\Delta G>0$ then $K_{ass}<1$ and equilibrium disfavours separated components.

If $\Delta G<0$ then $K_{ass}>1$ and equilibrium favours the formation of the complex.

By looking at equation 5, in order to obtain a favourable complexation, the ΔH and ΔS must produce a $\Delta G<0$.

The enthalpy (ΔH) defines the energy variation due to bond changes, which are non-covalent in the case of intermolecular interactions. Thus, the more bonds, or the stronger the bonds, the lower is the value of ΔH and consequently ΔG. Therefore, the strength or the number of interactions favours association.

The entropy (ΔS) defines the energy variation due to the changes in the freedom of movement of the components forming the host-guest system. Consequently, as the freedom increases, the higher is ΔS, the lower is ΔG. Therefore, a high positive value of ΔS favours association.

However, in the majority of the cases, host-guest complexes have less conformational freedom than when they are on their own, which is translated into a reduction in the entropy. Therefore, in order to achieve complexation ($\Delta G<0$), ΔH must be much more favourable than ΔS.

In reality, the application of equation 4 is not practical because in a host-guest system, there is not only one interaction as there can be many different types of intermolecular

forces involved in binding. Therefore, in order to calculate the net energy involved in complexation, all of the forces involved in binding must be additive.

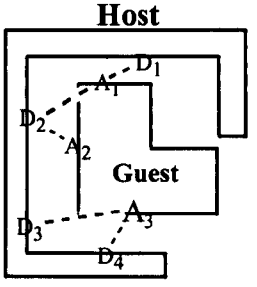

Figure 12: graphic of a host-guest multisite interaction.

The host guest system in Figure 12 shows different interactions between the host and guest. The total free energy (ΔG_t) involved can be described as the sum of single free energies (ΔG_{ij}), and the total binding constant (K_t) is the product of all equilibrium constants (K_{ij}). Each association constant (K_{ij}) occurs between pairs of species, each one bearing one binding group, as shown in the set of different equilibria below.[18]

$$R\text{-}A_1 + R'\text{-}D_1 \rightleftharpoons R\text{-}A_1\ldots D_1\text{-}R' \quad K_{11}$$

$$R\text{-}A_1 + R'\text{-}D_2 \rightleftharpoons R\text{-}A_1\ldots D_2\text{-}R' \quad K_{12}$$

$$R\text{-}A_2 + R'\text{-}D_2 \rightleftharpoons R\text{-}A_2\ldots D_2\text{-}R' \quad K_{22}$$

However, because the dimension of every K_{ij} is M^{-1}, the K_t would have M^{-n} dimensions, where "n" is the number of pair interactions. It is also incorrect to determine the total ΔG_t as a sum of all individual ΔG_{ij} because each ΔG_{ij} refers to the conversion of two species into one (in sizable entropic terms), whereas ΔG_t involves only one term for this.

To avoid this problem, the concentration of each species can be transformed into molar fractions (x), leading to dimensionless equilibrium constants. Taken into account that a 1M aqueous solution for a given solute corresponds to a molar fraction of about 1/55.6, the equilibrium equation transformed in molar fractions will lead to:

$$K_{ij}(M^{-1}) = \frac{[R-A_i.....D_j-R']}{[R-A_i][R'-D_j]} = \frac{([R-A_i.....D_j-R']/55.6)(1/55.6)}{([R-A_i]/55.6)([R'-D_j]/55.6)} =$$

$$K_{ij}(M^{-1}) = \frac{x_{R-Ai.....Dj-R'}\,(1/55.6)}{x_{R-Ai'}x_{R'-Dj}} = \frac{K_{ij}^{x}}{55.6} \qquad \text{Equation 6}$$

Thus, the product of every equilibrium constant is given by:

$$K_t^x = K_{11}^x K_{12}^x K_{22}^x ... = (55.6)^n K_{11} K_{12} K_{22} = 55.6 K_t \quad \text{Equation 7}$$

Finally, the total equilibrium constant will be:

$$K_t = (55.6)^{n-1} K_{11} K_{12} K_{22} \quad \text{Equation 8}$$

This equation shows that binding could be very strong even if the forces involved are very weak, providing there are a sufficiently large number of these interactions.

On the other hand, when the interactions are so weak that they cannot be studied experimentally, another approach has to be used. For these cases, the free energy of each interaction is represented by an increment calculated as a difference of the binding free energies in the host guest system, and without any given pair of sites.

Therefore, the total multisite complexation free energy ΔG_t should be represented as:

$$\Delta G_t = \sum \Delta\Delta G_{ij} + \Delta G_{ass} \quad \text{Equation 9}$$

$$\Delta\Delta G_{ij} = -RT \ln K_{ij}$$

And the total complexation constant would be:

$$K_t = K_{ass} K_{11} K_{12} K_{22} ..... \quad \text{Equation 10}$$

3.1.1. Solvent effect.[12]

The effect that the solvent has in host-guest interactions has been ignored in the previous treatment, however it is of extreme importance as a very effective host-guest interaction in one solvent may fail in another. Therefore, the solvent can have a large effect on stability, and can decrease or increase the number of binding sites. For example, Figure 13 shows how the value of the K_{ass} varies depending on the solvent used in the complexation of 18-crown-6 and Na^+ **22**. In this case, the stability constant of the complex increases as the solvating power of the solvent towards the cation decreases.

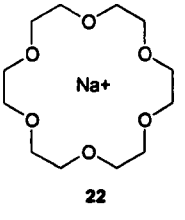

22

K_{ass}
63 in H_2O
22580 in MeOH

Figure 13: variation of the stability constant in the complex of 18-crown-6 with Na^+ in different solvents.[12]

3.2 Intermolecular interactions.[19]

The intermolecular interactions involved in host-guest systems possess a non-covalent nature. These forces normally involve energies from less than 1 to 15 $kJmol^{-1}$ and are therefore weak in comparison with ordinary chemical bonds. A summary of the bond energy involved is these interactions are illustrated in Table 1.[19]

INTERMOLECULAR INTERACTIONS			
Type of bond	**Bond energy ($kJ\ mol^{-1}$)**	**Type of bond**	**Bond energy ($kJ\ mol^{-1}$)**
Ion-Ion 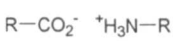	100-350	***Cation-π*** 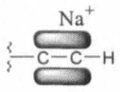	5-80
Ion-dipole 	50-200	***π-π*** 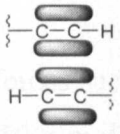	0-50
Dipole-dipole 	5-50	***Van der Waals*** 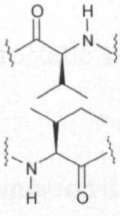	<5
H-bonding 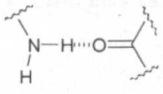	4-120		

Table 1: bonds energies involved in intermolecular interactions.[19]

Intermolecular interactions are induced by the electronic properties of each of the moieties that form the supramolecular entity, as well as the effect that their environment provokes in the system, that is the solvent effect. Thus, these interactions can be classified in the following five types.

3.2.1. H-bonding (4-120 $kJmol^{-1}$).[19]

Hydrogen bonding occurs between a proton donor group D-H and a proton acceptor A; where D is an electronegative atom, and the acceptor group A is a lone electron pair of an electronegative atom or a π-electron orbital of an unsaturated system.

Although the strength of this bond is about one tenth of the strength of a covalent bond (C_{sp3}-C_{sp3} is approximately 366 $kJmol^{-1}$ and C_{sp3}-H 400 $kJmol^{-1}$), it does however have significant effects on the physical properties. For example, in living organisms, hydrogen bonding occurs between bases in the chains of DNA (Figure 14).

The base pairing enables the molecule to be replicated and hence, be the blueprint for human life. Hydrogen bonding also occurs between the carbonyl and the N-H groups in proteins, and is responsible for maintaining the secondary structure.

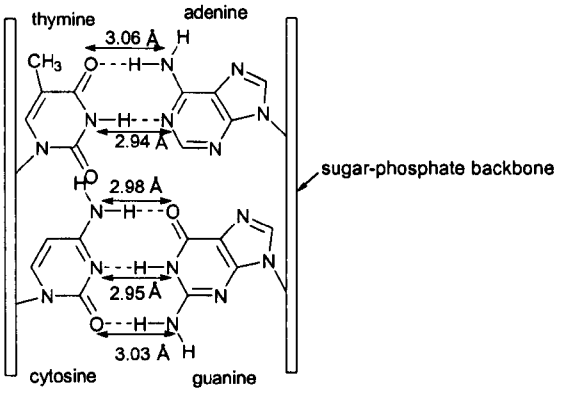

Figure 14: four bases of DNA showing H-bonding between base pairs.[20]

3.2.2. Electrostatic interactions.[19]

Electrostatic interactions involved different forces such as, ion-ion (100-350 $kJmol^{-1}$), ion-dipole (50-200 $kJmol^{-1}$), dipole-diole (5-50 $kJmol^{-1}$) and Van der Waals forces (<5 $kJmol^{-1}$).

The potential energy (F) concerned in electrostatic or coulomb interactions between two charges is described by equation 11.

$$F = \frac{q_1 q_2}{4\pi\varepsilon r^2} \quad \text{Equation 11}$$

$$\varepsilon = \varepsilon_r \varepsilon_o$$

Where q_1 and q_2 are the electric charge of two point masses at a distance r in a medium of permittivity ε_o, and ε_r the dielectric constant of the medium.

However, this approach cannot be used with organic ions since the charge is very delocalised. Bjerrum[18] suggested a solution to this problem, by applying the Debye-Hückel theory, considering the entire organic charged group as a spherical charged point. Thus, the association constants between the charges can be described as in equation 12.

$$K = \left(\frac{4\pi N}{1000}\right)\left(\frac{z_A z_B e^2}{\varepsilon kT}\right)^3 Q(b) \quad \text{Equation 12}$$

$$b = \frac{z_A z_B e^2}{2\varepsilon kTa}, \quad q = \frac{ab}{2} = \frac{z_A z_B e^2}{2\varepsilon kT}$$

Where N is the number density of molecules (the number per unit volume), z_A and z_B are the charges of the spherical ions A and B, and Q(b) depends on the distance of closest approach "a" (in Å) between A and B, whose (Q) values are tabulated.[21]

Ion-pairing occurs if the centres of the ions A and B approach each other at distances shorter or equal to q. Therefore, this distance becomes larger in solvents with a lower dielectric constant. With large ions where a>b, A and B do not associate at all.

Fuoss[18] developed equation 13 for contact ion pairs, however the experimental results did not show any difference between his equation and Bjerrum's.

$$K = 0.00252a^3 \exp(560 z_A z_B / \varepsilon a) \quad \text{Equation 13}$$

Although all these equations proved to give good results, they have to be handled with care because there are other parameters that must be taken into account when studying ion pair interactions. For example, smaller ions are more hydrated and participate in ion-pair formation with their hydrated shells, which make the size of the aggregation even larger than it would have been using larger ions, which are less hydrated. Although many approximations can be carried out when studying host-guest arrangements, in practice it is not easy to estimate the number of single interactions that occur in the whole system.

Figure 15 shows an example of ion pairing interaction between cyclophane **23** with different guests such as purine bases and the nucleoside ATP^{-4}.

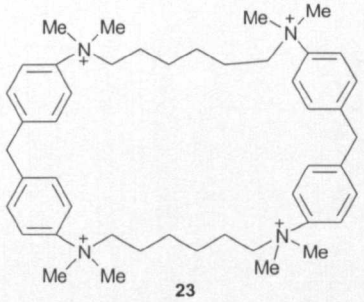

23

Guest	**log K (K in M^{-1})**
Adenine	1.70
ATP^{-4}	4.57
Cytosine	1.23

Figure 15: association constants for cyclophane **23** with different guests.[19]

3.2.3. Cation-π interactions.[19]

A cation-π interaction is a type of electrostatic interaction that occurs between a cation and a π-face of an aromatic structure as shown in Figure 16. This is of extreme importance for cation recognition and transport in proteins.

Figure 16: scheme of cation-π interaction.[19]

3.2.4. π-π interactions.[19]

Interactions between π-systems were studied in detail by Hunter and Sanders.[22] These forces occur when the attractive interaction between π-electrons and the sigma-framework compensate for the unfavourable contributions such as π electron repulsions.

The two types of interactions here are the face-to-face (offset rearrangement) and the edge-to-face, as shown below (Figure 17).

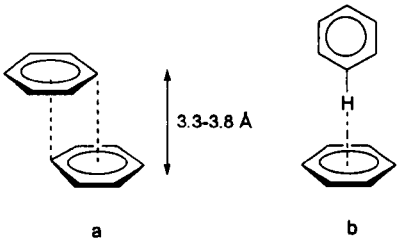

Figure 17: a) face-to-face orientation, b) edge-to-face orientation.[19]

The term edge-to-face will be used to describe the favourable T-shaped arrangement, which is the perpendicular arrangement of aromatic rings. The face-to-face arrangement minimises π-electron repulsion and maximises the attraction between the sigma-framework of one aromatic unit with the π -electrons of the aromatic unit immediately below it.

One example of offset stacked arrangement in porphyrin aggregation is shown below (Figure 18).

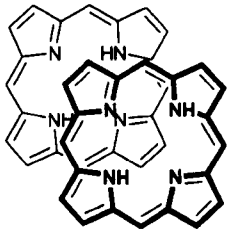

Figure 18: structure of the porphyrin-porphyrin aggregation.[22]

The face-to-face interaction is also responsible for the further stabilisation of the DNA double helix, due to the π-stacking between the aromatic rings of the bases.

3.2.5. Hydrophobic effects.

Hydrophobic effect refers to the fact that polar solvents (water, in general) repel non-polar particles. This has a direct effect on the non-polar groups because they associate in the aqueous solution reducing the contact area with the solvent.

Hydrophobic effect has two energetic components: entalphic and entropic. The enthalpic hydrophobic effect refers to the stabilisation between the water molecules that are released from a host after complexation with the guest, with the water molecules that surround the host. In the entropic hydrophobic effect, due to the solvatation of the host and guest, two cavities are created in the structure of the solvent. Therefore, when host and guest combine to form the complex, such cavities disappear. Thus, there is a gain in the entropy due to the minimisation of the interference that host and guest provoke separately in the water aggregate.

An example of enthalpic effect is shown in Figure 19.[18]

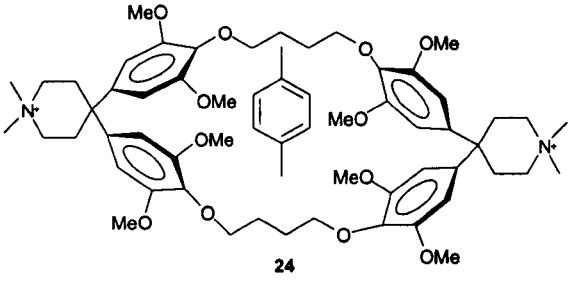

24

Figure 19: host guest complex between p-xylene and a cyclophane host **24.**[18]

The binding constant of the complex **24** in water is $K=9.3x10^3$ M^{-1}, and the complexation free energy is $\Delta G=-22$ $kJmol^{-1}$. Therefore, the favourable enthalphic stabilisation is $\Delta H=-13$ $kJmol^{-1}$, and the unfavourable entropic component is $T\Delta S=-9$ $kJmol^{-1}$. The forces involved in the complexation are π-staking and Van der Waals, which are too weak to give such a large ΔH value. Therefore, the hydrophobic effect is recognised as the driving force of the host-guest complexation.

3.3. Host-guest dynamics

Any host-guest system is characterised by its thermodynamic and kinetic parameters. When referring to kinetics, there are several motional processes than can occur in host guest systems, which must be taken into account when carrying out dynamic studies. These processes involve the translational movements (responsible for association and dissociation process), rotational processes (that affect the relative orientation of the guest in the cavity of the host) as well as the internal mobility of each component in the host-guest system.[23]

3.3.1 Guest exchange

There are numerous examples in which the encapsulation of a cation, in the cavity of the macrocyclic receptor, is produced by a strong coordination between the atoms in the inner cavity and the cation, resulting in a stable binding between them. However,

the contrary effect can also be observed. Once the guest molecule or ion is 'entrapped' by the macrocycle receptor, it does not necessarily remain in the inner cavity permanently, it can also depart from it. The process of cation exchange has been studied by using different NMR techniques.

The guest exchange can also be studied by looking at the variation of the chemical shift of the ligand after the complexation process. When this happens, a difference in the chemical shift is observed, as well as variations in the symmetry of the receptor. Therefore, when the host encapsulate the guest, the host loses its symmetry, which can be observed in the NMR spectrum. This information provides enough data to obtain the exchange rate by lineshape analysis, giving the measurement of the dissociation process.[24] The best known method used for the extraction of rate constants are the coalescence method.

3.3.1.1 Coalescence method.

The spectrum of a dynamic system depends on the particular dynamic process involved and the rate constant associated with it, as well as the temperature and the magnetic field of the NMR instrument.

For any process, there are four distinct temperature regimes: slow, intermediate, coalescence and fast exchange.[25] Dimethylformamide (Figure 20) is often used as a textbook example to illustrate conformational changes, that are energetically possible.

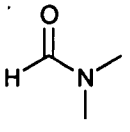

Figure 20: structure of dimethylformamide.

Slow exchange: occurs when an exchange process is slow on the NMR time scale. In this process, the signals of the free and complexed species appear in the NMR spectrum separately, and there is less than 20% overlap.

When T<Tc, where Tc is the coalescence temperature, the equation that applies to calculating the rate constant is equation 14.

$$k = \pi(h - h_0) \quad \text{Equation 14}$$

Where h_o is the width at half height of the peak at the low temperature limit and h is the width of the peak at the initial temperature.

Intermediate exchange: exchange resonances just merge into a broad peak with two crests in the spectra. The minimum between two peaks is at least 20% of peak intensity. The rate constant can be calculated from equation 15.

$$k = \frac{\pi}{\sqrt{2}}(\Delta\nu_0{}^2 - \Delta\nu^2)^{1/2} \quad \text{Equation 15}$$

Coalescence T=Tc. At this temperature, the peaks reunite in a broad band, and the rate constant can be calculated using equation 16.

$$k = \frac{\pi\Delta\nu_0}{\sqrt{2}} \quad \text{Equation 16}$$

Where $\Delta\nu_0$ is the chemical shift difference between the resonances in the low T limit.

Fast exchange: exchange process fast on the NMR time scale (T>Tc).

In the fast exchange (equation 17), the signal observed appear as an average of all species involved in the exchange process.

$$k = \frac{\pi\Delta\nu_0{}^2}{2(h - h_0)} \quad \text{Equation 17}$$

Figure 21 shows an example of a dynamic NMR for two equivalent exchanging groups, in dimethylformamide. The line shape analysis of the NMR spectra peaks allows the calculation of rate constants at different temperatures.

For a simple two-site, equal population exchange process (Figure 21), there is a straightforward formula linking $\Delta\nu_0$ and line widths to k. In a more complex situation, the extraction of data is more problematic, and requires a full simulation of the spectra at various temperatures.

The coalescence method is not only applicable to the exchange rate between protons of the same molecule, but also can be used in more complicated systems. In a supramolecular complex, the NMR study of the exchange of protons between the host-guest complex, can give important information about the exchange rate. The line shape reflects the exchange rate (k_A of either host or guest or k_B, for the host-guest complex) as well as their concentrations (p_A, p_B). Therefore, above the coalescence point either k_A or k_B can be calculated from equation 18:

$$k_A = \frac{4\pi p_A^2 p_B^2 \Delta\nu^2}{\Delta_A} \quad \text{Equation 18 } \textit{(Above coalescence)}$$

Where Δ_A is the observed line broadening of a signal, A, minus the half-height line width without exchange broadening ($h-h_o$).

Furthermore, p_A and p_B, can be also calculated from the equilibrium constant K measured by other methods.

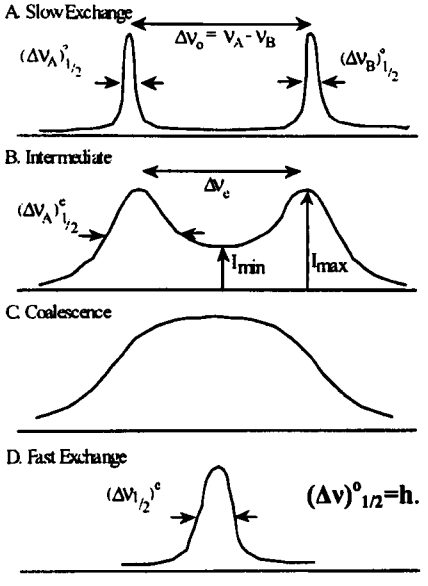

Figure 21: effect of the exchange of chemically equivalent nuclei on NMR line shapes. Where $(\Delta\nu)^o_{1/2}=h$.

However, below the coalescence point, the equation that must be applied is equation 15 shown above.

It should be pointed out that ΔG can be obtained directly at the coalescence temperature following equation 19 given below:

$$\Delta G^{\neq} = RT_c[23 + \ln(T_c / \Delta\nu)] = 8.3x10^{-3}T_c[23 + \log_{10}(T_c / \Delta\nu)]$$

Equation 19

Where Tc is in degrees Kelvin, ν in Hz and R is the gas constant (8.31 J $K^{-1}mol^{-1}$).

ΔG can also be obtained directly using the Eyring equation (Equation 20).

$$k = \frac{k_B T}{h} e^{-\Delta G^{\neq}/RT}$$ Equation 20

Where k_B=Bolzmann constant=$13.80x10^{-24}$ J K^{-1} and h=Plank's constant ($6.62x10^{-34}$ Jxs).

The disadvantage of this method it is not always correct for the multi-site systems that are frequently encountered in supramolecular chemistry.

3.3.1.2 Two Dimensional Exchange spectroscopy (2D-EXSY).[26]

The 2D EXSY can generate good results for more complicated systems than those shown above, when the system under study involves intermediate exchange.

The importance of this type of experiment is that it deals with the effects in a broad sense of chemical exchange between sites with different chemical shifts and/or different coupling constants.[26] Exchange rates should be faster than the longitudinal relaxation time but slow enough not to affect the lineshapes.

The EXSY spectrum can be interpreted in the same way as a ^{1}H-^{1}H-COSY, however the former shows the interchange of protons between molecules, whereas the latter shows coupling connectivity within the molecule.

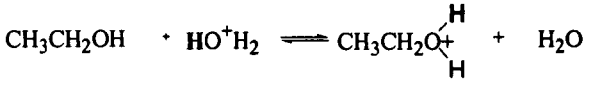

Figure 22: equilibrium exchange methanol-H_2O.

The simplest case of interchange, easily detected in an EXSY spectrum is the mixture of ethanol and water.[27] The ^{1}H-NMR spectrum shows the water peak at 2.8 ppm, and the OH peak at 3.3 ppm. In the 2D spectrum a cross peak is observed, which means that there is an interchange between the two protons.

The pulse sequence for measuring this chemical exchange is shown in Figure 23.

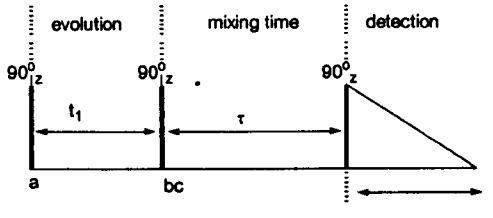

Figure 23: pulse sequence for EXSY.

For this experiment a 90° pulse is applied first. During the t_1 time, the proton chemical shift evolution takes place. Then the second 90° pulse rotates one component along the z-axes. The length and sign of the vector along z oscillates with the proton chemical shift frequency. During the mixing time (τ) coupled spins exchange magnetisation with each other, thereby transferring the chemical shift information from one proton to its exchanging partner. The final 90° pulse tests the length of the vector along the z-axes by rotating it into the x-y plane.

3.3.1.3 Host control of guest exchange.

The rate constant of complex formation does not necessarily depend on the flexibility or the size of the receptor. Some receptors possess a rigid hollow shell that contains a portal through which guests can enter in or depart from the inner cavity.

This transportation happens due to the (thermal) overcoming of the steric constraints imposed by the size and shape of the guest and of the portal, as well as the attractions of the inner part.

An interesting example of this type of aggregation was published by Cram and co-workers,[28] in which the term *"Constrictive binding"* was introduced to explain the steric repulsions that must be overcome for the dissociation of the receptor.

Hemicarcenad **25** (Figure 24), was tested with different guests such as $(CH_3)_2NCHO$ and $(CH_3)_2NCOCH_3$. The experiments were carried out in solutions of 0.3 M and the complexation ratio was determined by ^{1}H-NMR of free and complexed host. The results of the experiment showed that the guests can be expelled thermally by heating the complex to high temperatures in high boiling point solvents (too large to enter the cavity, like 1,2,4-$Cl_3C_6H_3$), leading to the free receptor and the guest.

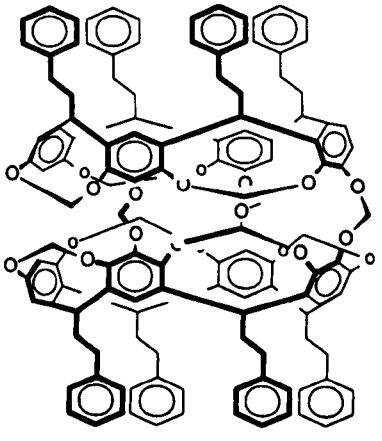

25

Figure 24: structure of hemicarcenand **25**.[28]

Another feature of importance in the host control of guest exchange is the variation in the size of the cavity by conformational modifications of the host. This is the case in Rebek's "self folding cavitants" **26-a** and **26-b**, shown in Figure 25.[23]

The cyclic array of hydrogen bonds introduces an element of chirality in the structure, and when the hydrogen bonding reversal is slow (in the NMR time scale), the $C(O)CH_2$ protons become diastereotopic.

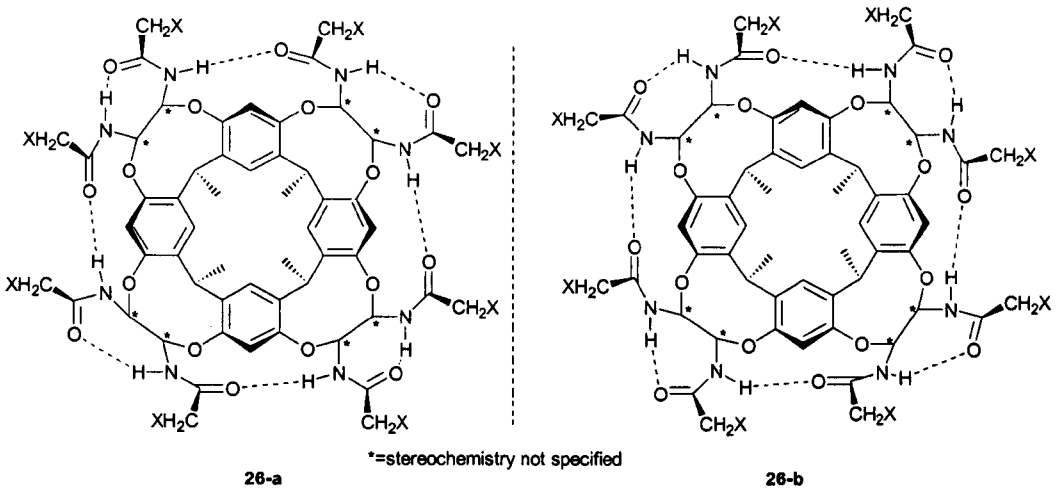

Figure 25: the cavity formed by the vase conformation of the self-folding cavitants **26** is extended by a cyclic array of H-bonds that renders the molecule chiral.[23]

When adamantane is used as a guest, the activation energy for the exchange (in and out of the cavity) was studied by EXSY and coincides with the activation barrier for the inversion of the bond array (70.4 kJ mol^{-1}, at 295K). Thus, when the guest is released, the cavitant "unfolds", and it self-folds again when the solvent exchanges the guest. This new rearrangement of the hydrogen bonds of the host interconverts one **26-a** into the diatereoisomer **26-b**.

The narrow entrance of the cavity is maintained by an intramolecular cyclic array of H-bonds that also result in non-equivalent amide NH groups. The H-bonding provokes the shifting of the NH signal downfield. The conformational modification of the host, also called *gating event*, involves a major conformational change because of the partial breaking of the H-bond. By using NMR techniques, its rate can be measured from the exchange of non-equivalent amide protons.

The release of the guests can also be due to the dissociation of the receptor, and in some cases once the guest is liberated, the receptor undergoes cyclisation to return to its original structure.

3.3.2 Effects of the guests in the dynamics of the hosts.

Instead of an increment of the flexibility in the receptor or host, this flexibility can be reduced after the complexation. This is the result of the non-covalent "cross-linking" introduced by simultaneous interactions of the guest with several binding sites. The guest complexation can also cause a change in the global shape of the molecule, thus modifying the hydrodynamic properties such as diffusion coefficients, relaxation times or viscosity of samples in solution.

An example of flexibility reduction in the host after complexation is shown in molecules such as **27-a** and **27-b** in Figure 26. In the absence of a guest, the methoxy groups can pass through the cavity. However, after complexation with sodium this flexibility is strongly reduced.[23]

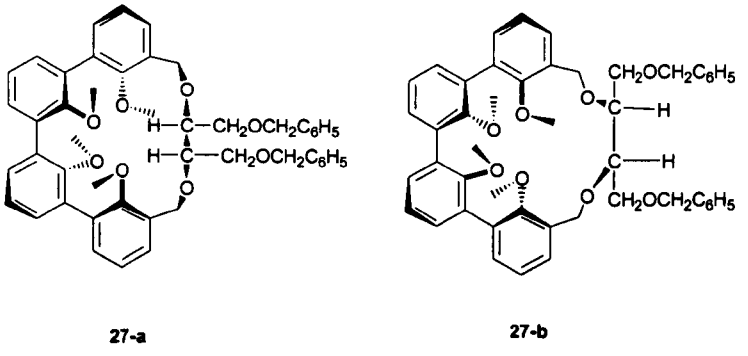

27-a 27-b

Figure 26: structure of different hemispherandes. The interconversion of 34 and 35 can be followed by NMR.[23]

The interconversion equilibrium between **27-a** and **27-b** results in coalescence at 0°C at 200 MHz in the ^{1}H-NMR spectrum. However, the presence of Na^+ inside the cavity eliminates the possibility of this interconversion, therefore no coalescence occurs and only the complex **27-a** is observed.

3.3.3 Dynamics of guests inside hosts.[23]

It was explained above how the presence of a guest molecule in the cavity of the host can provoke restrictions in the conformational mobility of the macrocycle. The same type of restrictions can occur in the complex as a whole. The restriction in conformational freedom upon host-guest complex formation has to be considered as one of the defining parameters for supramolecular complexes.

The dynamic coupling coefficient is defined as the ratio of correlation times of host and guest monitored by NMR. There are two types of complexes: [29]

Isodynamic complexes: the reorientation of the guest is strongly restricted, therefore the dynamic coupling posses a value of about 0.6.

Anisodynamic complexes, with a low value of this ratio (0.11-0.26) in which the guest reorients rapidly inside the cavities.

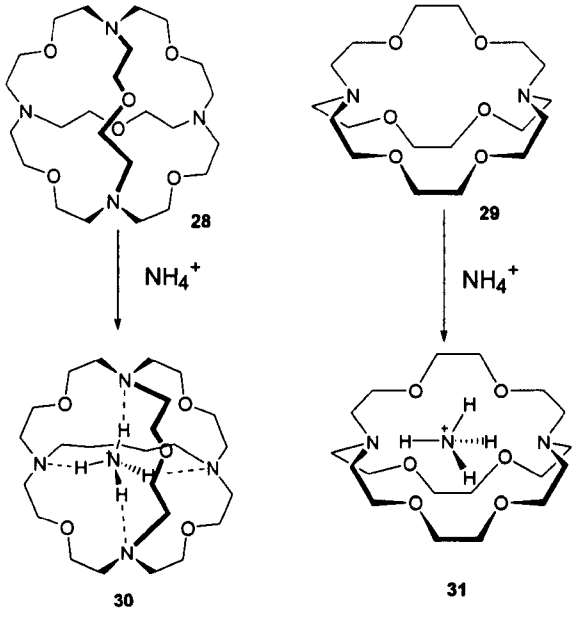

Figure 27: structure of criptands, and cryptates complexed with NH_4^+.[23]

An example of isodynamic and anisodynamic complexes is shown in Figure 27. Macrotricyclic cryptand **28** binds strongly with tetrahedral NH_4^+ to form cryptate **30** (Isodynamic complex). The ammonium ion fits into the cavity of the cryptand and is held by a tetrahedral array of $^+$N-H···N hydrogen bonds (the dynamic coupling coefficient is very large). However, the same guest in cryptate **31** (anisodynamic complex) does not undergo the same complexation, it is much weaker as there is not tetrahedral stabilisation. In cryptate **31** the NH_4^+ undergoes internal rotation inside the host.

Chapter II

BINDING STUDIES

Supramolecular chemists have developed various methods to understand the factors governing host-guest systems, such as binding constants, selectivity, solvent effect and quantification of binding energies between host and guest.

Each type of complexation or assembly between the macrocycle receptor and the target molecule has to be studied with the most suitable technique.

This section provides a short review of these techniques, in which NMR methods are described in more detail due the importance of this technique in this thesis.

4. Analytical methods for binding determination.

4.1. Electrochemical methods.

The majority of the studies related to the stability of complexes in molecular recognition involve a host receptor, which can be a neutral or charged macrocycle, and a charged guest (molecule or metal-ion). The best methods for the investigation of these complexes are based in the movement of charges generated in the assembly. The most important ones are *potentiometry* and *conductimetry*.[18]

Potentiometry, is a resourceful technique used for the determination of stability constants of metal-ion guests linked to macrocyclic hosts. In general, these methods involve a titration procedure (of different types depending on the array of equilibrium studied) carried out in a Galvanic cell.

Conductimetry, is used for the measurement of thermodynamic quantities (association constants, for instance) in reactions of electrolytes in solution, where only neutral hosts can be studied.

4.2. Calorimetry.[18]

This technique can determine the heat flow associated with a chemical reaction by measuring the temperature change it produces.

Titration calorimetry,[30,31] developed by Christiensen and Izatt, is a method for the determination of enthalpies of reaction and heat capacity in solution, when one reactant is titrated against another. The determination of ΔH values can be obtained by the application of the Van't Hoff equation (equation 21) to the temperature dependence of binding constant.

$$d(\log K)/dT = \Delta H/RT^2 \quad \text{Equation 21}$$

where T=temperature and ΔH the enthalpy of reaction.

The Van't Hoff equation for the chemical equilibrium relates the temperature dependence of the binding constant with the change in the standard enthalpy of the chemical reaction. This equation suggests that the standard enthalpy of the chemical reaction can be determined from two parameters, temperature and binding constant. Binding constants are relatively easy to determine experimentally, which makes this method very useful. Furthermore, as discussed above, using the binding constant, the standard Gibbs energy (ΔG) (equation 4) of the chemical reaction can also be calculated. Finally, the expression relating the Gibbs energy to enthalpy and entropy yields the standard entropy of the reaction (Equation 5).

$$\Delta G = \Delta H - T\Delta S \qquad \text{Equation 5}$$

4.3. Mass spectrometry.

The involvement of mass spectrometry in host-guest chemistry was triggered by the need to characterise complex molecules with higher molecular weight and lower volatility.[32]

The studies performed in host-guest chemistry using this technique can be carried out in two different ways. The **solution method** involves the dilution of the host and guests together, and the **gas phase method** concerns the evaporation of the reacting species separately in order to allow them interact in the absence of solvent.

The gas phase method was widely used with crown ethers, as this produces the best results, since the interactions are supported by sufficient solution data to allow the specific and precise evaluation of the parameters involved in these interactions. Another advantage of this method is that the results observed are not affected by the interactions that the solvents may cause in the system.

Figure 28 shows an example of the Mass spectrum of the calixarene Prop-Pyr **32**, which underwent an extensive complexation with isopropyl acetate *m/z* 1162 [Prop-Pyr+MeCOOiPr.H^+] and to a small extent with isopropyl alcohol at *m/z* 1120 [Prop-Pyr+iPrOH.H^+] under desorption chemical ionisation (DCI) conditions.

Brodbelt and co-workers[33] showed that in particular ESI-MS provided a good method for evaluation of binding selectivities in host-guest complexes.

In order to confirm the veracity of the results, they focused their study on known complexes already studied by traditional methods.

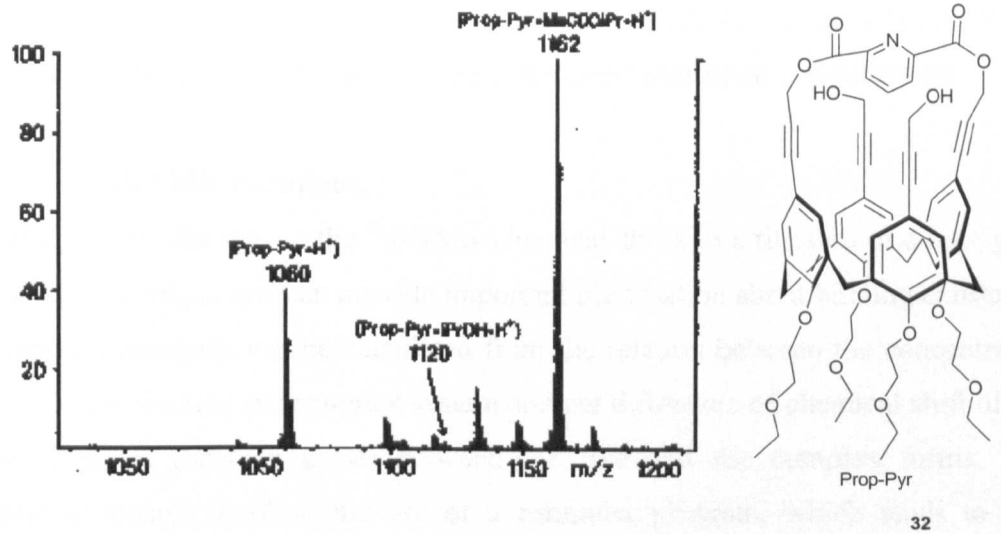

Figure 28: host-guest complexation process during DCI-MS experiment using a calixarene host and an equimolar mixture of propan-2-ol and isopropyl acetate in an excess of methane.[30]

One of the examples reported was the study of the selectivity binding of two hosts competing for the same guest, carried out by mixing two crown ethers (15-crown-5 and 18-crown-6) with Na^+. The results obtained showed a larger affinity for the Na^+ from the 18-crown-6, as expected.

Beauchamp and co-workers[34] published an example of molecular recognition using ESI-MS (Figure 29). The amino acid arginine **34** and 30-crown-10 (30-C-10) **33** formed a complex, because the protonated alkyl guanidinium side chain of arginine formed stable non-covalent bonds (H-bonding and ion-dipole) with the crown ether. In addition, it was demonstrated that **33** had more affinity with **34** than the related compound, 27-crown-9.

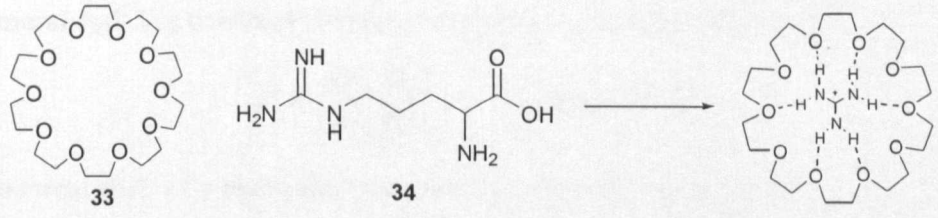

33
30-C-10

34
arginine

Figure 29: structures of 30-C-10 and arginine used in for a complexation study by ESI-MS.

5. Determination of binding by NMR.

5.1. One Dimensional NMR.

Techniques involving one dimensional NMR are used for characterising thermodynamic processes as the extraction of binding constants. The most common

method used for these proposals is the NMR shift titration, which is based on the change of the chemical shift that a given proton undergoes upon complexation.

5.1.1 ^{1}H-NMR Shift Titrations.

The study of the changes in the ^{1}H-NMR chemical shifts in a titration of a host-guest system is a technique that can provide important information about binding constants. The binding constants can be calculated from the relation between the concentration of the species forming the complex system and the difference of chemical shift of one of the samples (host or guest) between the free and the complex forms. This calculation always involves the use of a computer program, which tends to give reasonably accurate results, where the error can be around 10%.[18]

Host-guest process can occur in two different ways:

If it is slow in the NMR time scale, then two different set of signals are observed; one for the free and one for the bound (host or guest) proton.

If the complexation process is fast in the NMR time scale, then the chemical shift observed is a weighted average between the chemical shift of the free and bound species.

Programs such as EQNMR[35] is one of the methods used to evaluate binding constants in systems where all the species are in fast equilibrium, and where the chemical shifts vary with the degree of complexation.

Consider the system of 1:1 aggregation:

$$H_m + G_n \rightleftharpoons H_mG_n$$

The general stability constant (binding constant) is given by equation 22.

$$K = \frac{[H_m G_n]}{[H]_m [G]_n} \qquad \text{Equation 22}$$

The chemical shift of a particular resonance is given by equation 23.

$$\delta_{calc} = \sum_{m=1}^{m=i} \sum_{n=0}^{n=j} \frac{\delta_{mn} K_{mn} m[H]^m [G]^n}{[G]_{total}} \qquad \text{Equation 23}$$

Where δ_{calc}, is the average of the chemical shifts of the various species containing G, and i and j represent the maximum values of m and n respectively.

δ_{mn}, is the chemical shift of each species present, where *mn* is the ratio of H and G.

K_{mn}, is the stepwise binding constant.

The program resolves the optimum values for δ_{mn} and K_{mn}, which best fit in the experimental data.

In a typical ^{1}H-NMR shift titration experiment, the binding stoichiometry is firstly stabilised by the method of continuous variation or "Job-plot" analysis. Here the change of chemical shift (δ) is monitored on dependence of the molar ratio "x". The maximum in the curve indicates the binding stoichiometry. Thus when the maximum of the curve appears at 0.5 the relation host-guest is 1:1.

The graphic representation of a titration experiment can give different information. Thus, there are two types of plot (Figure 30): **The non-linear fitting,** which is used for the determination of binding constants and it is used for fast equilibrium, and **the job plot analysis**, for the investigation of the stoichiometry. [36,37]

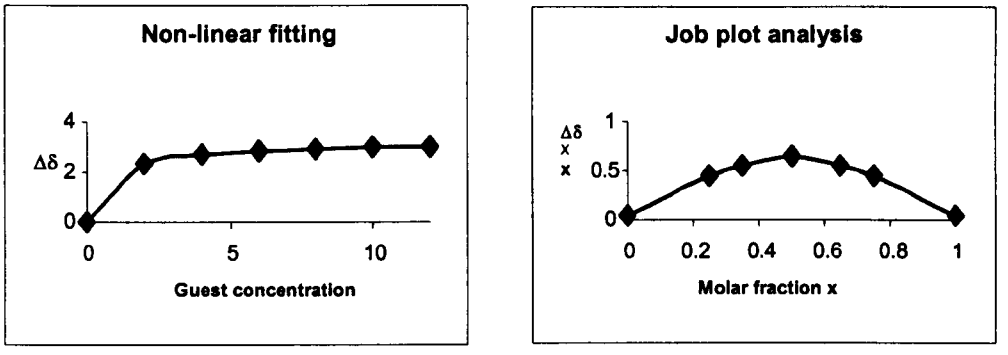

Figure 30: graphics obtained from NMR titrations.

The example given below is a titration[38] of slow exchange equilibrium. The information is obtained by plotting the molar relation of guest/host against the difference of chemical shift of the protons of the host.

In this example, the NMR titration is carried out using as host the calixarene (Figure 31) and the guest $La(CF_3SO_3)_3$ in $CDCN_3$ at room temperature.

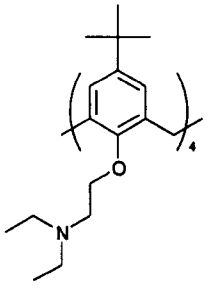

(La^{3+}/L)	$\underline{OCH_2}CH_2N$ Δδ
0.5	0.088
1.01	0.206
1.51	0.263
2.01	0.359

Figure 31: [tetrakis(N,N-diethylaminoethyl)oxyl]*p-tert*-butylcalix[4]arene.

The chemical shift changes occur gradually with an increase in the metal-ion salt concentration. For example, the chemical shift of the protons in the $O\underline{CH_2}CH_2N$ (in the free host) rises by a value of 0.106 ppm when complexing in a relation of 1:1 with the host, and reaches the 0.359 ppm in a 2:1 ratio.

The NMR shift titration method has two limitations due to the potential sources of error that can lead to wrong results. The first one is carrying out the titrations at concentrations unsuitable to the equilibrium. Typically titrations should be carried out between 20%-80% of complexation degree. The second one is confusion of acid-base equilibrium with binding. Figure 32 shows an example of the two possible interactions between the two species.

In order to resolve the ambiguity between binding and acid-base chemistry, carrying out a dilution ^{1}H-NMR experiment is sufficient. As proton transfer is independent of the concentration, as opposed to complexation, if proton transfer occurs, there will be no changes in the $\Delta\delta$ after dilution.

The methodology for the study of supramolecular complexes (i.e. dynamics of host-guest aggregates) involves more complicated parameters than the study of the variation of chemical shift. This is because the properties of each complex can vary depending on the species that are forming it.

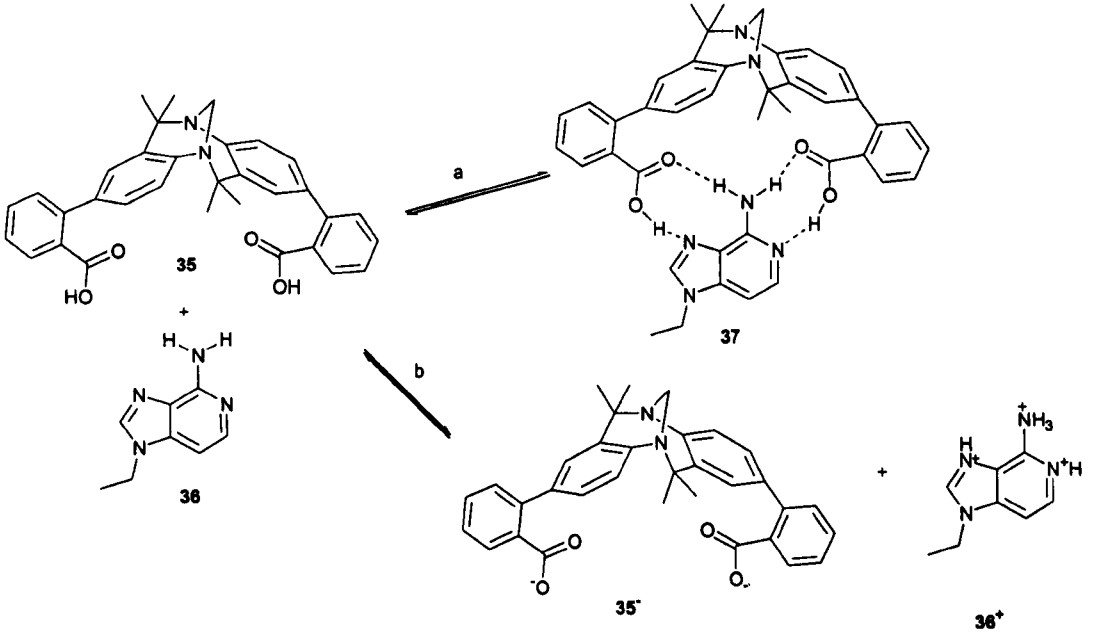

Figure 32: representation of the two possible interaction: complexation (a) and proton transfer (b).[18]

5.2 Two Dimensional NMR.

5.2.1 Diffusion ordered Spectroscopy (DOSY).

The latest progressions in supramolecular chemistry and host-guest systems have been improved due to the development of new spectroscopic techniques. This has enhanced its study due to the possibility of investigating new parameters that were impossible to access with classical methods. One of the most important tools is the study of diffusion coefficients using NMR.

Transport properties of molecules and ions are characterised by diffusion coefficients. The concept of diffusion appeared with the need to find new NMR dimensions (size, charge, mass...) to explain different properties of complex systems. The 'ordinary' NMR cannot provide information regarding these properties. The connection of 'diffusion' and structural properties arises because the diffusion coefficient D depends on friction factors and electrophoresis mobilities[18] according to the Debye-Einstein equation.[39]

$$D = k_B T / f_T \quad \text{Equation 24}$$

$$f_T = 6\pi\eta r_H$$

Where k_B is the Boltzman constant (1.38×10^{-23} J K^{-1}), T is the absolute temperature (K) and f_T is the friction factor, η is the viscosity, and r_H is the hydrodynamic radius.

Equation 24 shows that the hydrodynamic radius is inversely proportional to the diffusion coefficient, therefore molecules of different size possess different diffusion coefficients.

In order to understand how the diffusion coefficient is obtained, it is essential to understand the NMR parameters involved in this process.

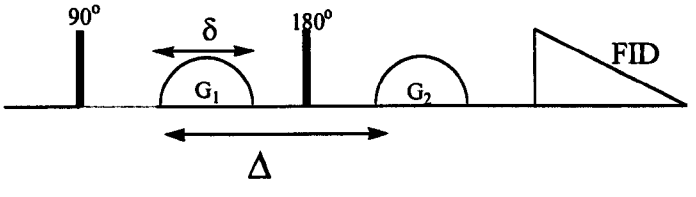

Δ: time separations between the process of dephase and refocus provoked by the gradients

δ: duration of the gradients, and G1, G2: gradient pulses

Figure 33: pulse sequence in diffusion NMR.

Diffusion ordered nuclear magnetic resonance is based on a pulse gradient spin echo (PGSE) technique. The 'gradient' (G_1 and G_2) is a period in which the magnetic field becomes deliberately non homogeneous, and the spin echo is a pulse sequence where first a 90° pulse is applied followed by a 180° pulse. (Figure 33).

If a gradient is applied, the refocusing proton can adopt a position different to the position that it had when the first gradient was applied, which means that it will not be refocused, therefore, it will be not detected or will be detected in a different position.

The diffusion coefficient is obtained relating the intensity of the signal of a specific nucleus in dependence of the intensity of the gradients.

The Stejskal-Tanner equation (equation 25) shows the relationship between the diffusion coefficient and the parameters introduced above.

$$I = I_o e[D(\gamma\delta g)^2(\Delta - \delta/3 - \tau/2)] \quad \text{Equation 25}$$

Where I_0 is the resonance intensity at zero gradient strength, I: observed intensity of the signal, D is the diffusion coefficient in the direction of the gradient, γ is the gyromagnetic ratio of the observed nucleus, δ is the duration of the gradient pulses, Δ: time separations between the process of dephase and refocus provoked by the gradients, δ: duration of the gradients and τ: correlation time.

The Diffusion coefficient can differentiate between large (host) and small (guest) molecules through the application of gradient magnetic field pulses. These gradient pulses are used to spatially determine the position of the molecules.

After the diffusion delay, a decoding gradient is applied. The magnetisation that is detected is primarily due to those molecules that do not diffuse during the diffusion delay. The larger the diffusion coefficient of a molecule, the larger the attenuation of the intensity of its NMR signals.

The diffusion coefficient (D) is obtained by measuring the NMR spectrum as a function of the square of the gradient area (or amplitude for pulses of fixed length), D can be obtained from the exponential decay of the resonance intensity.

The key principle is that small molecules diffuse faster than larger molecules. When the diffusion coefficient (D) of protons in a host-guest system is measured, the value of D obtained will be exactly the same for all nuclei that form the system (i.e. host and guest). If the encapsulation is not effective (the host does not bind the guest) those

values will be different. In this situation, the D of the guest will be higher than the D of the host.

Suppose a host-guest system composed by a Host and a Guest molecule in a 1:1 complex.[40]

$$nCD + mG \rightleftharpoons Gm:CDn$$

$$K_a = \frac{[G_m:CD_n]}{[CD]^n[G]^m} \qquad \text{Equation 26}$$

Where [CD]: concentration of the host; [G]: concentration of the guest molecule; $[G_m:CD_n]$: concentration of the inclusion complex.

If the free and bound hosts are in fast exchange on the NMR diffusion time scale, the D measured for the host will be a weighted average of the free and bound forms according to the equation:

$$D_{obs} = f \times D_{complex} + (1-f)D_{free} \quad \text{Equation 27}$$

$$f = \frac{D_{obs} - D_{guest}}{D_{complex} - D_{guest}} \qquad \text{Equation 28}$$

Where D_{obs} is the apparent (weighted average) diffusion constant of the guest, $D_{complex}$ is the diffusion constant of the host, D_{guest} is the diffusion constant of the guest, and f fraction of bound guest. Because experimentally $D_{complex}$ cannot be determinated, it is supposed that for small guest molecules $D_{complex} \approx D_{free}$.

Therefore, by plotting f versus [CD] the K_a is obtained.

$$f = \frac{K_a[G][CD]}{[G]+[G]K_a[CD]} \qquad \text{Equation 29}$$

$$f = \frac{K_a[CD]}{1+K_a[CD]} \qquad \text{Equation 30}$$

5.2.2 Two Dimensional Nuclear Overhauser Spectroscopy (NOESY)

All the experiments and techniques that have been explained so far, referred to the determination of binding constants. This section shows different procedures for the elucidation of structures in host-guest systems.

This experiment is based on the same pulse sequence EXSY spectroscopy,[26] where the cross peaks are observed for dynamic systems in the region of slow exchange between

the resonances of those nuclei, which are exchanging their frequencies. The exchange of magnetisation during the mixing time is based on the Nuclear Overhauser effect. Similar to the 1-D NOE experiments, when one multiplet is irradiated, protons close in space are affected. The strength of the NOE effect depends on intermolecular distances and molecular weight of the molecule under study.

This technique is useful for determining which signals arise from protons that are close in space but not connected by chemical bonds (for distances smaller that 5 Å). Thus, a NOESY spectrum provides crucial information about the geometry of molecules.[41] The NOESY experiment also determines cross peaks (which indicate the NOE effect) arising from chemical exchange.

Chapter III

SYNTHESIS OF HEXAIMINE MACROCYCLES

6. Synthesis of Hexaimine macrocycles.

Gawronski and co-workers[42] have recently introduced a new synthetic strategy for the synthesis of large poly-imine *meta*- and *para*-cyclophane type macrocycles. Using a [3+3]-cyclocondensation strategy, in which one equivalent of (1*R*, 2*R*)-diaminocyclohexane **38** reacts with one equivalent of an aromatic dialdehyde to give the macrocyclic structure. According to available databases, there has been no previous examples of [3+3]-cyclocondensation between diamines and aromatic dialdehydes reported, and only a few examples of [1+1][43] and [2+2][44] condensations between similar building blocks were found. It was shown however, that the achievement of such structures has been possible in the presence of templates. For example, the [2+2] cyclocondensation using 2,6-diformylpyridine, was successful in the presence of barium chloride.

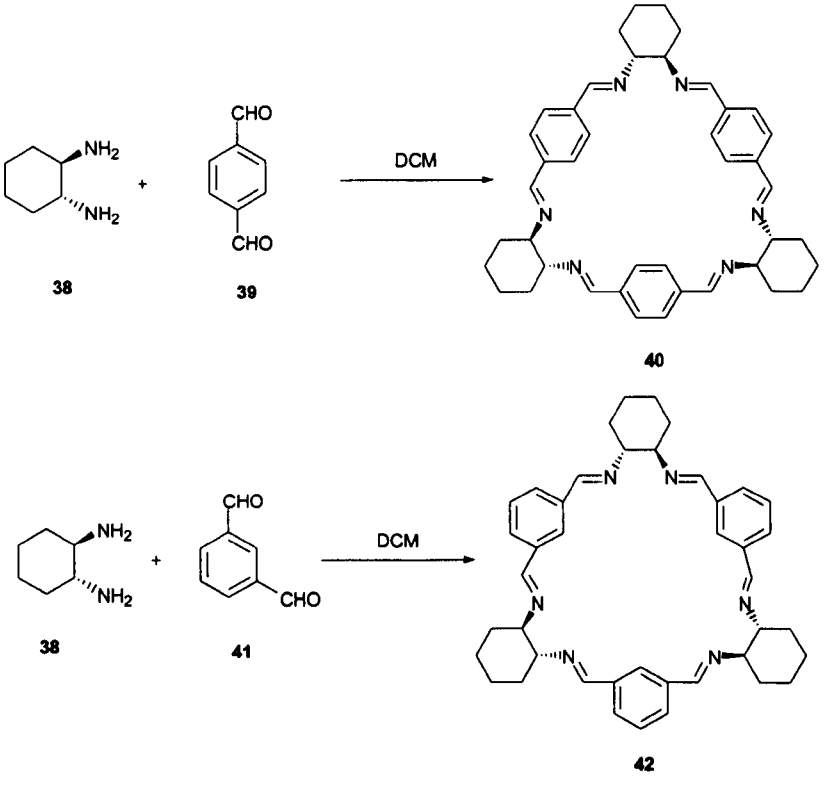

Figure 34: synthesis of hexaimine macrocycles.

In Gawronski's approach, the reaction between (1*R*, 2*R*)-diaminocyclohexane **38** and the aromatic dialdehydes isophthalaldehyde **39** and terephthalaldehyde **41**, gave the triangular macrocycles **40** and **42** in 90 % yield, in a standard 0.4 M concentration in dichloromethane, after stirring for 3 hours (Figure 34).

The mechanism in the synthesis of both triangle macrocycles proceeds *via* a normal imine or Schiff base formation (Figure 35).

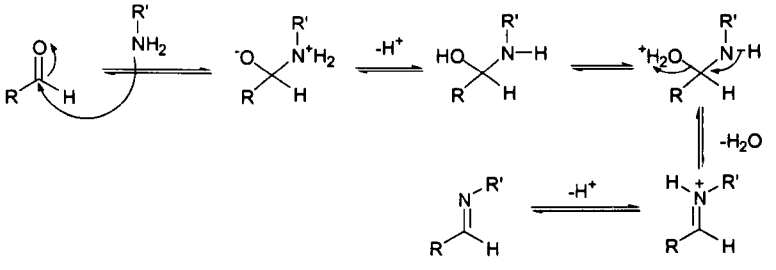

Figure 35: mechanism of imine formation.

The most remarkable characteristic of compounds **40** and **42** is the high symmetry they adopt in solution. This feature is observed in both ^{1}H-NMR and ^{13}C-NMR spectra, where the spectra only show one set of signals, corresponding to one repeated unit. The MS however reveals the molecular ion at *m/z* 636 M^{+} corresponding to the trimeric structure $(C_{14}H_{16}N_2)_3$.

Macrocycle **40** shows a very simple ^{1}H-NMR spectrum in which there is one sharp peak at 8.14 ppm, corresponding to the imine proton, another peak for the two equivalent aromatic protons and three peaks at 3.37, 1.80 and 1.48 ppm for the cyclohexane ring. Macrocycle **42** shows a slightly different spectrum, three signals for the aromatic ring at 7.28, 7.60 (broad) and 7.95 ppm, and at 8.20 ppm for the imine proton.

Both macrocycles exhibit a strong band in the IR spectrum corresponding to the C=N bond at ν 1642 cm^{-1}.

6.1 Principles of formation of macrocycles.

At first glance, the reaction product can be expected to be a linear polymeric chain formed by alternate diaminocyclohexane and aromatic groups. However both building blocks react to form the macrocycles exclusively.

The amino substituents in (1*R*, 2*R*)-diaminocyclohexane **38**, adopt the equatorial positions (Figure 36). Furthermore, it possesses a distinctive rigid structure that will facilitate the ring formation in the reaction with the aromatic dialdehydes, which have a planar structure.

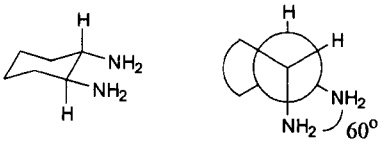

Figure 36: structure of (1*R*, 2*R*)-diaminocyclohexane.

In order to study the cyclisation, MMX molecular modelling was performed for the cyclohexylimine intermediate of the reaction.

Firstly, the structures of the intermediate products were investigated by studying the change of steric energy difference (ΔSE) in dependence of the dihedral angle ω (HC-N=C) that are determined by the rotational freedom of the C-N bonds, which connect the cyclohexane and the aromatic rings. (Figure 37).

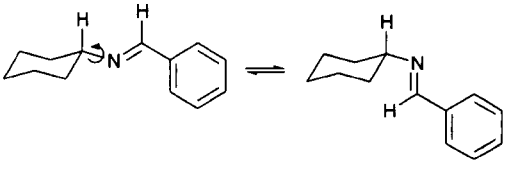

	43-syn	***43-anti***
ω(H-C-N=C) [deg]	0	7.50
ΔSE[kJ/mol]	0	3.83

Figure 37: possible imine conformers: *syn* or *anti*.

The conjugated N=C-C_{Ar}-C=N structural units lie on one plane, which means the structures of all possible conformational isomers result from the changes in the relative orientation of the imine bonds only. Therefore, the imine conformers can be simply characterised with the help of the dihedral angle H-C-N=C, ω, as *syn* or *anti* (Figure 37). MMX molecular modelling shows a preference for the **43**-*syn*, over the **43**-*anti* conformer.

Steric energy difference (ΔSE) calculation was carried out for the diimines **44** (Figure 38) and **45** (Figure 39). The results showed a SE preference of 7.50 and 10.41 $kJmol^{-1}$ for the respective *syn* conformers derived from terephthalaldehyde **39** and isophthalaldehyde **41,** over their *anti* counterparts, which for this reason will not be discussed further. Of all possible *trans* and *cis* conformations for the C=N bond in **44** and **45**, the (**44**-*syn-trans*) and (**45**-*syn, trans*) arrangement is favoured, leading to the corresponding macrocycles **40** and **42**.

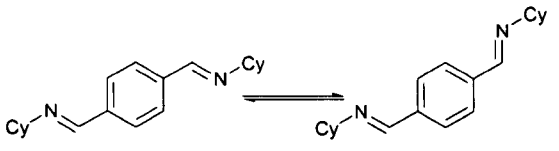

44-syn-trans 44-syn-cis

ΔSE [kJ/mol] (Preferred)	ΔSE [kJ/mol]
0	0.29

Cy=cyclohexyl

Figure 38: possible conformers and steric energies of *para*-diimines.

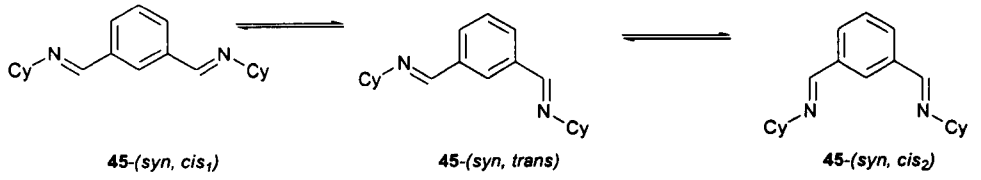

45-(syn, cis_1) 45-(syn, trans) 45-(syn, cis_2)

ΔSE [kJ/mol]	ΔSE [kJ/mol] (Preferred)	ΔSE [kJ/mol]
1.54	0	2.50

Figure 39: possible conformers and steric energies of *meta*-diimines.

In order to confirm that the cyclisation is the most favourable process, computational studies were also extended to the open-chain molecule **46**, shown in Figure 40.

The MMX steric minimisation of **46** reveals that the preferred conformational isomer is the all-*syn*, all-*trans* as it is the one with lowest energy and, therefore, supporting the argument for cyclisation of the macrocycle **40**.

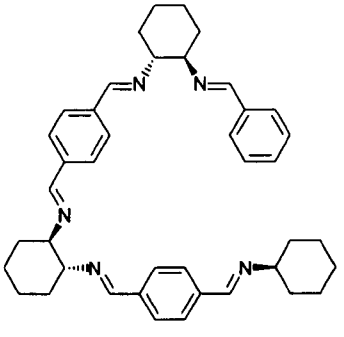

46

Figure 40: structures of open chain compound used in the cyclisation studies.

However, the analogous study carried out for the equivalent structure **42** did not give successful results.

In summary, the macrocyclisation precursor (3 amine and 3 aldehyde units) adopts a minimum energy conformation, in which cyclisation predominates over linear extension, thus giving a rational explanation for the formation of the macrocycles in

often quantitative yields. The macrocycle formation proceeded via a [3+3] diamine-dialdehyde addition, where the aromatic ring is situated on the sides and the cyclohexane on the vertex of the macrocycle.

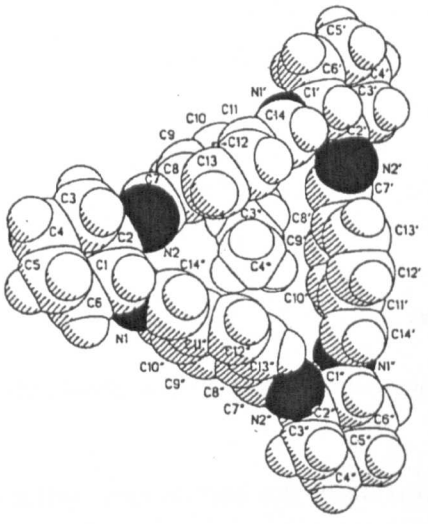

Figure 41: representation of the X-ray determination of macrocycle **40** containing one molecule of ethyl acetate.

The final confirmation for the structure of macrocycle **40** was obtained by X-ray crystallography (Figure 41). Curiously, it was found that the crystal structure shows a 1:1 complex of the macrocycle with ethyl acetate.

The reduction of the imine bond with $NaBH_4$ led to a new type of triangular hexaamines macrocycles **47** and **48** shown in Figure 42.

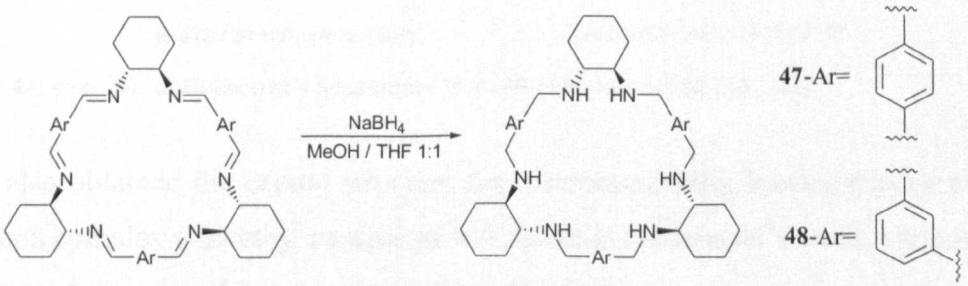

Figure 42: reduction of the hexaimine macrocycles to give the corresponded haxaamines.

Figure 42 shows the reaction scheme for the reduction of the triangular macrocycles. The reduced macrocycles also posses high symmetry in solution and, as in the case of their precursors, the NMR shows only one set of signals for each of the repeating units.

Based on Gawronski's initial studies, and during the course of this investigation, Hodacova and co-workers[45] extended the former's investigations by synthesising macrocycles from the enantiomeric and racemic forms of (1, 2)-diaminocyclohexane **38** with terephthalaldehyde **38** (Figure 43), producing the series of diastereomeric macrocycles represented in Figure 44 and 46.

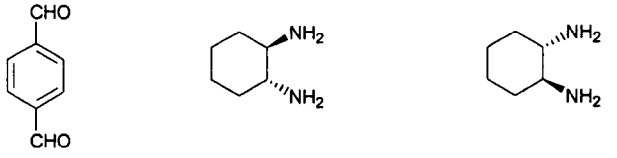

39 **38**-(*1R,2R*) **38**-(*1S,2S*)

Figure 43: structure of the building blocks used in Hodacová's research.

The cyclocondensation reaction was carried out in acetonitrile, dichloromethane and tetrahydrofuran, producing the target macrocycle in each of the solvents. It was also attested that the variation of the stoichiometric ratios of the starting materials did not change the course of the reaction. Compound **40-a** was obtained from **39** and **38**-(1*R*, 2*R*), and **40-b** from **39** and **38**-(1*S*, 2*S*).

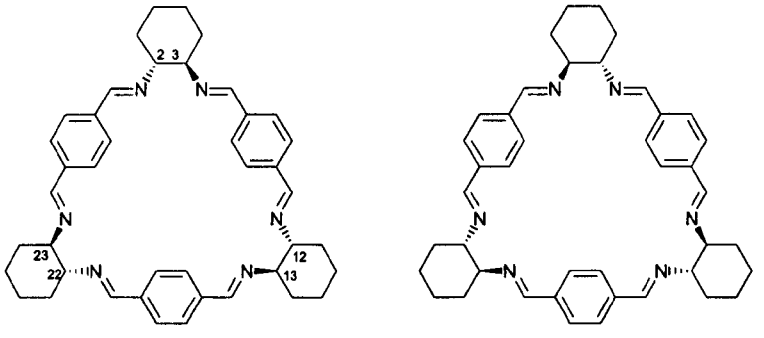

40-a-(2*R*,3*R*,12*R*,13*R*,22*R*,23*R*) **40-b**-(2*S*,3*S*,12*S*,13*S*,22*S*,23*S*)

Figure 44: structure of Hodacová's hexaimines from **38**-(1*R*, 2*R*) and **38**-(1*S*, 2*S*).

They also obtained the crystal structure for macrocycle **40-a** however there was no inclusion complex with ethyl acetate, as was found in Gawronski's work, although the unexpected crystal packing shown in Figure 45 was found.

Figure 45 shows the way in which the stack packing of the triangles forms columns. Also the rearrangement of each column in respect to the neighbouring one is shown to be oriented in an anti parallel way.

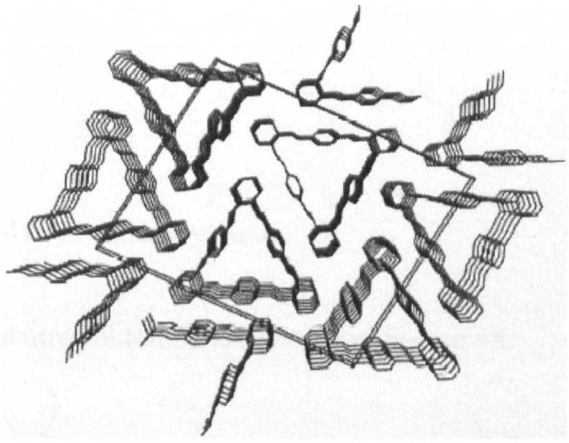

Figure 45: stack packing of the triangle **40**-a.

This feature was studied in depth by crystallising macrocycles from the racemic form of **38**. This investigation involved the recrystallisation of both enantiomers together **40-a** and **40-b.** The structure found was neither compound **40-a**, **40-b** nor the racemic mixture (2*RS*, 3*RS*, 12*RS*, 13*RS*, 22*RS*, 23*RS*). It was in fact a mixture of the two macrocycles formed by both (1*R*, 2*R)* and (1*S*, 2*S)*-diaminocyclohexane *i.e.* macrocycles **40-c** and **40-d**, shown in Figure 46.

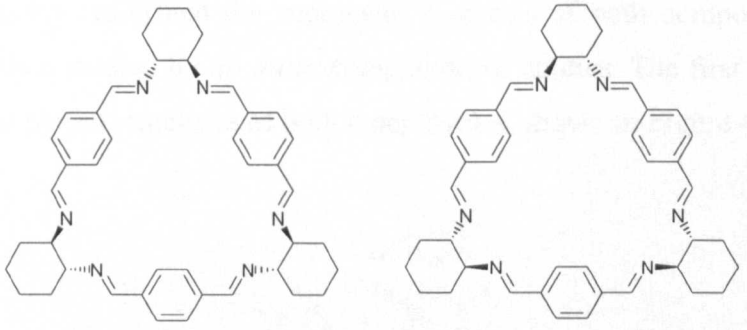

Figure 46: structure of Hodacová's hexaimines from the recrystallisation mixture of **40-a** and **40-b**.

Compounds **40-c** and **40-d** (together with **40-a** and **40-b**) were also obtained, from the reaction product from of terephthalaldehyde and the racemic form, (1*SR*, 2*SR)*-diaminocyclohexane.

Gawronski and Kwit[46] recently extended the study of these triangular-shaped macrocycles named as *calixsalenes* based on the same synthetic approach, but by reacting (1*R*, 2*R*)-diaminocyclohexane with the aromatic dialdehydes shown in (Figure 47).

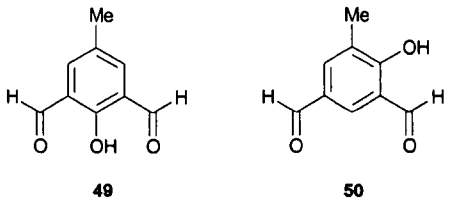

Figure 47: dialdehydes used for hexaimine synthesis.

The new triangular structures obtained are shown in Figure 48.

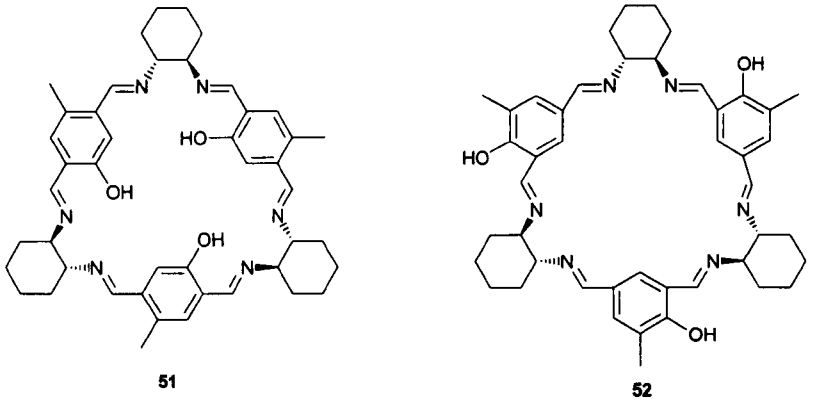

Figure 48: structure of the Gawronski's new hexaimines.

Mass spectrometry confirmed the successful synthesis of both compounds, and the structure was then studied by *ab initio* computational studies. The first approach was the study of the partial structures of both macrocycles, shown in Figure 49.

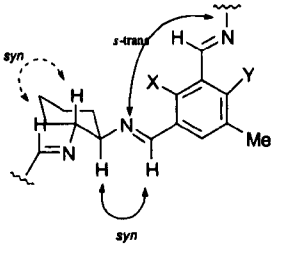

X=OH Y=H for **51**

X=H Y=OH for **52**

Figure 49: conformation of the partial structures of macrocycles **51** and **52**

It was found by Gawronski's previous analysis, the *syn* conformation of both the imine proton and the axial proton of the cyclohexane is preferred to the *anti* one, as well as the *trans* conformation of the diimine unit being preferred to the *cis*. Figure 50 shows the equilibrium for N-benzyledenecyclohexylamine. In the *anti* conformer, the

short distance between the axial proton of the cyclohexane, and the proton of the imine, produces a destabilisation of the structure ($\Delta E \geq 14.58$ kJ/mol).

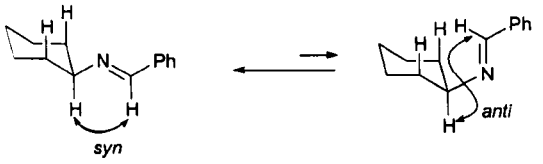

Figure 50: equilibrium for N-bencyledenecyclohexylamine.

The through space interaction for compounds **51** and **52** are summarised in Figure 51, displaying the NOE effects.

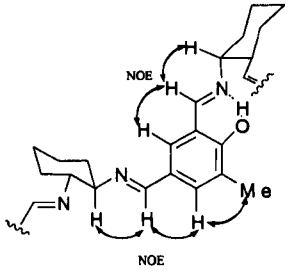

Figure 51: through space interaction for compounds **51** and **52**.

The increased interest in the study of these triangular macrocycles was clearly demonstrated by continued publications relating to modifications of those macrocycles already synthesised, such as that of Martell and co-workers.[47] During the course of this thesis the synthesis and protonation constants of known and new triangular macrocycles were studied, as well as various binding studies

The [3+3]-cyclocondensation of terephthalaldehyde with *cis*-(1, 2)-diaminocyclo-hexane was carried out to synthesise a new triangular macrocycle. Contrary to what would be expected, the reaction product of this cyclocondensation is reported to be only one macrocycle instead of the two diastereomeric structures expected. A by-product was also obtained upon cyclocondensation, which is the [2+2]-cyclocondensation product, and also was reported to be one diastereoisomer. The authors do not specify whether the other possible diastereoisomer was formed or not.

The reduction of the macrocycles obtained was carried out using sodium borohydride as reducing agent.

The overall protonation constant of the mixture of isomers was determined using potentiometric titrations, producing a value of $\Sigma \log K_i^H = 37.91$, which is much higher than that for (1*R*, 2*R*)-diaminocyclohexane (16.30). Additionally, the overall protonation constant for the macrocycle was determined as $\Sigma \log K_i^H = 38.86$. Comparing both results, as well as the value for (1*R*, 2*R*)-diaminocyclohexane, was demonstrated that the overall basicity of the macrocycles depends on the conformational properties.

As nitrogen containing chiral ligands had found widespread use in asymmetric catalysis, the authors also extended their investigations of the behaviour of macrocycle **47** as a Lewis base catalyst for the asymmetric aldol condensation between 4-nitrobenzaldehyde **53** and acetone (Figure 52).

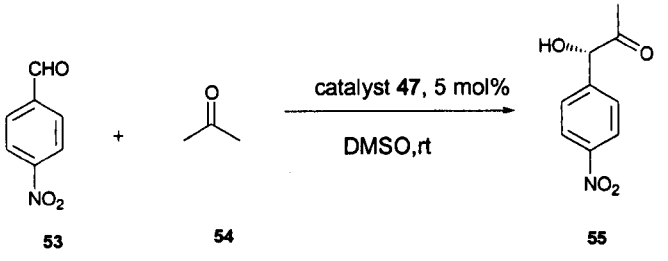

Figure 52: reaction of aldol-condensation between 4-nitrobenzaldehyde and acetone

It was found that the yield, and the enantiomeric excess (ee %), increased as the deprotonation of **47** (which was previously protonated with HBr) occurred (*ie,* more basic). However, once the deprotonation was completed (*ie,* only **47** pure), even adding more base, the yield and ee % did not improve. This means that it is not the basicity which is playing the catalysis role, therefore is the stereochemical properties of the molecule.

Nabeshima and co-workers[48] also investigated the synthesis of triangular macrocycles based on a diamine-dialdehyde condensation. However, the amino moiety used was 1,2-phenylenediamine **57** instead of the (1*R*, 2*R*)-diaminocyclohexane **38** used in the syntheses previously shown. The resulting macrocycles **58** and **60** (shown in Figure 53) posses a planar structure as well as high symmetry (C_3).

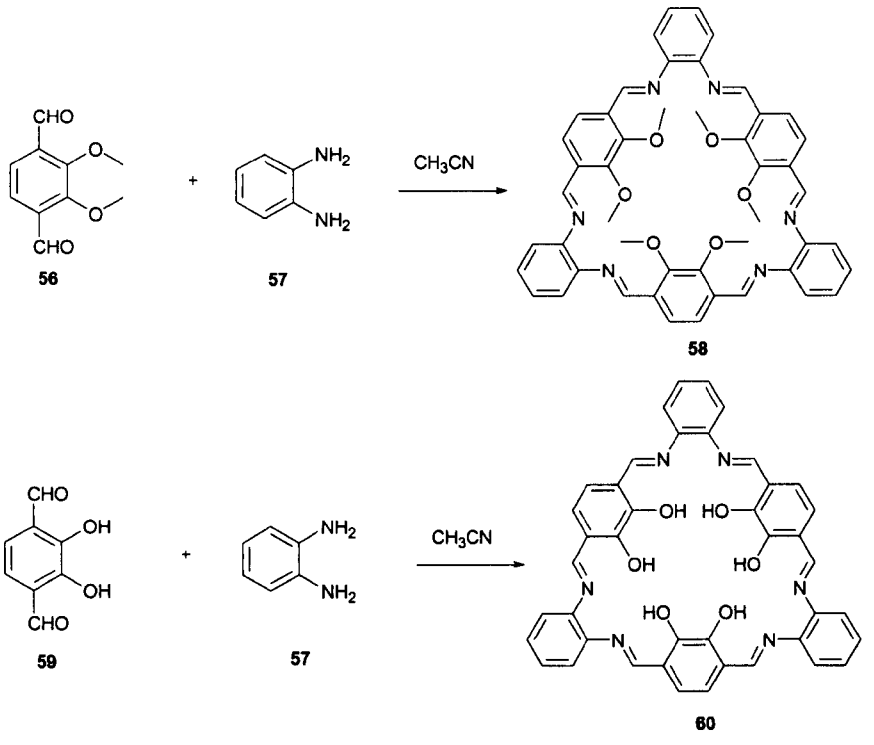

Figure 53: synthesis of Nabeshima's macrocycles.

Chapter IV

SYNTHESIS OF AROMATIC DIALDEHYDES. A REVIEW

From a synthetic point of view, aromatic aldehydes play a very important role in organic chemistry, because they can act as the building blocks for the synthesis of larger target molecules. The formyl group is of extreme importance in organic synthesis, as it possesses a wide versatility to undergo different transformations, in particular the formation of C-C bonds and nucleophilic additions.

A comprehensive review of related literature revealed that only isolated examples of aromatic dialdehydes have been prepared, and that no general method was available. Traditionally, the formyl group is introduced into an aromatic or heteroaromatic nucleus using a standard electrophilic aromatic substitution reaction. Unfortunately, these methods have a tendency to lead to poor yields, low regioselectivity, and require drastic reaction conditions, *etc.* However, other methods proved to give the same, or sometimes better, results.

The next section will show a review about the synthetic methods used in the synthesis of aromatic dialdehydes.

7. Electrophilic aromatic substitution

7.1 Vilsmeier-Haack reaction.[49]

The Vilsmeier-Haack reaction is the most common method used for the formylation of aromatic or heterocyclic compounds, using disubstituted formamides and an activating agent such as phosphorous oxychloride as formylating reagent. Unfortunately, this method is only suitable for highly activated substrates. For example, compounds such as amines and phenols undergo formylation, benzene and naphthalene are however unreactive under these conditions. The mechanism is believed to proceed *via* the main intermediates shown in Figure 54.

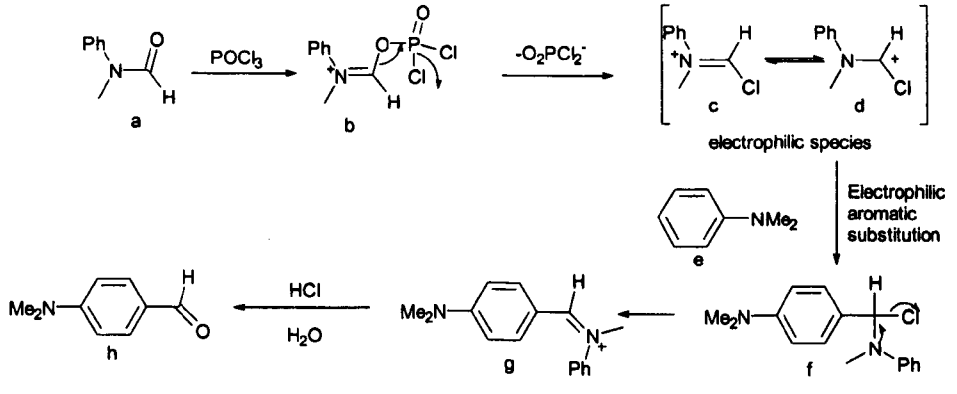

Figure 54: mechanism of the Vilsmeier-Haack reaction.

The original disubstituted formamide used in the Vilsmeier reaction was N-methylformanilide **a**. Nevertheless, the use of dimethylformamide is preferred due to the lower cost and the more convenient separation of by-products, therefore **a** is rarely employed.

Sessler and co-workers[50] used Vilsmeier conditions for the synthesis of the bis-formyl bipyrrole **61** (Figure 55) used as building blocks for the synthesis of sapphyrin **64** (Figure 56).

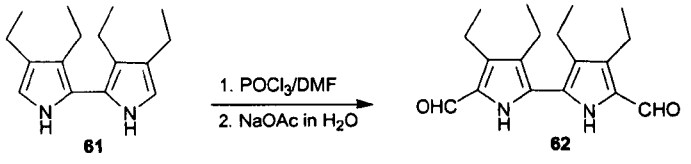

Figure 55: synthesis of bisformyl bipyrrole.

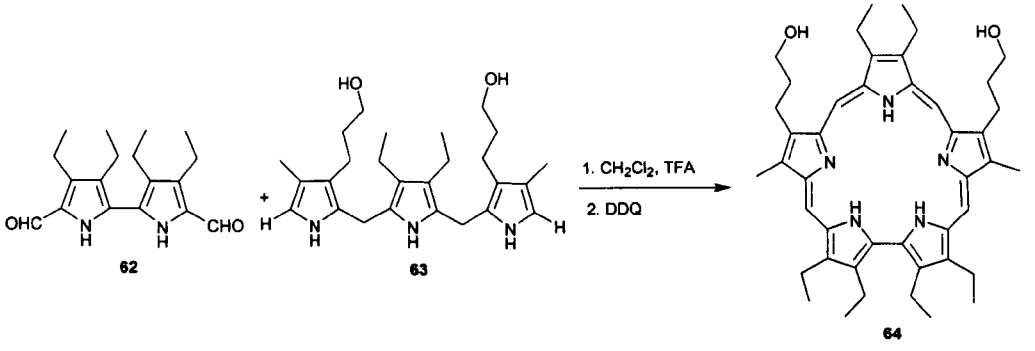

Figure 56: synthesis of sapphyrins.

Although the method of synthesis gave good yields (87 %), the whole process suffers from the disadvantage that the preparation of the starting material for the synthesis of the diformaldehyde **62** requires a six-step reaction.

Megati and co-workers[51] developed a singular approach for the synthesis of aromatic chlorobenzene-di and mono aldehydes using the Vilsmeier formylation of α,β-epoxy ketones. The process consisted of several steps thought to proceed *via* the mechanism shown in Figure 57.

The entire route involved first the synthesis of the epoxy-ketone **c**, from the corresponding α,β-unsaturated ketone using alkaline hydrogen peroxide. This is followed by the ring opening of the epoxide using the Vilsmeier reagent, to give one equivalent of the *o*-dichloro-intermediate. Finally, the formation of the aromatic dialdehyde is achieved under Vilsmeier conditions after iminoalkylation, followed by aromatisation. The final hydrolysis gave the dialdehyde product.

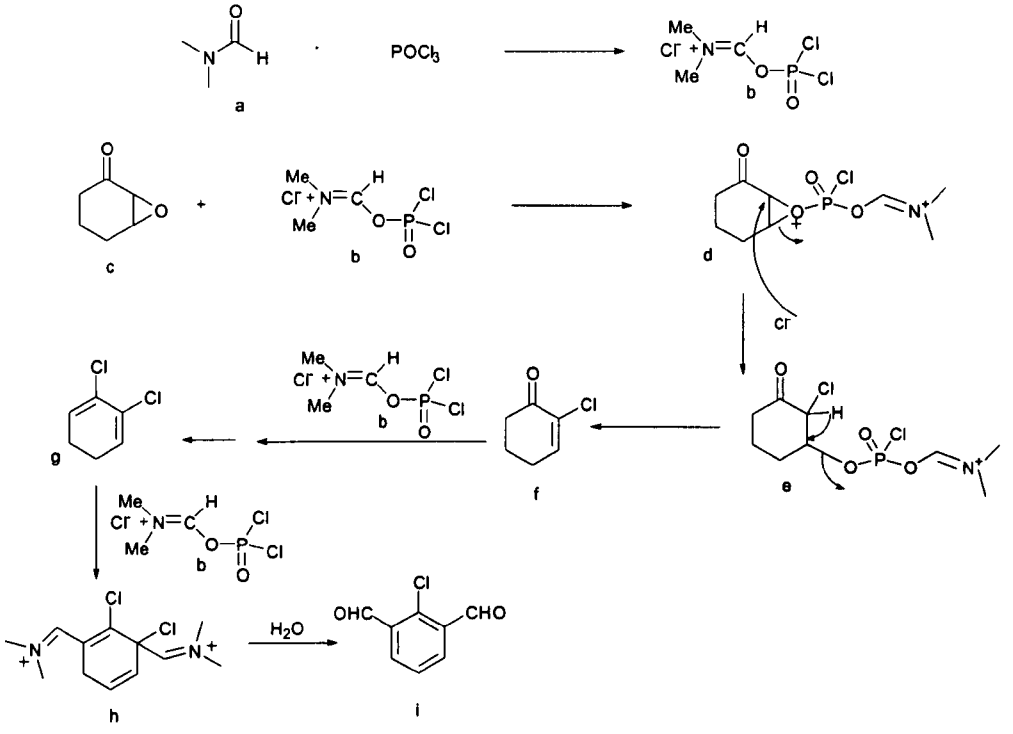

Figure 57: mechanism of Vilsmeier reaction in α,β-epoxy ketones.

Following this method, further four 1,3-aromatic dialdehydes were synthesised and they are shown in Figure 58.

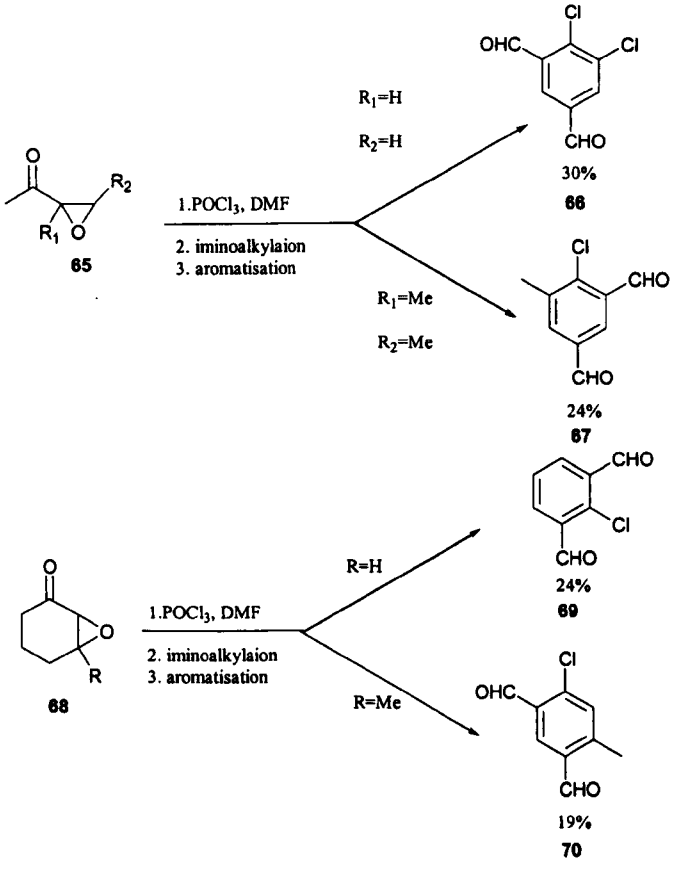

Figure 58: synthesis of 1,3-aromatic dialdehydes.

This method constitutes an innovative synthetic approach; yields, however, are disappointingly low.

Josemin and co-workers[52] also used Vilsmeier reaction for the synthesis of the aromatic formyl compounds shown in Figure 59.

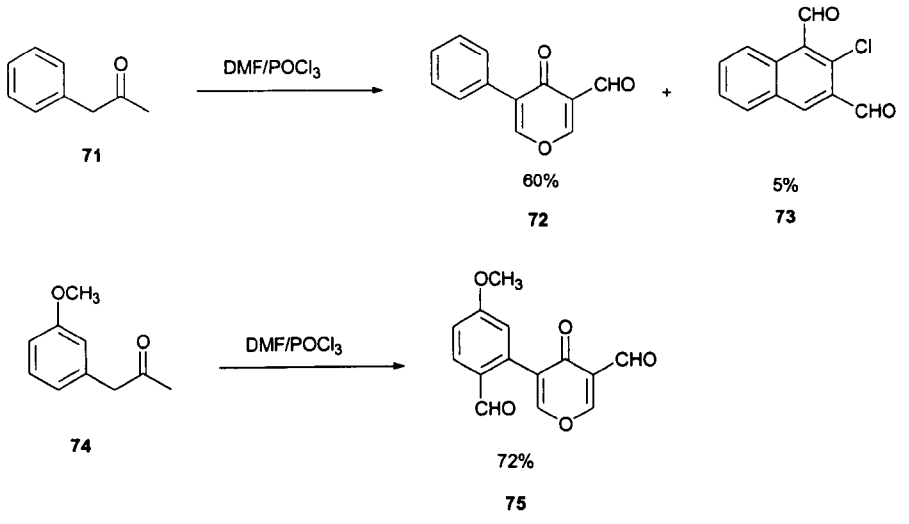

Figure 59: synthesis of dialdehydes *via* Vilsmeier reaction.

Dialdehyde **73** was obtained in extremely low yield (5 %), therefore the use of phenylpropan-2-one **71** as a starting material for diformylation is not the most appropriate. Nevertheless, compound **74**, appears to be a good precursor in the synthesis, giving the diformyl compound **75** in 72 % yield.

The synthesis of 3,6-diformyl-9-methylcarbazole[53] **77** and carbazole **79**,[54] was also achieved using Vilsmeier conditions, however, in very poor yields, 10 %, 31 %, respectively (Figure 60). In this case the original Vilsmeier reagent was used.

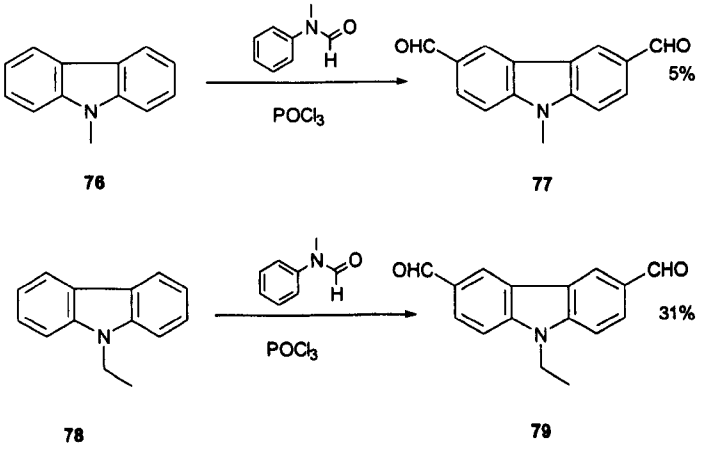

Figure 60: synthesis of diformylcarbazoles.

Evans and co-workers[55] synthesised dialdehyde **81** from **80** under the same conditions as above (Figure 61). Once again, the yields obtained did not seem very promising.

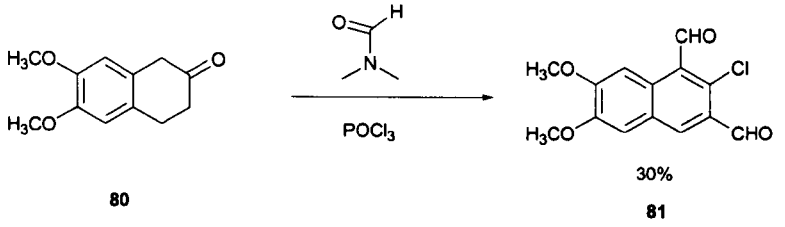

Figure 61: synthesis of 1-chloro-(6,7-dimethoxy)-naphtalene-1,3-dialdehyde.

Smith and co-workers[56] accomplished the synthesis of α,β- and α,γ-diformyl-porphyrins also under Vilsmeier conditions (Figure 62). The first set of diformyl porphyrins was obtained after 18 hours treatment with excess of Vilsmeier reagent at 50 °C to give **82**. The second set was obtained under similar conditions at 80°C to give **83**.

The mixture of the diformyl compound obtained in each set of compounds was separated by column chromatography, leading to the pure compounds in small yield.

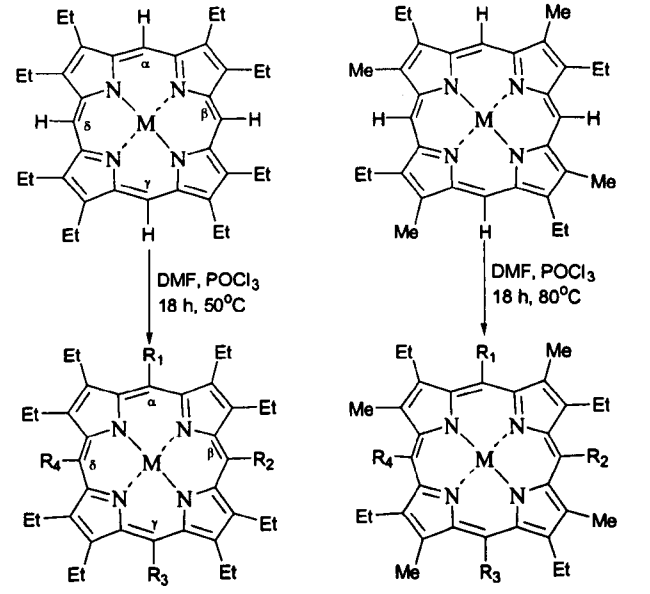

Figure 62: synthesis of diformyl porphyrins.

One of the best known examples of synthesis of aromatic dialdehydes is 1,3-diformylazulene[57] **85** (Figure 63), whose synthesis employs Vilsmeier reaction, giving the final product in good yield.

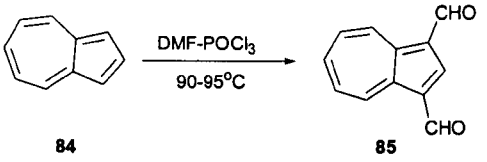

Figure 63: synthesis of diformylazulene **85**.

7.2 Gatterman-Koch reaction.[58]

In this reaction, the formylation of the aromatic compound is achieved using carbon monoxide and hydrogen chloride in the presence of aluminium chloride, at high pressure. Nevertheless, if CuCl is added, the reaction is reported to proceed at atmospheric pressure (Figure 64).

$$ArH + CO \xrightarrow{HCl,\ AlCl_3,\ CuCl} ArCHO$$

Figure 64: scheme of Gatterman-Koch reaction.

Though the mechanism of the reaction in not clear, it is believed that the electrophilic species is in fact the formyl cation[59] (Figure 65) formed without the mediation of formyl chloride.

$$HC{\equiv}O^+ \longleftrightarrow H^+C{=}O$$

Figure 65: formyl cation.

It is also thought that the role of the copper chloride is to aid the reaction between carbon monoxide and hydrogen chloride, *via* complex formation with carbon monoxide.

Tanaka and Souma[60] used the Gatterman-Koch reaction for the diformylation of polynuclear aromatic compounds shown in Figure 66 using, as catalyst, the HF-SbF_5 system, instead of the mixture of HCl and $AlCl_3$ (the role of SbF_5 in HF is to produce the fomyl cation as electrophilic reactive species).

In general, the Gatterman-Koch reaction is successful when used on moderately reactive aromatics, however it is unsuccessful with phenols or phenol ethers due to the formation of complexes with the Lewis acid.

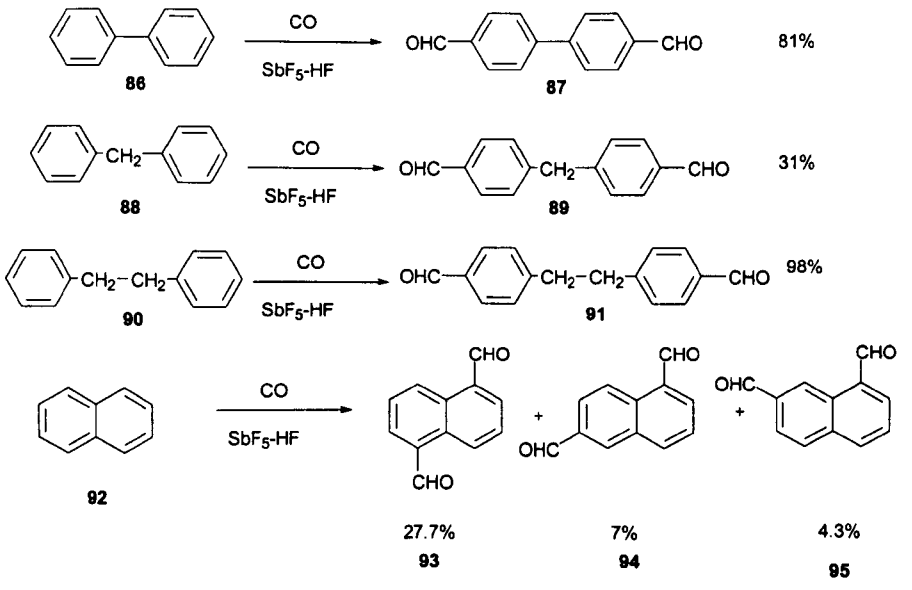

Figure 66: synthesis of aromatic dialdehydes *via* the Gatterman-Koch reaction.

7.3 Reimer-Tiemann reaction.[61]

Unlike the previous reactions mentioned, this method uses basic instead of acidic conditions. The reaction between chloroform and sodium hydroxide produces a carbene that will act as the electrophile in an electrophilic aromatic substitution. This is attacked by the phenoxide ion, and following the hydrolysis of the dichloromethyl moiety, the aldehydes **97** and **98** are obtained (Figure 67).

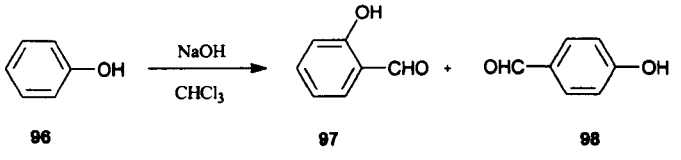

Figure 67: formation of phenolic aldehydes from phenols, chloroform and alkali.[62]

Although the use of the Riemer-Tiemann reaction was reported to be to be exclusive for the synthesis of monoformylated aromatics, Delmas and co-workers[63] found that the use of methanol as co-solvent led the simultaneous synthesis of the mono and the diformylated product (Figure 68). No yields were reported.

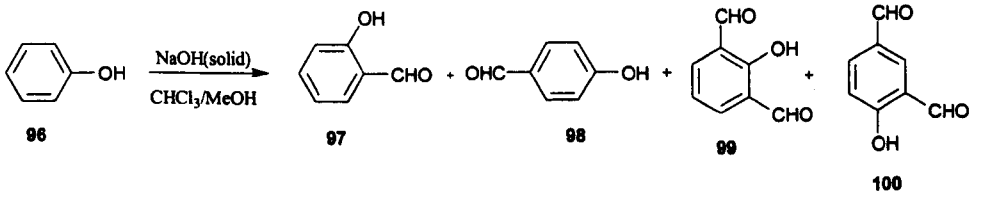

Figure 68: mono and di-formylated products using a variation of the Riemer-Tiemann reaction.

Another reaction involving the use of carbenes is employed in the synthesis of dialdehyde **104**,[64] which was achieved after the hydrolysis of **103**, previously obtained from the reaction of 3-acetamidophenol **102** with the carbene source **101**[65] (Figure 69).

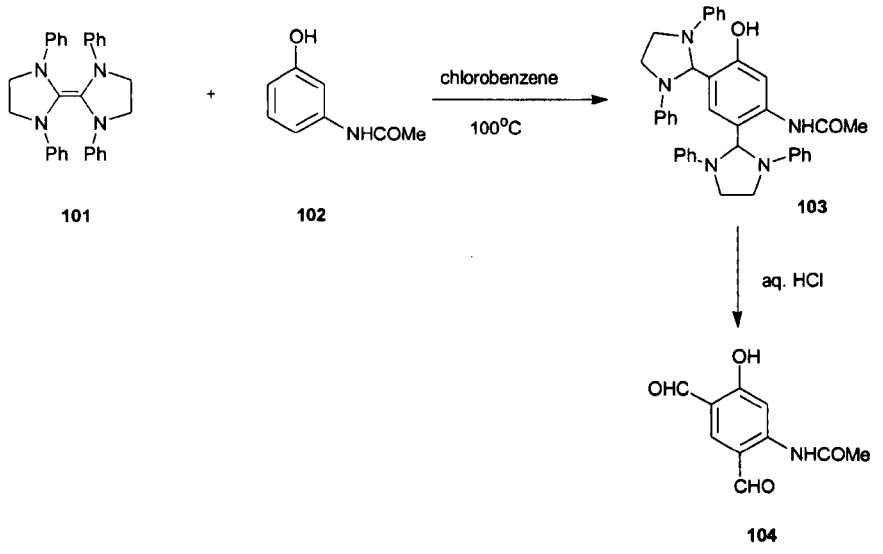

Figure 69: synthesis of *N*-(2,4-diformyl-5-hydroxyhenyl)acetamide.

The interesting feature of this reaction is the use of **101** because its dissociation leads to the nucleophilic carbenes, which can attack the aromatic ring to from an imidazolidine derivative, easily convertible by hydrolysis into an aldehyde.

7.4 Duff Reaction.[66]

The Duff reaction follows the same principle as the Reimer-Tiemann reaction, however, hexamethylenetetramine **105** is used in the presence of an acidic catalyst, instead of chloroform, and can only be applied to phenols and amines. *Ortho*-substitution is common, however, in the presence of anhydrous trifluoroacetic acid (TFA), regioselective *ortho* and *para* substitutions can be observed. (Figure 70, Figure 71).

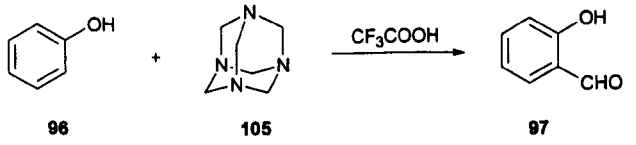

Figure 70: aromatic phenyl aldehyde synthesised *via* the Duff reaction.

In comparison to the Reimer-Tiemann reaction, the products obtained are generally of a higher purity and the reaction takes place in a shorter time.

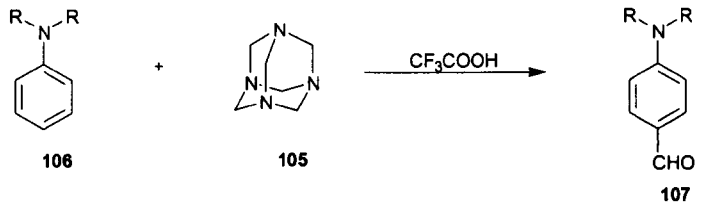

Figure 71: synthesis aromatic phenylamine aldehyde.

Lyndoy and co-workers[67] reported a series of dialdehydes synthesised from 4-substituted phenols based on the Duff reaction. This one pot reaction involved the use of two equivalents of hexamethylenetetramine in refluxing trifluoroacetic acid for 24 hours. The yields obtained vary depending on the substituent in the 4-position (Figure 72).

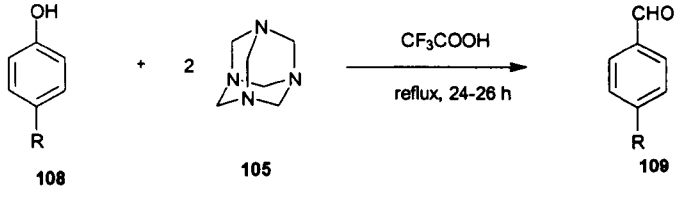

R= *tert*-Bu, Me, MeO, Br, NO_2 Yields: *tert*-Bu, 65 %; Me, 68 %; MeO, 42 %; Br, 41 %; NO_2, 5 %

Figure 72: aldehydes synthesised from 4-substituted phenols based on the Duff reaction.

Using the same conditions, dialdehyde **111** was synthesised as shown in Figure 73.

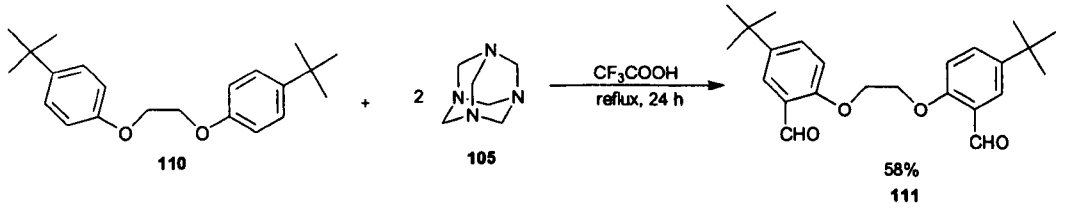

Figure 73: dialdehyde synthesised from biphenyl ether using the Duff reaction.

Stille and co-workers[68] used a similar approach to synthesise 2,4-diformylphenol **100**. Hexamethylenetetramine **105** was added to a solution of *p*-formylphenol **98** and trifluoroacetic acid, followed by ethanol led to a pure crystalline product. Although the advantage of this method is that no chromatographic purification is needed, the yield is low (39 %) (Figure 74).

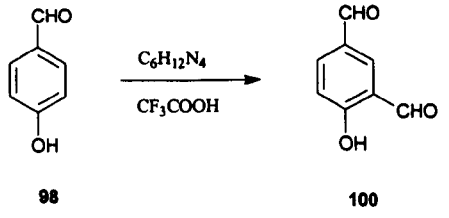

Figure 74: synthesis of 2,4-diformylphenol.

Concentrated hydrochloric, instead of trifluoroacetic acid, and **105** were used by Ackerman and co-workers[69] for the synthesis of isophthalaldehyde **41** from 1,3-methylaminebenzene **112** (Figure 75) in 62 % yield.

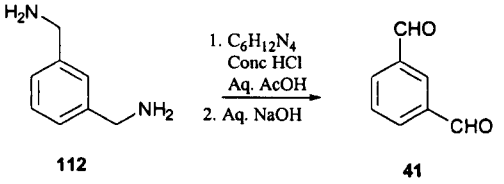

Figure 75: synthesis of isophthaldehyde by Ackerman and co-workers.

7.5 Other types of electrophilic aromatic substitution reactions.

Using the electrophilic aromatic substitution approach, Nishimura and co-workers[70] reported the formylation of *syn*-[2.n]metacyclophanes **114, 115** and **116,** (Figure 76) which were used as potential building blocks for the failed synthesis of multi-briged cyclophanes. Dialdehydes were synthesised from dimethoxy-[2.n]metacyclophanes **113** using as formylating agent dichlorodimethylether and $SnCl_4$ in dry dichloromethane for 4-48 h at room temperature. The yields obtained varied between 4.6 and 19 %.

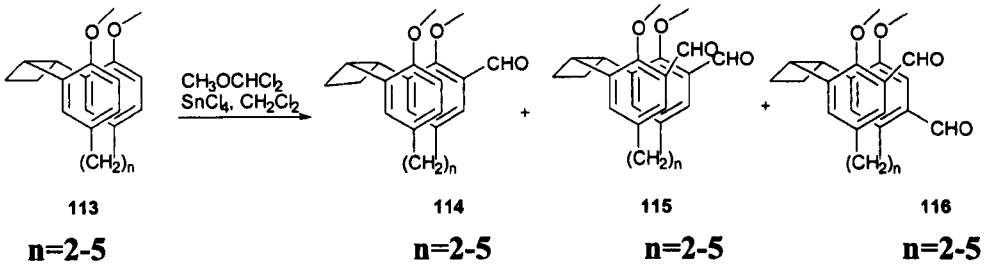

Figure 76: synthesis of aldehydes from *syn*-[2.n]metacyclophanes.

The same approach was used by Sereda and co-workers[71] for the synthesis of di- and trifromyl trypticene **118** and **119** shown in Figure 77.

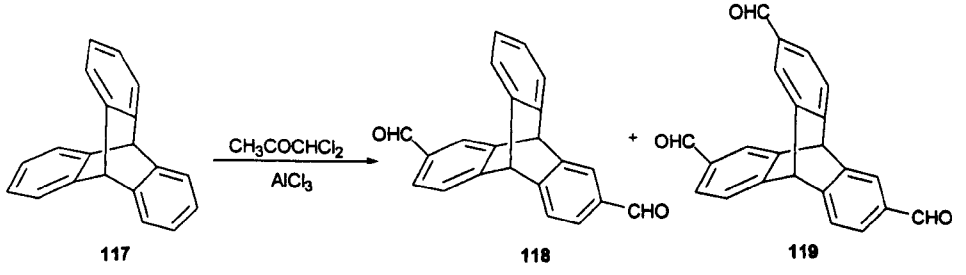

Figure 77: synthesis of di and tri-formyl trypticene.

All previous formylation processes described above proceed *via* an electrophilic aromatic substitution mechanism. The substrate therefore requires electron-donating substituents. Consequently, the use of these reaction procedures is very restricted because diformylation can only be achieved in exceptional cases and yields are generally low.

Other methodologies to synthesise dialdehydes rely on functional group interconversions using difunctionalised aromatic compounds as starting materials. These methods are reviewed in the following section.

8. Dilithiation procedures.

The substitution of an aromatic hydrogen or halogen for a metal atom is of extreme significance in organic synthesis. The importance is not derived from the carbon-metal bond, but rather in the organometallic intermediate species that is produced.

Special attention will be paid to both the halogen-lithium and hydrogen-lithium interchange, which are the most commonly used. In general, the aryl-lithium reagents are obtained from either *n*-butyllithium or *tert*- butyllithium and are easy to handle.

The success achieved using these procedures in synthesis of dialdehydes is due to the generation of a negative charge in the aromatic ring. The aromatic dialdehyde is obtained by the nucleophilic attack by the phenyl ion on the formyl compound, which has to contain the necessary leaving group.

8.1 Dilithiation by double Lithium-Bromine exchange.

The lithium halogen exchange reaction was discovered by the groups of Wittig[72] and Gilman[73] in 1938 and has, ever since, proven extremely useful.

Dilithiations using a double lithium-halogen exchange have first been reported by the group of Worden using resorcinol dibromides[74] in 1970 (Figure 78).

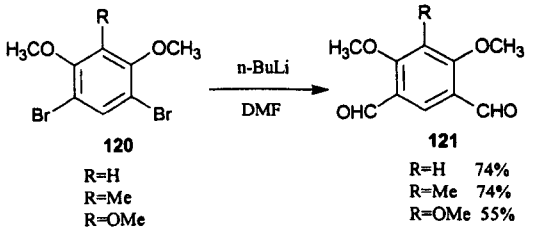

120

R=H
R=Me
R=OMe

121

R=H 74%
R=Me 74%
R=OMe 55%

Figure 78: synthesis of dialdehydes *via* Br-Li interchange.

In all cases, the dibromide precursor was treated with *n*-butyllithium in dry ether, followed by dimethylformamide. The dialdehydes were obtained by filtration after acid hydrolysis.

Syper and co-workers[75] synthesised a series of dialdehydes from commercially available dimethoxy benzenes, following different routes. One of the examples of diformylation shown in this paper involves a 3-step reaction. Aldehyde **124** was obtained from tetramethoxy benzaldehyde **122** by protection of the formyl group *via* acetalisation followed by bromination (with NBS in trifluoroacetic acid). Finally, the second formyl group was introduced by lithiation with *n*-BuLi followed by quenching with dimethylformamide (Figure 79).

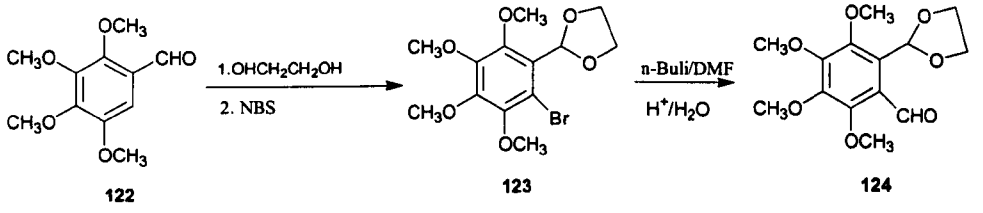

Figure 79: synthesis of dialdehydes *via* Br-Li interchange.

The synthesis of diformylnaphthalenes shown in Figure 80, was performed by Sylvester-Hvid and co-workers[76] using the same synthetic procedure. 1,6-Dimethoxy naphthalene **125** was treated with bromine in carbon tetrachloride and two dibrominated compounds were obtained. After separation and further treatment with *n*-butyllithium and dimethylformamide, the desired dialdehydes **127** and **129** were obtained in 17.1 and 78 % yield respectively.

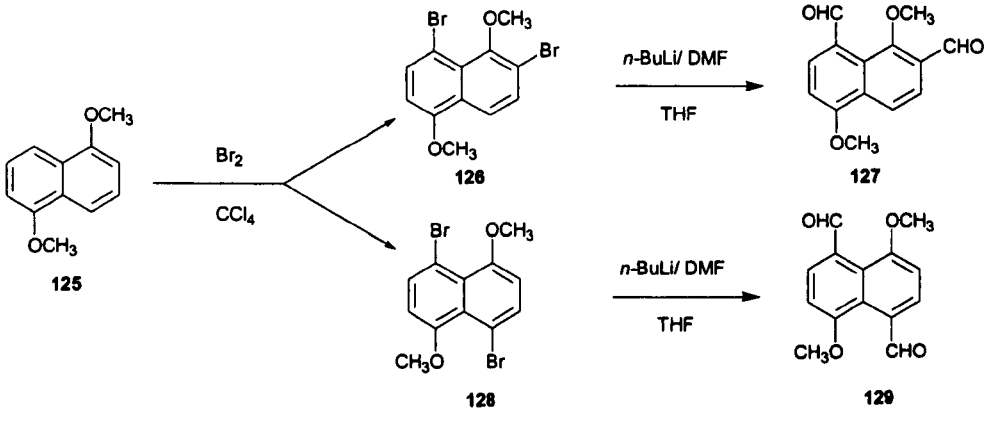

Figure 80: diformyl-dimethoxy naphtalene synthesis.

The same approach was used for the synthesis of dialdehyde **132**, from **130**. The whole scheme included the protection of the hydroxyl groups, followed by dibromination and finally formylation (Figure 81).

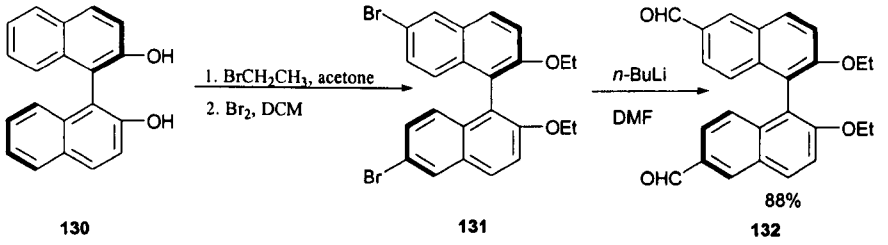

Figure 81: synthesis of 2,2'-diethoxy-6,6'-dialdehyde-1,1'-binaphtyl.

8.2 Dilithiation by double directed *ortho* metalation.

The directed *ortho*-metalation reaction was published one year after the Br-Li exchange reaction, again alongside the groups of Wittig and Gilman.[77,78] It has been developed into one of the most fundamental methodologies in the functionalisation of aromatic compounds over the last two decades.[79] The dilithiation of aromatics using a double directed ortho lithiation on a single aromatic nucleus has been reported by Snieckus and co-workers using the O-carbamate directing group, and by Sundberg[80] using the methoxy directing group (Figure 82).

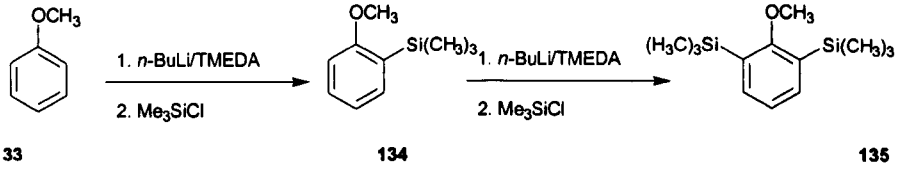

Figure 82: directed ortho-metalation.

As in the case of the halogen-lithium interchange, here it is also *n*-butyllithium used to achieve the metalation. However, tetramethylethylenediamine (TMEDA) is needed to increase the rate of the reaction. This tertiary amine can chelate the lithium, that is, it 'solvates' the organometallic species and reduce the aggregation in solution, producing a complex (Figure 83) capable of accelerating the deprotonation process.

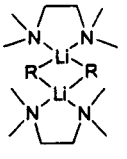

Figure 83: TMEDA complex.

The most important synthetic utility of the lithiation procedure is that it gives the *ortho* isomer when an *ortho* directing group is present (Figure 84).

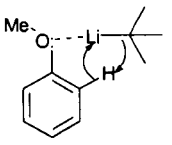

Figure 84: scheme or interaction between the lithiating agent and the methoxy group.

Regardless of the numerous publications using hydrogen-lithium exchange for further derivatisation of aromatics, only a few examples exist for diformylation.

One of them was the synthesis of 1,1'-diformylferrocene **137** from ferrocene (Figure 85) that is widely used as building block for different types of macrocycles and other derivatives. Fröhlich and co-workers[81] and Carrol and co-workers[82] have published the most recent papers using this synthetic method.

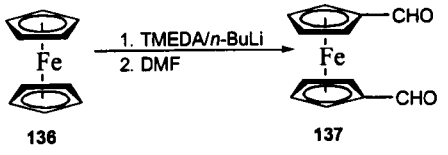

Figure 85: synthesis of 1,1'-diformylferrocene.

Feringa[83] used this procedure for the synthesis of dialdehyde **139** (Figure 86), using a mixture of *n*-butyllithium with TMEDA and potassium *tert*-butoxide in pentane. The final product was obtained after quenching the reaction with dimethylformamide in 80 % yield.

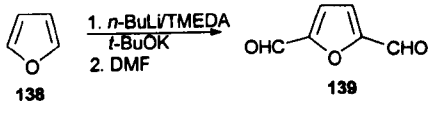

Figure 86: synthesis of 2,5-diformylfurane.

Dilithiation of 1,2-dimethoxybenzene **140** followed by the reaction with dimethylformamide (Figure 87), was also reported by Nabeshima and co-workers [84] for the synthesis of dialdehyde **56**. The deprotection of the hydroxyl groups was achieved by treatment with boron tribromide to achieve the dialdehyde **59** in 92 % yield.

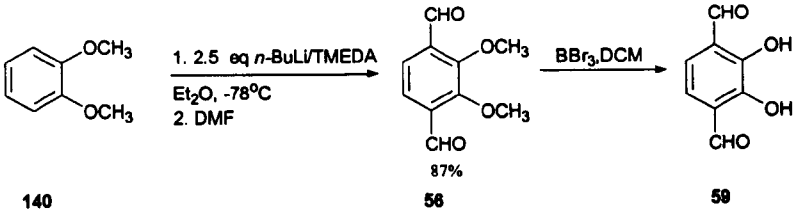

Figure 87: synthesis of dimethoxy and dihydroxy dialdehydes.

Märkl and co-workers[85] also used this method for the synthesis of dialdehyde **142** (Figure 88) for building blocks in the synthesis of annulene **144** (Figure 89). However, the use of TMEDA was not reported.

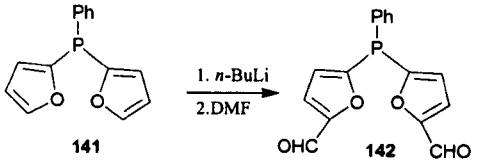

Figure 88: synthesis of bisfuranedialdehyde.

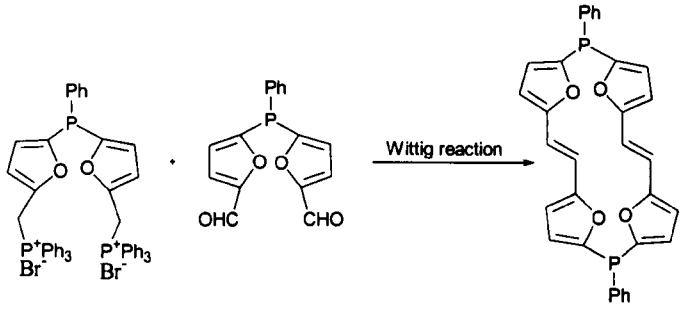

Figure 89: synthesis of 5,16-dihydro-5,16-diphospa-tetraepoxy annulene.

The synthesis of the different types of dialdehydes following this approach is reported in a paper published by our research group and will be discussed in detail in the results and discussion chapter.

9. Synthesis of dialdehydes *via* Oxidation.

9.1 Sommelet Reaction.[86]

The Sommelet reaction can formally be classified as an oxidative process in which a benzyl halide is transformed *via* the benzylic ammonium salt, into an aldehyde (Figure 90).[86]

The quaternary ammonium salts, which do not need to be isolated, are prepared from benzyl halides and hexamethylenetetramine **105**. Then, these salts are decomposed by heating in the presence of water, to give the arylmethylamine **147**. Finally the dehydrogenation of the amine, followed by hydrolysis, produces the aldehyde.

This is a general reaction for the synthesis of aromatic aldehydes, and usually gives satisfactory yields.

Wood and co-workers[87] used this procedure to synthesise **155, 156, 157, 158** and **159** from hexa-methylenetetramine-bis-(chloromethyl)-benzene salts, shown in Figure 91.

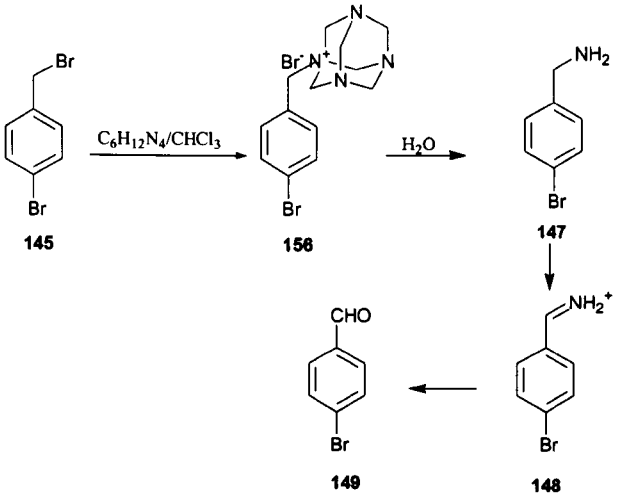

Figure 90: mechanism of the Sommelet reaction.

The synthesis of aromatic dialdehydes from this method is not always successful because the hydrolysis of the salt depends on the location of the substituents with respect to the chloromethyl groups, as well as their location in respect to each other.

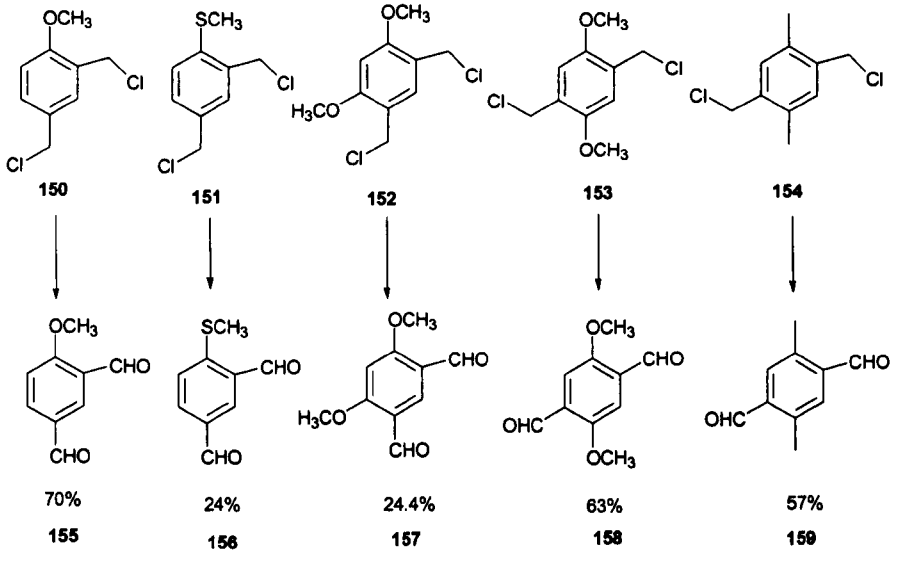

Figure 91: synthesis of aromatic dialdehydes *via* Sommelet reaction.

Gelling and Feringa[88] also used Sommelet reaction for the synthesis of dialdehyde **161** in 33 % yield, from 2,6-bis(bromomethyl)-4-methoxyphenol **160** (Figure 92).

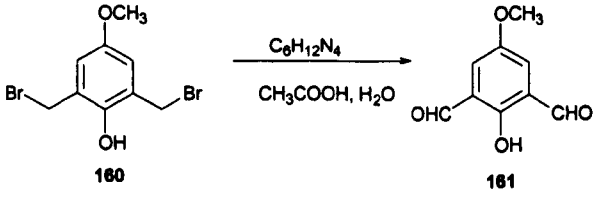

Figure 92: synthesis of 1-hydroxy-4-methoxybenzene-2,6-dialdehyde.

9.2 Oxidation *via* selenium derivative compounds.

Heterocyclic aromatic dialdehydes can be easily obtained *via* oxidation from readily available starting materials such as alcohols. For example, Jin and co-workers[89] found that the use of selenium dioxide in dioxane provided the best method for the synthesis of 2,6-diformylpyridine **163** from 2,6-dipyridinedimethanol **162**, and in very good yield (85 %) (Figure 93).

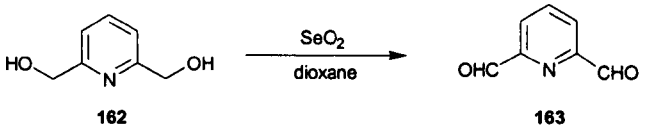

162 **163**

Figure 93: synthesis of 2,6-diformylpyridine.

As well as the use of the lithiation procedure to synthesise aldehydes, Syper and co-workers[75] also reported two different synthetic routes using selenium derivatives in the oxidation processes.

Figure 94 shows a scheme of synthesis of dialdehydes from halomethyl compounds. The reaction involves a reaction, heated under reflux, with potassium phenylselenite ($PhKSeO_3$) and dipotassium hydrogen phosphate in acetonitrile. The dialdehydes are obtained by filtration after aqueous work-up (Figure 94).

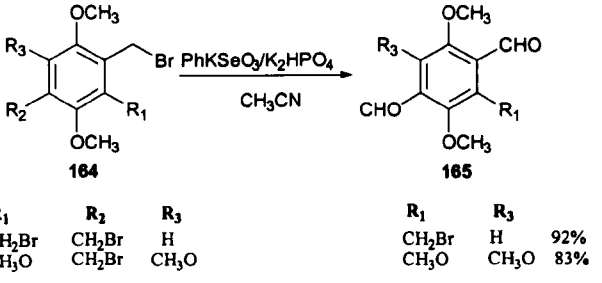

164 **165**

R_1	R_2	R_3		
CH_2Br	CH_2Br	H		
CH_3O	CH_2Br	CH_3O		
R_1		R_3		
CH_2Br		H	92%	
CH_3O		CH_3O	83%	

Figure 94: synthesis of dialdehydes from halomethyl compounds.

Another method of diformylation, where chlorine instead of bromine was used as halomethyl group is shown in Figure 95. In this case the diformyl derivative is obtained using potassium phenylselenite, dipotassium hydrogen phosphate and 18-crown-6-ether, to give the final product **166** in 90 % yield.[75]

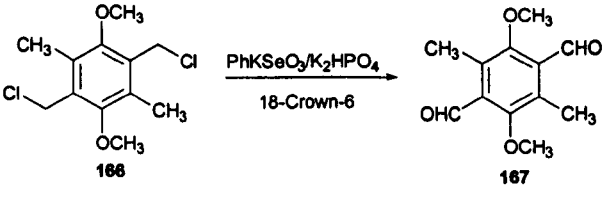

166 **167**

Figure 95: synthesis of dialdehydes from chloromethyl compounds.

9.3 Oxidation *via* Manganese derivative compounds.

Manganese dioxide was the oxidising agent used by Ogawa and co-workers[90] for the synthesis of **169** from 2,4-bis(hydroxymethylene)-3-benzoxepin (**168**) in a 50 % yield (Figure 96).

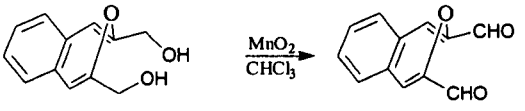

168 169

Figure 96: synthesis of dialdehydes by oxidation with manganese dioxide.

The use of manganese dioxide and molecular sieves in hexane, proved to be a straightforward procedure for the oxidation of aromatic alcohols to aldehydes. Using this methodology Hirano and co-workers[91] synthesised isophthalaldehyde **41** and terephthalaldehyde **39** in 98 and 99 % yield respectively, in a 3-hour reaction (Figure 97).

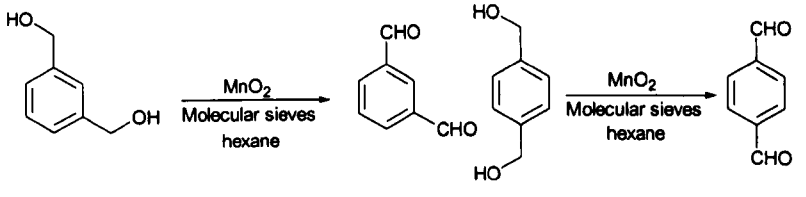

170 41 171 39

Figure 97: synthesis of dialdehydes *via* manganese dioxide.

The synthesis of **173** in 93 % yield was reported by Sahade and co-workers,[92] using barium permanganate with **172** in dichloromethane (Figure 98).

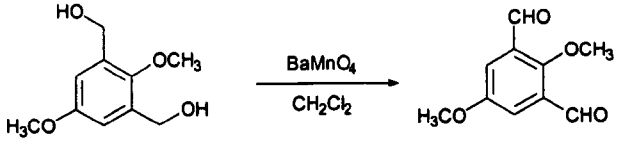

172 173

Figure 98: synthesis of 1,3-diformyl- 2,5-dimethoxybenzene.

9.4 Oxidation *via* carbonates and bicarbonates.

Mataka and co-workers[93] published the synthesis of aromatic dialdehydes, involving the hydrolysis of dibromomethyl aromatic precursors for the preparation of 1,3-formylbenzenes. Hydrolysis of bis(dibromomethyl)-benzenes **174** was carried out with a mixture of sodium acetate, calcium carbonate and tetrabutylamonium chloride

in water, refluxing for different reaction times depending on the starting material (Figure 99).

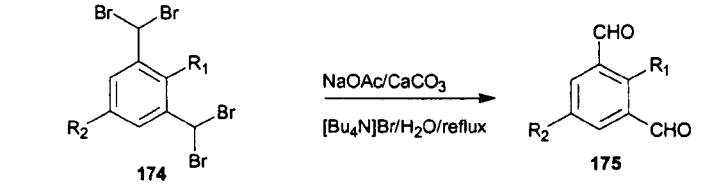

a)R_1=R_2= H; b)R_1=Br, R_2=H; c) R_1=H, R_2=Br; d)R_1=Br, R_2= MeO; e) R_1=MeO, R_2=H; f)R_1=EtO, R_2=H; g) R_1=PrO, R_2=H

a), b), c), d),e), f),g)= 64%; 82%; 75%; 48%; 79%; 80%; 76% Respectively

Figure 99: aromatic dialdehydes synthesised by Makada and co-workers.

The yields obtained by this method are good, but it has the disadvantage, as many to of the methods already shown, that the starting materials are not readily available. Kornblum oxidation[94] was the method chosen by Lippard and co-workers[95] for the synthesis of **176** for use as a building block for the synthesis of macrocyclic dicarboxylate compounds **178** (Figure 100).

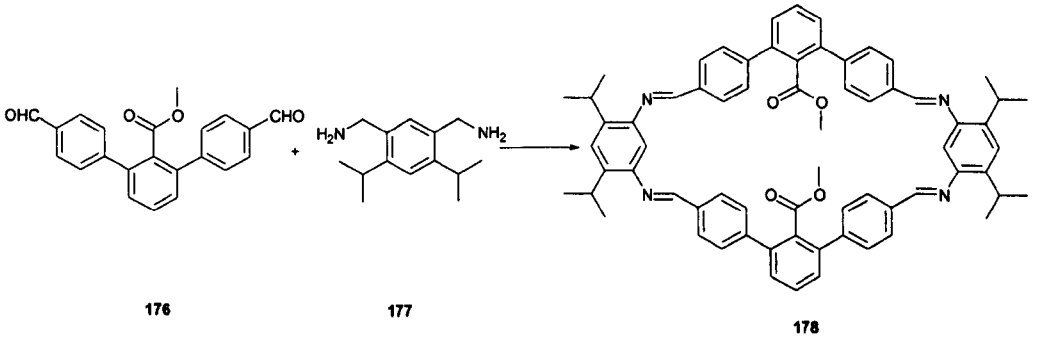

Figure 100: synthesis of macrocyclic dicarboxylates.

The dialdehyde was synthesised from the benzylic bromide precursor **180** employing dimethylsulphoxide and sodium bicarbonate to transform the carbon-halogen bond to the carbonyl compound (Figure 101).

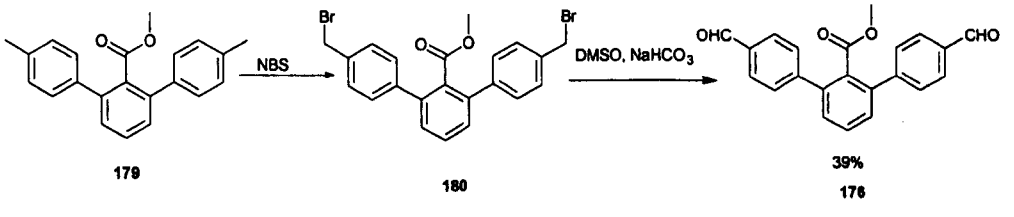

Figure 101: synthesis of methyl-4,4''-diformyl[1,1';3',1'']terphenyl-2'-carboxylate **176**.

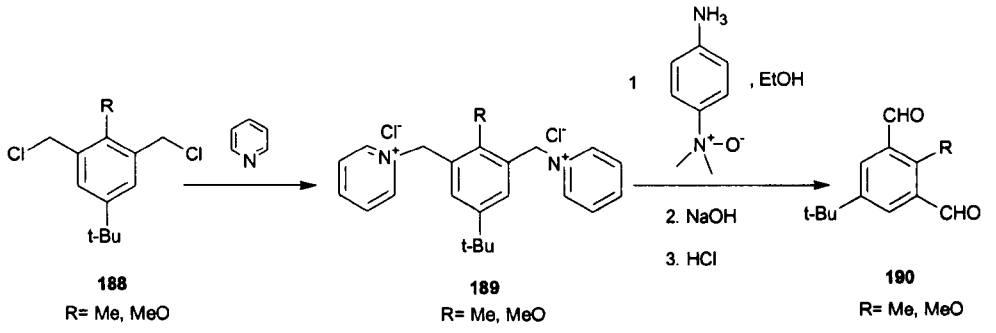

Figure 104: synthesis of 2-methyl-5-*tert*-butyl-1,3-benzenedialdehyde and 2-methoxy-5-*tert*-butyl-1,3-benzenedialdehyde.

These 1,3-benzenedialdehydes were used as building blocks for the synthesis of tetrahydroxy[2.2]metacyclophanes **192** (Figure 105).

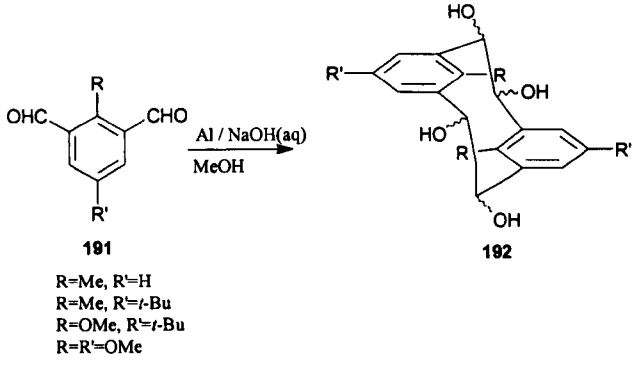

Figure 105: synthesis of tetrahydroxy[2.2]metacyclophanes.

Takada and co-workers[99] published an alternative method of carrying out the synthesis of dialdehydes by using DDQ in dichloromethane as oxidising agent in the biphenylether **193** (Figure 106).

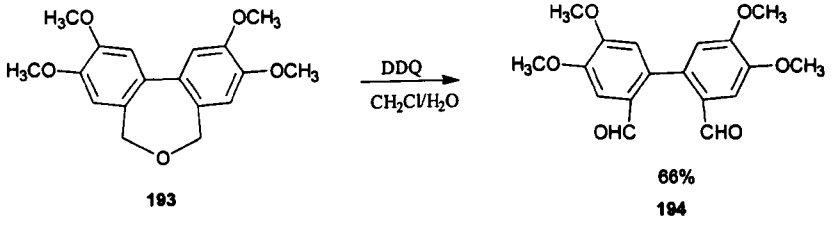

Figure 106: synthesis of dialdehydes *via* DDQ.

9.7 Oxidation involving catalysis.

Different authors achieved the synthesis of terephthaldehyde **39** using oxidation procedures from different starting materials. For example, Green and co-workers[100] obtained **39** in 98 % yield using a ruthenium catalyst in dichloromethane (Figure 107). This method has the advantage over other oxidants of cleanly oxidising a wide range of alcohols to aldehydes without the attack of double bonds.

9.5 Oxidation *via* transition metal derivative compounds.

Gagne and co-workers,[96] and later Chang and co-workers,[97] synthesised 2,6-diformyl-*p*-cresol **184** from **181** in a three-step reaction using, as oxidising agent, sodium dichromate in acetic acid (Figure 102).

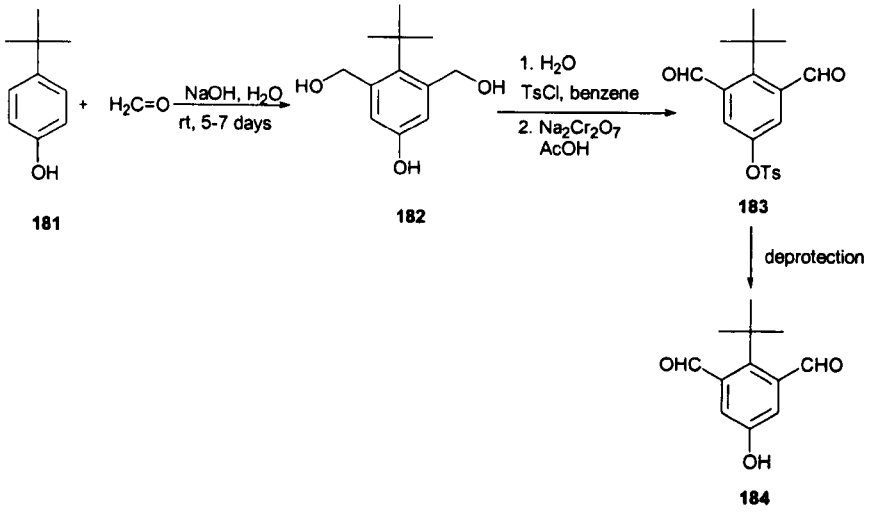

Figure 102: synthesis of 2,6-diformyl-*p*-cresol.

This procedure suffers the disadvantage of extremely long reaction time for the first step of the synthesis.

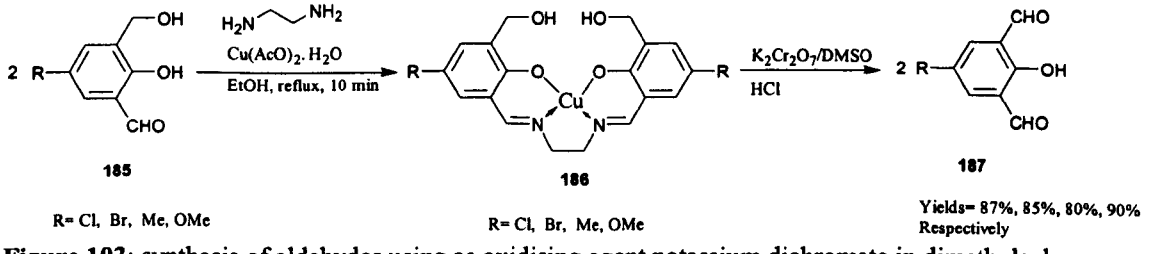

Figure 103: synthesis of aldehydes using as oxidising agent potassium dichromate in dimethylsulfoxide.

Another method to obtain dialdehydes by oxidation was published by Hu co-workers[98] using, as oxidising agent, potassium dichromate in dimethylsulfoxide (Figure 103). The synthesis includes the transformation of **185** into **186** using ethanol, ethylendiamine and copper acetate. Further oxidation leads to the dialdehydes **187** in high yield.

9.6 Oxidation *via* formation of pyridinium salts and DDQ.

Sahade and co-workers[92] also synthesised the series of dialdehydes **190** from chloromethyl benzenes **188** *via* pyridinium salts **189**. Figure 104 shows the scheme for the synthesis.

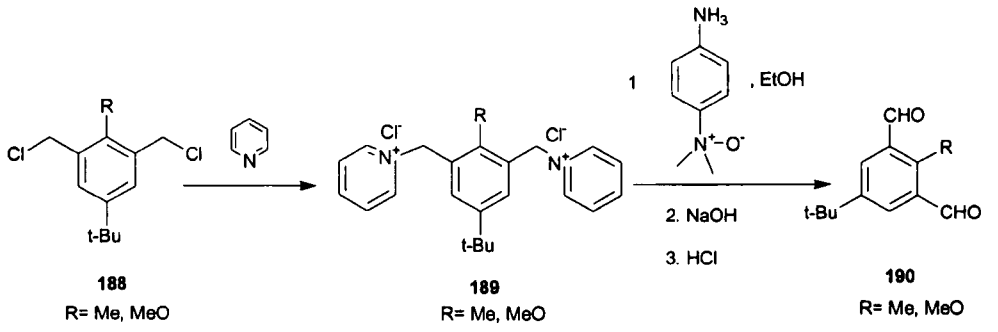

Figure 104: synthesis of 2-methyl-5-*tert*-butyl-1,3-benzenedialdehyde and 2-methoxy-5-*tert*-butyl-1,3-benzenedialdehyde.

These 1,3-benzenedialdehydes were used as building blocks for the synthesis of tetrahydroxy[2.2]metacyclophanes **192** (Figure 105).

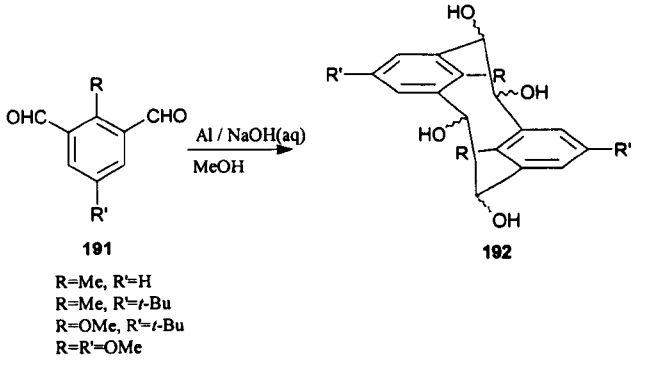

Figure 105: synthesis of tetrahydroxy[2.2]metacyclophanes.

Takada and co-workers[99] published an alternative method of carrying out the synthesis of dialdehydes by using DDQ in dichloromethane as oxidising agent in the biphenylether **193** (Figure 106).

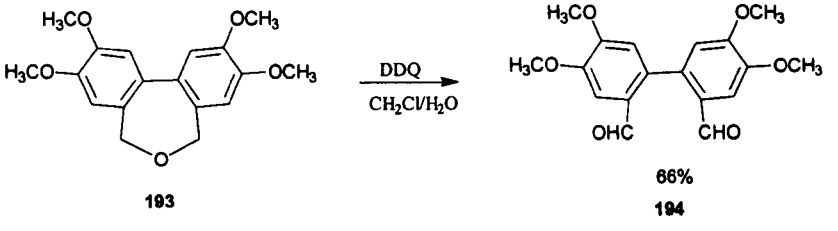

Figure 106: synthesis of dialdehydes *via* DDQ.

9.7 Oxidation involving catalysis.

Different authors achieved the synthesis of terephthaldehyde **39** using oxidation procedures from different starting materials. For example, Green and co-workers[100] obtained **39** in 98 % yield using a ruthenium catalyst in dichloromethane (Figure 107). This method has the advantage over other oxidants of cleanly oxidising a wide range of alcohols to aldehydes without the attack of double bonds.

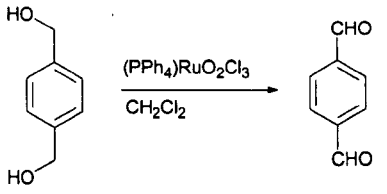

171 39

Figure 107: synthesis of terephthalaldehyde **39**.

A 95 % yield was obtained in the synthesis of **39** using different reaction conditions. In this case (Figure 108), N-chlorosuccinimide and [2,2,6,6-tetramethyl-1-piperidinyloxy, free radical] (TEMPO) was used under phase-transfer conditions with tetra-*n*-butylammonium chloride, which catalyses the oxidation of the primary alcohol to aldehyde.[101]

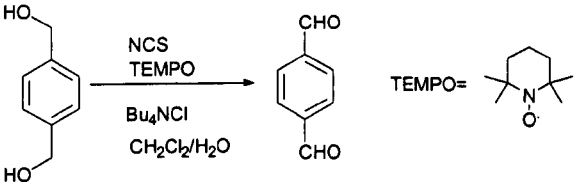

171 39

Figure 108: synthesis of terephthalaldehyde under phase-transfer conditions.

Under these conditions, primary alcohols are quantitatively oxidised to aldehydes, without any noticeable overoxidation to carboxylic acid.

Isophthalaldehyde **41** and terephthalaldehyde **39** in 75 and 53 % yield respectively were obtained from **195** and **196** (Figure 109), using catalytic oxidation with n-hydroxyphtalamide and NO in acetonitrile.

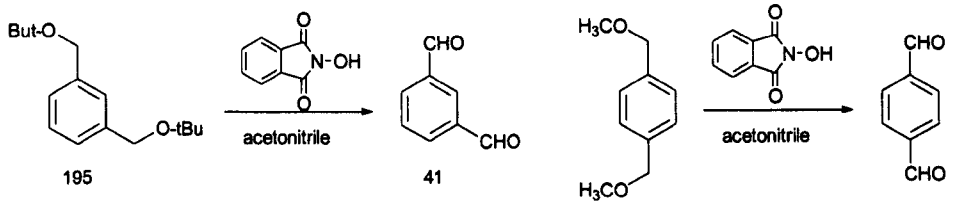

195 41 196 39

Figure 109: synthesis of dialdehydes *via* catalytic oxidation with n-hydroxyphtalamide and NO.

9.8 Oxidation *via* Silver salts and strong acids.

Kochegin and co-workers used a two-step reaction, using silver nitrate in acetonitrile and ethanol in sodium ethoxide,[102] for the same purpose, however the yield obtained for the synthesis of **39** was higher than the previous example (60 %) (Figure 110).

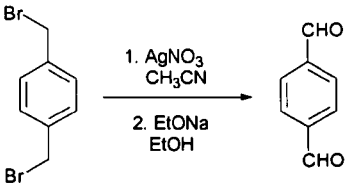

197 39

Figure 110: synthesis of therephthalaldehyde using silver nitrate in acetonitrile

Although the yields obtained using the following method (Figure 111) are not as good as those previously presented (41-83 %), several authors published the transformation of dimethylbenzene **198** into **39** using bromine and sulphuric acid as oxidising agent.[103] The transformation proceeds *via* side chain bromination of the methyl group followed by oxidation.

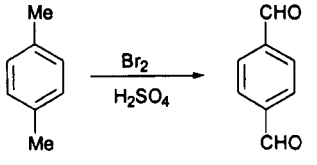

198 39

Figure 111: synthesis of terephthalaldehyde *via* bromination followed by oxidation.

Similar conversion was used by Ferringa and co-workers[88] for the synthesis of **200**, from the aromatic tetrabromide **199**, in 53 % yield (Figure 112).

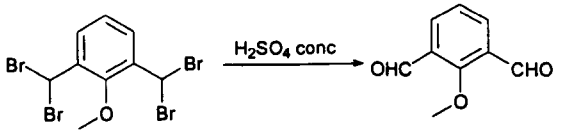

199 200

Figure 112: the synthesis of 1-methoxy -2,6-diformylbezene.

9.9 Oxidation *via* other methods.

Le Bozec and co-workers[104] successfully achieved the synthesis of diformylbipyridines **203** from dimethyl-2,2'-bipyridine derivatives **201**, *via* the oxidative cleavage of enamine groups by sodium periodate in a two step reaction (Figure 113).

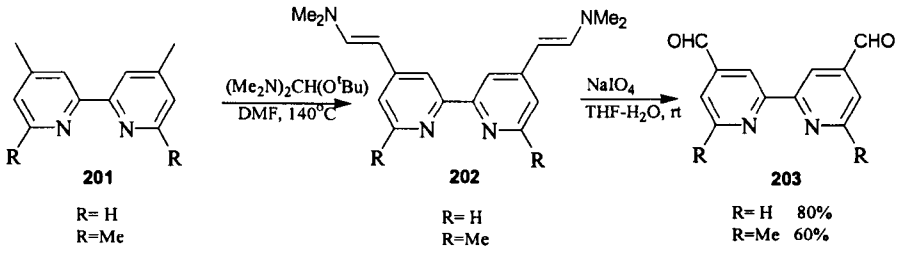

Figure 113: synthesis of 4,4'-diformyl-2,2'-bipyridines.

The reaction involves the use of *tert*-butoxybis(dimethylamino)methane (Brederck's reagent) and compound **201** in dimethylformamide to give the corresponding dienamine **202**. The second step involves oxidative cleavage with sodium periodate in aqueous THF at room temperature to give the dialdehyde **203** in high yield (R=H, 80 %, R=Me, 60 %).

The synthesis of 2,5-diformylfurane **139** has been reported previously from different stating materials. In Figure 114 an example of the synthesis of **139** designed by Skowrónski and co-workers[105] using electrochemical oxidation with a platinum anode in a biphasic system of an inorganic salt solution and dichloromethane is shown. The maximum yield obtained with this method was reported to be 57 %.

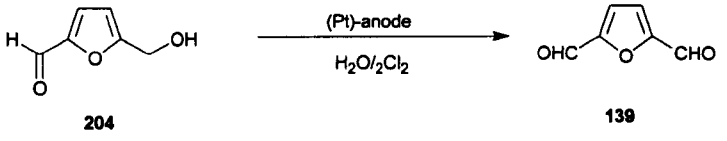

Figure 114: 2,5-diformylfurane using electrochemical oxidation.

10. Synthesis of dialdehydes *via* Reduction.

De las Heras and co-workers[106] synthesised **41** from acyl chlorides *via* imidazonium salts **207** (Figure 115). Unfortunately there are not more examples of the synthesis of 1,3-diformylbenzenes with other substitutions in the aromatic ring and, although the yield obtained is reasonably good (83 %), the product obtained is commercially available.

1,3-diformylbenzenes can also be obtained by direct hydrogenation of the 1,3-dicarboxylic acid **208** precursor with trimethylacetic anhydride (pivalic anhydride) and palladium (0) catalyst[107] (Figure 116).

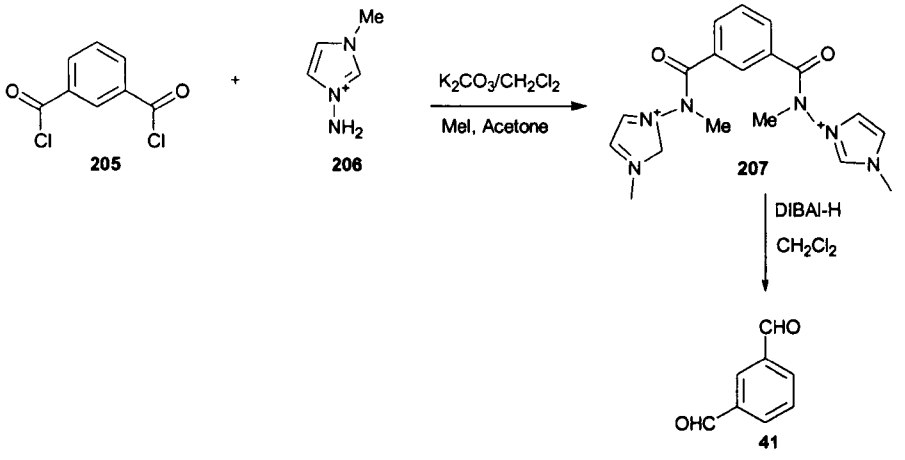

Figure 115: synthesis of **41** *via* 1-(acylmethylamino)-3-methylimidazonium salts.

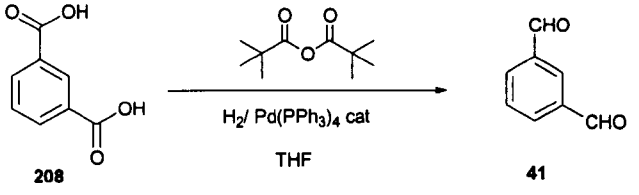

Figure 116: synthesis of **41** by direct hydrogenation.

Furanediacylchloride[108] was the starting material for another method of synthesis of **139**. The reducing reagent used for this approach was Bu_3SnH in xylene (Figure 117), and the yield obtained was 59 %.

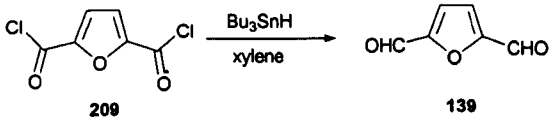

Figure 117: synthesis of diformylfurane **139** using Bu_3SnH.

Zaluski and co-workers[109] obtained better yield for the synthesis of the same compound, but through a different approach. Using as starting material **210**, and after reaction with *iso*-butylaluminium hydride, **139** was obtained in 66 % yield (Figure 118).

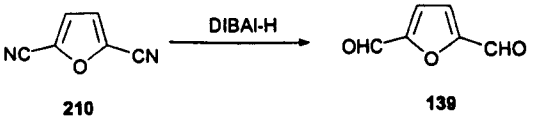

Figure 118: synthesis of diformylfurane *via* DIBAl-H.

Another reductive method to obtain aromatic dialdehydes was published by Zagotto and co-workers[110] for the synthesis of 3,6-diformyl-2,7-dimethoxynaphthalene **213**

from the dimethoxy precursor **211**. This procedure involved a three-step reaction. First, **211** is treated with *n*-butyllithium in diethyl ether and carbon dioxide to obtain **212**. This compound is then reduced with a mixture of RedAl and morpholine in toluene, to give the dialdehyde with a yield of 56 % (Figure 119).

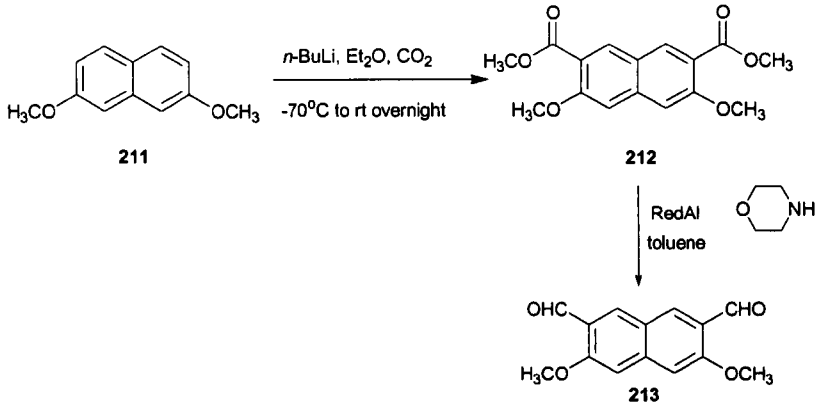

RedAl= $NaAlH_2(OCH_2CH_2OCH_3)_2$.

Figure 119: synthesis of 2,7-dimethoxy-3,6-diformylnaphthalene.

Using the same approach, Hagiya and co-workers[111] synthesised a series of aromatic dialdehydes from diesters. In this case, N-methylpiperazine instead of morpholine, was used to form the reducing reagent. The products obtained are shown in Figure 120.

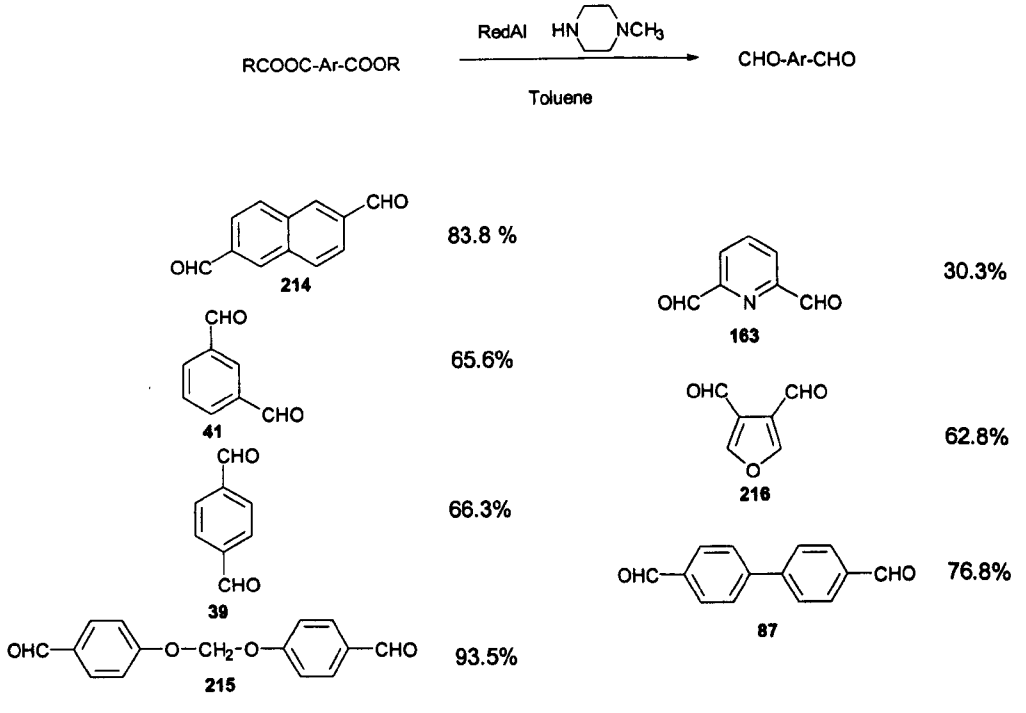

Figure 120: synthesis of aromatic dialdehydes from diesters using N-methylpiperazine.

11. Synthesis of aldehydes *via* coupling methods.

Colon and Kelsey[112] investigated the couplings of aryl chlorides to form byphenyls to synthesise aldehydes (Figure 121). The coupling reagent was a catalytic mixture of anhydrous nickel salt and triphenylphospine in the presence of a reducing metal that, in the case of the synthesis of **87**, was zinc (Figure 121). This synthetic method gave a 94 % yield.

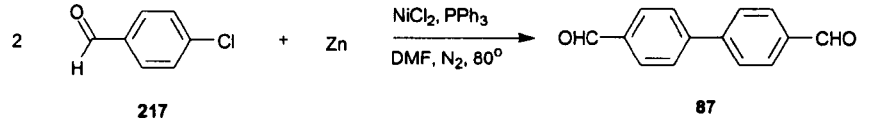

217 **87**

Figure 121: synthesis of 4,4'-biphenyldialdehyde.

Another method of synthesis using a coupling a strategy was published by Itsuno and Kumagai (Figure 122).[113]

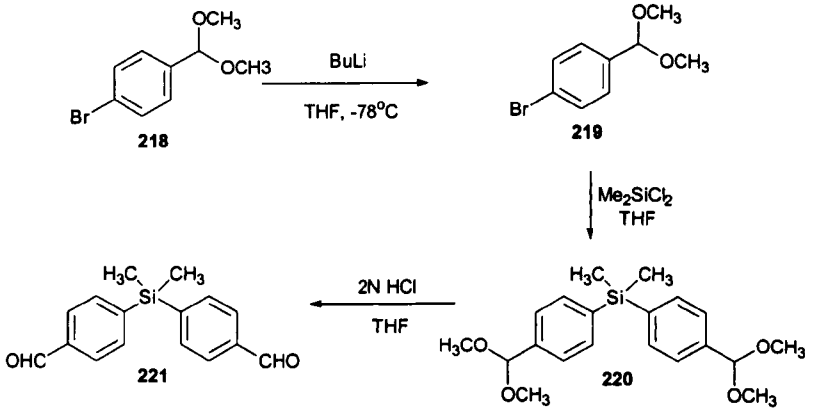

218 **219** **220** **221**

Figure 122: synthesis of dialdehydes *via* coupling of *p*-lithiobenzaldehyde hemiacetal with dichloro-methylsilane.

In this method of synthesis, dialdehyde **221** (64 %) is obtained by coupling of *p*-lithiobenzaldehyde hemiacetal with dichloromethylsilane, followed by deprotection of the acetal moiety.

Simion and co-workers[114] published another example of synthesis of dialdehydes using the coupling approach in the synthesis of cyclophanes **223** from salicylaldehyde **97** (Figure 123).

The synthesis of the diformyl derivative **222** involves a one-pot reaction of salicylialdehyde, the corresponding dibrominated compound and NaOH in boiling ethanol.

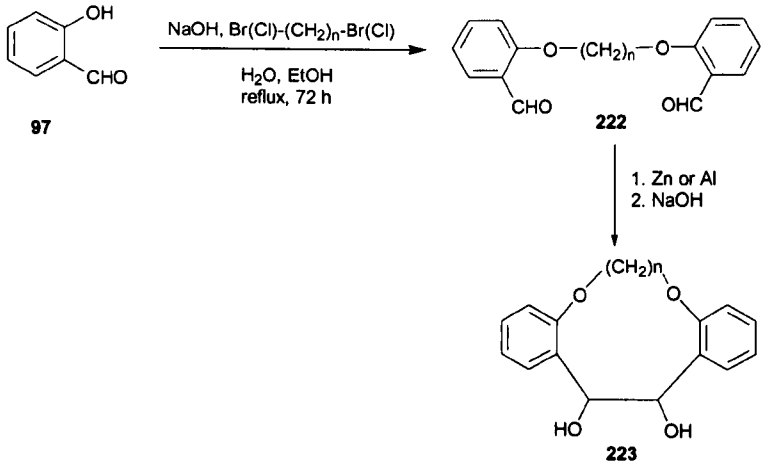

Figure 123: synthesis of dihydroxy-dioxygenated *ortho*-cyclophanes.

Suzuki coupling was the approach used by Krebs and Spanggaard[115] for the synthesis of polyfluorinated aromatic dialdehydes **225** in yields that varied between 63 % and 25 % (Figure 124).

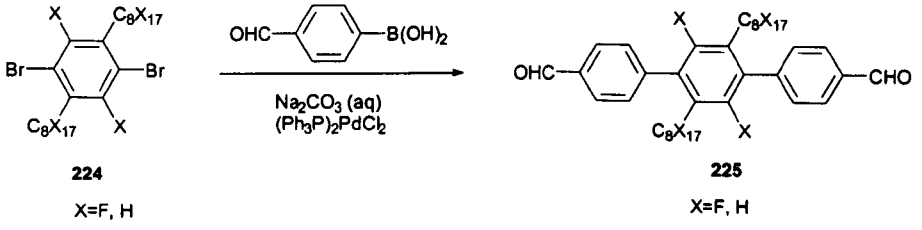

Figure 124: the synthesis of polyfluorinated aromatic dialdehydes.

The condensation of the dialdehyde **225** with 9,10-phenanthrenequinonegave the dye molecule **226** (Figure 125).

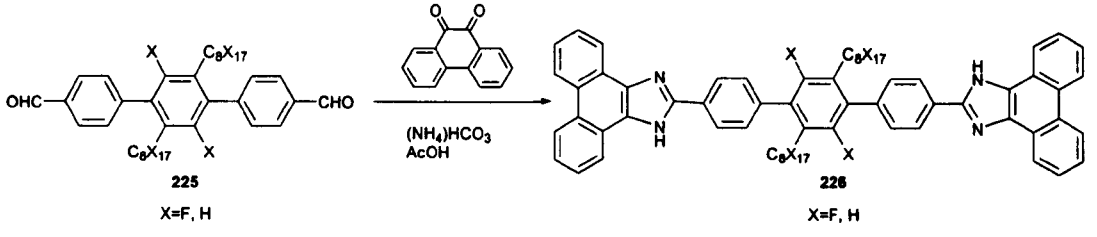

Figure 125: condensation of the dialdehyde **225** with 9,10-phenanthrenequinone.

12. The use of dialdehydes.

As it has been shown above, there are several methods of synthesis of dialdehydes and, although they are very useful as building blocks of many systems, there is not a general procedure for their synthesis.

The use of the aldehydes shown above refers to pure organic synthesis however, there are numerous occasions where their use is related to other areas such as biology or polymer chemistry.

The general use of aldehydes in biology is as fixating agents for tissues removed from a body and in polymer chemistry as building blocks (monomers or oligomers) for the synthesis of polymeric materials.

12.1 Chemical fixation.[116]

When a fraction of tissue is extracted from the body, the cells that compose it die in a process of self-destruction caused by the action of the intracellular enzymes, resulting in the total decomposition of the tissue.

The objective of fixation is to preserve the cells and tissue components suffering from this decomposition and maintain them in a condition suitable for their study.

The use of aldehydes plays an important role in the study of tissues because they are used, among some other substances, as fixating agents. Their role is to combine covalently with the biochemical constituents and 'fix' them into place. Aldehydes form intermolecular imine linkages causing a change in the sol form of the cytoplasm, transforming it into a transparent gel, therefore they behave as a non-coagulative fixative. The three most important aldehydes used for this purposes are formaldehyde (H_2CO), gluraraldehyde (HOC-$(CH_2)_3$-CHO), and acrolein (H_2C=CH-CHO).

Although the precise details of chemical fixation are not known, the general principle is thought to be creation of a gel by the formation of cross-links between the aldehyde and the protein, mainly between the amine groups, leading to the conservation of the cellular constituents.

12.2 Dialdehydes in polymer chemistry.

Using a modified Williamson ether synthesis, Jiang and co-workers[117] synthesised a series of 4,4'(1,n-dioxaalcane)-bisbenzaldehydes **223** from 1,n-dibromoalkanes and the lithium salt of **98** (Figure 126). These dialdehydes have potential applications as oligomers for the synthesis of different polymers.

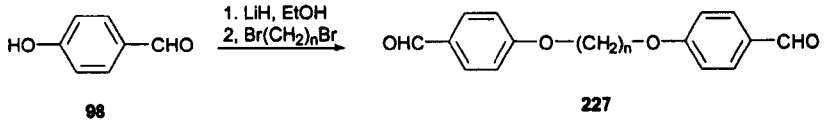

Figure 126: synthesis of 4,4'(1,n-dioxaalcane)-bisbenzaldehydes.

One example of aromatic aldehydes used in polymer chemistry is the synthesis of polymer *salen* compounds. The synthesis of tetradentate Schiff-base[118] polymers was carried out by condensation of **230** and the appropriate diamines in 31-97 % yields (Figure 127). The dialdehyde building blocks were prepared using Suzuki coupling.

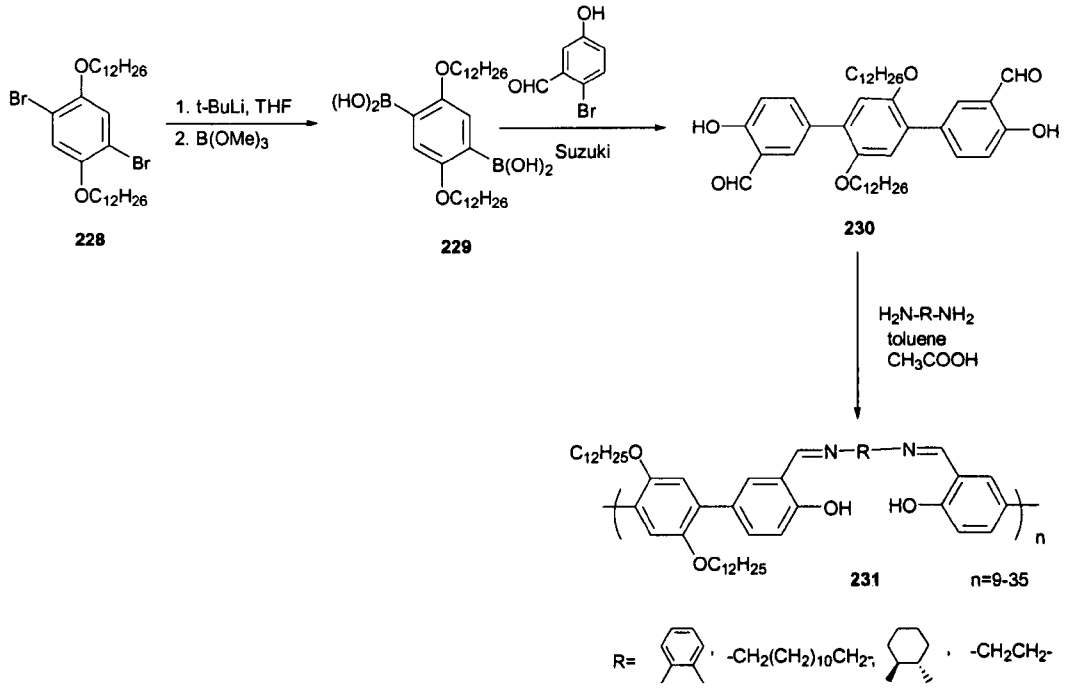

Figure 127: synthesis of tetradentate Schiff-basepolymers.

AIMS AND OBJECTIVES

Aims and objectives

The initial goal of this research is to synthesise a novel type of triangular macrocyclic hosts or *trianglimines*. These enantiomerically pure macrocycles are formed from a [3+3]-cyclocondensation reaction between (1*R*, 2*R*)-diaminocyclohexane and various aromatic dialdehyde building blocks.

The aromatic dialdehydes required for the trianglimine synthesis must have two formyl groups located in a certain way with respect to each other to allow macrocyclisation. As the number of commercially available aromatic dialdehydes suitable for the trianglimine synthesis is limited to a few examples, the development of a strategy for the synthesis of such aromatic dialdehydes was also set as an objective.

In addition to the synthesis of a series of trianglimines with different cavity sizes, another objective was to study the trianglimine formation. Whether different reaction conditions, or the modification of the stoichiometry of the trianglimine building blocks, provokes any variation in trianglimine synthesis will be evaluated, along with a short study into the thermodynamic control of trianglimine synthesis.

As an imine group can be easily reduced to amine, the synthesis of reduced trianglimines or *trianglamines* will be set as another objective for the synthetic part of this research.

The final goal of this project is to test these trianglimines as supramolecular receptors for the entrapment of pesticides. These binding studies will be carried out using two different strategies: ^{1}H-NMR shift titrations and DOSY-NMR.

PART II

RESULTS AND DISCUSSION

Chapter V

SYNTHESIS OF AROMATIC DIALDEHYDES

13. Synthesis of aromatic dialdehydes.

13.1 Dilithiation by Double Lithium-Bromide Exchange.

The first approach followed for the synthesis of dialdehydes was the direct dilithiation by double lithium-bromide exchange from, with a few exceptions, commercially available substrates.

In all cases, the formylation follows the same pattern, which involves the treatment of an aromatic dibromide with *n*-BuLi in dry tetrahydrofuran at –78°C, followed by the addition of dimethylformamide at the same temperature. Finally, the addition of hydrochloric acid and water at room temperature led to the dialdehyde, which in some cases, was obtained by precipitation and in other cases was separated by aqueous extraction with diethyl ether.

Figure 128 shows the double lithium bromide exchange reaction on 1,4-dimethoxy-2,5-dibromobenzene **232**, that proceeded smoothly at –78 °C in 20 ml of THF. The addition of *n*-BuLi gave the dialdehyde **158**[91] after treatment with dimethylformamide and 3N HCl in 60 % yield.

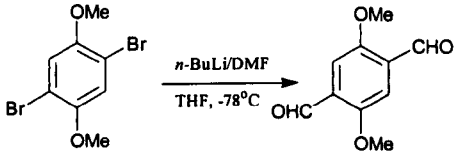

232 158

Figure 128: synthesis of 1,4-dimethoxy- 2,5-diformylbenzene **158**.

The spectroscopic features of dialdehyde **158** were easy to analyse due to the simplicity of its structure. The ^{1}H-NMR spectrum showed one singlet at 10.52 ppm for the two formyl groups, at 7.55 ppm another singlet corresponding to the aromatic protons was seen, and finally another singlet at 4.03 ppm corresponding to the methoxy groups. The IR spectrum showed a strong peak at 1682 cm^{-1} corroborating the presence of the aldehyde group, as did the signal of the formyl carbon at 189.6 ppm in the ^{13}C NMR spectrum.

Similarly 4,4'-dibromo-biphenyl **233** and 9,10-dibromoanthracene **234** gave the corresponding dialdehydes **87**[64] and **235**[119] under identical conditions and in 50 % and 40 % yield, respectively (Figure 129). In these three cases the dialdehydes precipitated directly from the reaction mixture, as pure products requiring no further purification steps, upon addition of HCl.

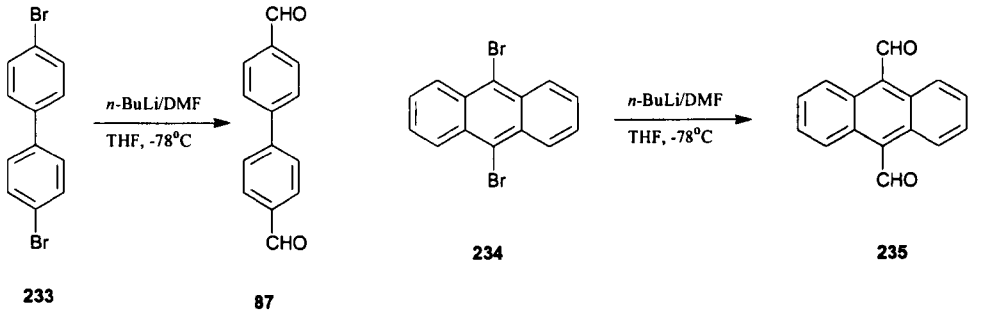

Figure 129: synthesis of dialdehydes *via* Br-Li exchange.

Compound **87** was obtained as white crystals and, as in the case of **158**, the symmetry of its structure was confirmed by the appearance of one set of signals in both ^{1}H and ^{13}C-NMR spectra. The formyl group of **87** appeared as a singlet at 10.13 ppm and the non-equivalent aromatics appeared as two doublets at 8.00 and 7.81 ppm (J 8.1 Hz). The IR spectrum showed a strong peak at 1686 cm^{-1} also confirming the presence of the formyl group, as well as the mass spectrum exhibiting the molecular ion peak at *m/z* (EI) 210 M^{+}.

The structure of 9,10-diformylanthracene **235**,[119] which was obtained as a orange powder, was confirmed by ^{1}H-NMR showing one singlet at 11.50 ppm for the two formyl groups, and at 8.71 and 7.63 ppm the signals corresponding to an AA'XX' spin system. The structure was corroborated by mass spectrum showing the molecular ion at *m/z* (EI) 234 M^{+}.

The synthesis of bis-4-formylphenyl-ether **237** (27.3 %) from bis-4-bromophenyl-ether **236** was carried out in the same way as the previous dialdehydes. However, the pure product was not obtained by precipitation, therefore the extraction with diethyl ether was necessary.

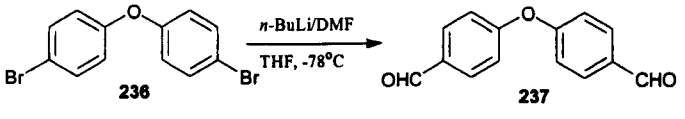

Figure 130: synthesis of 4,4'-bis(formyl)phenyl-ether **237**.

The identity of this compound was confirmed by mass spectrometry showing the molecular ion in CI at *m/z* 227 M^{+}. The ^{1}H-NMR spectrum showed the high symmetry of the molecule with one singlet corresponding to the aldehyde protons at 9.98 ppm, and two doublets for the aromatic protons at 7.92 and 7.18 ppm. The single crystal X-Ray structure of **237** obtained is shown in Figure 131. The data for the crystal structure is presented in appendix A.

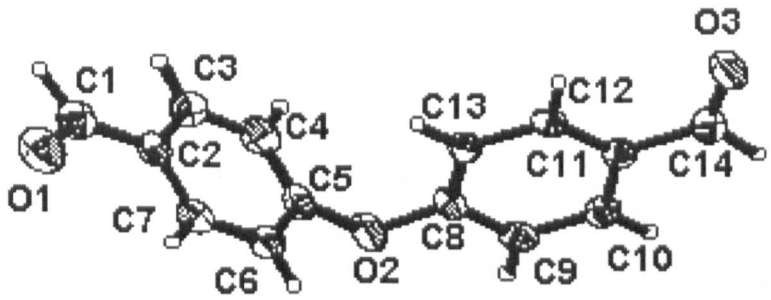

Figure 131: crystal structure of dialdehyde **237**.

The crystal structure of **237** has been compared with the aromatic dialdehyde shown below (Figure 132).

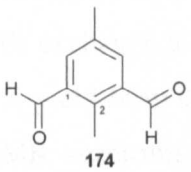

174

Figure 132: structure of 2,5-dimethylisophthalaldehyde **174** compared to compound **237.**

The C-C(O) bond length of **237** (1.478 Å) is practically the same as the bond length of **174** (1.477 Å). The distance between the oxygen and the carbon of the carbonyl group is also very similar in compounds **237** (1.207Å) and **174** (1.192 Å). The bond distance is also the same in both compounds for the respective bond distance between the aromatic carbon (attached to the carbonyl group) and the adjacent, unsubstituted, aromatic carbon, (1.402 Å) for **237** and (1.378 Å) for **174**. In contrast, the dihedral angles are quite different. In **237**, the C(7)-C(2)-C(1) is 121.40°, whereas in **174**, the C(6)-C(1)-C(7) is 115.40°.

The sum of the bond angles around an atom gives an indication of the geometry exhibited by an atom within the molecule. In the case of **237**, the sum of the dihedral angles of C(7)-C(2)-C(1), C(7)-C(2)-C(3) and C(3)-C(2)-C(1) whose values are 121.40°, 119.08 °, 119.53° respectively, gives a value of 360°, which means that geometry is planar.

Unfortunately, the number of commercially available dibrominated aromatic precursors was quite limited. As a consequence new strategies were developed involving the functionalisation of the available substrates to make them suitable for further transformations into dialdehydes.

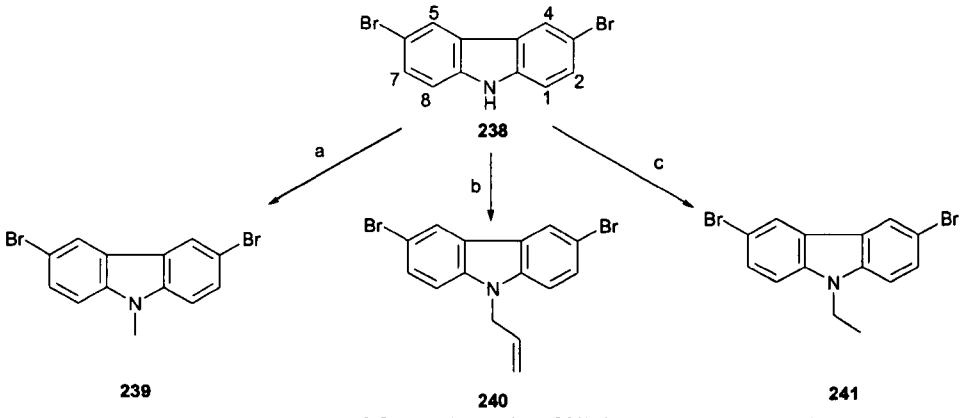

Figure 133: a) 1.NaOH/Acetone, 2.Me_2SO_4, **b)** 1.$BnNEt_3Cl$/2-butanone, 2.NaOH/$BrCH_2CH_2{=}CH_2$ **c)** 1.$BnNEt_3Cl$ / 2-butanone, 2.NaOH/EtBr.[120]

This functionalisation is illustrated in Figure 133, in which the NH group of carbazole **238** had to be protected prior to Li-Br exchange to avoid deprotonation by the *n*-BuLi. Carbazole **239** was obtained in 56 % yield from carbazole **238** and dimethyl sulphate in acetone and NaOH. The ^{1}H-NMR spectrum showed one set of signals, which demonstrated the symmetry of the molecule with the following characteristic signals: at 3.76 ppm, a singlet belonging to the methyl group, another singlet at 8.13 ppm for the proton adjacent to the bromine ($H_{4,5}$) and two doublets (at 7.22 and 7.53 ppm) of the protons $H_{1,8}$ and $H_{2,7}$ respectively.

Carbazole **240** was obtained in 59 % yield from carbazole **238** after the reaction at 50 °C for two hours with allyl bromide, benzyltriethylammonium chloride (catalytic) and aqueous NaOH in 2-butanone. The ^{1}H-NMR spectrum confirmed the structure by showing the characteristic peaks of the allyl group at 4.85, 5.13 and 5.80 ppm. The ^{1}H-NMR spectrum also showed one set of aromatic signals corresponding to the 3 aromatic protons, demonstrating again the symmetry of the molecule.

Carbazole **241** (98 %) was obtained using the same procedure as before but, instead of allyl bromide, 1-bromoethane was used. The characteristic signals of the compound by ^{1}H-NMR spectrum showed the CH_3-CH_2- moiety at 1.40 ppm for the CH_3- group and 4.31 ppm for the -CH_2-. The signals (one set of peaks again) of the aromatic ring are shown in detail in the experimental section.

Having successfully modified the carbazoles, the synthetic strategy followed for the diformylation involved, again, the dilithiation by double lithium-bromide exchange using *n*-BuLi and dimethylformamide.

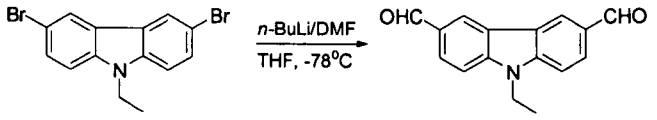

241 79

Figure 134: synthesis of diformyl carbazole **79**.

The treatment of 3,6-dibromo-N-ethyl-carbazole **241** with *n*-BuLi followed by dimethylformamide gave, under identical conditions as before, a 9:1 mixture of monoaldehyde and diformaldehyde **79**[58] (28 %) that was separated easily by recrystallisation using a mixture of 3:1 diethyl ether: petroleum ether (Figure 134).

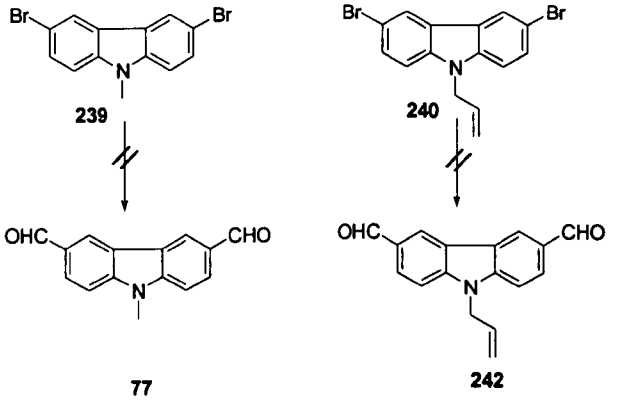

Figure 135: failed attempts to synthesise carbazoles dialdehydes.

The same reaction was attempted on carbazoles **239** and **240** under the same conditions (Figure 135).

The formylation of the carbazoles **239** and **240** was repeated several times using slightly different conditions, but the results were not as satisfactory as expected. The reaction products in both cases resulted in a mixture of compounds whose separation and identification was unsuccessful.

In case of the allyl substituted derivative, deprotonation in the double activated benzylic position seems to compete with the Li-Br exchange, leading to a variety of products.

For the synthesis of the naphthalene dialdehyde **246** (Figure 136), functionalisation of the commercially available starting material was necessary. Firstly, dibromination of **243** with bromine in glacial acetic acid gave **244**.[121] Secondly this was followed by methylation of the hydroxyl groups[122] of **244** using MeI in DMSO to obtain **245**.[123]

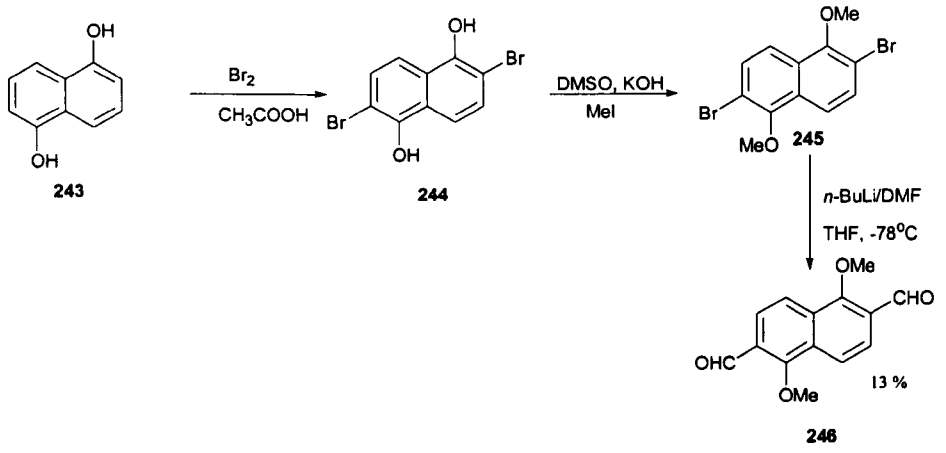

Figure 136: synthesis of 1,5-dimethoxy- 2,6-diformylnaphthalene.

The dibrominated naphthalene **245** was then formylated using the standard conditions, obtaining the final product **246** as a yellow precipitate. The high symmetry of this compound was verified by ^{1}H-NMR spectroscopy. The formyl proton appeared as one singlet at 10.61 ppm, the aromatic protons appeared as a pair of doublets at 8.08 and 7.96 ppm (J 8.8) and the two OCH_3 groups appeared as a singlet at 4.14 ppm.

The same approach was attempted for 2,7-dihydroxynaphthalene **247** and 2,3-dihydroxynaphthalene **248**. The first step of the synthesis, that is the alkylation using MeI (or EtI) in DMSO and KOH, was accomplished successfully to give **211**,[124] **249**[125] and **250**.[126] However, the dibromination failed, giving as a final product a mixture of mono, di and tri-bromination products, as deduced from the mass spectrum. The crude mixture of reaction could not be separated (Figure 137).

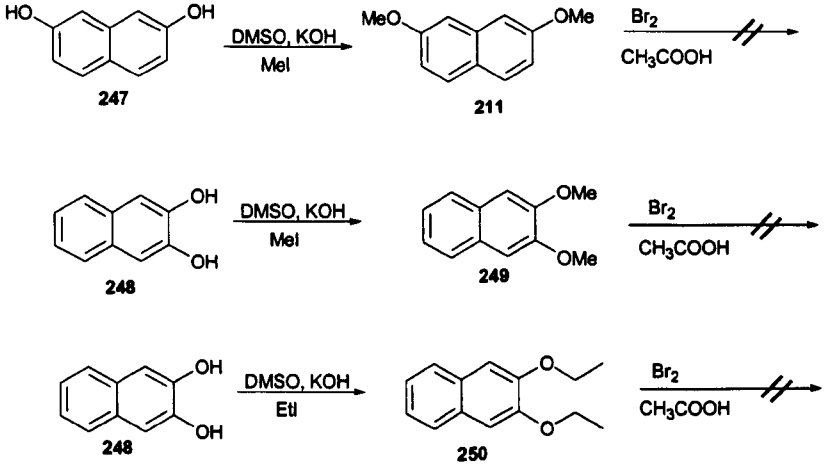

Figure 137: failed attempts to synthesise dibromide-naphthalenes from hydroxyl precursors.

It was attempted to reverse the order of the synthetic procedure, by carrying out the synthesis of the dibromo-dimethoxynaphthalenes (Figure 138). In this case, bromination of **248** was performed successfully in the first step to give **252**[127] (this

was unsuccessful in the case of **247**), followed by the methylation, that was not achieved.

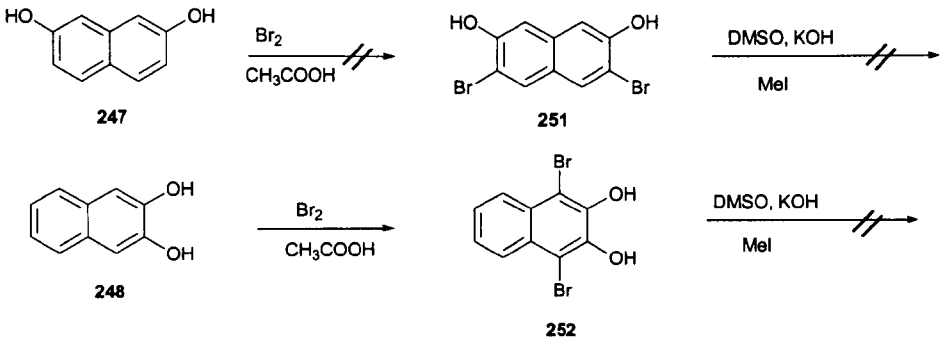

Figure 138: failed attempts to synthesise naphthalene dialdehydes.

Double lithiation of fluorinated dibromides failed to yield any dialdehydes. Surprisingly the first lithium-bromide exchange step on **259** and **262** shown in Figure 139, carried out as a control reaction, proceeded smoothly and yielded the monoaldehydes **260** and **263** in almost quantitative yields (no further purification and characterisation was carried out for **260** and **263**, as these compounds were not of relevance for this thesis). Addition of more than 1 equivalent of *n*-BuLi, however, produced what can only be described as complete and utter decomposition of all materials involved.

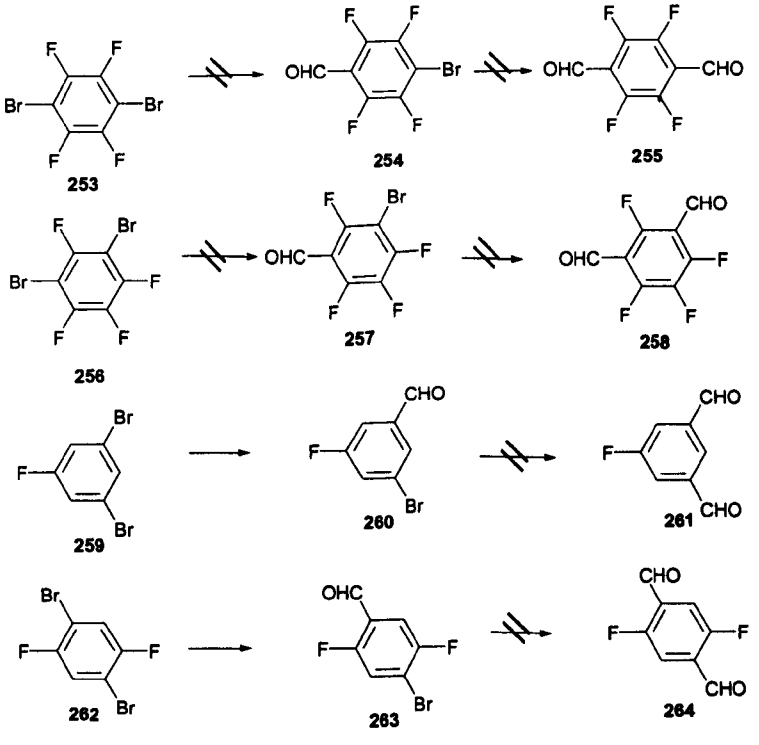

Figure 139: structure of the fluorinated dibromides used for diformylation.

Table 2 summarises the results obtained for the synthesis of these dialdehydes obtained *via* lithium-bromide exchange.

Substrate	Product	m/z	^{1}H-NMR (C*H*O)	^{13}C-NMR (*C*HO)	Yield %
232	**158**	194	10.50	189.6	60
233	**87**	210	10.10	192.1	50
234	**235**	234	11.50	194.7	40
236	**237**	227	9.98	190.8	27
241	**79**	251	10.14	191.7	28
243	**246**	245	10.61	189.6	13

Table 2: summary of spectroscopy data for the aldehydes obtained *via* lithium-bromide exchange.

13.2 Sequential Dilithiation by Lithium Bromide Exchange.

Since a number of substrates failed to undergo the direct double lithiation it was reasoned that a sequential route might be beneficial, moving the negatively charged centre in **265** away from the central aromatic nucleus and hence reduce any charge-charge repulsion. The figure below illustrates this approach.

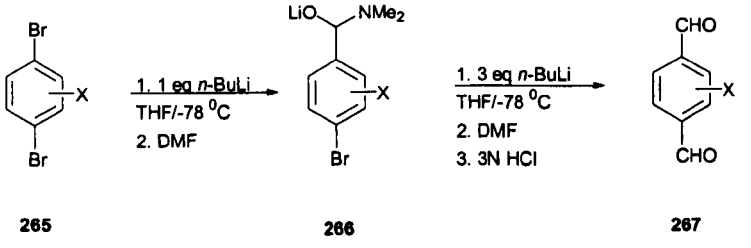

Figure 140: sequential Dilithiation by Lithium Bromide Exchange.

The sequential route followed for dibromide **268** gave dialdehyde **269** in low yield (11 %) (Figure 141). The spectroscopic data showed the formyl proton at 10.12 ppm and the aromatic protons at 8.21 and 7.99 ppm in the ^{1}H-NMR spectrum. The mass spectrum showed the molecular ion by EI at *m/z* 149.1.

The sequential route followed for **270** gave **271** (Figure 141) in excellent yield (99 %). The first attempt to synthesise **271** was carried out with *n*-BuLi, but the yield obtained was very low. However, when the reaction was carried out with *tert*-BuLi, the result was surprisingly different, as the yield obtained was much higher. The ^{1}H-NMR spectrum of **271** showed two different peaks for the two non-equivalent protons of the formyl groups at 10.38 and 10.08 ppm.

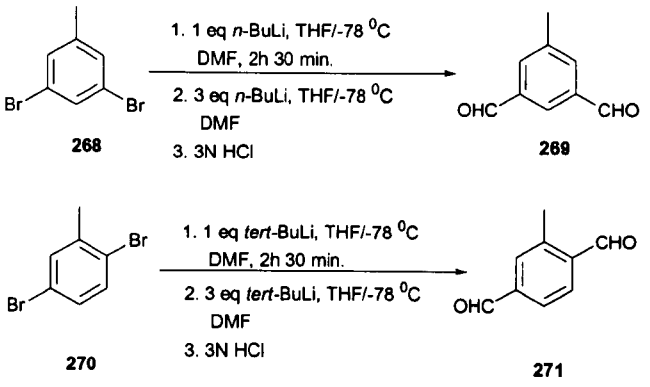

Figure 141: sequential Dilithiation by Lithium Bromide Exchange.

Table 3 summarises the results obtained for the synthesis of these dialdehydes.

Substrate	Product	m/z	^{1}H-NMR (CHO, $-CH_3$)	^{13}C-NMR (CHO, $-CH_3$)	Yield %
268	269	149.1	10.10, 2.56	191.7, 21.5	11
270	271	148.0	10.38, 10.08, 2.76	192.8, 192.5, 19.9	99

Table 3: summary of spectroscopy data for the aldehydes obtained *via* sequential lithium-bromide exchange.

13.3 Dilithiation by Double Directed *Ortho* Metalation.

In a previous section (**13.1**), the synthesis of dialdehydes *via* bromide-lithium exchange was introduced involving, in some cases, the bromination of the starting materials. However, this is not always necessary because the hydrogen-lithium exchange is reported to work effectively in the presence of *ortho*-directing substituents at the aromatic ring.

The dilithiation was carried out with the *n*-BuLi-TMEDA complex in diethyl ether, and with different molar ratios according to the aromatic precursor (Figure 142). Elevated temperatures and/or long reaction times were often necessary to achieve dilithiation (see table 5). In this case (unlike that of the formylation of the brominated precursors) it was necessary to use TMEDA because it is reported to coordinate to the lithium thereby reducing the aggregation of the lithium reagent employed and hence producing a more reactive organolithium species.

This synthetic procedure has the characteristic (in comparison with the formylation of the brominated precursors) that it does not require low temperatures.

In all reactions carried out, the purification of the compounds was necessary because of the presence of by-products, principally monoformylated compounds. The crude reaction products were orange oils (in the three cases) that were treated with a mixture of (3:1) diethyl ether: petroleum ether leading to a mixture of a precipitate and a

solution. The pure product was obtained by filtration and recrystallisation from diethyl ether.

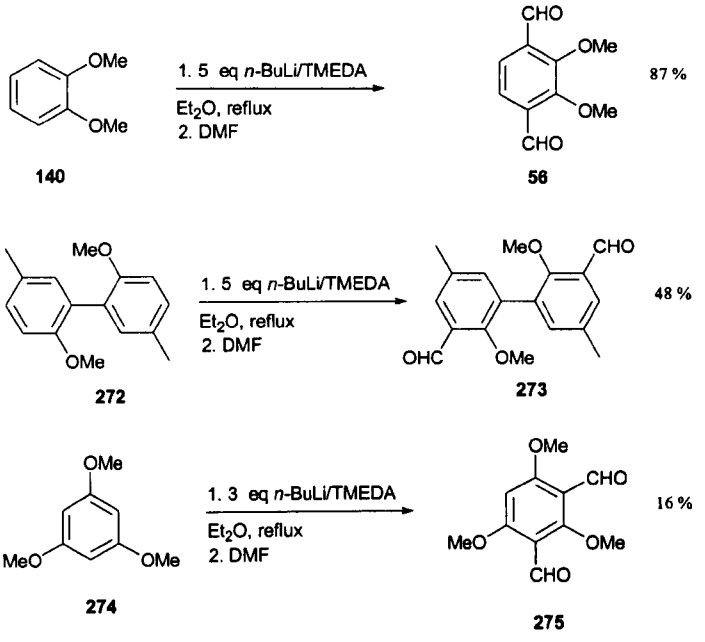

Figure 142: synthesis of dialdehydes *via* *n*-BuLi/TMEDA.

The double directed *ortho*-lithiations of 1,2-dimethoxybenzene **140** and 1,1'-dimethoxy-4,4'-dimethylbiphenyl **272** were carried out with 5 equivalents *n*-BuLi/TMEDA complex in diethyl ether at reflux. After quenching with dimethylformamide followed by 3N HCl, the dialdehydes **56**[88] and **273** were obtained in satisfactory yields (Figure 142). For the synthesis of compound **275**[79], three equivalents of *n*-BuLi/TMEDA were needed.

As in the previous cases, the dialdehydes synthesised showed very simple ^{1}H-NMR spectra. 1,2-dimethoxy-3,6-diformylbenzene **56** showed three singlets, one at 10.44 ppm for the formyl groups, 7.63 ppm for the aromatic protons and 4.05 ppm for the –OCH_3 protons.

The ^{1}H-NMR spectrum of 1,1'-dimethoxy-2,2'-diformyl-4,4'-dimethylbiphenyl **273**, showed one set of signals for each aromatic moiety: 10.41 ppm a singlet corresponding to the two formyl groups; at 7.72 and 7.43 ppm two singlets corresponding to protons H_6 and H_4, respectively, and at 3.57 and 2.41 ppm, another two singlets for the methoxy and methyl groups, respectively.

1,3,5-trimethoxy-2,4-diformylbenzene **275** showed also three singlets, one for each different proton. Thus, one singlet for the two formyl groups at 10.32 ppm and one more singlet for the aromatic proton at 6.27 ppm, and only one signal (with intensity nine), appeared for the three OCH_3 groups at 4.00 ppm.

In Figure 143 is shown the synthesis of 1,1'-diformylferrocene **136**, which was prepared under the same conditions found in the literature[86] in 40 % yield.

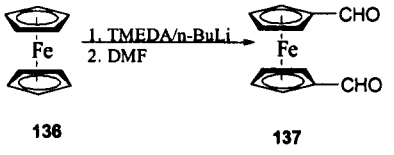

Figure 143: synthesis of 1,1'-diformylferrocene.

The ^{1}H-NMR spectrum of **137** showed the expected values for the chemical shifts found in the literature. Thus, the formyl proton appeared at 9.93 ppm, and the aromatic protons appeared at 4.87 and 4.66 ppm.

In the section of synthesis of dialdehydes by dilithiation by double lithium-bromide exchange (**13.1**), one successful synthesis of a diformyl naphthalene derivative was shown along with various failed attempts of synthesis. As this approach failed, the dilithiation by double directed *ortho* metalation was tried instead. This approach employed the methylation of the two phenolic OH groups with methyliodide, and further reaction with *n*-BuLi and TMEDA in the same way as the examples described above (Figure 144).

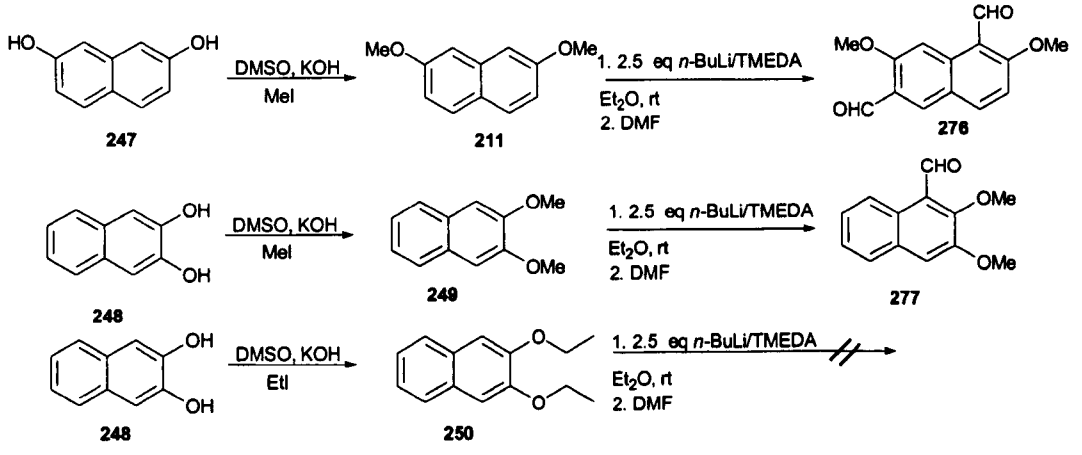

Figure 144: synthesis of dialdehydes *via* methylation followed by *n*-BuLi /TMEDA.

Compound **276** was obtained *via* the double directed *ortho*-metalation procedure from 2,7-dimethoxynaphthalene **211**[124] using 2.5 equivalents of TMDA and *n*-BuLi in diethyl ether at room temperature for 6 hours, followed by quenching with dimethylformamide and further hydrolysis with hydrochloric acid.

Unlike the previous dialdehydes synthesised, the ^{1}H-NMR spectrum of 2,7-dimethoxy-1,6-diformylnaphthalene **276** illustrates the lack of symmetry of the compound, leading to one signal for each proton in the molecule. In this case, two signals for the two-formyl groups are present (10.84 and 10.52 ppm), as well as for the two non-equivalent OCH_3 groups at 4.07 and 4.06 ppm.

The attempt to synthesise 1,4-diformyl-3-dimethoxynaphthalene failed and the monoformylated compound **277**[128] was obtained instead. The reaction was attempted several times varying temperatures and reaction times, however, the outcome was either a mixture of compounds that could not be separated and identified, or the monoformylated product.

Table 4 summarises the results obtained for the synthesis of these dialdehydes.

Substrate	Product	m/z	^{1}H-NMR (*CHO*, -OC*H*$_3$)	^{13}C-NMR (*C*HO)	Yield %
140	**56**	194.1	10.44, 4.05	189.5	87
272	**273**	298.2	10.41, 3.57	190.4	48
274	**275**	225.2	10.32, 4.00	187.4	16
247	**276**	244.0	10.84,10.52, 4.07	191.6,189.7	44

Table 4: summary of spectroscopy data for the aldehydes obtained *via ortho*-metalation.

13.4 Synthesis of dialdehydes *via* oxidation.

The oxidation of 5-hydroxymethylfurfural **204** (Figure 145) was carried out using manganese dioxide in toluene, giving 2,5-diformylfurane **139** in 89 % yield using the literature procedure.[94]

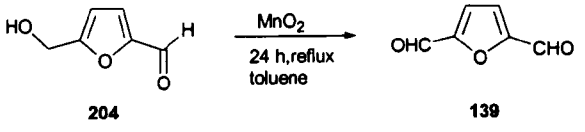

Figure 145: oxidation of 5-hydroxymethylfurfural *via* manganese dioxide.

The spectroscopic features seen were one singlet at 9.70 ppm for the two formyl groups and one singlet for the aromatic protons at 7.32 ppm.

Dioxidation with selenium dioxide in dioxane was carried out on 2,6-hydroxymethylpyridine **162**, leading to 2,6- diformylpyridine **163** using the literature procedure[92] (Figure 146). The ^{1}H-NMR spectroscopic data showed the peak corresponding to the formyl group at 10.22 ppm and the aromatic protons appeared as a multiplet at 8.23 ppm.

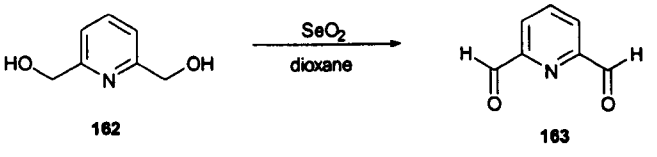

Figure 146: synthesis of 2,6- diformylpyridine.

13.5 Synthesis of dialdehydes *via* Vilsmeier-Haack reaction.

The 1,3-diformylazulene **85**[61] was prepared from azulene **84** using the Vilsmeier-Haack reaction. Although the crude reaction contained a mixture of mono and di-formylated product, **85** was isolated in 40 % (Figure 147).

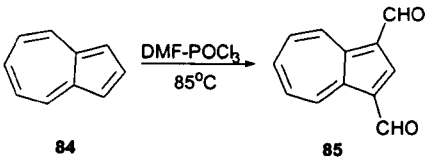

84 85

Figure 147: synthesis of 1,3-diformylazulene by using Vilsmeier-Haack reaction.

The diformylated compound showed in ^{1}H-NMR the chemical shifts given in Figure 148.

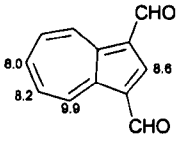

Figure 148: structure of 1,3-diformylazulene showing the chemical shift.

Table 5 summarised all the conditions used in all diformylations carried out.

Entry	Substrates	Conditions	Product	Method	Yield
1	**232**	1.3 eq *n*-BuLi, -78 ^{0}C, THF, 2 h; 2. 3 eq DMF, -78 ^{0}C,THF, 30 min; 3. 3 N HCl	**158**	A	60
2	**233**	1.4 eq *n*-BuLi, -78 ^{0}C, THF, 2 h; 2. 4 eq DMF, -78 ^{0}C,THF, 30 min; 3. 3 N HCl	**87**	A	50
3	**234**	See entry 2	**235**	A	40
4	**236**	1.2,5 eq *n*-BuLi, -78 ^{0}C, THF, 2 h; 2. 2,5 eq DMF, -78 ^{0}C,THF, 30 min; 3. 3 N HCl	**237**	A	27
5	**241**	1. 4 eq *n*-BuLi, -78 ^{0}C, THF, 2 h; 2. 4 eq DMF, -78 ^{0}C,THF, 30 min; 3. 3 N HCl	**79**	A	28
6	**243**	See entry 2	**246**	A	13
7	**268**	1.1 eq *n*-BuLi, -78 ^{0}C, THF, 30 min; 2. 1 eq DMF, -78 ^{0}C,THF, 30 min; 4. 3 eq *n*-BuLi, -78 ^{0}C, 2 h;5. 3 eq DMF, -78 ^{0}C, 30 min; 6. 3 N HCl	**269**	B	11
8	**270**	1.1 eq *tert*-BuLi, -78 ^{0}C, 30 min; 2. 1 eq DMF, -78 ^{0}C, 30 min; 4. 3 eq *tert*-BuLi, -78 ^{0}C, THF, 2 h; 5. 3 eq DMF,-78 ^{0}C, 30 min; 6. 3 N HCl	**271**	B	99
9	**140**	1.5 eq *n*-BuLi/TMEDA, -78 ^{0}C, Et_2O, 2 h; 2. 5 eq DMF, rt, THF, 30 min; 3. 3 N HCl	**56**	C	15
10	**272**	See entry 9	**273**	C	30
11	**274**	See entry 9	**275**	C	16
12	**136**	See entry 9	**137**	C	40
13	**247**	1.2,5 eq *n*-BuLi/TMEDA, -78 ^{0}C, Et_2O, 2 h; 2. 2.5 eq DMF, rt, THF, 30 min; 3. 3 N HCl	**276**	C	44
15	**204**	1.5 eq. MnO2/toluene, reflux, 2. $CHCl_3$	**139**	D	89
16	**162**	1.2 eq SeO_2/dioxane, reflux. 2. CH_2Cl_2	**163**	D	40
17	**84**	1.3 eq $POCl_3$/DMF, 85°C, 2. H_2O/NaOH, 3.$CHCl_3$	**85**	E	40

a) Method A (double LiBr-exchange), Method B (sequential dilithiation), Method C (double *ortho* lithiation); Method D (oxidation), Method E (Vilsmeier-Haack).

Table 5: summary of the reaction conditions for the synthesis of all the dialdehydes.

Chapter VI

SYNTHESIS OF TRIANGLIMINES

In the literature review chapter, a new synthetic strategy was presented for the synthesis of large poly-imine *meta*- and *para*-cyclophane type macrocycles using a [3+3]-cyclocondensation strategy, which was introduced for the first time by Gawronski and co-workers and followed by the group of Hodacova. The fascination for this approach led to start the investigation of the scope and limitation of these macrocycles in significant extension based on Gawronski's scheme, synthesising novel, exciting and unusual macrocycles. Due to their unique triangular shape it was suggested to name these new classes of macrocycles *trianglimines*.

The synthesis of the new trianglimines consisted in the cyclocondensation of (1*R*, 2*R*)-diaminocyclohexane with aromatic diketones and acyl halide derivatives as well as aromatic dialdehydes synthesised in the previous section.

14. Synthesis of (1*R*, 2*R*)-diaminocyclohexane.[129]

The synthesis of (1*R*, 2*R*)-diaminocyclohexane involved a two-step reaction process, being, the synthesis of the (1*R*, 2*R*)-diaminocyclohexane tartaric salt followed by the decomposition of the salt to yield the enantiomerically pure diaminocyclohexane.

(1*R*, 2*R*)-diaminocyclohexane tartrate salt **279** was obtained as white crystals, after half an hour reaction at 100°C, between the racemic form (1*RS*, 2*RS*)-**38** with L-tartaric acid **278** in water (Figure 149).

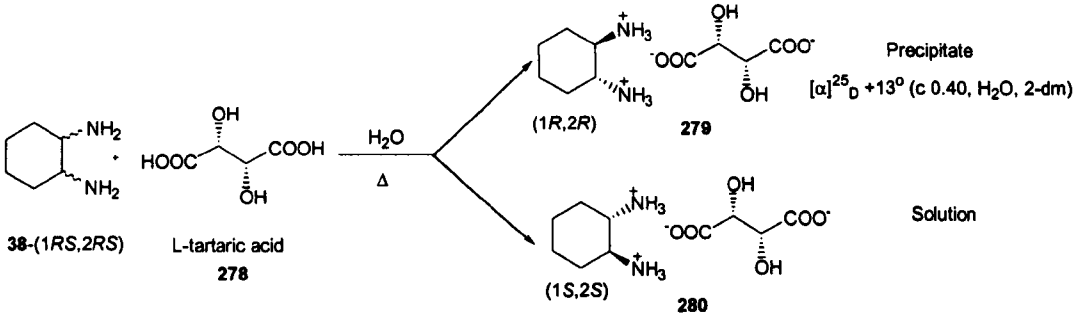

Figure 149: synthesis of diaminocyclohexane tartrate salt.

The reaction mixture led to a white precipitate in a yellow solution. The pure salt was obtained after filtration and recrystallisation from water. In order to confirm the enantiomeric purity of the tartrate salt, its optical rotation was determined using polarimetry. In comparison with commercial catalogue values, it can be stated that the (1*R*, 2*R*)-**38**-tartrate salt **279** synthesised possess a 98.5 % enantiomeric excess.

(1*R*, 2*R*)-**38** was obtained after dissolving 1 equivalent of the tartrate salt **279** in a solution of 2 equivalents of sodium hydroxide aqueous solution, followed by

extraction with chloroform (Figure 150). After evaporation of the solvent, the enantiomerically pure (1*R*, 2*R*)-diaminocyclohexane was obtained as white needles. The measurement of the optical rotation by polarimetry gave a value of $[\alpha]^{25}_{D}$ –23.7° (c 4, HCl, 1-dm), which compared with literature[129] values (lit. $[\alpha]^{25}_{D}$ –23.7° (c 4, HCl, 1-dm) gives a 98 % enantiomeric excess.

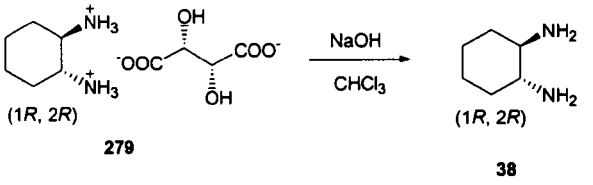

Figure 150: decomposition of the diaminocyclohexane tartaric salt to obtain (1*R*, 2*R*)-diaminocyclohexane (63%).

15. Synthesis of trianglimines from aromatic ketones and acyl halides.

As an extension to the [3+3]-cyclocondensation first reported by Gawronski, the cyclocondensation between (1*R*, 2*R*)-diaminocyclohexane and the commercial available 1,4-diacetylbenzene **281** and 1,3-diacetylbenzene **282** were attempted (Figure 151).

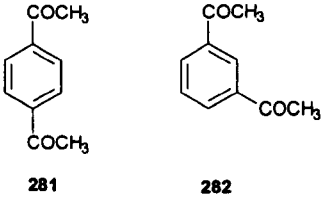

Figure 151: structures of the diketones used in trianglimine synthesis.

Both carbonyl compounds show a considerably reduced reactivity in comparison to the unsubstituted dialdehydes published by Gawronski.

The [3+3]-cyclocondensation between **281** and **38** gave the macrocyclic trianglimine **283** (Figure 152) after a 24 hour reaction at reflux in dichloromethane, along with a number of tetrameric linear condensation products, as showed in the LSIMS spectrum.

Although the reaction product was insoluble, the macrocycle could be obtained after recrystallisation in moderate yield (28 %). The LSIMS spectrum confirmed the structure of the macrocycle shown by the molecular ion at *m/z* 720.3 [M+H]. Also, the ^{1}H-NMR spectrum illustrated the spectroscopic characteristics of the macrocycle proposed.

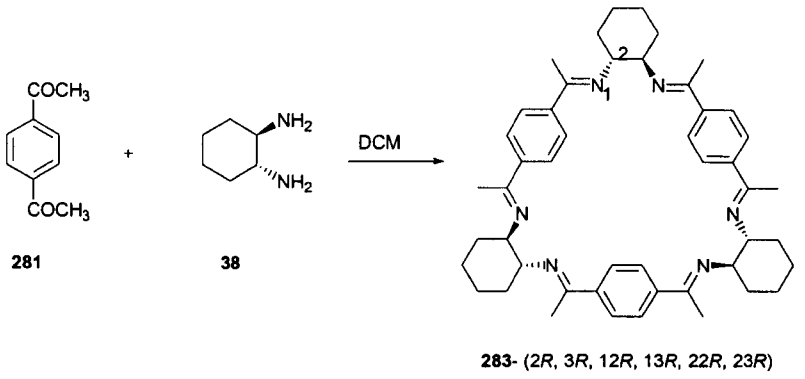

281 38 283- (2*R*, 3*R*, 12*R*, 13*R*, 22*R*, 23*R*)

Figure 152: reaction between 1,4-diacetylbenzene and (1*R*, 2*R*)-diaminocyclohexane.

The most important characteristic signals are a singlet at 7.95 ppm, due to the presence of the aromatic protons, as well as a singlet at 2.09 ppm, corresponding to the six methyl groups.

The second attempt to synthesise a macrocycle, or trianglimine, from 1,3-diacetylbenzene **282** was unsuccessful (Figure 153). The reaction resulted in a complex mixture of [2+2] and [3+3]-cyclocondensation products as well as open chains of different lengths and unknown compounds, as judged by the mass spectrum obtained for the crude reaction product.

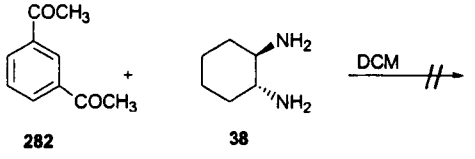

282 38

Figure 153: failed attempt to synthesise a trianglimine from **38** and **282**.

The [3+3]-cyclocondensation between **38** and terephthaloylchloride **284** (Figure 154) in dichloromethane using DMAP, NEt_3 or K_2CO_3 did result in the formation of a white material displaying an amide C=O band at 1631 cm^{-1} in the infrared spectrum. Due to its complete insolubility in all solvents employed, a definite structure could not be assigned. However, the reaction product showed the mass spectrum molecular ion in FAB major signal of the [2+2]-cyclocondensation product **285** at *m/z* 490 [M+H], and [3+3]-cyclocondensation product **286** at *m/z* 734 [M+H]. Further characterisation was precluded by the lack of solubility.

Although there was not further spectroscopic evidence to prove the structure of the reaction product, macrocycle **288** (Figure 155) was proposed as the most probable product of reaction.

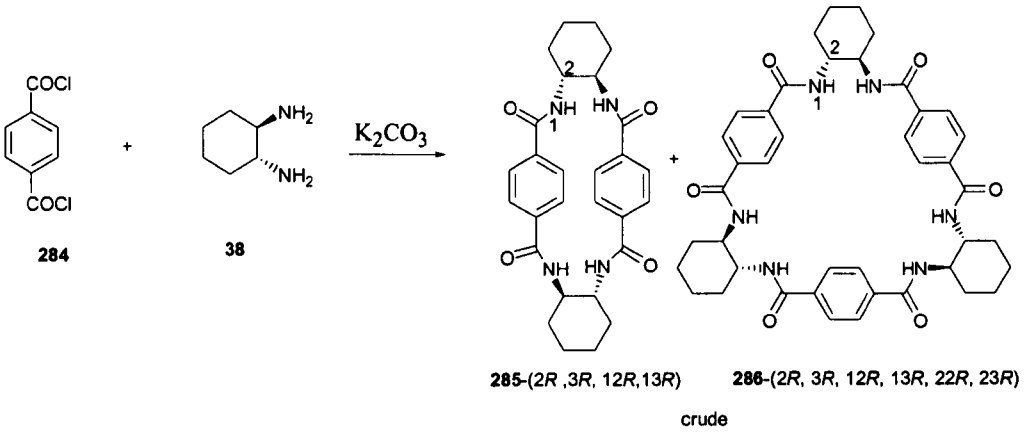

Figure 154: cyclocondensation between therephthaloyl chloride and **38** gave a mixture of products.

The first synthetic approach for the synthesis of trianglimines from diketones or acyl halide derivatives gave in all cases products of reaction with extremely low solubility that made them unsuitable for characterisation and further investigation.

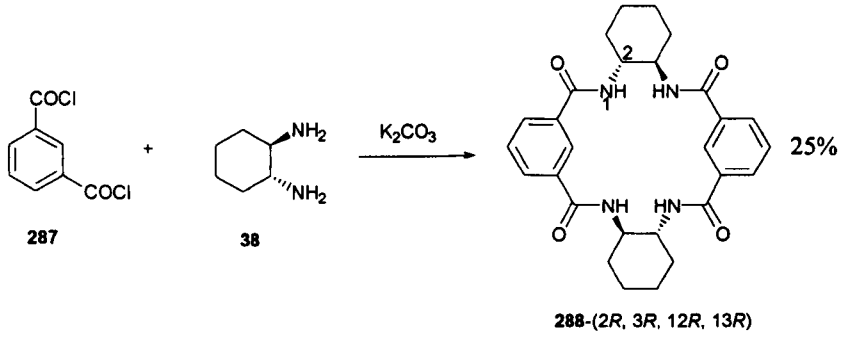

Figure 155: cyclocondensation between **287** and **38** gave [2+2]-cyclocondensation product **288**.

Thus, a new strategy was employed, and instead of continuing the synthesis of ketone trianglimines, it was decided to focus on the synthesis of trianglimines from the aromatic dialdehydes synthesised and presented in the previous chapter.

16. Synthesis of trianglimines from aromatic dialdehydes.

The first synthetic approach taken was the synthesis of the same trianglimines carried out previously by Gawronski[42]and Hodacova.[45] The synthetic procedure used was the same as reported by Gawronski (Figure 156).

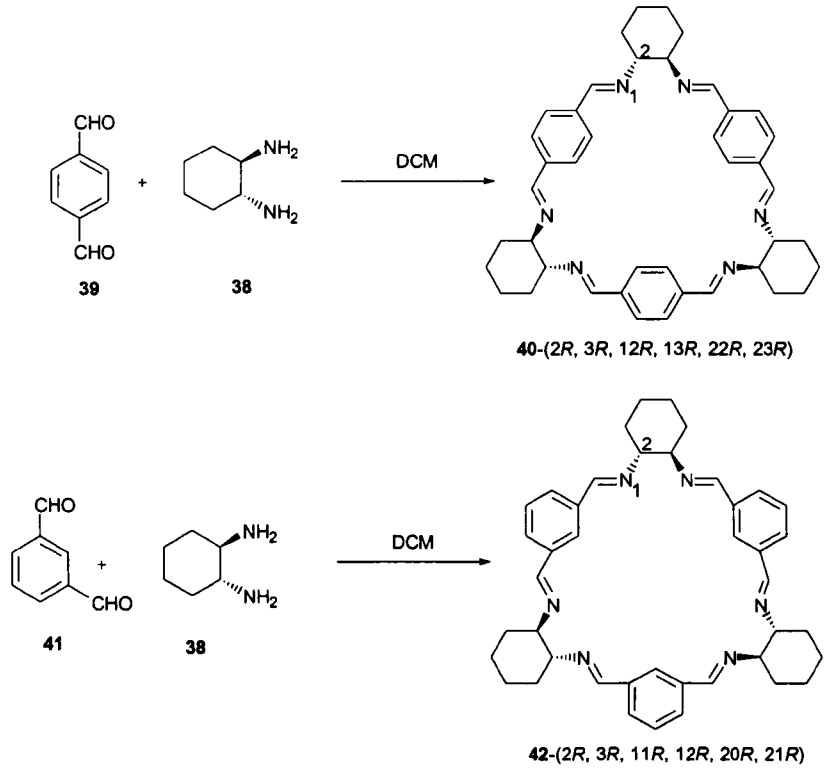

Figure 156: synthesis of Gawronski's trianglimines **40** and **41**.

Trianglimine **40** (89 %) was obtained after a 3 hour reaction at room temperature between one equivalent of **39** and one equivalent of **38** in dichloromethane. The spectroscopic features obtained agree with those published in the literature.[42] Figure 156 also showed the synthesis of trianglimine **42** (74 %) using the same synthetic procedure as for trianglimine **40**. The spectroscopic data also obtained coincided with the data reported by Gawronski.

After successfully repeating the synthesis of the first trianglimines published, the synthesis of a new set of trianglimines using the dialdehydes previously synthesised was carried out. Trianglimine **289** was obtained from 1,4-dimethoxy-2,5-diformylbenzene **158** and (1*R*, 2*R*)-diaminocyclohexane **38** in dichloromethane after 3 hour reaction at room temperature (Figure 157). The trianglimine was obtained as a pure product in 90 % yield.

The reaction gave exclusively the trianglimine **289**, as shown by the LSIMS mass spectrum, which showed only the expected molecular ion at *m/z* 817.4 [M+H]. The simplicity of the ^{1}H-NMR spectrum showed that the compound posses high symmetry in solution, showing only one set of signals for each of the three repeating units of the structure (Figure 158).

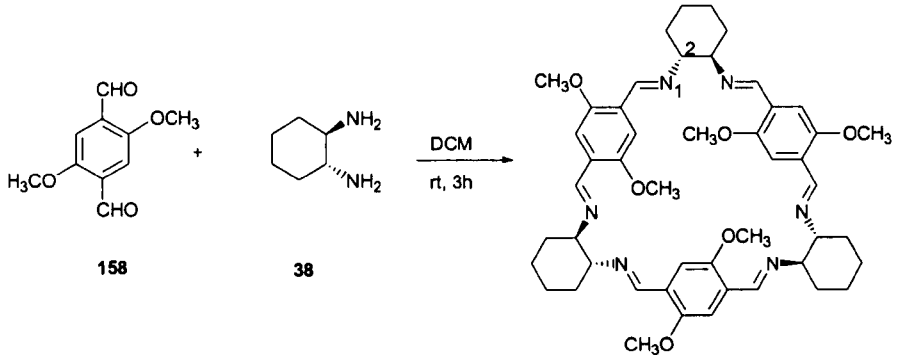

Figure 157: synthesis of trianglimine **289**.

There was only one peak corresponding to the six imine protons at 8.40 ppm, one peak for the six aromatic protons at 7.23 ppm, a sharp peak matching the six methoxy groups at 3.64 ppm, a broad band for the six protons adjacent to the nitrogens in the cyclohexane ring at 3.35 ppm, and finally two broad signals for the remaining protons of the cyclohexane ring at 1.91-1.22 ppm. The ^{13}C-NMR spectrum also showed one set of signals. At 155.6 ppm, the peak of the imine carbon was seen at 132.1 ppm the aromatic carbon attached to the methoxy group, at 128.8 ppm the aromatic carbon attached to the imine bond, and at 100.5 the signal of the non-substituted aromatic carbon. The signal corresponding to the diaminocyclohexane carbon attached to the nitrogen of the imine bond appeared at 82.3 ppm, the carbon of the methoxy group at 46.8 ppm, and finally the two remaining carbons of the cyclohexane ring, appeared at 29.1 and 13.4 ppm.

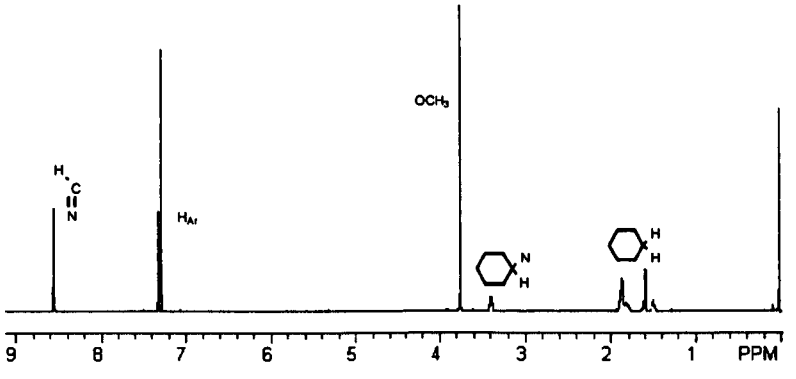

Figure 158: ^{1}H-NMR spectrum of trianglimine **289** ($CDCl_3$, 500 MHz).

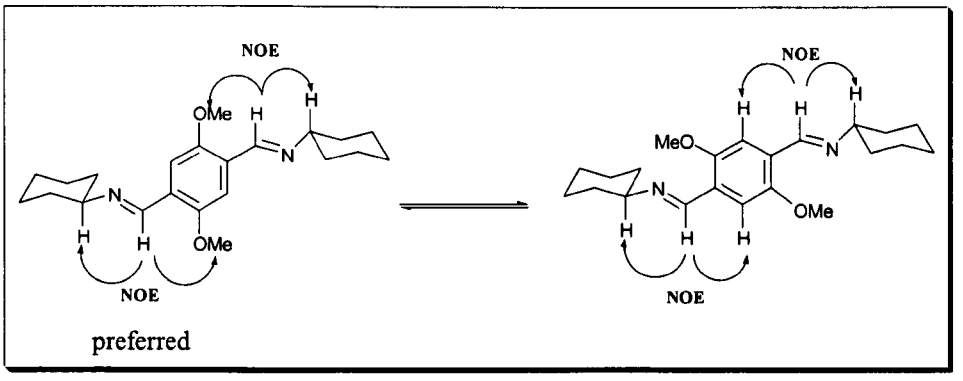

Figure 159: possible conformations in solution of trianglimine **289**.

In order to determine the conformation that trianglimine **289** adopts in solution, ^{1}H-^{1}H-NOESY experiments were carried out. The two possible conformations in solution are shown in Figure 159. The conformer on the left illustrates the preferred conformation, showing a strong NOE effect between imine protons and the methoxy protons, which are aligned in the same plane. In the conformer illustrated on the right, the NOE effect between the aromatic protons and the imine protons is considerably weaker, indicating that both conformers are in equilibrium in solution. The overall symmetry of **289** is D_{3h}.

Similarly to trianglimine **289** described in Figure 157, an isomeric trianglimine was synthesised from 3,6-diformyl-1,2-dimethoxybenzene **56** and **38**, whose structure is shown in Figure 160.

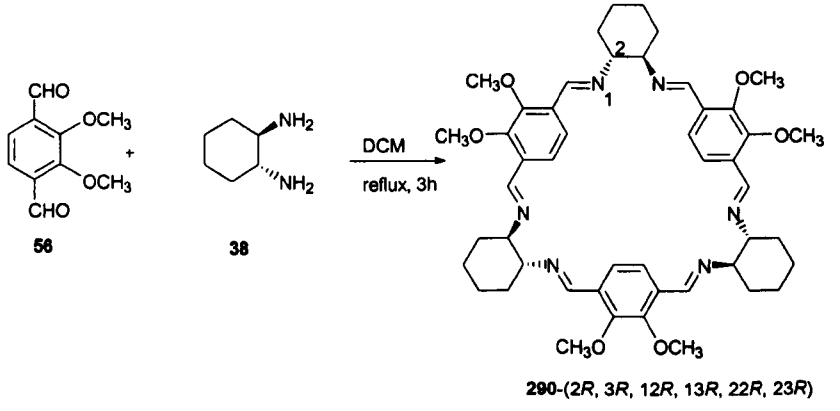

Figure 160: synthesis of trianglimine **290**.

Unlike the previous trianglimine synthesised, the reaction did not proceed at room temperature and heating under reflux for two hours was required. The LSIMS spectrum of **290**, with a molecular ion *m/z* of 817.3, confirmed that the trianglimine was obtained as the reaction product. After the recrystallisation of the crude reaction mixture from ethyl acetate, **290** was obtained in 25 % yield. The ^{1}H-NMR spectrum

showed, as in the previous trianglimine **289**, that **290** displays high symmetry (C_3-symmetry) in solution.

The spectroscopic data showed only one set of signals for each of the three repeating units: a singlet at 8.35 ppm for the imine protons, another singlet at 7.42 corresponding to the aromatic protons, and at 3.50 ppm an additional singlet for the six methoxy groups. The IR spectrum also displayed the characteristic band at 1635 cm^{-1} for the C=N bond.

In order to gain insight into the dimensions of the trianglimine, approximate values using molecular modelling at the MM2 level (CS Chem3D Pro®, Cambridge) were obtained (Figure 161).

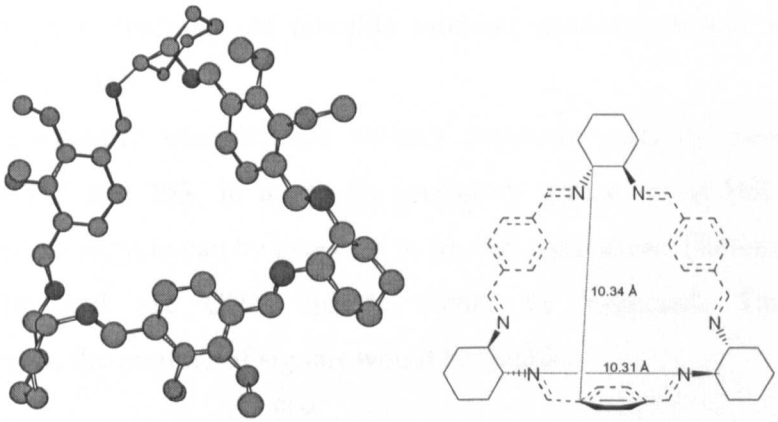

Figure 161: conformational structure of **290**, and approximated dimensions.

The reaction of 1,3,5-trimethoxy-2,4-diformylbenzene **275** with **38** was carried out for 3 hours at room temperature in dichloromethane (Figure 162). The crude reaction product was recrystallised from ethyl acetate to give trianglimine **291** in moderate yield (26 %).

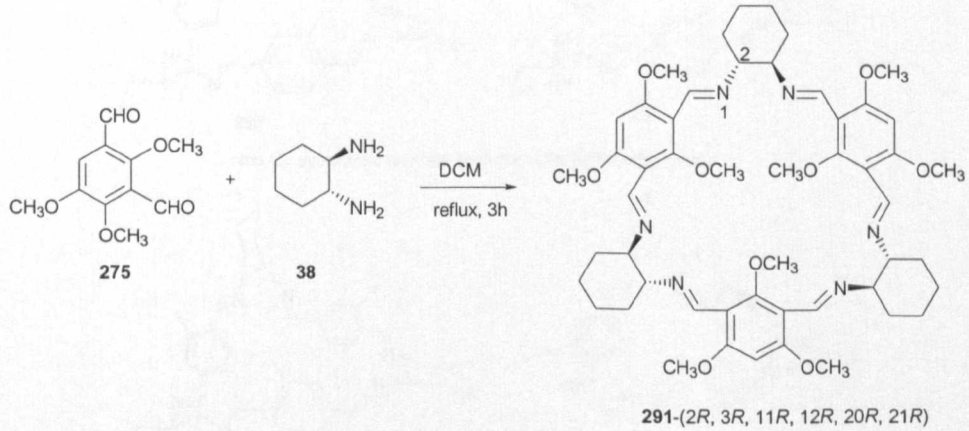

Figure 162: synthesis of trianglimine **291**.

The same symmetry pattern as in the previous trianglimines was observed, which is the appearance of only one set of signals in ^{1}H-NMR spectrum for each of the three repeating units. In this case, the signals of the imine protons were found at 8.71 ppm, the aromatic proton at 8.39 ppm and the methoxy protons at 3.24 ppm. The LSIMS spectrum showed also a major peak corresponding to the molecular ion at *m/z* 907.2.

The use of the non-symmetric dialdehyde **271** gave, as cyclocondensation product, a molecule with a complex ^{1}H-NMR spectrum. Although the CI mass spectrum only showed one peak corresponding to the molecular ion at *m/z* 679 [M+H] it was evident that more than one isomer was formed in the reaction.

The reaction between the non-symmetric dialdehyde **271** and **38** gave therefore, a series of isomeric structures as possible reaction products whose structures are proposed in Figure 163.

Firstly, non-symmetric trianglimines without symmetry can be expected that is trianglimines **292** and **293**. In a non-C_3 symmetry isomer as in **292** and **293**, all protons in the macrocycle can be expected to be non-equivalent. Therefore, six imine, nine aromatic and six CHN signals would be expected. Thus, for two diastereoisomers, the number of signals would be double.

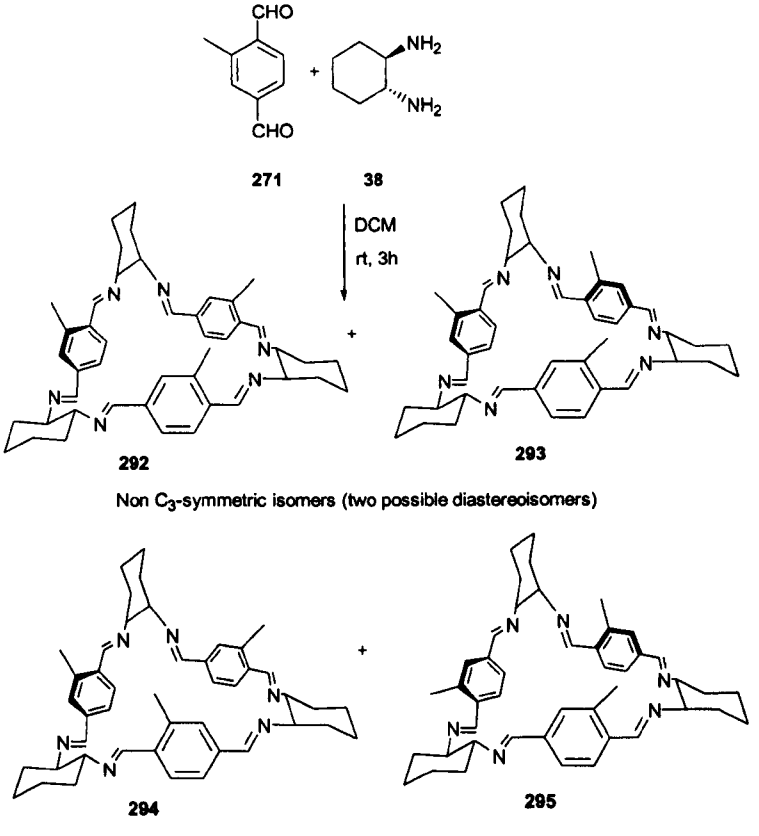

Figure 163: possible reaction products for the cyclocondensation between **271** and **38**.

In the case of C_3 symmetric trianglimines as in **294** and **295** (two diastereoisomers are possible), two non-equivalent imine protons and two sets of signals for all other protons would be expected for each of the two possible diastereoisomers.

The ^{1}H-NMR spectra in two different solvents are shown in Figure 164. The ^{1}H-^{1}H-NOESY spectrum in C_6D_6 showed the same cross peaks between signals as compared to that measured in $CDCl_3$. The ^{1}H-^{1}H-NOESY spectrum in $CDCl_3$ showed a very strong NOE effect between the triplet at 8.45 ppm and the doublet of doublets at 8.14 ppm, with the broad CyH-N peak at 3.36 ppm. From this data, it was deduced that these two groups of peaks belong to the C<u>H</u>N imine peaks.

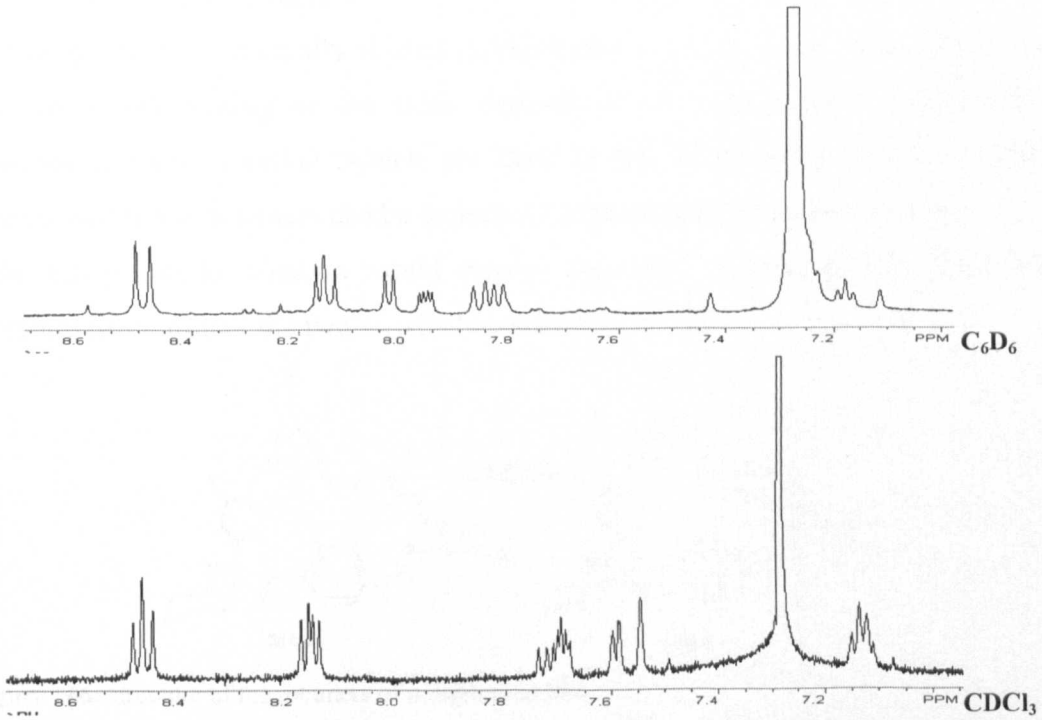

Figure 164: expanded ^{1}H-NMR spectrum observed in C_6D_6 and $CDCl_3$ (500 MHz).

The ^{1}H-^{1}H-COSY spectrum in $CDCl_3$ showed the coupling between the multiplets at 7.66 and 7.11 ppm, corresponding to the aromatic groups; therefore, the two other peaks at 7.55 and 7.51 ppm belong to the aromatic moiety in *ortho* to the aromatic methyl group (Figure 165).

The overall number of signals for the HC=N proton is a total of eight signals, which suggest two possible explanations.

Firstly, if the reaction products are supposed to be two non-C_3 symmetric macrocycles showing six imine signals and one C_3 symmetric macrocycle (showing 2 imine signals), they would be formed with exceptionally high diastereoselectivity (75:25:0:0, according to the integration of the ^{1}H-NMR).

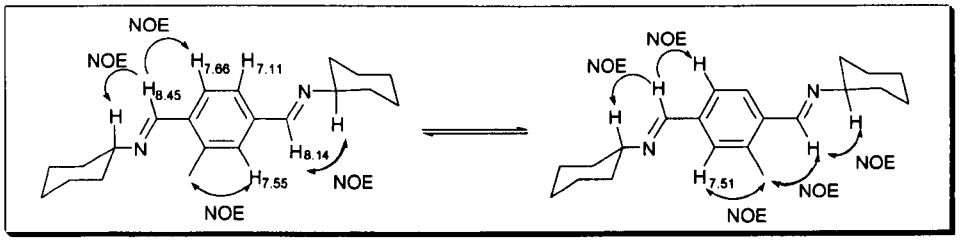

Figure 165: NOE effect observed.

Alternatively, it has to be taken into account, that there can be possible different rotamers in a C_3 symmetric diastereoisomer, and these can have strong implications in the elucidation of the structure.

In analogy to the structually related calix[4]arenes, which show interconversion of conformers (depending on the steric demand of the narrow rim substituents) by 'through annulus' rotation, which are slow in the NMR time scale.[23] A similar interconversion of rotamers can be expected for the trianglimine macrocycles.

This through anulus rotation would involve concerted rotation of one of the three aromatic rings around the two C_{Ar}-C=N bonds (Figure 166).

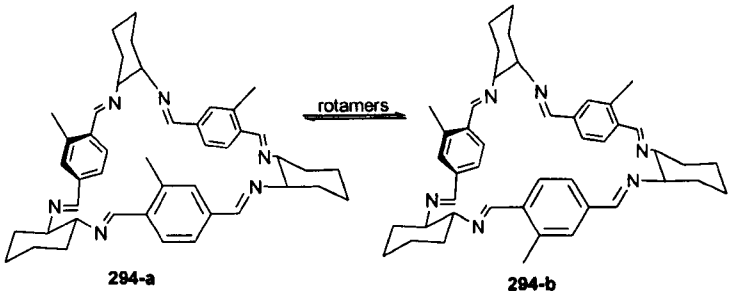

Figure 166: structure of the rotamers of trianglimine **294.**

The rotation of the aromatic ring without involving the C_{Ar}-C=N bonds is not possible due to steric hinderance as is shown in the figure below (Figure 167).

As a result, assuming that this process is slow in the NMR time scale, both rotamers of a single C_3-symmetric diastereoisomer would give rise to the observed eight signals, six for the non-symmetric rotamer and two for the symmetric rotamer.

However, in order to confirm either of these two theories, more experiments were necessary.

In order to distinguish conformation changes in the spectrum two experiments at high temperature (up to 338 K) were carried out (Figure 168). The first one was carried out in d^6-DMSO but it did not show significant spectral changes and therefore gave no valuable information.

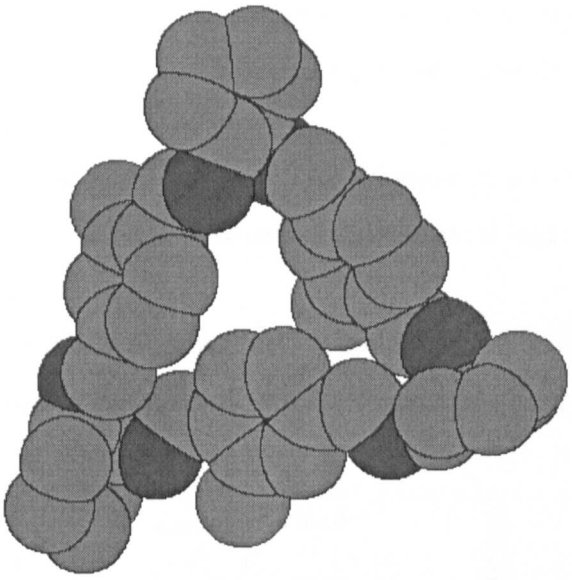

Figure 167: structure of trianglimine **294-a**, showing the limited cavity size to allow ring rotation without the rotation across the imine bond.

The high temperature ^{1}H-NMR spectrum carried out in d^6-C_6D_6 (Figure 168), showed interesting changes. The two imine singlets (8.63 and 8.55 ppm) became a broad band, the 7.90(t) became a singlet and the aromatics were transformed into two doublets and one triplet (see Figure 169).

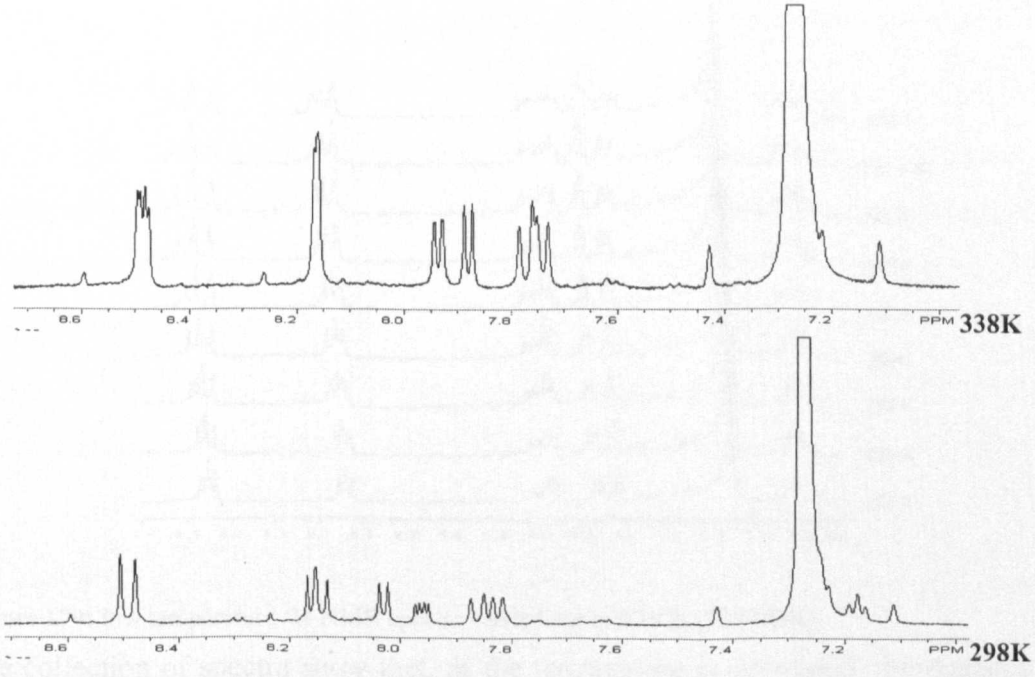

Figure 168: ^{1}H-NMR spectrum in d^6-C_6D_6 (500 MHz).

These spectral changes point towards coalescence of the signal and towards the conformational interchange of the two rotamers, rather than co-existence of two distinct diastereoisomers.

Based on the NOE experiments with strong NOE effects between the aromatic methyl group and the imine protons, the diastereoisomer formed with high stereoselectivity is assigned to be compound **294-a**.

The rationale behind this diastereoselectivity is based on the repulsion between the sterically demanding methyl group and the nitrogen lone pair disfavouring the formation of **294-b**.

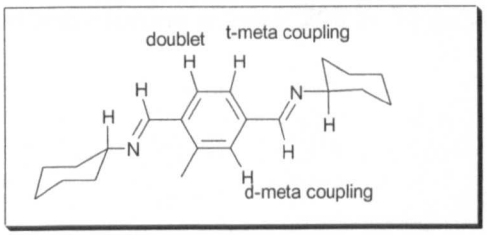

Figure 169: aromatic couplings produced in the high temperature 1H-NMR experiment.

To further elucidate the final structure, a last experiment was performed at low temperature (up to 223 K) ^{1}H-NMR experiment in $CDCl_3$ (Figure 170).

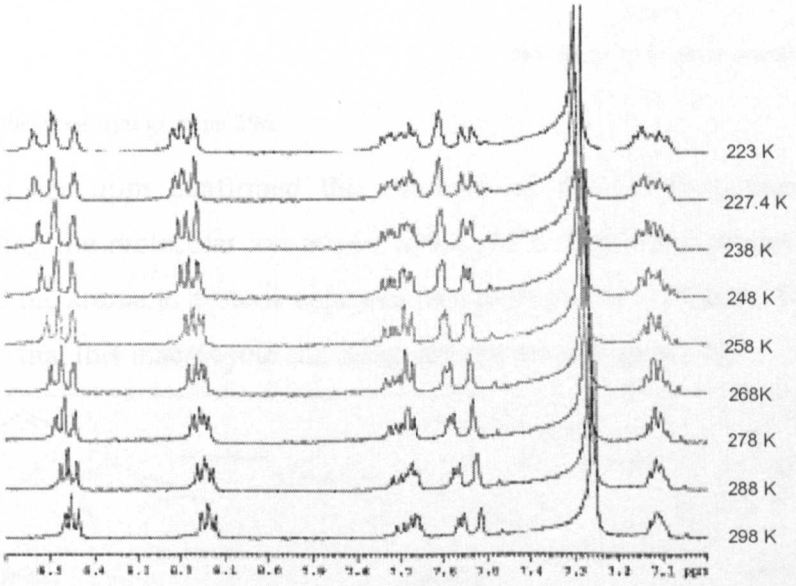

Figure 170: low temperature ^{1}H-NMR spectra carried out in $CDCl_3$ (500 MHz).

The collection of spectra show that, as the temperature is decreased, the distance (in ppm) between the imine peaks becomes larger. There is also variation in the aromatic region as there is an inversion in the chemical shift of the doublet at 7.55 ppm and singlet at 7.51 ppm (in the room temperature spectrum) when the temperature reaches

223 K. These changes in the spectra seem to show again that conformation interchange is the origin of the observed spectroscopic behaviour, rather than co-existence of two different diastereoisomers. The final support for either of the two theories would have to come from single crystal X-ray analysis.

It is worth noting that similar spectroscopic behaviour has been observed for a series of non-symmetrical hydroquinone derived trianglimine macrocycles.[130]

In order to study the scope and limitation of the macrocyclisation reaction, a new series of trianglimines were synthesised from heterocyclic dialdehydes.

In this way, the [3+3]-cyclocondensation of diformyl pyridine **163** with (1*R*, 2*R*)-diaminocyclohexane gave trianglimine number **296** in 70 % yield (Figure 171).

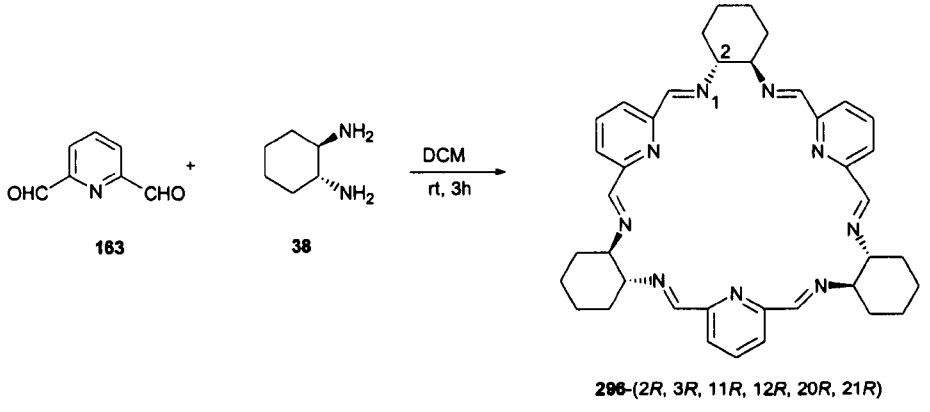

Figure 171: synthesis of trianglimine **296**.

The CI Mass spectrum confirmed the structure of the [3+3]-cyclocondensation product showing the molecular ion at *m/z* 639.4 (M^+). The imine proton appears at 8.22 ppm, and the aromatic protons appeared as a multiplet at 7.79 ppm. The possible conformations that this macrocycle can adopt are shown in Figure 172.

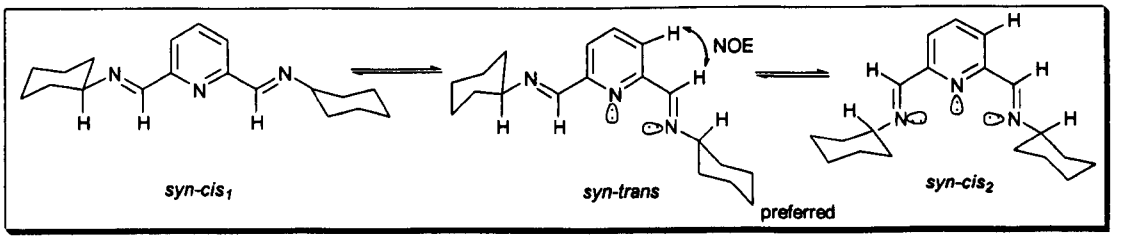

Figure 172: possible conformation of trianglimine **296.**

In order to confirm which rotamer is present in solution, ^{1}H-^{1}H-NOESY experiments were carried out. The ^{1}H-^{1}H-NOESY spectrum showed the correlation between the imine peak and a doublet corresponding to one of the aromatic protons. This result

immediately eliminates rotamer *syn-cis*$_1$. The presence of two spatially close nitrogen atoms (in the case of the *syn-trans* conformation) and three (in the case of the *syn-cis*$_2$ conformation), appears to cause a destabilisation due to the expected repulsive interactions of the nitrogen lone pairs. However, this distortion seems to overcome the ring strain in *syn-cis*$_1$ orientation.

Nevertheless, there is no spectroscopic evidence that allow to distinguish between the *syn-cis*$_2$ or *syn-trans* conformers because both of them can result in the same through space NOE interaction. As a consequence, there is not any final indication of whether the structure is one rotamer, the other or the equilibrium of both, which can interchange fast in the NMR time scale.

Continuing with the synthesis of the heterocyclic trianglimines, trianglimine **298** (Figure 173) was obtained from 2,5-diformylthiophene **297** and **38** in dichloromethane in 35 % yield.

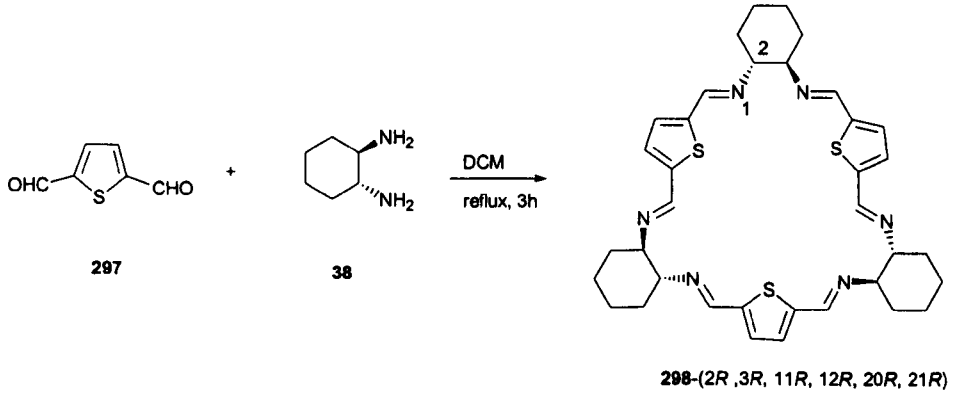

Figure 173: synthesis of trianglimine **298**.

Although this trianglimine showed very low solubility ([α] could not be determined), it was possible to obtain the ^{1}H-NMR spectrum without difficulties. The imine protons were observed as a singlet at 8.06 ppm, and the aromatic proton as another singlet at 9.92 ppm. The CI mass spectrum showed, exclusively, the expected peak of the molecular ion at *m/z* 655.2 [M+H].

The last example of heterocyclic trianglimine **299** synthesised from furanedialdehyde **139** is shown in Figure 174.

In this case, the reaction was carried out at room temperature for four hours. The reaction product obtained was a brown oil, whose CI mass spectrum showed the molecular ion at *m/z* 607 [M^+] corresponding to the expected [3+3]-cyclocondensation product.

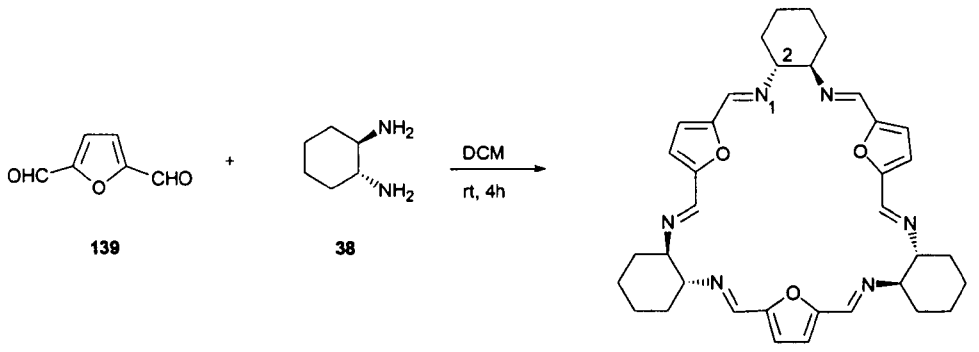

Figure 174: synthesis of trianglimine **299**.

The ^{1}H-^{1}H-NOESY experiments of **298** and **299** revealed the preferred conformation, shown in Figure 175, where there is a NOE effect between the imine protons and the diaminocyclohexane protons. In contrast with **296**, there is no through space interaction between these protons and the aromatic protons of the thiophene and furan ring. A plausible explanation for this effect is that, in the conformation represented on the right (*syn-cis*$_2$), there is a strong repulsion between the lone pair of electrons of the nitrogen and the oxygen (or sulphur), producing a destabilisation of the structure.

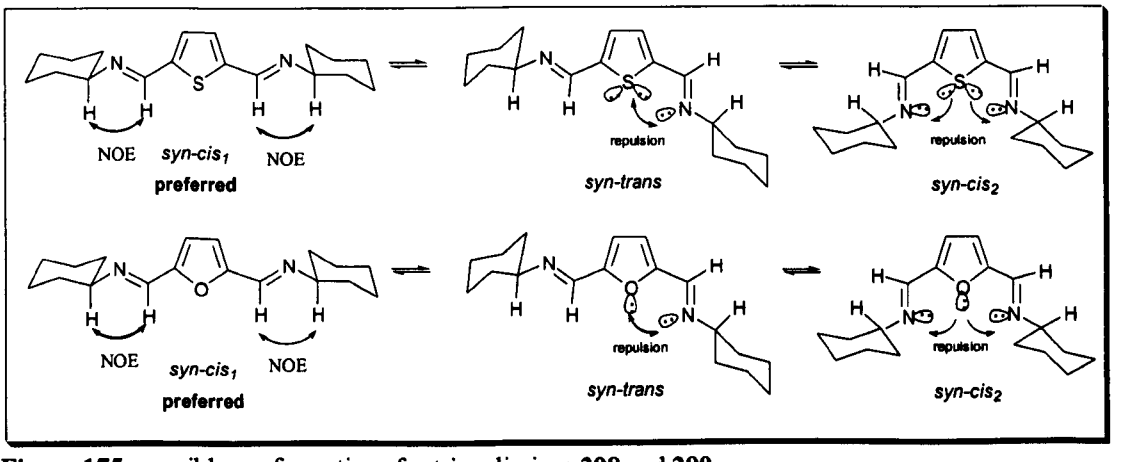

Figure 175: possible conformations for trianglimines **298** and **299**.

To study the scope and limitations of the macrocyclisation reaction in depth, it was decided to use a series of dialdehydes of larger size.

The use of 9,10-diformylanthracene **235** was chosen to increase the height of the aromatic wall of the trianglimine.

Trianglimine **300** was obtained after a 3 hour room temperature reaction between 9,10-diformylanthracene **235** and **38** in dichloromethane. After recrystallisation from ethyl acetate, **300** was obtained as an orange solid in 30 % yield (Figure 176).

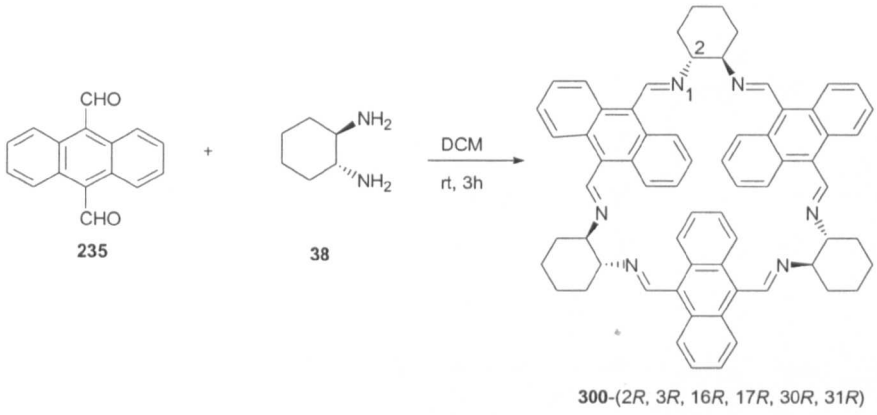

Figure 176: synthesis of trianglimine **300**.

The IR spectrum showed the typical band corresponding to the C=N bond at 1632 cm^{-1}. The ^{1}H-NMR spectrum demonstrated the symmetry of the structure, showing the characteristic imine peak at 9.45 ppm. In the aromatic region the two distinctive sets of signals corresponding to the AA'XX' spin system at 8.14 and 6.56 ppm, were observed.

Similarly to trianglimine **290**, MM2 (CS Chem3D Pro®, Cambridge) studies were performed for this molecule, showing the interesting structure in Figure 177.

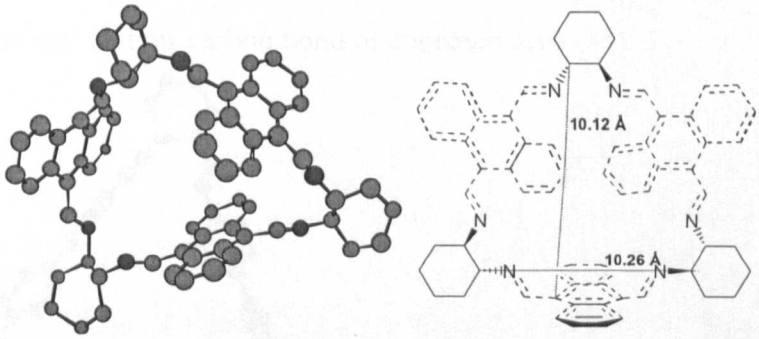

Figure 177: MM2 (CS Chem3D Pro®, Cambridge) structure of trianglimine **300**.

The dialdehydes shown in Figure 178 possess a greater distance between the two formyl groups, compared with the previous dialdehydes presented, and they were used for the formation of trianglimines with increased cavity sizes.

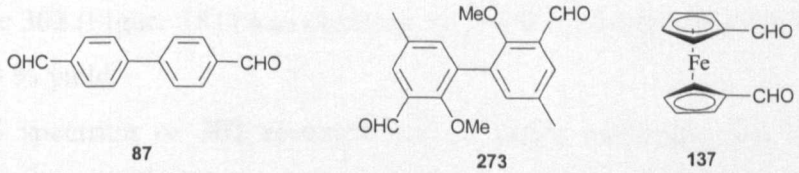

Figure 178: dialdehydes used for the synthesis of trianglimines with large cavities.

Trianglimine **301** (32 %) (Figure 179) was obtained from a 0.1 M solution of 4,4'-diformylphenyl **87** and **38** in a 3 hour reaction at room temperature.

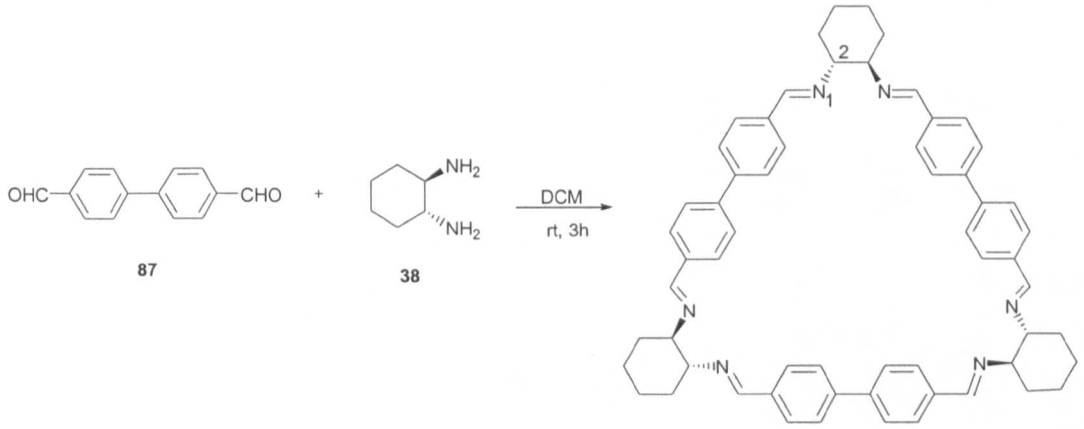

301-(2*R*, 3*R*, 16*R*, 17*R*, 30*R*, 31*R*)

Figure 179: synthesis of trianglimine **301**.

The ^{1}H-NMR spectrum showed the imine peak at 8.14 ppm as a singlet, and the aromatic protons appeared as a pair of doublets at 7.52 and 7.39 ppm. The LSIMS showed exclusively the [3+3]-cyclocondensation product at *m/z* 866.3 [M+H]. The structure in Figure 180, obtained by minimisation at the MM2 level (CS Chem3D Pro®, Cambridge), shows the estimated dimensional structure of trianglimine **301**. The model shows the non-coplanarity of the two aryl groups, and a torsion angle between the sp^2-sp^2 carbon-carbon bond of approximately 35°.

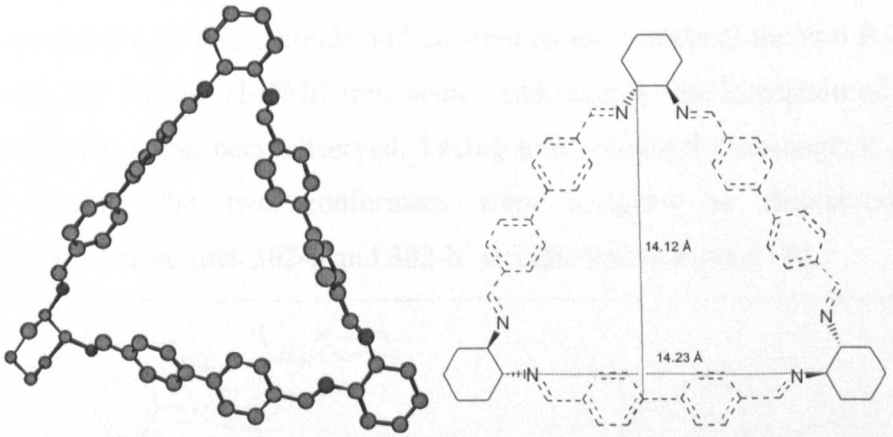

Figure 180: MM2 (CS Chem3D Pro®, Cambridge) structure of trianglimine **301**.

Trianglimine **302** (Figure 181) was obtained by [3+3]-cyclocondensation between **273** and **38** in 34 % yield.

The LSIMS spectrum of **302** revealed only a single molecular ion at *m/z* 1130. However, the ^{1}H and ^{13}C-NMR spectra in $CDCl_3$ showed two distinct sets of signals in a ratio of 2:1.

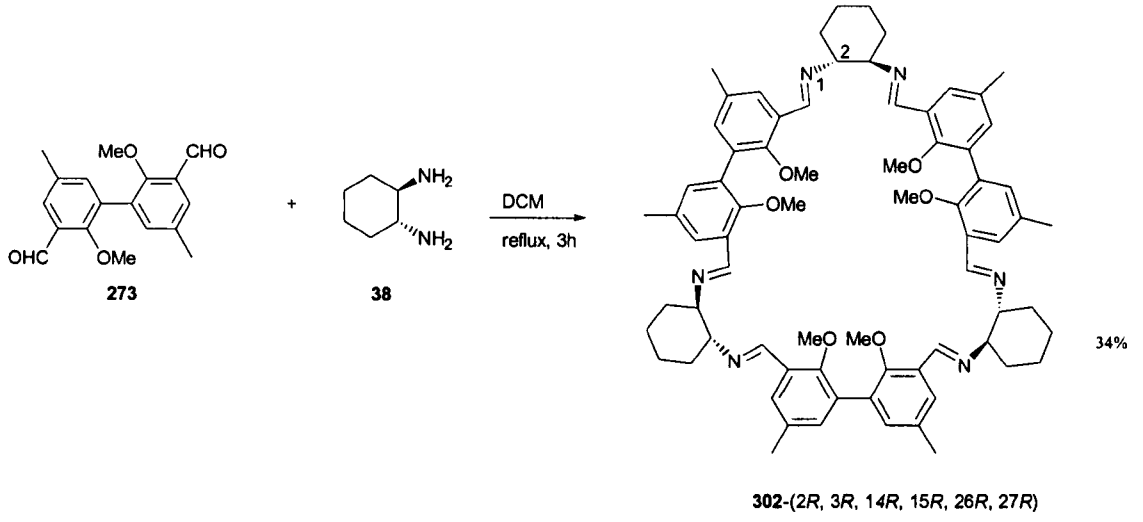

Figure 181: synthesis of trianglimine **302**.

Each set represented a full set of signal indicating a biphenyl moiety and a 1,2-cyclohexane-diimine moiety. In order to observe possible changes in the ^{1}H-NMR spectrum, a high temperature ^{1}H-NMR experiment was carried out, however, the lines did not broaden even at 100 °C in d^6-DMSO. Consequently, trianglimine **302** must adopt two distinct highly symmetrical conformations in solution, which interconvert slowly on the ^{1}H-NMR-time scale. This slow interconversion of the two conformers was confirmed using 2D-EXSY spectroscopy. Previous investigation showed that rotation around the N=C-C_{Ar} bonds and *anti-syn* isomerisation of the two R-N=C-C_{Ar} moieties are fast on the ^{1}H-NMR time scale. Additionally, the formation of (*Z*)-C=N bond isomers has never been observed. Taking into account the stereogenic nature of the biaryl axis, the two conformers were assigned as diastereomeric or *atropisomeric*[131] structures **302-a** and **302-b**, as indicated in Figure 182.

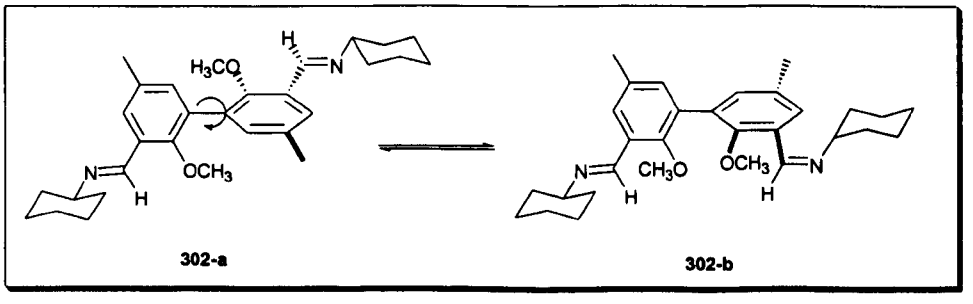

Figure 182: structure of the two possible conformers of trianglimine **302**.

One diastereomer is characterised by an *all-(R)* biaryl axis (**302-a**) (three axes with *R* configuration), whereas the second diastereomer **302-b** is characterised by an *all-(S)* biaryl axis. From molecular models at the MM-2 level it seems, however, impossible

to assign the major and minor diastereomeric conformers unambiguously by ^{1}H-^{1}H-NOESY, or any other spectroscopic method.

Trianglimine **303** was obtained in 13 % yield after 45-h reaction at room temperature between 1,1'-diformylferrocene **137** and **38** in dichloromethane (Figure 183).

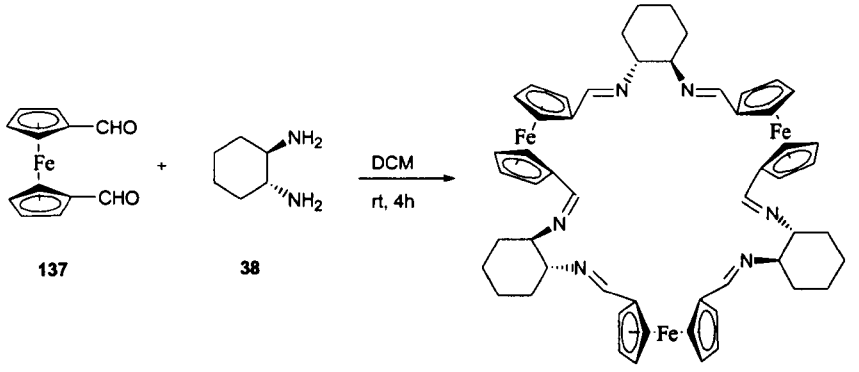

Figure 183: synthesis of trianglimine **303**.

Despite the apparent complexity of this structure, the trianglimine showed high symmetry in solution. The ^{1}H-NMR spectrum (Figure 184) shows one signal for the six imine protons at 8.17 ppm and four signals for each of the non-equivalent aromatic ferrocene protons at 4.45, 4.36, 4.04 and 3.85 ppm. This non-equivalence can be rationalised in term of slow rotation around the C-C=N-C bonds. The ^{1}H-^{1}H-NOESY spectroscopy allows unambiguous assignment of all ferrocene protons.

Figure 185 shows the ^{1}H-^{1}H-NOESY spectrum of the ferrocene trianglimine and the through space correlations observed experimentally. As in the previous trianglimines, a NOE effect between the imine proton (8.17 ppm) and the proton of the amine-cyclopentadienyl moiety (3.41 ppm) is observed. Simultaneously, these two protons correlate with the proton (H_1, 4.45 ppm), as expected. The ^{1}H-^{1}H-NOESY spectrum also shows correlation between the previously mentioned protons and other hydrogen of the cyclopentadienyl ring at 4.36 ppm, which would not theoretically correlate.

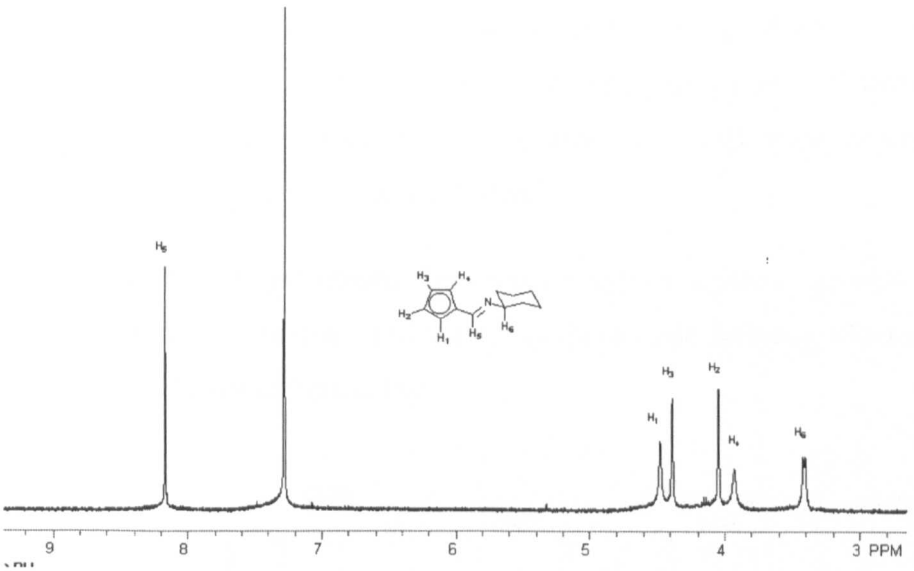

Figure 184: expansion of the ^{1}H-NMR spectrum of trianglimine **303** ($CDCl_3$, 500 MHz).

However, ^{1}H-^{1}H-NOESY spectroscopy can determine through space correlation up to 5 Å, and the distance between the two cyclopentadienyl rings is about 3.29 Å.

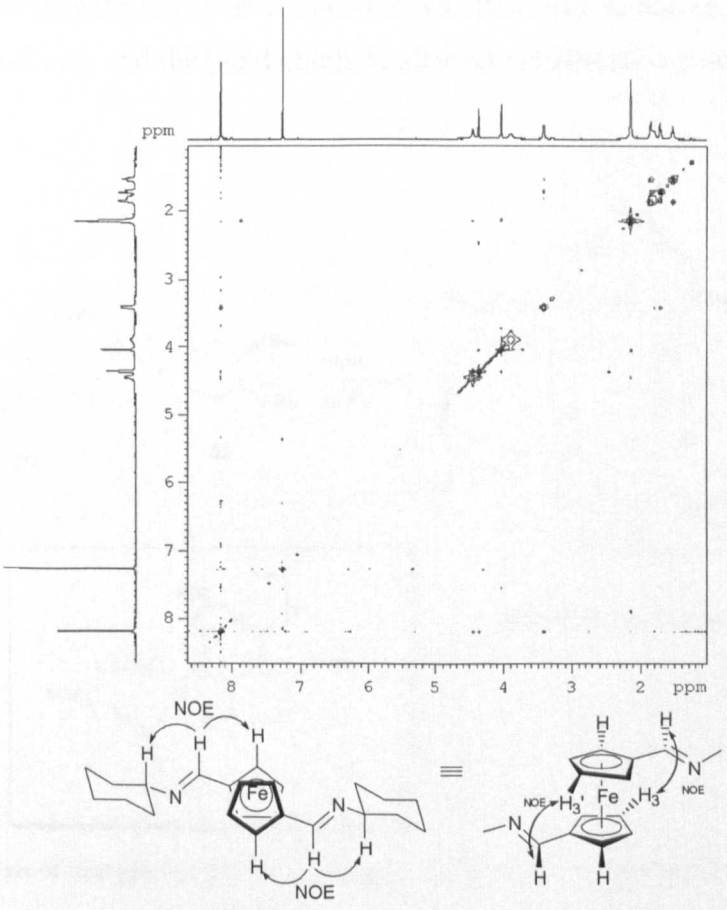

Figure 185: ^{1}H-^{1}H-NOESY spectrum of trianglimine **303** and scheme of the through space correlation between protons.

Hence, it can be expected that the NOE effect seen in the ^{1}H-^{1}H-NOESY spectrum is due to the interaction with a proton on the counterpart cyclopentadienyl ring. Furthermore, [3+3]-cyclocondensation was confirmed by FAB mass spectrometry showing the expected molecular ion at *m/z* 961M$^+$.

Trianglimines also can be synthesised from more complex aromatic groups. This is the case in the use of naphthalene derivatives as dialdehyde building blocks. These aromatic groups are shown in Figure 186.

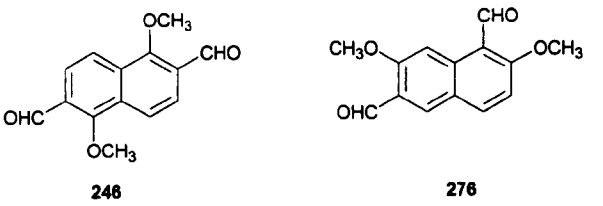

Figure 186: structure of the naphthalene dialdehydes used in trianglimine synthesis.

Trianglimine **304** (Figure 187) was obtained in a similar way as before, from **276** and **38** in dichloromethane, and the yield obtained after recrystallisation from ethyl acetate was 18 %.

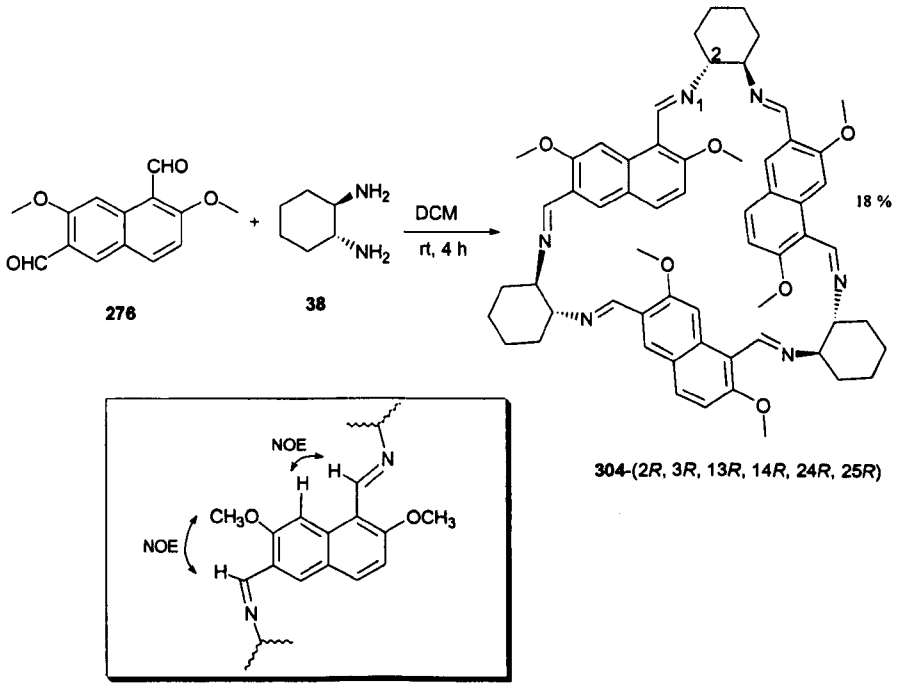

Figure 187: synthesis of trianglimine **304** and correlation shown in the ^{1}H-^{1}H-NOESY spectrum.

The spectroscopic data showed two peaks for the non-equivalent imine protons at 9.01 and 8.84 ppm. The methoxy group also presented two sets of signals at 3.93 and 3.86

ppm. The through space correlation between the different protons observed from the ^{1}H-^{1}H-NOESY experiment, is also shown in Figure 187.

The cyclocondensation between **38** and dialdehyde **246** gave the trianglimine **305** in 14 % yield (Figure 188). Contrasting the ^{1}H-NMR spectrum for the previous trianglimine **304**, the ^{1}H-NMR spectrum of **305** exhibits only one peak for the imine proton at 8.64 ppm and another single peak for the methoxy at 3.71 ppm. The ^{1}H-^{1}H-NOESY experiments showed the through space interaction between both methoxy protons with the imine peak.

This trianglimine can be compared with trianglimine **289** due to the similar orientation of the methoxy groups in relation to the proton of the imine. Therefore, it can be supposed that trianglimine **305** posses the same D_{3h} symmetry.

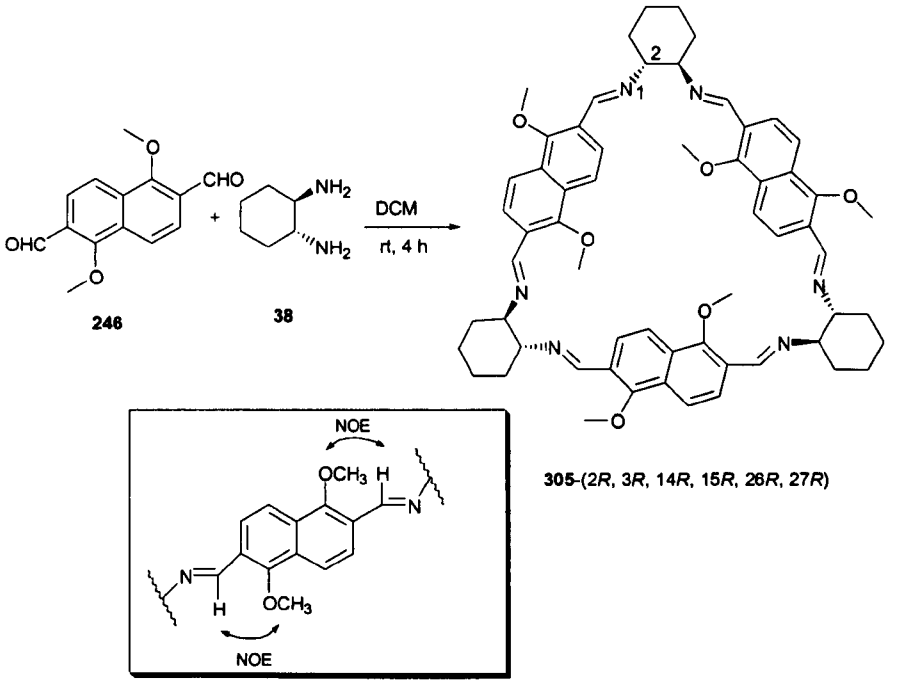

Figure 188: synthesis of trianglimine **305**.

17. Synthesis of [2+2]-cyclocondensation products.

All macrocycles obtained and described so far, were formed exclusively *via* [3+3]-cyclocondensation. This was not always the case as, on several occasions mixtures of [3+3] and [2+2]-cyclocondensation products were obtained, and in some cases, the final product was exclusively the [2+2]-cyclocondensation product.

The first example, in which mixtures of the two possible macrocyclisation products were obtained, is shown in Figure 189. In this case the separation was not possible.

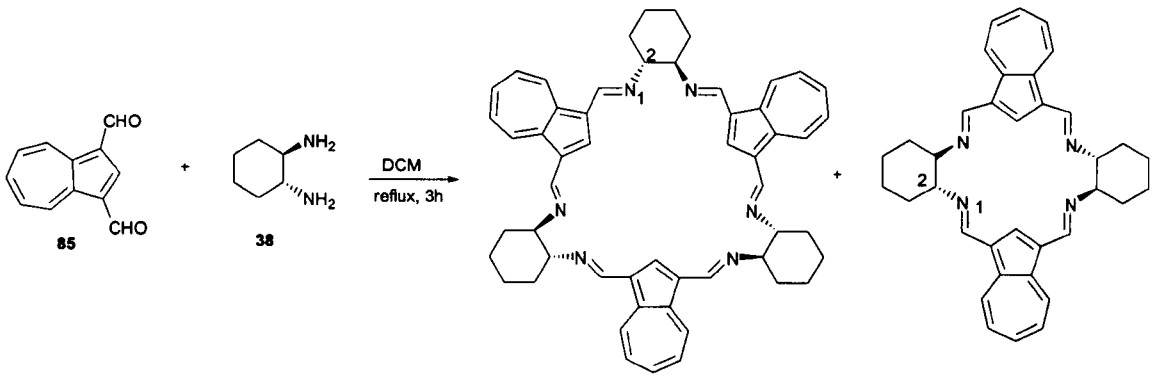

Figure 189: synthesis of the crude trianglimine **306** and dimer **307.**

The reaction between 1,3-diformylazulene **85** and (1*R*, 2*R*)-diaminocyclohexane **38** gave as shown in Figure 189, the mixture of the trianglimine **306** and the macrocyclic dimer **307** in a ratio 4:1. The LSIMS spectrum revealed the presence of both products showing the molecular ions at *m/z* 788.0 (M+H) and 526.4 (M^+).

Although the separation was unsuccessful, the assignment of every proton could be achieved by ^{1}H-^{1}H-COSY–NMR experiments.

The reaction between bis-4-formylphenyl-ether **237** and **38** was attempted several times using the standard conditions as in the previous cases. All these attempts failed to give the desired product. However, the reaction gave the [2+2]-cyclocondensation product **308** in 42 %, after a 24 hours reaction at room temperature in dichloromethane. The FAB spectrum showed the molecular ion of the reaction product **308** at *m/z* 609 (M+H) exclusively.

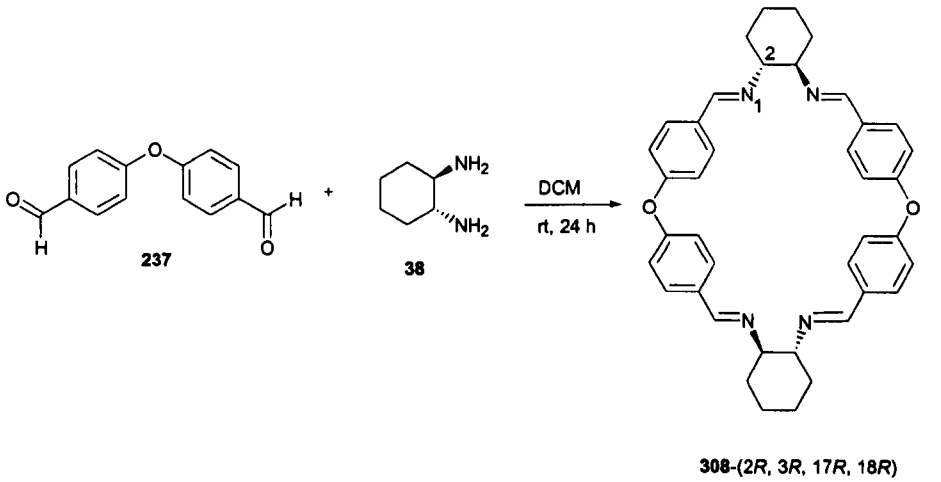

Figure 190: synthesis of trianglimine **308.**

The last example of synthesis of a dimer is shown in Figure 191, where the cyclocondensation between **38** and the carbazole dialdehyde **79** gave the [2+2]-cyclocondensation product **309** exclusively.

Through careful monitoring of the reaction by ^{1}H-NMR spectroscopy, it was revealed the appearance of a highly symmetric intermediate, which was believed to be the [3+3]-cyclocondensation product. However, the isolation of this intermediate failed.

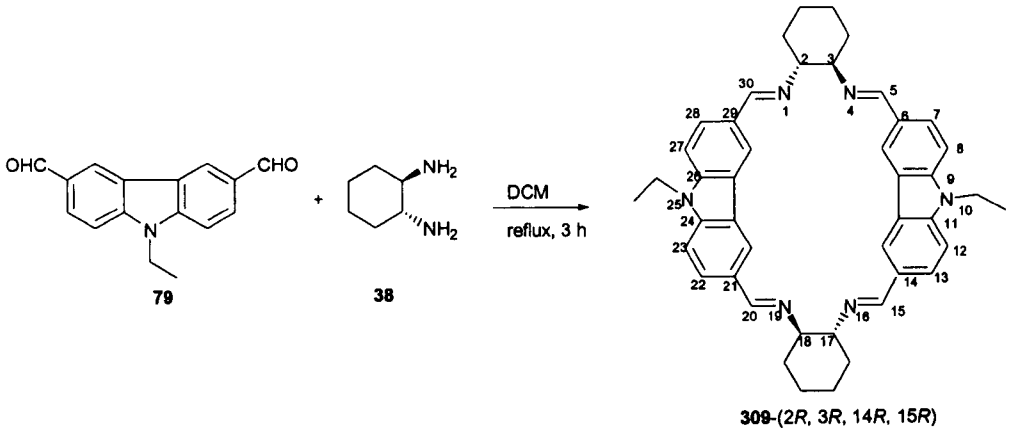

Figure 191: synthesis of dimer **309**.

The [2+2]-cyclocondensation product **309** appears to be thermodynamically favored over the [3+3]-cyclocondensation product under the reaction conditions.

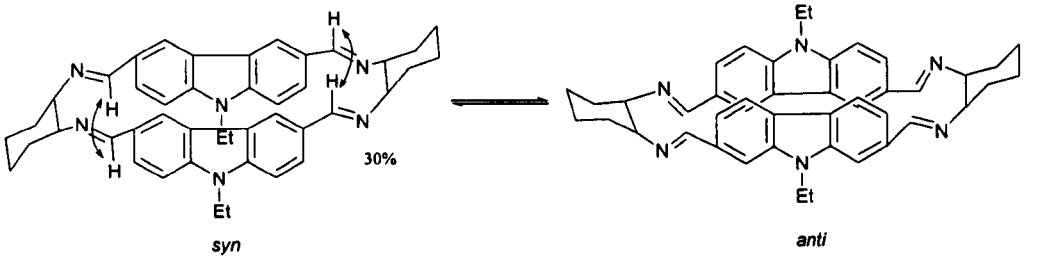

Figure 192: conformation adopted by macrocycle **309**.

Unlike most of the imine macrocycles, this compound displayed temperature dependent ^{1}H-NMR spectrum. In the room temperature spectrum, two sets of signals for the non-equivalent carbazole units are clearly visible. Similarly, the two signals corresponding to the non-equivalent NCH protons coalesce into one signal. Upon increase of temperature, the two sets of signals coalesce into one set of signals. (Figure 193).

The change in the spectra was attributed to a ring inversion induced by a concerted rotation around two (N=C)-Ar bonds. This isomerisation is equivalent to change from a *syn* isomer to an *anti* isomer (illustrated in Figure 192).

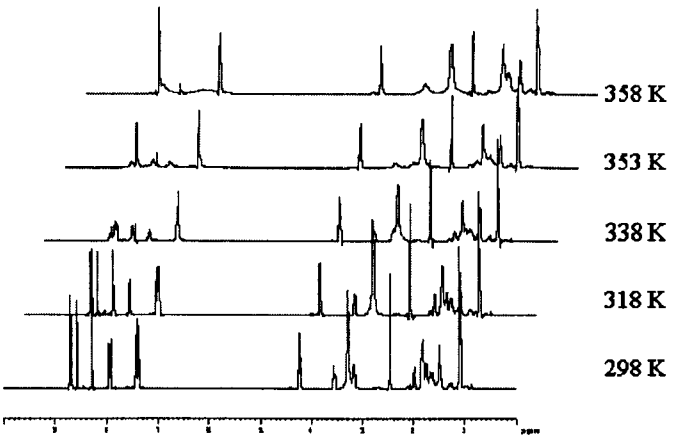

Figure 193: ^{1}H-NMR temperature dependence spectra of carbazole dimer **309** (d^{6}-DMSO, 500 MHz).

^{1}H-^{1}H-NOESY spectrum of the isomer preferred at room temperature displayed NOE effects between the non-equivalent pairs if imine protons (H-5 to H-30 and H-15 to H-20) as well as from H-7' to the H-5 HC=N of the imine. Molecular models at the MM-2 levels for both *syn* and *anti* isomers clearly indicate that the observed NOE interactions can only occur in the *syn* isomer. The energetically preferred isomer at room temperature was assigned to be the *syn* with the N-Et moieties are in a *syn* arrangement.

Table 6 shows the spectroscopic data and yields of the macrocycles synthesised.

Dialdehyde	^{1}H-NMR CHN	^{13}C-NMR CHN	Products	*m/z*	Yield %
158	8.40	155.6	289	817.0	90
56	8.35	159.3	290	817.2	25
275	8.71	155.3	291	907.2	26
271	8.45; 7.14	161.0; 160.9	294	679.0	46
163	8.22	161.2	296	639.4	70
297	8.06	153.4	298	655.2	35
139	8.22	152.8	299	607.0	14
235	9.4	160.8	300	938.3	80
87	8.14	160.9	301	866.3	32
273	8.58; 8.45	158.7	302	1130.5	50
137	8.12	160.0	303	961.0	13
276	9.01; 8.84	158.3; 158.2	304	967.0	18
246	8.64	157.3	305	967.0	14
85	8.49	--	306-307	788.5	15
237	8.33	160.0	308	609.0	42
79	8.73; 8.48	162.9; 161.5	309	658.4	30

Table 6: spectroscopic data and yields of the macrocycles synthesised.

Chapter VII

MECHANISM OF TRIANGLIMINE FORMATION

18. Effect of the stoichiometry in macrocycle synthesis.

The synthesis of trianglimines presented in the previous chapter was carried out *via* a [3+3]-cyclocondensation reaction between **38** and a given aromatic dialdehyde.

As three repeating units of each building block form the trianglimine, in order to obtain an effective macrocyclisation, the stoichiometry used was always equimolar with respect to the two reagents.

In order to investigate whether or not the variation in the stoichiometry can modify the results of the cyclocondensation reaction, such as the formation of oligomers, and the increase or reduction of the yield, several stoichiometric experiments were carried out. Hence, the [3+3]-cyclocondensation reaction was carried out altering the stoichiometric proportions of the starting material.

Thus, different stoichiometries of **158** and **38** (Figure 194) were used. When an excess of **38** (3 equivalents) was used, all of **158** was consumed in the formation of the trianglimine **289** and the excess of diaminocyclohexane remained unreacted with no formation of oligomers observed. Thus, the isolation of the pure trianglimine **289** was achieved by washing the reaction product with distilled water to remove the excess of amine. On the other hand, when an excess of dialdehyde **158** (3 equivalents) was used, the reaction also gave **289** as the only reaction product. There were no other reactions with the dialdehyde forming by-products. In this case, the isolation of the trianglimine was achieved by washing the reaction products with dichloromethane.

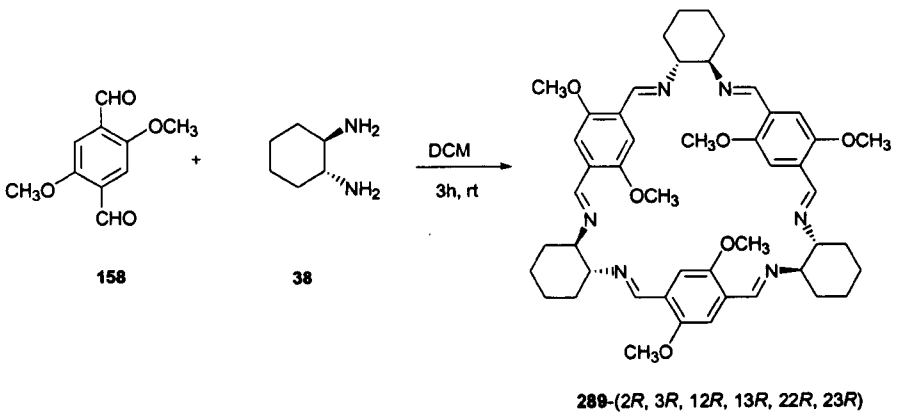

Figure 194: synthesis of **289** using different stoichiometries of **158** and **38**.

In this solvent, the trianglimine has low solubility, whereas the dialdehyde is very soluble. The separation was straightforward because the trianglimine is a white powder, whereas the dialdehyde **158** has a bright yellow colour. In this way, once the yellow colour has disappeared from the solid, it can be considered as fully pure.

In this particular cyclocondensation reaction, the stoichiometry does not play an important role in the synthesis of the trianglimine **289**, as it is always formed regardless of the stoichiometry of the building blocks.

19. Synthesis of trianglimines from mixtures of aldehydes.

The experiment reported in the previous section (**18**) showed that, in the synthesis of trianglimine **289**, the modification of the stoichiometry did not interfere with the progress of the reaction. In order to continue the investigation into the scope and limitations of the building blocks stoichiometry in trianglimine synthesis, a series of experiments were performed using mixtures of dialdehydes in different molar ratios. The following experiments were designed in order to experimentally determine whether [3+3]-macrocyclisation of mixtures of dialdehydes produce an equilibrium mixture of macrocycles or, alternatively, show selectivity in the formation of one trianglimine over another.

In order to follow this approach, three experiments were carried out.

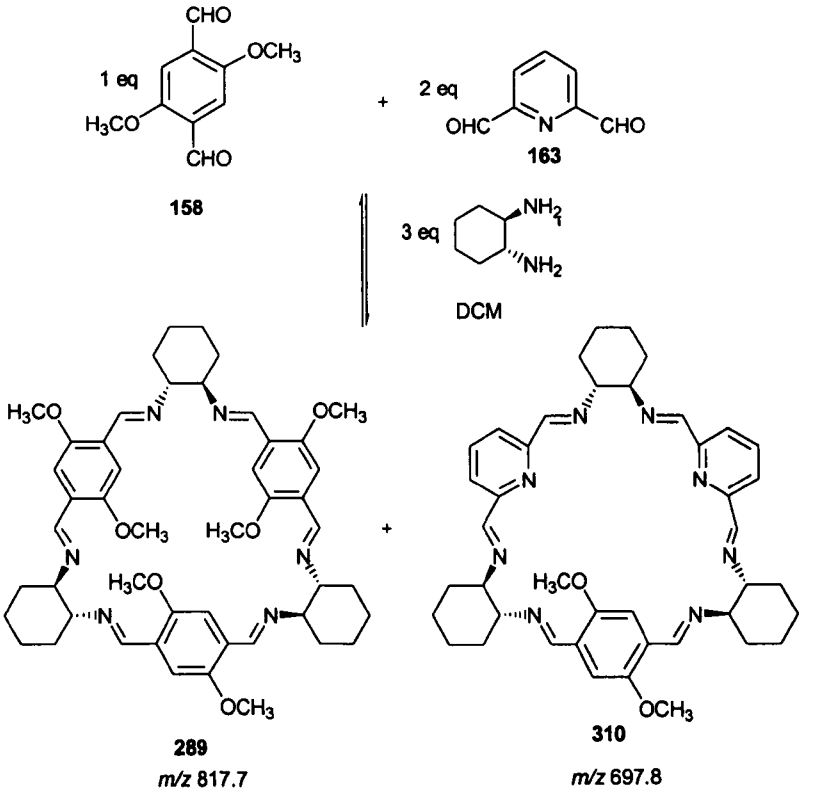

Figure 195: cyclocondensation **163** (2 equivalents) and **158** (1 equivalent) with **38** (3 equivalents).

Firstly the cyclocondensation of 2,6-diformylpyridine **163** (2 equivalents) and 1,4-dimethoxy-2,5-diformylbenzene **158** (1 equivalent) with **38** (3 equivalents) in a 0.1 M concentration was carried out over three hours (Figure 195). The reaction did not give

the trianglimine **310** exclusively, as would be expected taking into account the stoichiometry of the reagents, it produced a mixture of compounds instead. The reaction products obtained were then analysed by the standard procedures. Firstly, they were analysed by ^{1}H-NMR spectroscopy. The aldehyde, aromatic, and imine region showed a large number of peaks, making the unambiguous assignment of signals very difficult. The ^{13}C-NMR spectrum did not provide any further insight, showing again a large number of peaks. However, the ESI spectrum, showed the presence of two products. There was a peak, with 100 % intensity, corresponding to the molecular ion at *m/z* 817.7 (M+H), which can be assigned as the molecular ion of trianglimine **289**. The second product was assigned as the target trianglimine **310**, that is, the cyclocondensation between one equivalent of **158** and two equivalents of **163** at *m/z* 697.8 (M+H) (7 %). Unfortunately the attempt to isolate both compounds failed.

Although the reaction gave two products, the formation of **289** appeared to be more favourable than the formation of any other product.

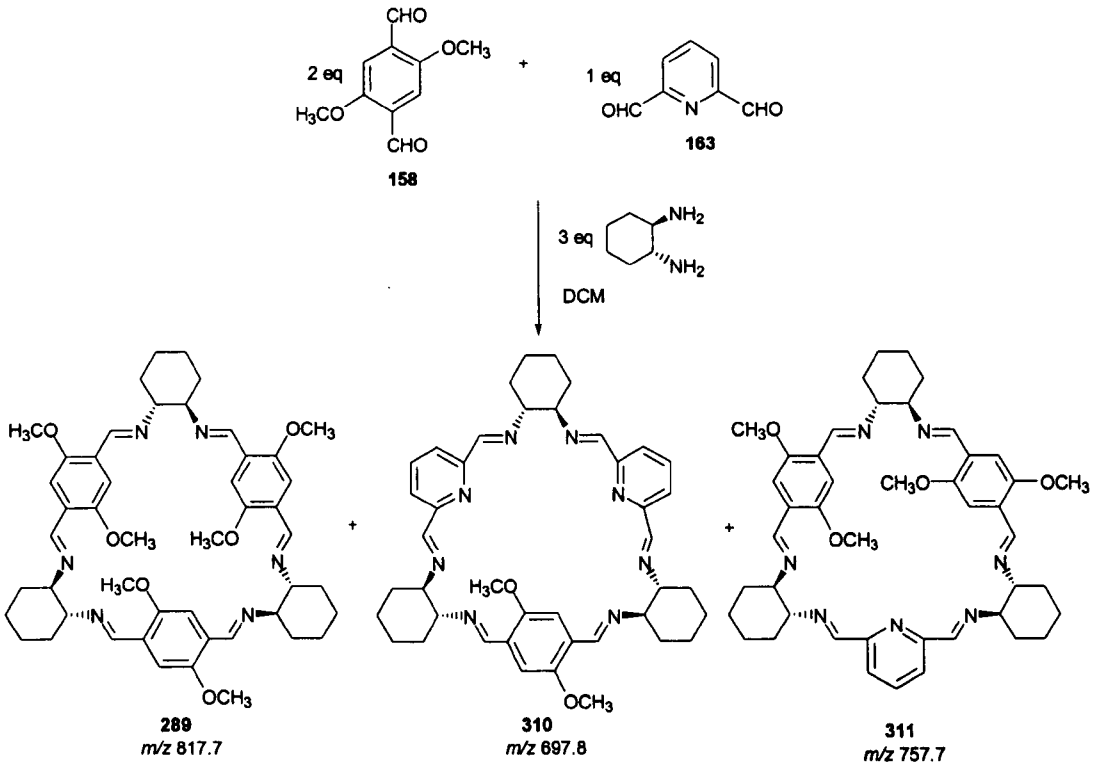

Figure 196: cyclocondensation **163** (1 equivalents) and **158** (2 equivalent) with **38** (3 equivalents).

A second reaction was carried out, but in this case, the molar ratio of the dialdehyde building blocks was inverted. Thus, the cyclocondensation of 2,6-diformylpyridine **163** (1 equivalent) and 1,4-dimethoxy-2,5-diformylbenzene **158** (2 equivalents) with

38 at 0.1 M in dichloromethane over three hours, formed a mixture of **289**, **310** and **311** (Figure 196).

As in the previous case, there were signals of the free dialdehydes in the ^{1}H-NMR spectrum, and both the aromatic and the CH=N- region showed a large number of peaks that could not be assigned. Nevertheless, the ESI mass spectrum revealed the formation of several trianglimines (Figure 197). As in the reaction carried out above (Figure 195), the major product produced was trianglimine **289** with a molecular ion at *m/z* 817.5 (100 %). The next peak corresponded to macrocycle **311** at *m/z* 757.7 (20 %) M^+. With a very small difference in intensity (19 %), a peak at *m/z* 697.8 (M^+) revealed the presence of the trianglimine formed by one equivalent of **158** and 2 equivalents of 2,6-diformylpyridine **163**. This is macrocycle **310**.

The isolation of the trianglimines obtained also failed.

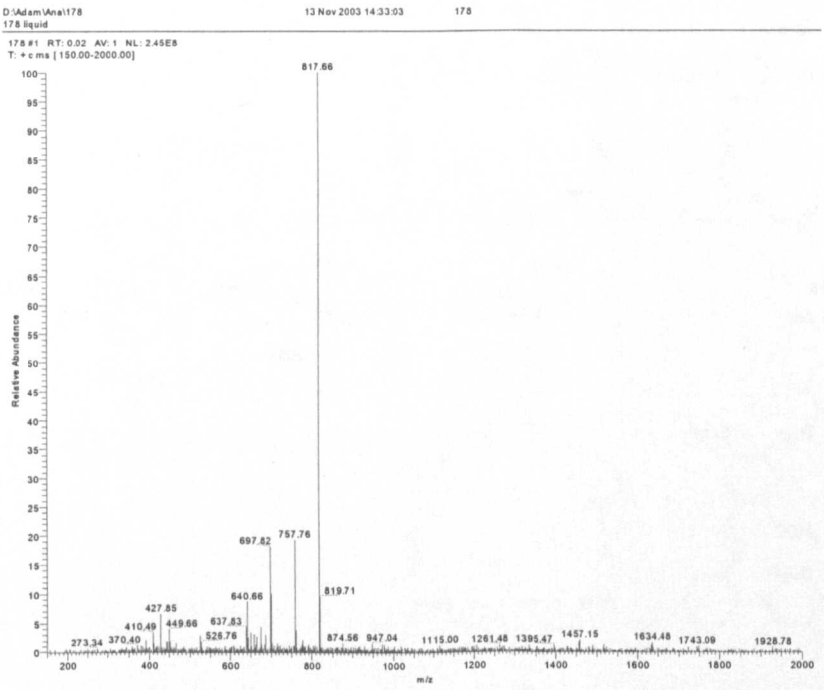

Figure 197: ESI spectrum for the mixture of compounds obtained from the reaction between **163** (1 equivalent) and **158** (2 equivalents).

Another attempt to obtain a trianglimine formed by different dialdehydes was carried out for the [3+3]-cyclocondensation of **39** (2 equivalents) and **158** (1 equivalent) with **38** in dichloromethane (0.1 M) (Figure 198).

The reaction product showed, as in the preceding cases, a very complex ^{1}H-NMR spectrum whose signals could not be assigned. It is worth noting that the number of imine and methoxy signals considerably increased.

Once again, ESI mass spectrum (Figure 199) showed the reaction products obtained. In this case, the major product obtained was the target macrocycle **312**, showing a peak for the molecular ion at *m/z* 697.8 (M+H, 100 %). A second major product, a peak at *m/z* 757.6 M^+ (53 %) which agrees with the trianglimine formed by two equivalents of **158** and one equivalent of **39** (**313**) was also observed. The third major product was found to be the trianglimine **40**, formed by three equivalents of terephthalaldehyde at *m/z* 637.9 (M+H, 20 %). Finally, the molecular ion of trianglimine **289** was observed at *m/z* 817.6 (M+H, 15 %). The observed mass spectrum corresponds closely to that of a statistical 1:3:3:1 mixture of all possible macrocycles.

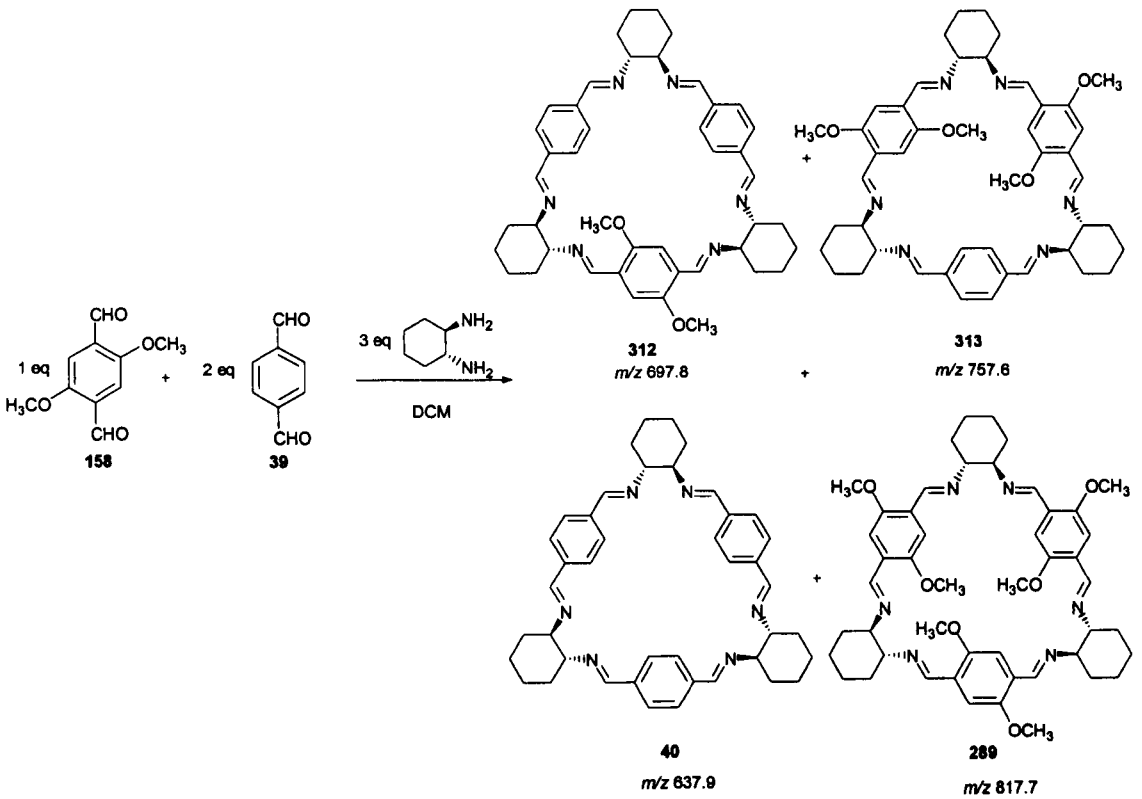

Figure 198: reaction scheme for the synthesis of trianglimine **312, 313, 40, 289**.

In contrast to the earlier synthesis, the mixed trianglimine **312** could be isolated through recrystallisation, and the ^{1}H-NMR spectrum illustrates the C_2 symmetry of the trianglimine **312**.

Three singlets were found for the imine peak at 8.50, 8.17 and 8.15 ppm. The aromatic protons belonging to the terephthalaldehyde moiety showed a multiplet at

7.56 ppm. A singlet at 7.11 ppm matched the aromatic proton of the dimethoxyarene moiety. The methoxy protons appeared as a singlet at 3.58 ppm.

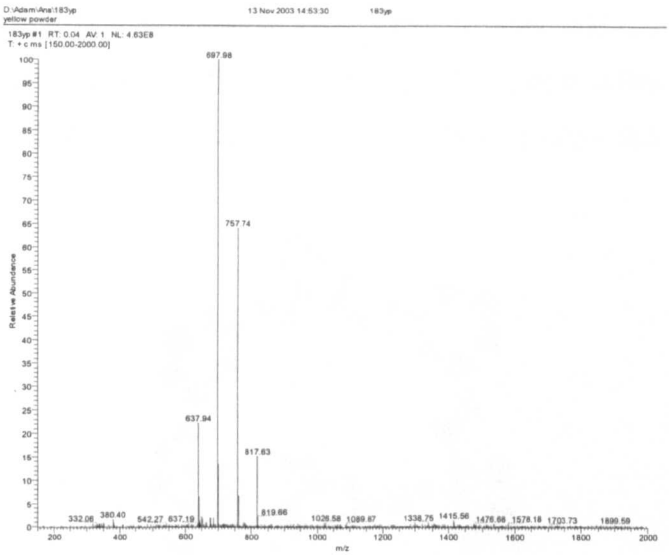

Figure 199: ESI mass spectrum for the mixture of compounds obtained from the reaction between **158** (1 equivalent) and **39** (2 equivalents).

All the experiments carried out above showed that the resulting products of the cyclocondensation were in, all cases, trianglimines and, in no case was the presence of a [2+2]-cyclocondensation product observed.

20. Formation of trianglimines: Thermodynamic versus Kinetic control.

Initial studies carried out by Gawronski,[42] pointed out that the macrocyclisation precursors (3 amine and 3 aldehyde units) adopt a minimum energy conformation in which cyclisation predominates over linear extension, thus giving a rational explanation for the formation of the trianglimines in kinetic terms.

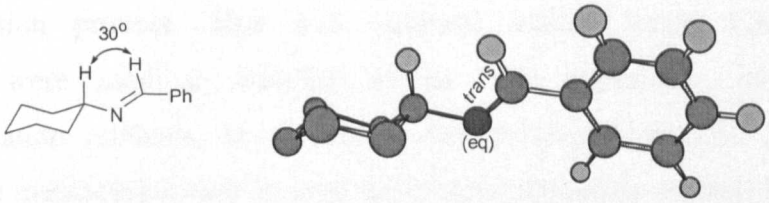

Figure 200: structure and MM2 model of cyclohexylimine 90.

In order to confirm this finding, molecular modelling (Figure 200) at the MM2 level (CS Chem3D Pro®, Cambridge) was performed to understand more about the geometry of the starting materials and intermediates.

Minimisation of the energy of a simple cyclohexylimine revealed that the imine moiety is placed into the equatorial position and the C-N=C-C_{Ar} moiety adopts a *trans*

geometry. Due to repulsive 1,3 interactions between the axial cyclohexyl hydrogen and the N=CH hydrogen the H-C=N-C-H dihedral angle was found to be around 30°. An extension of this geometry along three units (Figure 201), 3 diamines and 3 aromatic dialdehydes, led to a minimum energy conformation in the macrocyclisation precursor, in which the -CHO and -NH_2 functional groups are in close spatial proximity (2 to 3 Å).

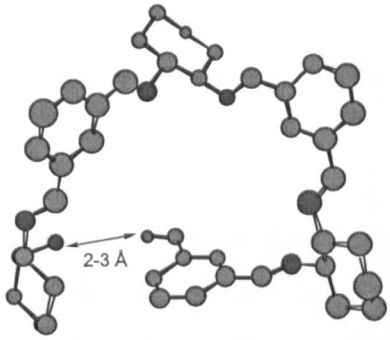

Figure 201: conformation of minimum energy at the MM2 level for the 3 diamine and 3 dialdehyde units.

Hence, macrocyclisation can occur efficiently and under kinetic control (the products are formed through the transition state of lowest energy). This can be rationalised by identifying the minimum energy conformation of the direct macrocyclisation precursor, in which one free amine and one free aldehyde functionality are very close in space.

In the previous chapter, trianglimines synthesised *via* [3+3]-cyclocondensation were reported. However, some of the experiments demonstrated that the [3+3]-cyclisation is not a general reaction. Indeed, in some cases, mixtures of [3+3] and [2+2]-cyclocondensation products were obtained, and in some other occasions, exclusively a [2+2]-cyclisation product. This was observed mainly when 1,3-disubstituted dialdehydes were used as building blocks. The appearance of the [2+2]-cyclocondensation products, in particular after prolonged reaction times, points towards these macrocycles were formed under thermodynamic control. In addition, it also has to be taken into account the reversible nature of the imine bond, which reinforces even more the likelihood of a thermodynamic equilibrium.

As a general rule, in a thermodynamically controlled process, the product distribution depends only on the relative stabilities of the final products. In the kinetically controlled case, however, it is the free activation energy differences between two or

more competing transition states leading to the products that determine their relative proportions.[132]

However, the covalent bonds can form, break, and reform again reversibly under equilibrium conditions. If the equilibrium process is sufficiently fast, the efficient formation of products under thermodynamic control can be observed. In these reactions, it is the stability of the resulting products, and not the energy of the transition states, which controls the reaction.

In order to study which process is involved in trianglimine synthesis, several experiments were carried out.

20.1 Product distribution over time in the synthesis of trianglimines.

The general procedure followed in the synthesis of trianglimines involved a 3 hour reaction between **38** and a given dialdehyde in equimolar proportions, at room temperature. However, several examples in which the trianglimine was not obtained were shown in the previous chapter, as in various cases, the [2+2]-cyclocondensation product was obtained after a prolonged reaction time.

An interesting example is the cyclocondensation product obtained from isophthalaldehyde **40** and (1*R*, 2*R*) diaminocyclohexane **38**, which after a 3 hour reaction at room temperature, led to the trianglimine **42**. However, when the sample was kept in solution in $CDCl_3$, the ^{1}H-NMR spectrum showed two sets of signals instead of the one observed in the original product. The mass spectrum revealed that these signals corresponded to the molecular ion of the [3+3]-cyclocondensation **42** at *m/z* 636.5 M^+, and a peak at *m/z* 424.0 M^+ corresponding to the [2+2]-cyclocondensation product **314** (Figure 202).

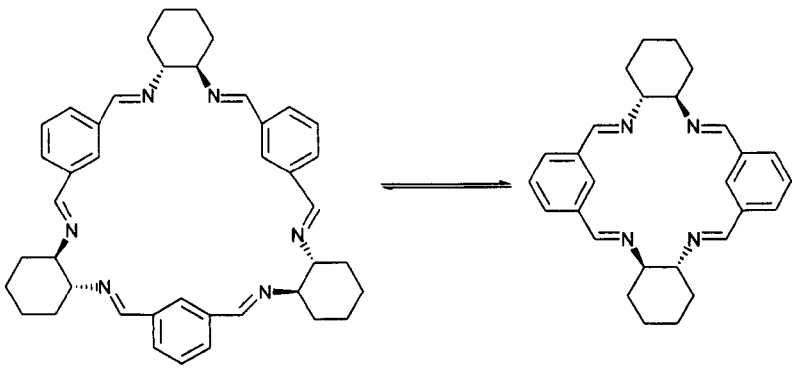

Figure 202: equilibrium formed between trianglimine **42** and dimer **314**.

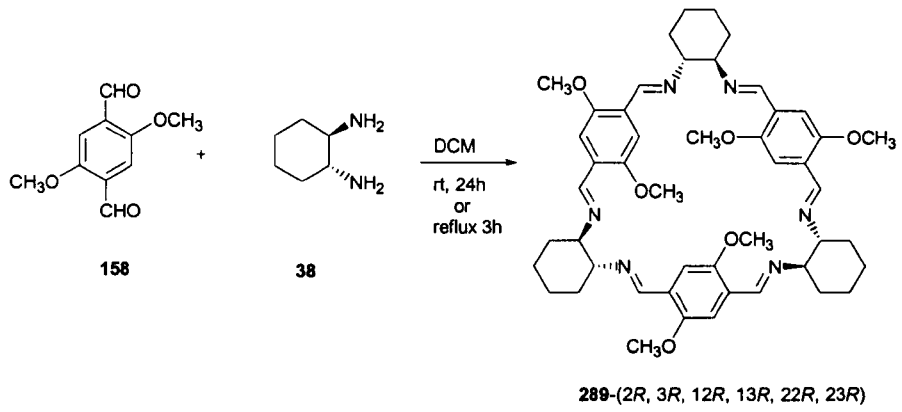

Figure 203: synthesis of **289** using different reaction times.

With the aim of testing whether other trianglimines undergo ring contraction to form the [2+2]-cyclocondensation product, trianglimine **289** was kept in solution in $CDCl_3$ for several days. After this time, the ^{1}H-NMR spectrum showed no changes and, furthermore, the mass spectra did not show any signal for the [2+2]-cyclocondensation product, since the molecular ion of the trimer at *m/z* 817 [M+H] was the only peak observed. In order to verify that trianglimine **289** was the only reaction product that can be obtained, the synthesis was carried out using longer reaction times (up to 24 hours) and under reflux for three hours (Figure 203). Once again, the only product obtained was **289**.

The two examples shown above present a different behaviour in solution that can be rationalised in terms of kinetic and thermodynamic processes. Thus, the reaction product of the cyclocondensation between **40** and **38** can be either **42** or **314** depending on the reaction conditions. As a first approximation, it appears that **42** is the product obtained under kinetic control and **314** is the product obtained under thermodynamic control. Trianglimine **289** appears, however, to be only the thermodynamic product.

Nevertheless, these experiments do not allow ultimate assumption of thermodynamic control, as a proof of reversibility of the reaction is required.

21. Study of the reversibility of the trianglimines synthesised.

21.1 Mixture of trianglimines with dialdehydes.

In order to demonstrate the reversibility of the trianglimine synthesis and therefore the thermodynamic control in the synthesis of trianglimines, a series of exchange experiments were carried out. Thus, the reversibility of the trianglimines was studied

by mixing three equivalents of each trianglimine with one equivalent of a given dialdehyde. The progress of the exchange of groups was monitored by ^{1}H-NMR spectroscopy and ESI mass spectrometry.

The first experiment carried out consisted of the mixture 3:1 of trianglimine **40** and dialdehyde **158** in 5 ml of $CDCl_3$ (13 mM) (Figure 204).

The first ^{1}H-NMR experiment (after three hours of carrying out the mixture) did not show any indication of exchange between aromatic moieties of the free dialdehyde and macrocycle.

However, the ^{1}H-NMR experiment recorded after one week showed clearly the exchange between the aromatic groups; between the aromatic moieties in the free dialdehyde and in the macrocycle, as well as the probable decomposition of the trianglimine. This is shown by the numerous signals, which appeared in the aldehyde, aromatic and methoxy regions, of the ^{1}H-NMR spectrum. The third ^{1}H-NMR spectrum recorded (15 days later) did not show any substantial changes from the second ^{1}H-NMR spectrum recorded.

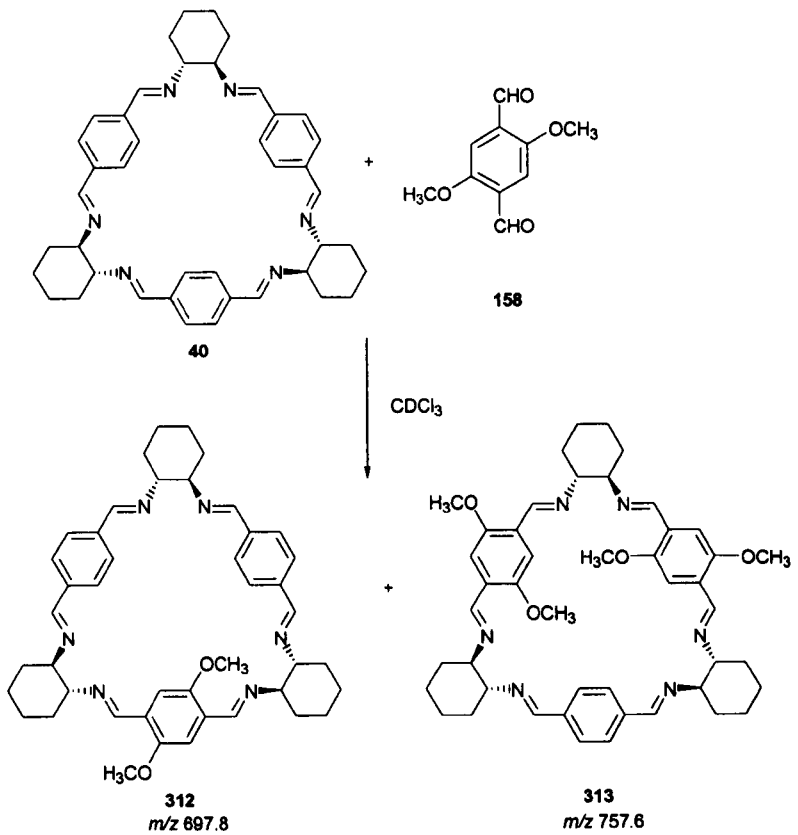

Figure 204: structures of the trianglimines obtained from the mixture of **40** and **158**.

The signals observed in the ^{1}H-NMR spectrum of this reaction coincide with the signals obtained from **313** and **312** from the previous experiment (page 119, Figure 198).

The ESI mass spectrum obtained after 15 days of the reaction mixture (Figure 205) showed the major peak corresponding to the trianglimine **40** at *m/z* 638.0. At very small intensity but still appreciable, there were the two peaks corresponding to the trianglimines **312** and **313**, at *m/z* 697.8 (18 %) and *m/z* 757.7 (15 %) respectively.

The next exchange experiment carried out used a mixture 3:1 of trianglimine **42** and dialdehyde **163** (Figure 206).

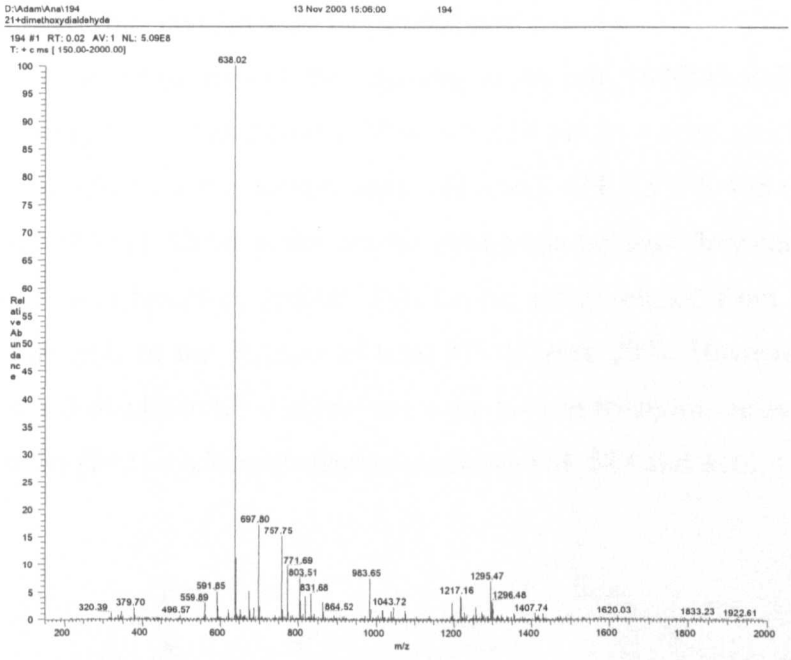

Figure 205: ESI spectrum obtained from the mixture of **40** and **158** after 15 days of the mixture.

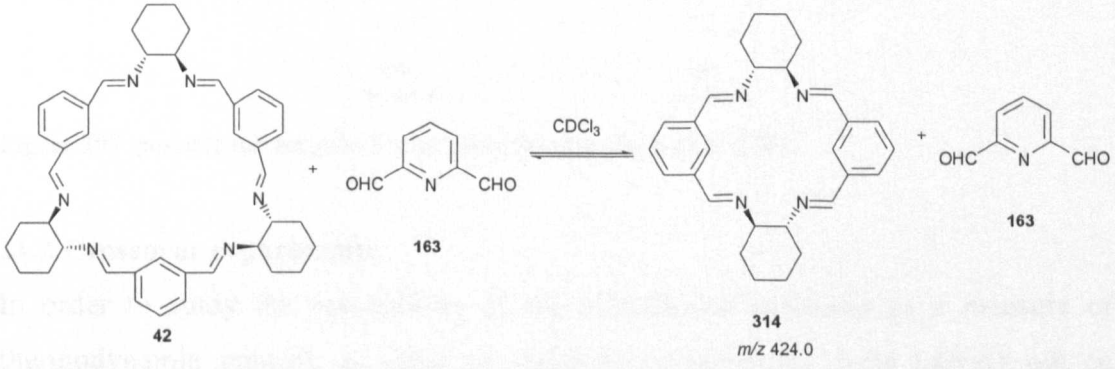

Figure 206: mixture experiment between **163** and **42**.

In this experiment, three equivalent of trianglimine **42** were mixed with one equivalent of dialdehyde **163** in 7 ml of $CDCl_3$ (11.11 mM).

The first ^{1}H-NMR experiment (three hours after mixing both compounds) did not show any exchange between aromatic moieties in the free dialdehyde **163** and macrocycle **42.** The next spectrum recorded (one week later), showed a pair of singlets of both the 2,6-diformylpyridine **163** and isophthalaldehyde **40**, at 10.10 and 9.99 ppm, respectively. The aromatic region showed a large number of peaks of different intensities, however, these intensities of the new peaks emerged were very small (less than 1 %). The third ^{1}H-NMR spectrum recorded (15 days later) did not show any changes when compared to the second one.

The CI mass spectrum (carried out the same day as the last ^{1}H-NMR did) showed the peak corresponding to the trianglimine **42** at *m/z* 638 but in a very low intensity (15 %). At higher intensity, various signals appeared at *m/z* 424 (15 %), 425 (100 %), 426 (50 %), and 427 (10 %). These peaks can be ambiguous because they can correspond to the [2+2]-cyclocondensation product **314**, to the dimer formed from two units of diformylpyridine **313**, or the mixture of both **316** (Figure 207). However, it is clear that, whenever 1,3-disubstituted dialdehydes were used in trianglimine synthesis, they transform into the [2+2]-cyclocondensation products **314, 313** and **316.**

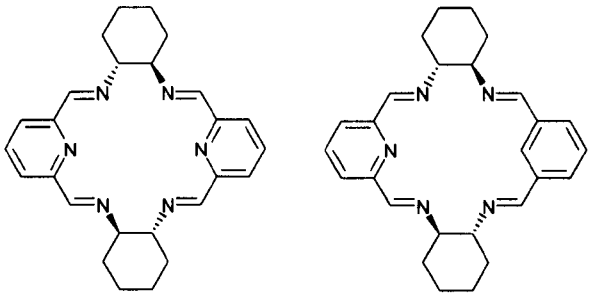

315
m/z 426.0

316
m/z 425.0

Figure 207: possible macrocycles formed from the mixture of **42** and **163.**

21.2 Crossover experiments.

In order to study the reversibility of the trianglimine synthesis as a measure of thermodynamic control, a series of crossover experiments were carried out to investigate if there is any exchange between the aromatic moieties due to a reversible imine interchange reaction. These experiments consisted of mixing different pairs of trianglimines in a 1:1 ratio and monitoring the progress of the reaction mixture by ^{1}H-NMR experiments.

The first experiment carried out combined trianglimines **289** and **296** in equal proportions (Figure 208). One equivalent of trianglimine **296** was mixed with one equivalent of trianglimine **289** in 2 ml of $CDCl_3$ (3 mM). The first spectra recorded (three hours after mixing both compounds) showed a negligible interchange of groups between the two macrocycles. After a week in solution, the signals corresponding to the aromatic region and the signals belonging to the imine group were multiplied, and up to 8 singlets of different intensities were detected in the spectrum between 8.35 and 8.55 ppm.

The aromatic region showed an increased number of signals; from a singlet (7.21 ppm in **289**) a triplet and doublet (7.78, 7.79 respectively in **296**) to a large group of signals and again, of different intensities. The most evident demonstration of interchange between macrocycles is shown in the region of the methoxy group. In the isolated spectra of **289** the OCH_3 signal appears as a singlet at 3.6 ppm. In the mixture sample, three singlets with different intensities appeared instead.

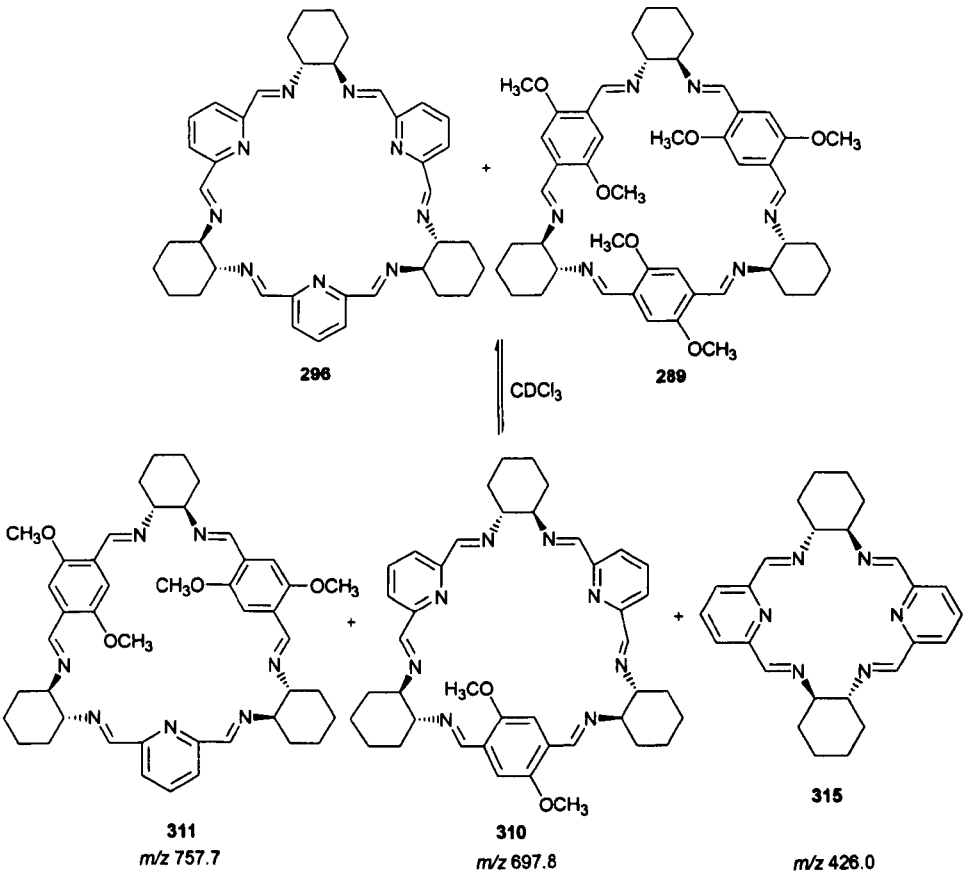

Figure 208: structures of trianglimines involved in experiment of mixture of **296** and **289**.

Further ^{1}H-NMR spectrum was carried out one month later and no changes were observed in the chemical shift or intensity of the signals. A CI mass spectrum was

obtained after one month of this crossover experiment and showed the exchange between the aromatic moieties of the two trianglimines. With an intensity of 100 % the peak at *m/z* 699.3 (M+H) showed the trianglimine formed from two units of **163** and one unit of **158**, which was assigned as trianglimine **310**. At *m/z* 758.0 (M+H) with an intensity of 90 % is the peak corresponding to the trianglimine **311** formed from two units of **158** and one **163** unit. With a very small intensity (10 %) the signal of the [2+2]-cyclocondensation product **313** was also present. As in the case of the ring contraction of **42** to give **314**, it appears that **296** also undergoes ring contraction to give the dimer **313** when the sample is kept in solution over a longer period of time. The result of this experiment indicates that trianglimines **289** and **296** open their rings and break down to smaller fragments in order to reorganise themselves to form the new set of trianglimines **311** and **310**.

The results of the mixing experiment of the two trianglimines (**296** and **289**), compared with the stoichiometry experiments (cyclocondensation between **158** and **163** in different proportions) showed great similarity, as the resulting products were the same trianglimines **311** and **310** (page 117, Figure 196).

A similar experiment was carried out by mixing trianglimines **42** and **289** (Figure 209).

In this experiment, one equivalent of trianglimine **42** was mixed with one equivalent of trianglimine **289** in 2 ml of $CDCl_3$ (2.3 mM)

The first spectra recorded after 3 hours showed very little change however, the signals increased in number in the aromatic and in the methoxy region. The second spectra recorded (one week later) showed clearly the decomposition of **42** to give **314**, and also many other signals that could not be assigned.

The last ^{1}H-NMR spectrum carried out (15 days later) showed a spectrum with no exchange between groups at all. This spectrum revealed that the signals of **289** and the signals of the [2+2]-cyclocondensation product **314** formed from **42** had the highest intensity. The CI mass spectrum (carried out the same day as the last ^{1}H-NMR spectrum) of the trianglimines involved in the mixing experiment of **42** and **289** showed, as the peak of highest intensity (100 %), the molecular ion of **314** at *m/z* 425.0 (M+H). Following in intensity (50 %) is the peak of the molecular ion of **318** at *m/z* 697.1, corresponding to the trianglimine formed by two units of **40** and one unit of **158**. Lastly and at almost equal intensity (47 %) as for **314**, there were the peaks

corresponding to the trianglimine formed from by two units of **158** and one unit of **40,** with a molecular ion at *m/z* 757.0 M^+ that was assigned as trianglimine **317**.

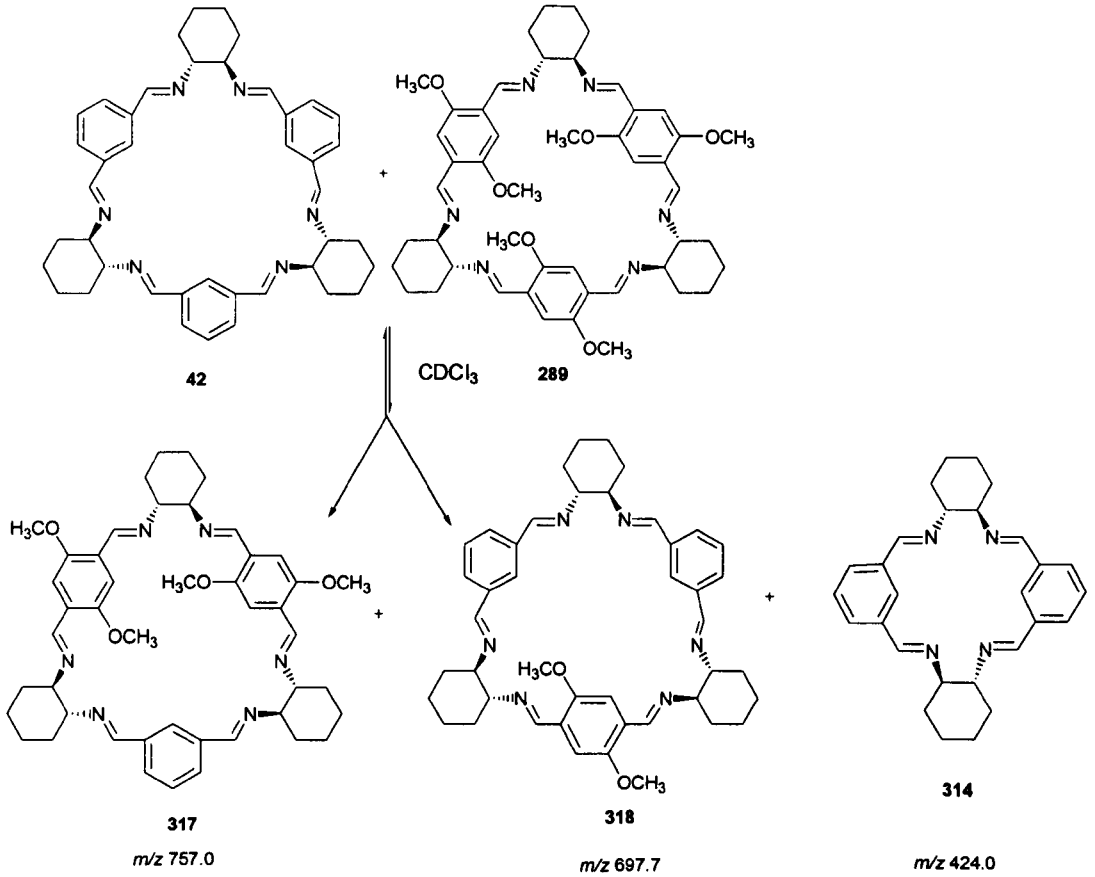

Figure 209: structures of trianglimines involved in the mixing experiment of **42** and **289**.

The 1:1 crossover experiment between trianglimines **40** and **289** (3 mM in $CDCl_3$) (Figure 210) did not show interchange between the aromatic moieties of the two trianglimines in the ^{1}H-NMR spectrum (three hours after the mixture). After one week, the ^{1}H-NMR spectrum showed considerable exchange between the aromatic moieties of the two trianglimines, with a series of very well distinguished set of signals.

The ^{1}H-NMR spectrum showed a mixture the trianglimines **40, 312, 313, 289** and again this ratio of the macrocycles formed corresponds roughly to a statistical equilibrium of 1:3:3:1.

No changes were observed with respect to the previous ^{1}H-NMR spectrum, in the ^{1}H-NMR spectrum obtained after 15 days.

The ESI mass spectrum (Figure 211) (obtained after 15 days of the reaction time) showed, at almost the same intensity, one peak at *m/z* 697.9 (100 %) associated to the molecular ion of trianglimine **312** and at *m/z* 757.6 (99 %) a signal corresponding to

the molecular ion of the trianglimine obtained with inverted proportions of the dialdehydes, that is **313**. The signal of the molecular ion of trianglimine **289** (24 %), and the signal corresponding to the molecular ion of trianglimine **40** at *m/z* 637 (10 %), could also be observed. The ^{1}H-NMR signals of **40, 312, 313** and **289** coincide with those obtained in the crossover experiments on page 119 (Figure 198) and page 124 (Figure 204).

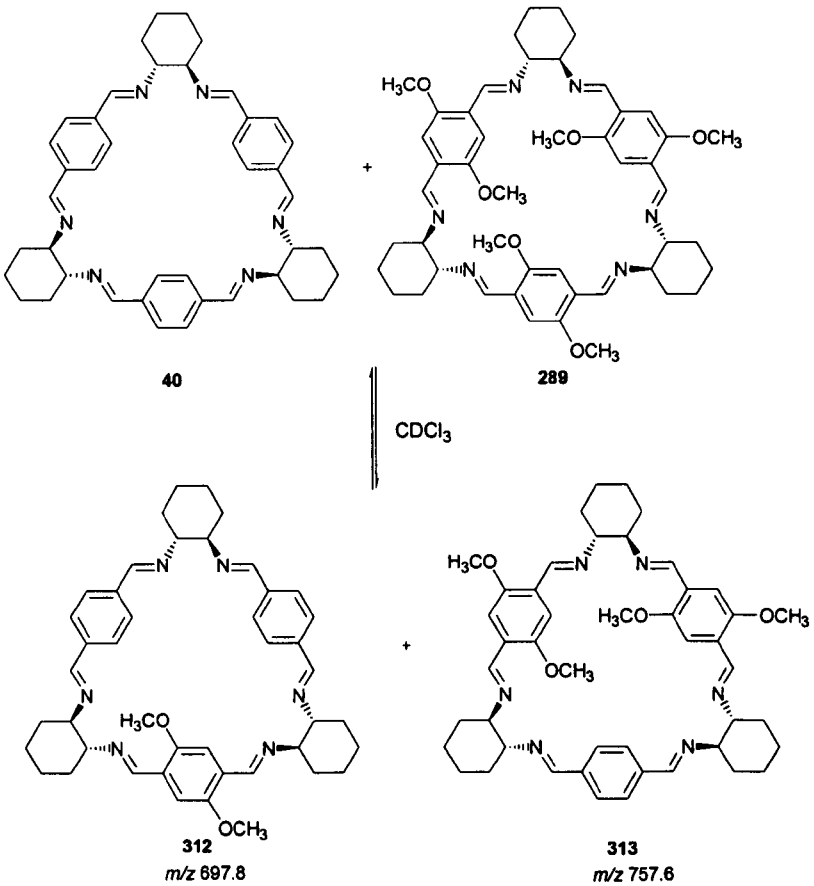

Figure 210: structures of trianglimines involved in the mixture of **40** and **289**.

Table 7 shows the values of the molecular ions of the trianglimines and [2+2]-cyclocondensation products obtained in the all experiments carried out in this chapter.

Compound	*m/z*	Compound	*m/z*
40	639.9	**313**	757.6
42	637.5	**314**	424.0
289	817.7	**315**	426.0
310	697.8	**316**	425.0
311	757.7	**317**	757.0
312	697.8	**318**	697.1

Table 7: values of the *m/z* obtained for the macrocycles synthesised.

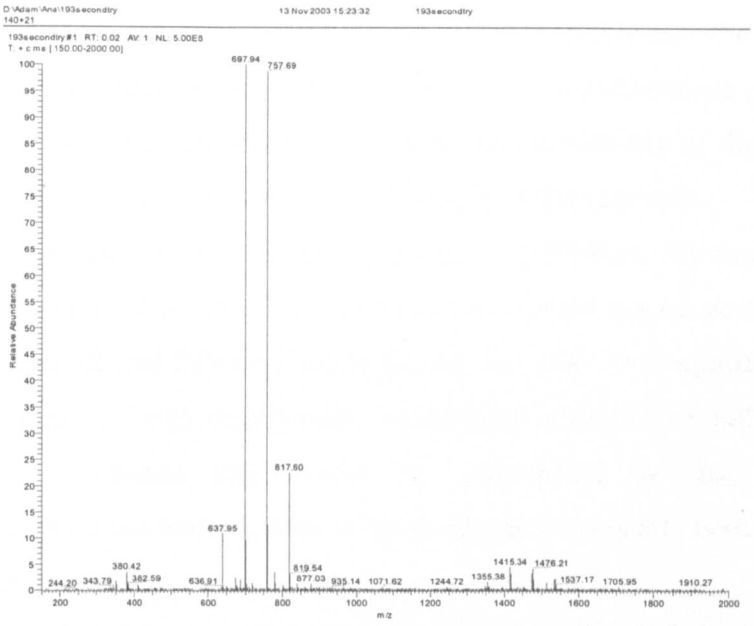

Figure 211: ESI mass spectrum of the mixture of **40** and **289**.

The computational studies carried out by Gawronski suggested that the trianglimines were formed under kinetic control and this was explained in terms of the transition state with lowest energy. However, the appearance of [2+2]-cyclocondensation products (when 1,3-disubstituted dialdehydes were the building block used in the reaction) indicated that thermodynamic control might be the reason why these [2+2]-cyclocondensation products were formed.

The most obvious case that shows kinetic *versus* thermodynamic control is the trianglimine **42** formed under kinetic control (page 122) and the [2+2]-cyclocondensation product **314** formed under thermodynamic control. When the reaction was carried out for three hours at room temperature, the resulting product is the [3+3]-cyclocondensation product **42**. However, when the reaction was carried out for longer reaction times or under reflux, the reaction gave the [2+2]-cyclocondensation product **314**. The same circumstance occurs with the trianglimine **296**, which also undergoes ring contraction to give **315** when the sample is kept in solution for a long period of time (7 days). These experiments illustrate that, depending on the conditions used, the reaction can proceed under kinetic control, to give **42** or **296** or, under thermodynamic control, to give **314** or **315** respectively.

In analogy to Gutsche's experiments with calixarenes,[133] and Sanders'[134] with macrocycles synthesised from quinine oligomers, the most consistent theory, as to why **42** is transformed into **314** is because **42** (formed under kinetic control)

undergoes a defragmentation into its building blocks, followed by the recombination into the more thermodynamic stable compound, which is in this case the dimer **314**.

The crossover experiments showed that the [3+3]-cyclocondensation products were not, in all cases, formed under kinetic control as the reversibility of the reaction was demonstrated, confirming the thermodynamic nature of the reaction.

Most importantly, the same almost statistical equilibrium mixture of [3+3]-cyclocondensation products was obtained from two distinct set of starting materials, either macrocycles **42** and **289** or dialdehydes **40** and **158**. This equilibrium mixture seems to correspond to the thermodynamic equilibrium of this set of building blocks

In conclusion, a general rule cannot be established to state that [3+3]-cyclocondensation occurs under kinetic or thermodynamic control, as each case has to be studied independently.

It is worth noting that these experiments demonstrated for the first time the reversible nature leading to thermodynamic control in the synthesis of imine macrocycles.[132]

One of the great advantages of the synthesis of trianglimines containing 1,3-disubstituted aromatic moieties, is that the reaction can be controlled (kinetically or thermodynamically) in order to obtain the desired macrocycle. Therefore the resulting reaction product can be selected as being either a trianglimine or a [2+2]-cyclocondensation product.

The [3+3]-cyclocondensation products obtained under thermodynamic conditions also provide benefit for the synthesis of new trianglimines as the imine bond can be regarded as a dynamic covalent bond. Therefore, under controlled reaction conditions, it would be possible to carry out an effective synthesis of a desired macrocycle. In addition, the reversible nature of the trianglimines can provide the possible generation of dynamic combinatorial libraries.

Chapter VIII

SYNTHESIS OF TRIANGLAMINES

22. Synthesis of trianglamines.

The imine group of the trianglimines previously synthesised can be easily reduced to produce new types of macrocyclic hexamines. By doing so, a new collection of macrocycles was synthesised, and named *trianglamines*, in analogy to their precursors.

The reduction procedure was straightforward and all trianglimines were treated under the same conditions unless stated otherwise. The general reaction scheme is shown in Figure 212.

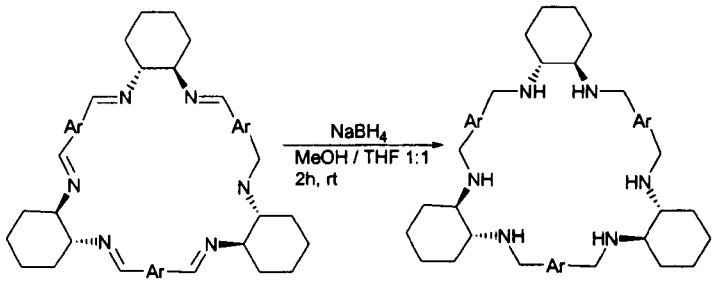

Figure 212: general scheme of trianglamine synthesis.

Trianglamine **319** (Figure 213) was obtained in 80 % yield after treating **289** with sodium borohydride in THF:MeOH at room temperature for 2 hours. After removing the solvents under vacuum, the residue was extracted three times with CH_2Cl_2 and water, the organic extracts were combined, and the solvent removed.

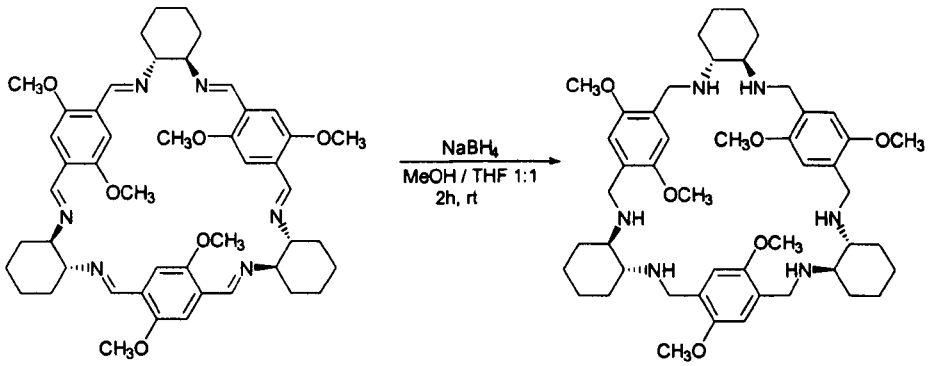

289-(2*R*, 3*R*, 12*R*, 13*R*, 22*R*, 23*R*)

319-(2*R*, 3*R*, 12*R*, 13*R*, 22*R*, 23*R*)

Figure 213: synthesis of trianglamine **319**.

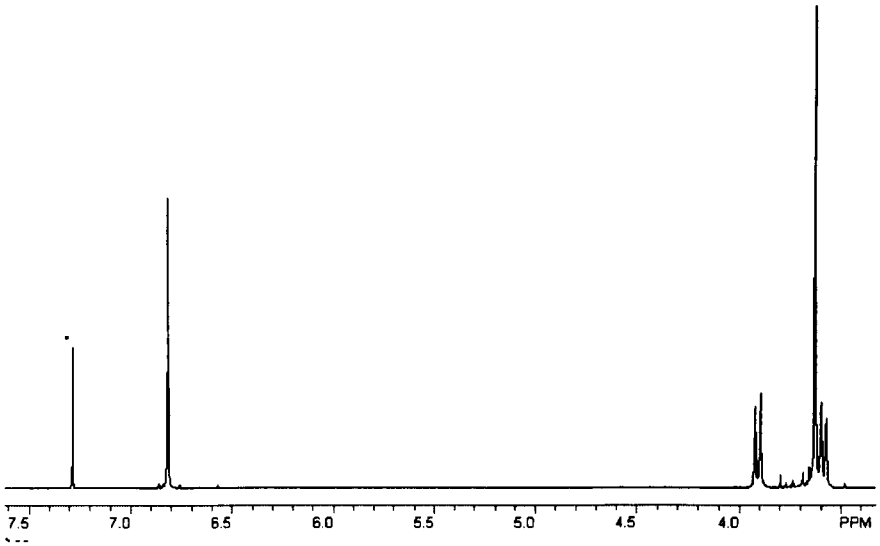

Figure 214: spectrum of trianglamine **319** expanded ^{1}H-NMR ($CDCl_3$, 500 MHz).

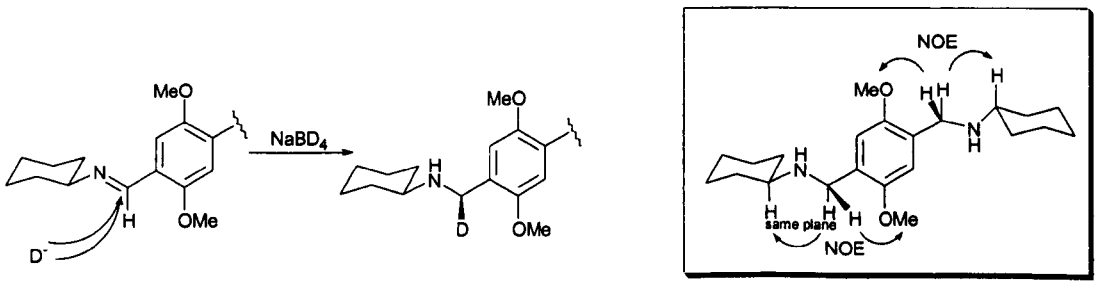

Figure 215: reduction of **289** with $NaBD_4$ and of NOE interactions.

The reduction of the imine bond of the trianglimine was shown to be complete as indicated by the spectroscopic data. The IR spectrum revealed the disappearance of the imine bond at 1630 cm^{-1}. The ^{1}H and ^{13}C-NMR spectra showed the absence of the imine at 8.40 and 155.6 ppm respectively. The ^{1}H–NMR spectrum (Figure 215) showed the new CH_2N moiety formed by the reduction of the imine, as two set of doublets corresponding to the diastereotopic protons at 3.81 and 3.56 with a typical $^{2}J_{HCH}$ geminal coupling of 13.0 Hz.

The reduction of trianglimine **319** with $NaBD_4$ (Figure 215) allowed the assignment of the two diastereotopic CH_2N signals in the ^{1}H-NMR. Under the assumption that the attack of the "D^-" nucleophile occurs from the outside of the macrocycle, as opposed to the inside cavity, the 'in plane' hydrogen was found at 3.56 ppm whereas the 'out of plane' hydrogen is observed at 3.81 ppm. This theory is supported by the ^{1}H-^{1}H-NOESY experiment. This spectrum shows the strong NOE effect between the axial proton of the cyclohexane ring and the proton that appears in the same plane (at 3.56

ppm). The second doublet (3.81 ppm), which corresponds to the hydrogen that is pointing out of the plane, and the methoxy group, also show a strong NOE effect.

The definitive confirmation of the structure of trianglamine **319** was obtained by the LSIMS spectrum, showing the molecular ion at *m/z* 829.3 (M + H).

As with the trianglimine precursor, trianglamine **319** proved to have high symmetry in solution demonstrated by the appearance of one set of signals for each of the three repeating units, in both ^{1}H and ^{13}C-NMR spectra.

Trianglamine **320** (Figure 216) was obtained in 15 % yield from trianglimine **290** following the same synthetic approach as for the previous example.

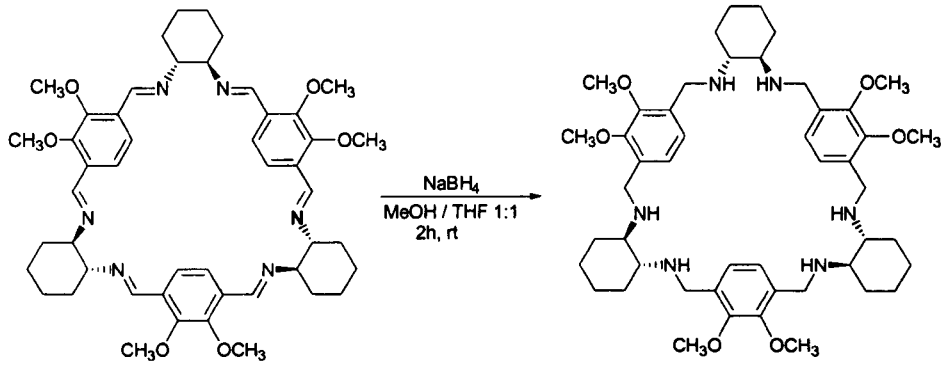

290-(2*R*, 3*R*, 12*R*, 13*R*, 22*R*, 23*R*)

320-(2*R*, 3*R*, 12*R*, 13*R*, 22*R*, 23*R*)

Figure 216: synthesis of trianglamine **320**.

For **320**, the IR spectrum showed the new peak corresponding to the -NH at 3415 cm^{-1}, indicating total reduction of the imine into the amine. In addition, the ^{1}H-NMR spectrum showed the two diastereotopic protons of the CH_2N group as an AB quartet at 3.52 ppm (*J* 13.3 Hz). This was confirmed by the ^{13}C-NMR spectrum showing the peak of the CH_2N at 46.1 ppm. In addition, the LSIMS spectrum showed the molecular ion at *m/z* 831.0 (M+H), confirming the achievement of the target compound **320**.

Trianglamine **320** also proved to have high symmetry in solution, as demonstrated by the appearance of one set of signals in both ^{1}H and ^{13}C-NMR spectra.

Following the same reaction scheme, trianglamine **321** was obtained from trianglimine **291** in 13 % yield (Figure 217).

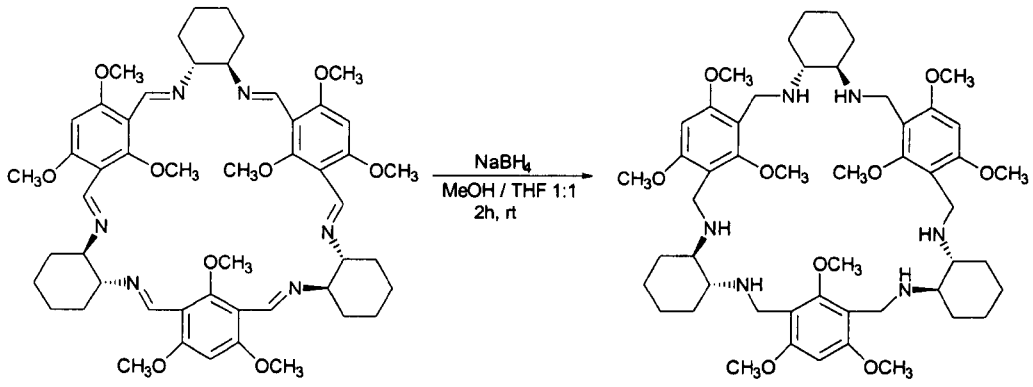

291-(2*R*, 3*R*, 11*R*, 12*R*, 20*R*, 21*R*) **321**-(2*R*, 3*R*, 11*R*, 12*R*, 20*R*, 21*R*)

Figure 217: synthesis of trianglamine **321**.

The spectroscopic data obtained in the IR spectrum showed a broad band at 3320 cm^{-1}, confirming the presence of the –NH bond and the complete reduction of the imine. However, the ^{1}H-NMR spectrum did not display a clear distinction of signals. In contrast to the trianglamines shown above, broad bands were present. Nevertheless, the AB quartet could be distinguished at 3.74 and 3.72 ppm (*J* 12.7 Hz) showing the presence of the CH_2N group. In addition, the CI mass spectrum showed the molecular ion of trianglamine **321** at *m/z* 919.0 (M^+).

The broad bands in ^{1}H-NMR spectrum were attributed to either an increased conformational flexibility of the macrocycle on the NMR time scale, or a possible aggregation of various units of trianglamine **321**.

The appearance of broad bands in the ^{1}H-NMR spectrum was also observed for trianglamine **322**, which was obtained in 90 % yield after reduction of the trianglimine precursor **296** (Figure 218). Although the molecular ion at *m/z* 651.47 (M^+) in the EI-MS spectrum confirmed the formation of trianglamine **322**, the ^{1}H-NMR spectrum showed the presence of broad bands in the aromatic region.

The IR spectrum showed a broad band at 3340 cm^{-1} identifying the -NH amine bond. The ^{1}H and ^{13}C-NMR spectra showed the CH_2N group at 3.80 and 3.73 ppm as an AB quartet in the ^{1}H-NMR spectrum, and at 52.7 ppm in the ^{13}C-NMR spectrum. Furthermore, the EI-MS spectrum confirmed the structure of **322** by showing the molecular ion at *m/z* 651.47 (M^+).

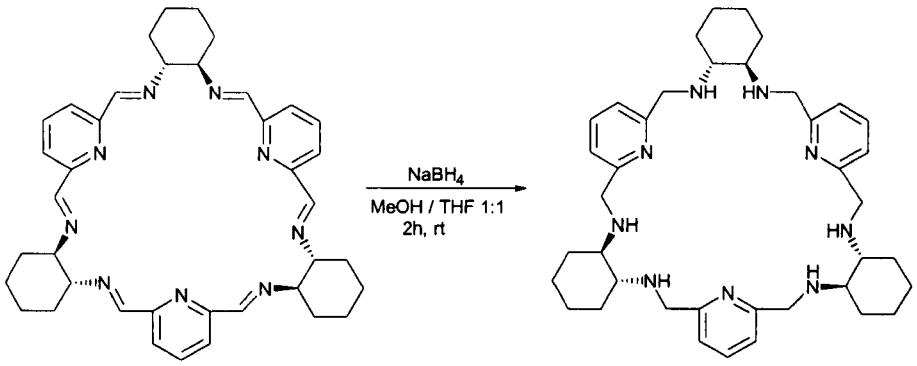

296-(2*R*, 3*R*, 11*R*, 12*R*, 20*R*, 21*R*) **322**-(2*R*, 3*R*, 11*R*, 12*R*, 20*R*, 21*R*)

Figure 218: synthesis of trianglamine **322**.

Under identical conditions to previous examples, trianglimine **299** was reduced to obtain trianglamine **323** (Figure 219).

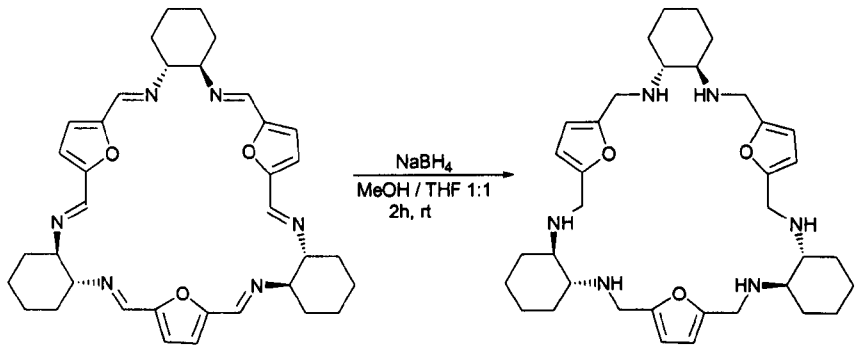

299-(2*R* ,3*R*, 11*R*, 12*R*, 20*R*, 21*R*) **323**-(2*R* ,3*R*, 11*R*, 12*R*, 20*R*, 21*R*)

Figure 219: synthesis of trianglamine **323**.

The ^{1}H-NMR spectrum was characterised by the appearance of broad bands in the aromatic, amine and alkyl regions of the spectrum. Although the ^{13}C-NMR spectrum did not give all the information necessary to confirm the structure (as one of the quaternary peaks was not detected due to poor solubility), the ESI spectrum showed only one peak for the expected molecular ion at *m/z* 619.5 (M+H) revealing the presence of trianglamine **323**.

The reduction of trianglimine **300** (Figure 220) with sodium borohydride gave trianglamine **324** in 80 % yield and, as with the trianglamines synthesised above, this one also presented broad bands in the aromatic region, however, the two doublets of the CH_2N group were clearly differentiated. Between 8.02 and 6.95 ppm there was a broad band for the aromatic protons and, at 4.88 and 4.56 (*J* 12.3 Hz) ppm (AB system), the two protons of the alkyl group. The LSIMS spectrum confirmed the structure of trianglamine **324** by showing a peak at *m/z* 949.4 (M + H).

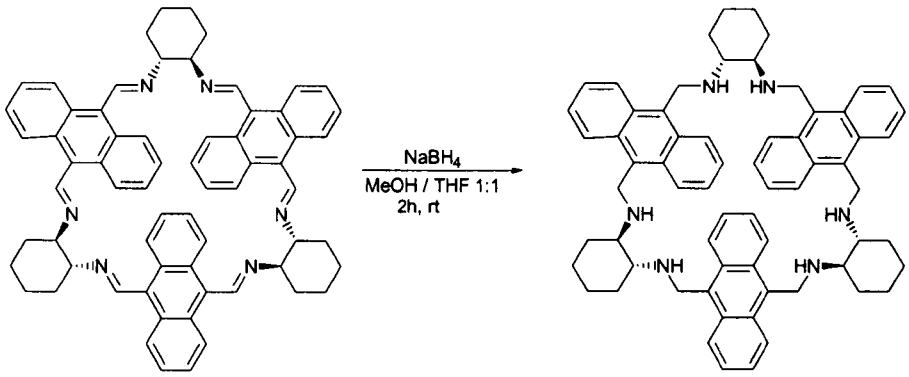

300-(2*R*, 3*R*, 16*R*, 17*R*, 30*R*, 31*R*)

324-(2*R*, 3*R*, 16*R*, 17*R*, 30*R*, 31*R*)

Figure 220: synthesis of trianglamine **324**.

Broad bands also appeared in the aromatic region for trianglamine **325,** obtained in 40 % yield from **301** (Figure 221), and as in trianglamine **324**, the two doublets of the alkyl group were clearly differentiated. The aromatic signals were observed between 7.22-7.61 ppm, and the CH_2N doublets appeared at 3.99 and 3.80 ppm (AB system) with a coupling constant *J* 12.4 Hz. In the ^{13}C-NMR spectrum the $-CH_2$ peak appeared at 43.5 ppm. The LSIMS spectrum showed the molecular ion of the trianglamine **325** at *m/z* 877.3 (M +H).

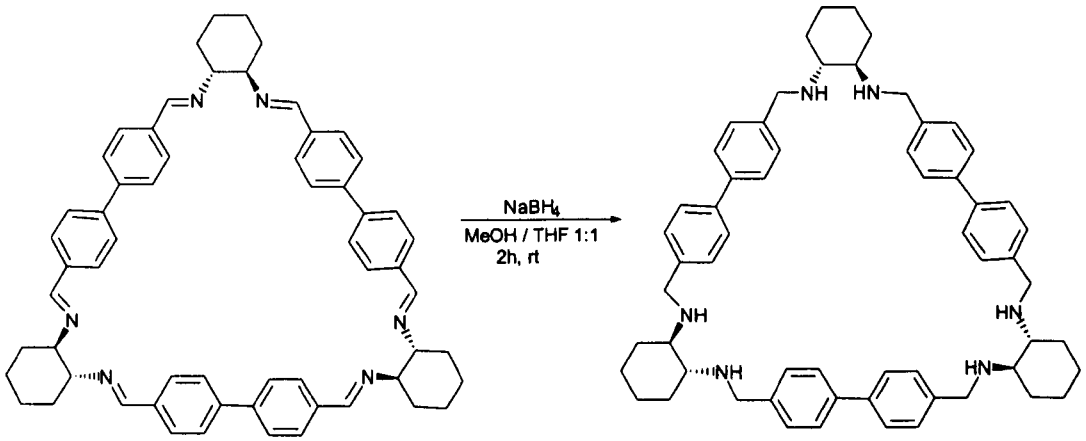

301-(2*R*, 3*R*, 16*R*, 17*R*, 30*R*, 31*R*)

325-(2*R*, 3*R*, 16*R*, 17*R*, 30*R*, 31*R*)

Figure 221: synthesis of trianglamine **325**.

The reduction of trianglimine **302** was completed as revealed by the spectroscopic methods used. The HC=N band in IR spectrum that appeared at 1635 cm^{-1} in the precursor **302** is missing in the IR spectrum of the new compound **326**, as well as the two imine peaks that appeared at 8.58 and 8.45 ppm in the ^{1}H-NMR spectrum.

The ^{1}H-NMR of the starting material **302** showed the presence of two diastereomeric structures due to restricted rotation (slow on the NMR time scale) of the biaryl system. This effect is not observed in the ^{1}H-NMR of the reduced form since only one set of signals was observed.

However, the product obtained was not the trianglamine expected, the [2+2]-cyclocondensation product **326** was formed instead (Figure 222). The FAB spectrum showed the [2+2]-cyclocondensation product peak at m/z 760.1 M^+ and 783 (M^++Na) and a small trace of trimer at *m/z* 1141.5 (M^+).

The aromatic region showed two singlets at 6.85 and 7.17 ppm corresponding to the aromatic protons. The new CH_2N group came out as an AB quartet at 3.93 ppm (*J* 13.2 Hz) and the methoxy and methyl groups appeared as two singlets at 3.95 and 2.30 ppm respectively. The ^{13}C NMR spectrum showed these three signals very clearly, at 46.6 (CH_2-), 61.6 (-OCH_3) and 21.0 (-CH_3) ppm.

As was mentioned above, the ^{1}H-NMR spectrum of **326** showed, unlike the trianglimine precursor, only one set of signals. This result can be explained as a fast rotation phenomenon on the NMR time scale since there was more rotational freedom in **326** as compared to **302**.

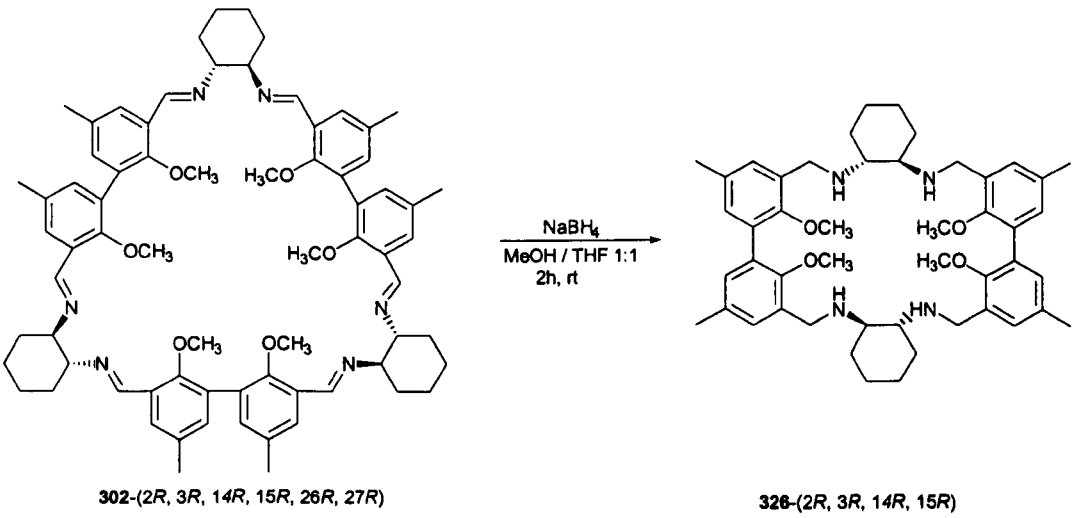

302-(2*R*, 3*R*, 14*R*, 15*R*, 26*R*, 27*R*)

326-(2*R*, 3*R*, 14*R*, 15*R*)

Figure 222: synthesis of trianglamine **326**.

The reduction of the trianglimine **303** (Figure 223) was carried out under the standard reaction conditions, however, the reaction did not proceed to completion as the ^{1}H-NMR spectrum exhibited a remaining imine peak. The reaction was repeated increasing the reaction time to 24 hours. As in the previous examples, the ^{1}H-NMR

spectrum showed broad bands in the ferrocene region, as also in the CH_2N and N-CH. The ^{13}C-NMR spectrum could not be obtained due to lack of solubility of **327**.

The ESI mass spectrum confirmed that the reaction product was not the trianglamine as the only peak present appeared at *m/z* 650.0 (M+H, 100%). This value corresponds to the formation of **327** (Figure 223).

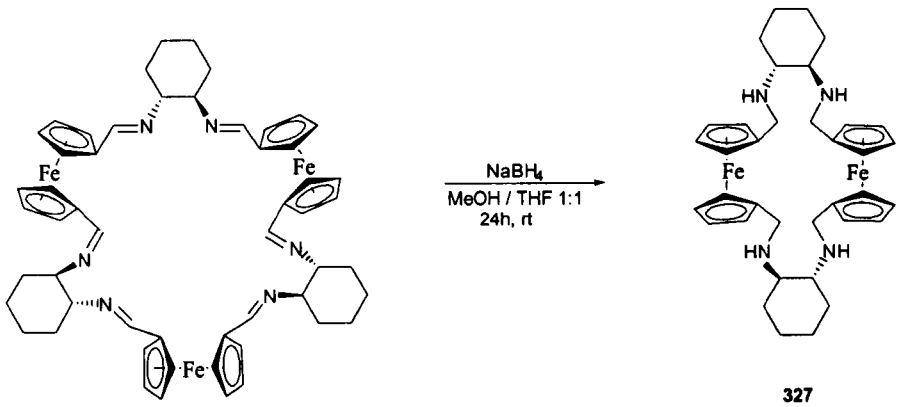

Figure 223: synthesis of [2+2]-cyclocondensation product **327**.

In the previous chapter it was explained that some trianglimines were the kinetic product of the cyclocondensation, however, when the reaction was carried out for longer reaction times, the major product obtained is the thermodynamic one, that is the [2+2]-cyclocondensation product. In this case, the reaction was carried out for 24 hours and thus the product obtained was the [2+2]-cyclocondensation product **327**. This experiment demonstrated that ring contraction can occur under the reduction conditions, forming the smaller macrocycle. This may occur because of the reversible breaking and reforming of the imine linkage being faster than the reduction.

The reduction of trianglimine **304** gave a dark yellow oil as final product. The structure of the proposed product obtained was trianglamine **328** shown in Figure 224. The characterisation of this compound was extremely difficult as the ^{1}H-NMR spectrum showed broad bands in the aromatic region as well as in the region in which the chemical shift of the CH_2N, OCH_3 and N-CH emerge. In addition, the ^{13}C-NMR experiment did not provide a satisfactory spectrum, due to lack of solubility.

However, the major peak in ESI spectrum appeared at *m/z* 1042.0, which corresponds to trianglamine **328** containing one molecule of sodium borohydride and a sodium atom, and the second major peak at *m/z* 1056, which corresponds to the trianglamine molecular ion containing two molecules of sodium borohydride.

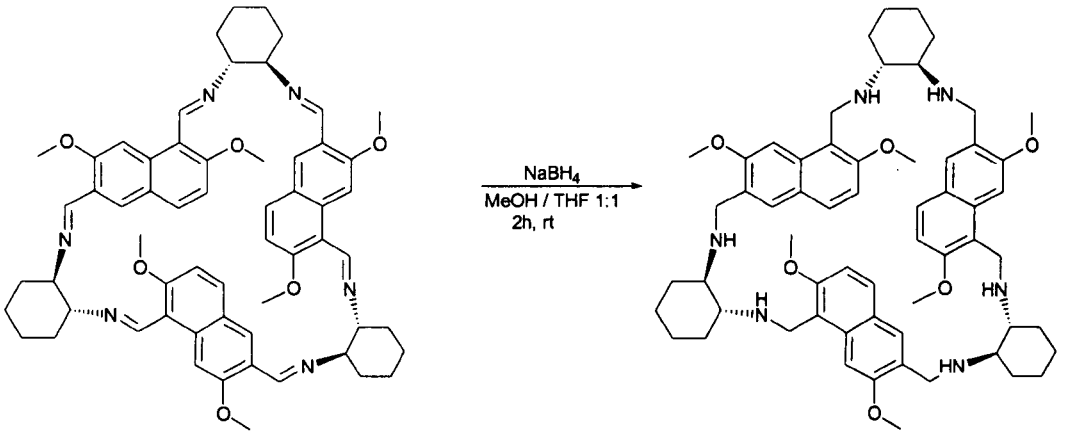

304-(2*R*, 3*R*, 13*R*, 14*R*, 24*R*, 25*R*)

328-(2*R*, 3*R*, 13*R*, 14*R*, 24*R*, 25*R*)

Figure 224: synthesis of trianglamines **328**.

Although the spectroscopic data did not justify the structure proposed, the mass spectrum appears to confirm the structure of trianglamine **328**.

In the same way, the ^{1}H-NMR spectrum of trianglamine **329** (Figure 225) showed broad bands and multiplets, again making the assignment of the signals very difficult. Due to the lack of solubility, the ^{13}C-NMR spectrum carried out did not produce conclusive results. However, the ESI mass spectrum showed a peak with higher intensity at *m/z* 1049.6 which corresponded to trianglamine **329** containing one molecule of THF. The second major peak at *m/z* 979.7 corresponded to the trianglamine **329** molecular ion.

Trianglamines **328** and **329** presented broad bands in the ^{1}H-NMR spectrum making the assignment of the signals very difficult. For this reason, and in order to clarify the results obtained, experiments at low temperature NMR were performed.

A set of ^{1}H-NMR spectra in $CDCl_3$ were carried out following the same procedure for both samples **328** and **329**. The experiment was started at room temperature (298 K) and was decreased in stages of 20 degrees, running a ^{1}H-NMR spectrum at each interval, until the temperature reached 223 K (-50°C). Unfortunately, no spectral changes were observed with the temperature variation. This did not help in the elucidation of the structural features that these molecules possess.

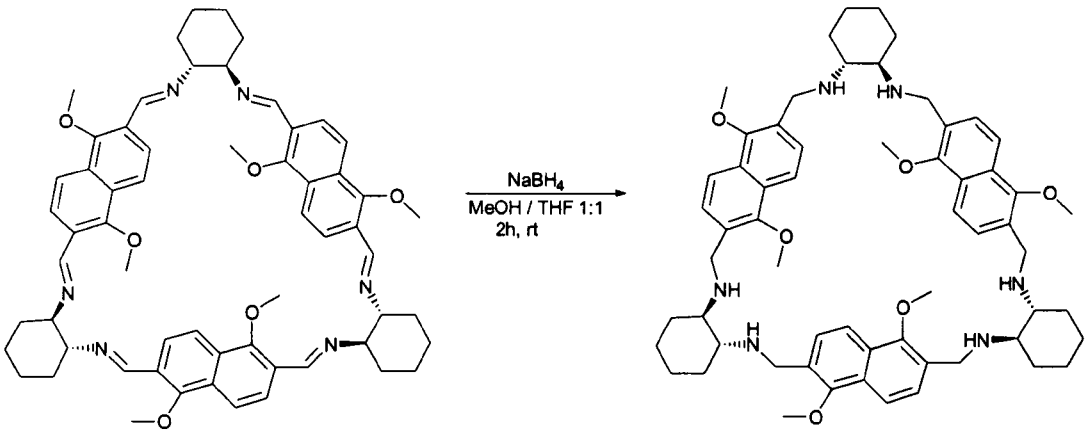

289-(2*R*, 3*R*, 14*R*, 15*R*, 26*R*, 27*R*)

329-(2*R*, 3*R*, 14*R*, 15*R*, 26*R*, 27*R*)

Figure 225: synthesis of trianglamines **329**.

The [2+2]-cyclocondensation products that were obtained in the attempted synthesis of the trianglimines were also treated with sodium borohydride under standard reaction conditions.

Unexpected results were obtained from [2+2]-cyclocondensation product **308** in Figure 226. The cyclocondensation product of bis-4-formylphenyl-ether **219** and (1*R*, 2*R*)-diaminocyclohexane **38** gave exclusively the [2+2]-cyclocondensation product **308**, without showing any signal of trimer in either ^{1}H-NMR or mass spectrometry. When the reduction was carried out, the outcome was the tretraamine macrocycle confirmed by the ESI mass spectrum showing the molecular ion at *m/z* 617.5 (M+H, 100%). However, the trianglamine (**331**) peak was also observed at *m/z* 925.5 (M+H, 40 %), which was unexpected.

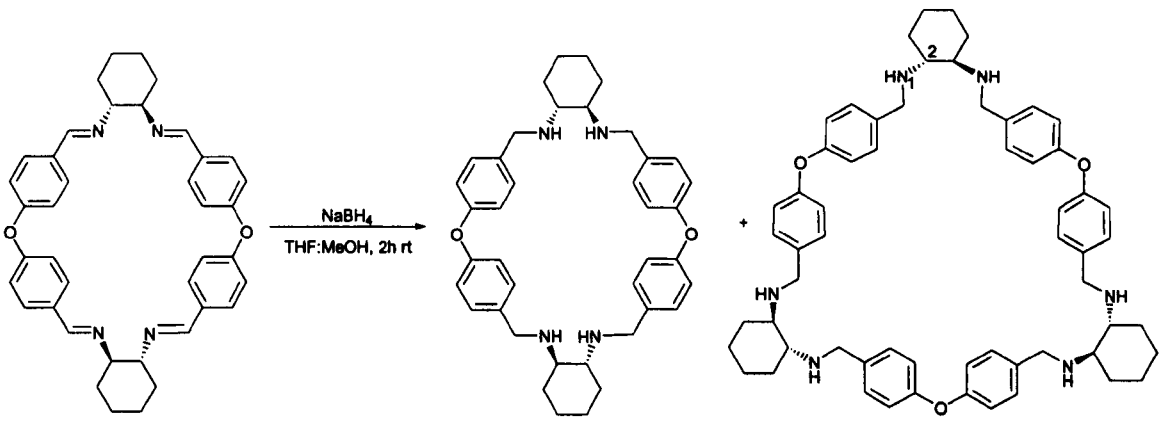

308- (2*R*, 3*R*, 17*R*, 18*R*)

330- (2*R*, 3*R*, 17*R*, 18*R*)

331- (2*R*, 3*R*, 17*R*, 18*R*, 32*R*, 33*R*)

Figure 226: synthesis of trianglamine **331** and [2+2]-cyclocondensation product **330**.

This result suggests that during the reduction process, the ring of the imine [2+2]-cyclocondensation product opens to produce an open chain intermediate. This intermediate undergoes ring expansion to give the trimer followed by reduction.
Although the characterisation in the ^{1}H-NMR spectrum was straightforward for each peak, the assignment of these signals to the corresponding molecule (**330** or **331**) was not possible. The aromatic protons were found at 7.16 (*J* 8.0 Hz), 7.15 (*J* 8.5 Hz), 6.84 (*J* 8.4 Hz) and 6.83 (*J* 8.4 Hz) ppm. However, the diastereotopic -CH_2 signals were not easily distinguished, as they appeared as broad bands.

The reduction of the macrocycle **309** gave exclusively the [2+2]-cyclocondensation product **332** as shown in Figure 227. As with trianglimine **302**, macrocycle **309** also showed two sets of signals in the ^{1}H-NMR spectrum. The same pattern also follows upon reduction, where only one set of peaks for **332** was observed.

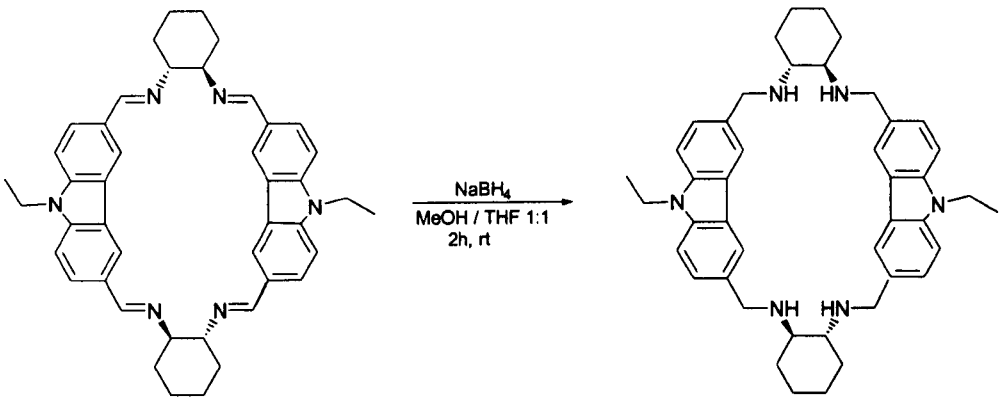

Figure 227: synthesis of [2+2]-cyclocondensation product **332**.

The reduction of the tetraamine **309** was complete since neither of the two imine peaks (8.73 and 8.48 ppm) were present in the ^{1}H-NMR of the reaction product. This result was corroborated by the IR spectrum, which did not show the imine band at 1620 cm^{-1}, instead it showed the -NH peak at 3402 cm^{-1}.
The ^{1}H-NMR spectrum showed a singlet for one of the aromatic protons at 8.19 ppm and the remaining two non-equivalent protons appeared as an AB quartet, at 7.29 ppm (*J* 8.1 Hz). Another AB quartet emerged at 4.05 and 3.78 ppm (*J* 13.5 Hz) for the CH_2N moiety. Furthermore, the achievement of **332** was revealed by the FAB mass spectrum showing the molecular ion at *m/z* 666.4 (M^+).

The last example of the synthesis of trianglamines was carried out from trianglimine **294** (Figure 228). The ^{1}H- NMR spectrum showed clearly the complete reduction of the trianglimine precursor. The imine protons disappeared and the -CH_2N diastereotopic protons appeared at 3.88 and 3.56 (*J* 13.5 Hz) ppm. However, these two AB system signals were not clearly shown as a pair of sharp doublets. The aromatic region showed an interesting feature that, at first sight, did not match the structure of the trianglamines expected. Three pairs of doublets appeared at 7.27, 7.75 and 7.22 ppm (*J* 8.0, 7.0, 7.0 Hz, respectively), and three singlets at 7.18, 7.15 and 7.12 ppm. In addition, the methyl region (2.13 ppm) appeared as a broad band. In contrary, the ^{13}C-NMR spectrum showed one set of signals only. The ESI spectrum also showed three main peaks at *m/z* 691.9, 754.6 and 761.8. The peak at *m/z* 691.9 corresponds to the molecular ion (M^+, 100 %), the peak at *m/z* 754.6 (97 %) matches the value of one trianglamine **333** containing a molecule of $NaBH_4$ and a sodium atom. The last peak at *m/z* 761.8 (80 %) corresponds to the trianglamine **333** containing a tetrahydrofuran molecule.

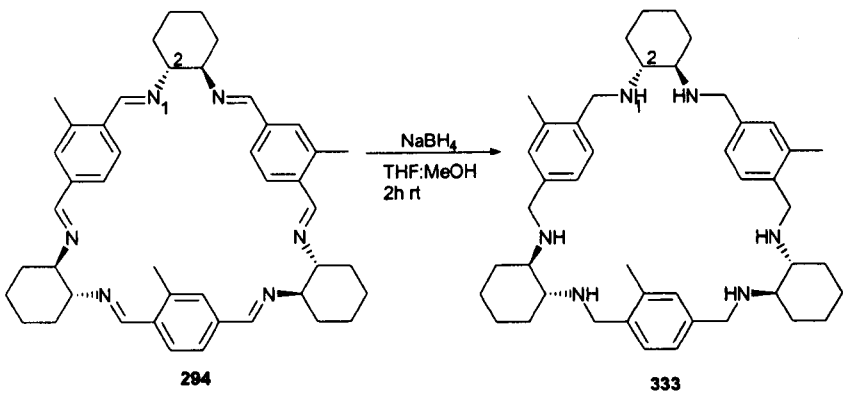

Figure 228: synthesis of trianglamine **333**.

The results obtained from the ESI spectrum, where the macrocycle entraps different molecules, can help to explain the data extracted from the ^{1}H-NMR spectrum. One possible explanation for the appearance of the three pair of doublets and three singlets in the aromatic region, is that the reaction product was only trianglamine **333**, and no rotational isomer is observed. As the trianglamine entraps different solvent and reagent molecules, it provokes variation in the chemical shift of the protons of the molecule. Therefore, the three sets of signals observed may represent the same trianglamine in the free form, and the two different complexed forms. Nevertheless, in order to confirm this theory, further experimentation would be required.

Table 8 summarises the spectroscopic data obtained for the trianglamines and tetraamines synthesised.

Substrate	Products	^{1}H-NMR CH_2N	^{13}C-NMR CH_2N	*m/z*
289	319	3.56	45.8	829.3
290	320	3.52	46.1	831.0
291	321	3.74-3.73	58.9	919.9
296	322	3.80-3.73	52.7	651.7
299	323	broad	43.7	619.5
300	324	4.88-.56	43.5	949.4
301	325	3.99-3.43	43.5	877.3
302	326	3.93	46.6	783.1
303	327	broad	-	650.0
304	328	broad	-	1042.0
305	329	4.28-4.03	-	979.7
308	330,331	3.84-3.46	50.4	617.5-925.5
309	332	4.05-3.78	55.8	648.4
294	333	3.88-3.56	50.7	691.9

Table 8: spectroscopic data obtained for the trianglamines and tetraamines synthesised.

Chapter IX

BINDING STUDIES

23. Introduction.

All of the macrocycles synthesised (both trianglamines and trianglimines), possess distinctive characteristics that make them suitable to act as a good receptors in a host-guest system. These characteristics include; a cavity capable of binding an aromatic group, a site capable of binding a polar group and hydrogen bonding motifs. However, these characteristics are not universal for binding every different type of guest molecule. Other elements also have to be taken into account, the most important being the complementarity between host and guest, which is determined by the electronic properties and the size and shape of both. For example, a binding site too small for a guest is detrimental to binding, as is a site that is too big.

Of the possible candidates to act as guest molecules for the macrocycles synthesised, it was found that various types of pesticides contain the complementary features that can potentially establish a host-guest system. These types of pesticides are characterised by an aromatic group, a polar group and a liphophilic group.

Thus, the use of the trianglimines and trianglamines synthesised, promises to be a good tool to remediate the problems these toxins cause.

Furthermore, the problem of contamination caused by the use of old generation pesticides requires urgent remediation as large amounts of toxic pesticide residues have entered the food chain, provoking serious health concerns to both humans and animals. This is of particular significance in several regions of the former Soviet Union and Vietnam, where the indiscriminate use of such pesticides, is still causing major health problems.

With the increasing use of pesticides for both industrial and domestic purposes, the amount of accidents and intoxications associated with their use has increased simultaneously. According to the World Health Organisation[135] two million people are intoxicated by direct or indirect exposure to pesticides every year. The contact with pesticides and their entrance into the human body (though the skin, respiration or ingestion) is generally a result of exposure in the work place, their improper use and from crop dusting. It was also found, in some cases, that the pesticide residue in humans could only be explained by assuming ingestion.

The pesticides chosen in this project for testing the macrocycle receptors were:

2,4-D: 2,4-dichlorophenoxyacetic acid.

2,4,5-T: 2,4,5-Trichlorophenoxyacetic acid.

2,4-DP: 2-(2,4)- dichlorophenoxypropionic acid.

2,4-DCP: 2,4-dichlorophenol.

Atrazine: 2-chloro-4, 6-bis-isopropylamino-1, 3, 5-triazine.

Propazine: 2-chloro-4, 6-bis-isopropylamino-1, 3, 5-triazine.

Sencor: 4-amine-6-tbutyl-3-methylthio-1, 2, 4-triazinone.

Chlorsulfuron: n-[{4-methyl-6-methoxy-1,3,5-triazin)-2-aminocarbonyl]-2-chlorobenzenesulfonamine.

Thiofensulfon: methyl3-[[[[(4-methoxy-6-methyl-1,3,5-triazin-2-yl)amino] carbonyl]amino]-sulfonyl]-2-thiophenecarboxylate.

The structures of all these pesticides are shown in Figure 229.

Atrazine, propazine, sencor and thiofensulfon are herbicides belonging to the group of triazines, which are widely used to control broadleaf and grassy weeds in corn, pineapple, and in conifer reforestation planting.[136] Their use has been greatly extended due to the improvement in the production and quality of the crops.

Nevertheless, the treatment of laboratory animals with these chemicals has been shown to result in toxic effects such as mammary gland tumours in female rats, attenuation of the lutenizing hormone (LH), altered pregnancy maintenance and delayed puberty development.

Further studies for the Environmental Protection Agency[137] (EPA) revealed the carcinogenic effect of atrazine and propazine in female rats.

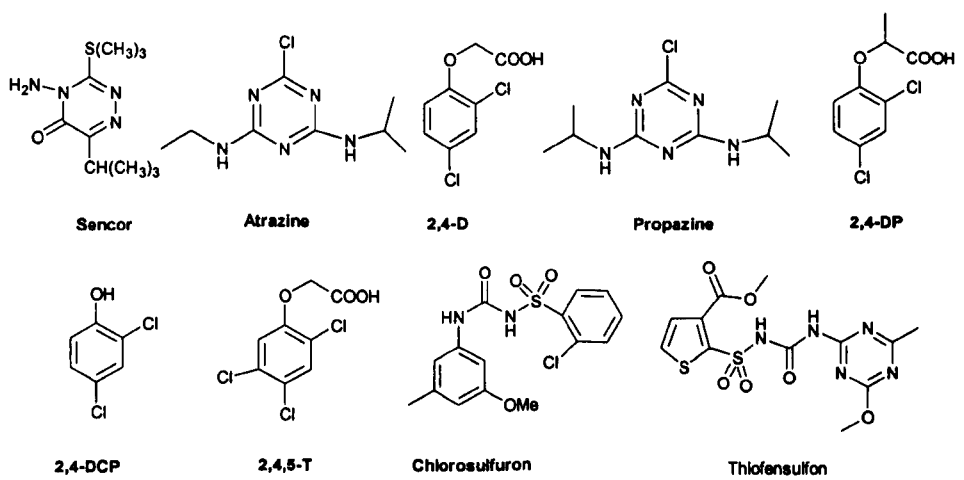

Figure 229: pesticides used as guest for the binding studies.

All of the macrocycles synthesised possess the appropriate characteristics to act as potential receptors for the entrapment of the pesticides presented above. However, a small number of selected compounds were chosen for binding studies. The

macrocycles were selected according to the ease of synthesis of the starting materials (that is the dialdehydes) as well as the yield obtained after recrystallisation of the macrocycles.

The macrocycles chosen are shown in Figure 230.

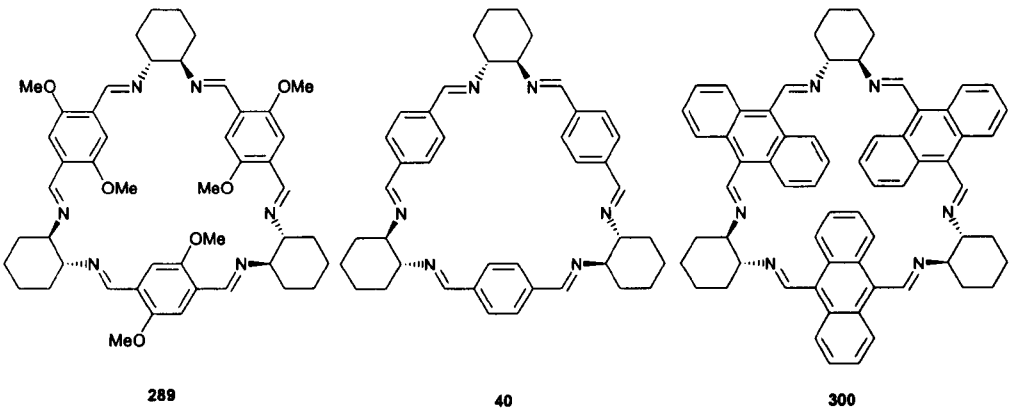

Figure 230: macrocycles used in the binding studies.

24. General measurements of ^{1}H-NMR complexation and DOSY experiments.

The methodologies employed to investigate the possible binding between these pesticides and the synthesised macrocycles, were ^{1}H-NMR shift titrations and diffusion NMR. The experimental work carried out in this section is by no means extensive enough to determine with certainty that binding is occurring.

24.1 General ^{1}H-NMR measurements.

^{1}H-NMR measurements were recorded at 298K in a Bruker 500 MHz pulsed transform NMR spectrometer.

The solutions of the samples with a typical concentration in the milimol scale were prepared in $CDCl_3$ using (0.01 %) TMS as internal reference.

The methodology followed for the titration was as follows. To a NMR tube containing a solution of a known concentration of the macrocycle receptor, it is added stepwise a solution of the pesticide (concentration depending on the solubility of the pesticide), increasing the amount of pesticide in each addition. ^{1}H-NMR spectra were recorded after each addition of the pesticide. The concentration of the receptor is kept constant during the titration process.

In order to perform reliable ^{1}H-NMR shift titrations, several considerations have to be taken into account. In high-resolution instruments, reliable K values can be obtained even if $\Delta\delta<0.03$ ppm.[18]

The most insoluble component (in $CDCl_3$) in all the titrations carried out was the macrocycle, whose concentration was kept constant along the titration. In order to obtain reasonable good spectra, the solubility of the macrocycle should be, in theory, above 0.001 mol/l to allow a complexation degree between 20 % and 80 %. However, in the majority of the cases, the concentration of the macrocycle used was lower.

24.2 General DOSY-NMR measurements.

DOSY-NMR measurements were recorded at 298K in a Bruker 500 MHz pulsed transform NMR spectrometer. The typical operations for a normal diffusion NMR involve:

Spectral frequency 500.15 MHz

Acquisition time 5.34 sec.

δ= 3.00 ms

Δ=35.0 ms

The solutions of the samples were prepared in $CDCl_3$ using TMS as internal reference.

$$I = I_o e[D(\gamma\delta g)^2(\Delta - \delta/3 - \tau/2)] \quad \text{Equation 25}$$

Equation 25 gives the relationship between the Diffusion constant "D", the gradient strength "g" and the measured signal intensity "I".

The only parameters kept constant were the gradient duration (δ), the diffusion delay time (Δ). The gradient strength (g) was varied from 5 % to 95 % in 16 steps. The software package XWin NMR (Bruker Biospin, Rheinstetten) analysed the results giving, the diffusion coefficients (D) by curve fitting using the equation shown above.

The experiment consists of measuring the diffusion coefficient of a sample in a 1:1 proportion (Host:Guest) dissolved in the appropriate deuterated solvent (in all cases $CDCl_3$).

In order to have accurate and reliable results in DOSY experiments, it is essential to ensure that the correct δ and Δ parameters are used. δ and Δ were chosen in order to obtain 90 % signal attenuation for the slow diffusion component in a preliminary experiment.

By plotting I/Io against the gradient strength, a curve as shown in Figure 231 is observed. Curve fitting allows the determination of the diffusion coefficient from the experimental curve.

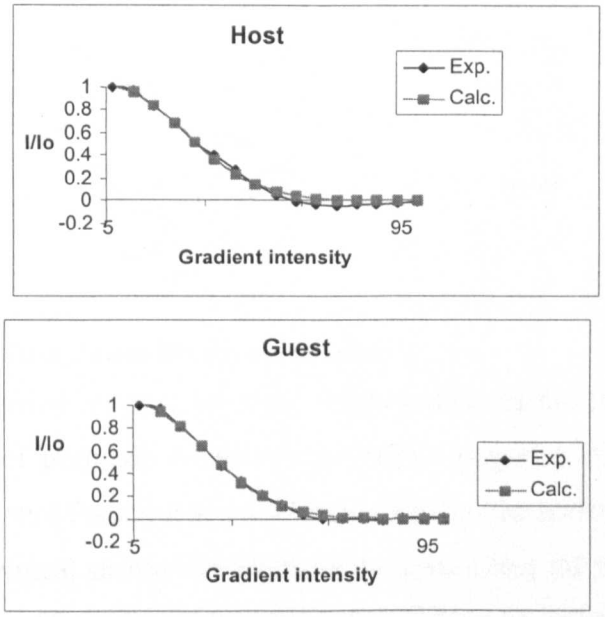

Figure 231: diffusion decay curves of host and guest. These curves correspond to real examples. The host curve corresponds to trianglimine **289** and the guest to the pesticide **sencor**.

In the DOSY-NMR method only singlets and sharp peaks can be measured in order to obtain reliable diffusion coefficients. This is due to the determination of peak height for I/Io measurements. Other software allows proper integration for I/Io measurements.

Therefore, the imine peak for example, which is always a broad band, does not give the same value of diffusion coefficient as the remaining protons of the trianglimine.

Although what follows, in respect to the DOSY experiments, shows a certain degree of positive results, they are only based on a single 1:1 trianglimine: pesticide relationship.

Therefore, the diffusion NMR experiments allow qualitative determination of binding, rather than a quantitative evaluation of a binding constant.

The values of the diffusion coefficients presented an error of 10% estimated based on the capabilities of the NMR spectrometer.

25. Binding studies.

25.1 Trianglimine 289 and Sencor.

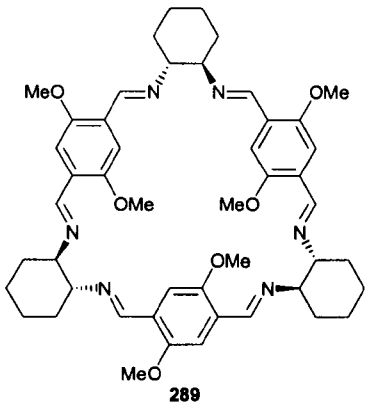

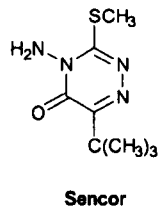

Figure 232: structures of trianglimine **289** and pesticide **sencor**.

The titration was carried out at a constant concentration of the trianglimine of 2.33 mM. The aliquots of pesticide solution were added stepwise starting with a ratio **sencor**: **289** of 0.28, and finishing at a 4.52 ratio, in a 10-step addition process.

The variation in chemical shift of the pesticide protons along the titration was almost imperceptible, giving $\Delta\delta$ values in the order of 10^{-03} ppm. In addition, there was only one peak observed for the pesticide protons, which can be interpreted as no complexation between host and guest, therefore no variation in the chemical shift was produced. The representation of the titration curve (non-linear fitting curve), in which the $\Delta\delta$ of the pesticide was plotted against the concentration of the guest, is omitted due to the lack of information it provides, as there was not variation in the chemical shift in any of the protons of the pesticide. The same occurs in the job-plot, in which the desired curve that shows the stoichiometry of complexation was not obtained.

In order to confirm the result obtained from the titration, a DOSY experiment was carried out. 1 equivalent of trianglimine **289** and 1 equivalent of pesticide **sencor** (Figure 232) were dissolved in 2.5 ml of $CDCl_3$. ([**289**]=[**sencor**]= 6.12 mM)

The results obtained confirmed those of the previous NMR titration, which is to say that no encapsulation is observed. The values of the diffusion coefficients of the receptor and the guest are far too different. The DOSY spectrum showed that the signals of the diffusion coefficient belonging to the pesticide are quite separated from the host (if the complexation is effective, both signals should appear in the same region), which means that the diffusive flux is higher (as expected from small molecules).

Figure 233 shows the DOSY spectrum of the mixture. The x-axis of the spectrum shows the chemical shift (δ) in ppm, and the y-axis represent the diffusion coefficient, however the plot shows a scale from -8.1 to –9.0. These values must be read as "*log D*" values in m^2/s. For example, -8.6 ppm means a diffusion coefficient of $10^{-8.6}$= $2.5x10^{-09}$ m^2/s. [138]

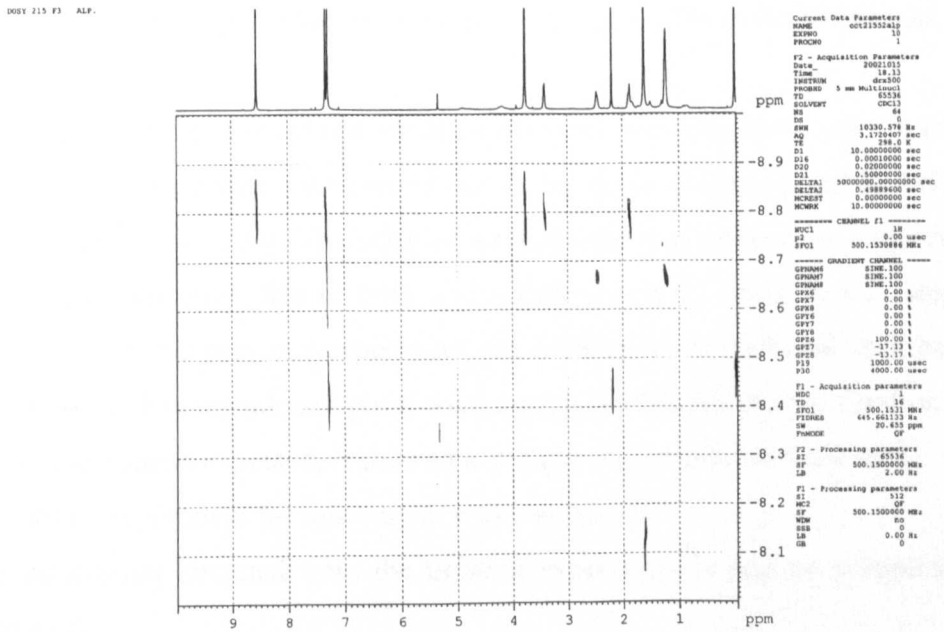

Figure 233: DOSY-NMR spectrum of the 1:1 mixture of trianglimine **289** and **sencor**

The diffusion coefficients of the trianglimine **289** appeared in the region of (as is shown in the plot) log D=–8.8 ($D=1.58x10^{-9}$ m^2/s), whereas the diffusion coefficients of the pesticide (2.44 and 1.10 ppm) appear at around log D=–8.65 ($D=2.23x10^{-9}$ m^2/s). The values of the diffusion coefficient obtained from the pesticide (at the same concentration) in this experiment are the same as the values of the diffusion coefficients obtained from DOSY experiments of the free pesticide. This means that the presence of the trianglimine does not affect the diffusion of the pesticide. In the spectrum the diffusion coefficients for the solvent $CDCl_3$ is $3.98x10^{-9}$ m^2/s, for the TMS is $3.54x10^{-9}$ m^2/s and for H_2O is $7.94x10^{-9}$ m^2/s can also be seen. As can be seen in the spectra, the lines corresponding to the diffusion coefficient of the trianglimine and the pesticide appeared at different heights, which mean that they do not diffuse together, therefore, no binding is produced.

As the use of **sencor** as guest was unsuccessful, the same trianglimine **289** was used with other triazine pesticide.

25.2 Trianglimine 289 and Atrazine.

Atrazine is a selective triazine herbicide used to control broadleaf and grassy weeds in corn, sugarcane, pineapple, Christmas trees, and other crops, and in conifer reforestation plantings. Atrazine is slightly to moderately toxic to humans and other animals.[137]

The binding studies carried out for this system were concentrated only in the titration procedure. The titration was carried out at the same concentration of **289** as above (2.33 mM) (Figure 234). The addition of pesticide was carried out stepwise starting with a ratio, **atrazine**: **289** of 0:08, and finishing at a 4:1 ratio, in a 11 step addition process. As in the previous experiment, the differences of chemical shift between the free and possibly complexed guest were negligible. Therefore, the titration curve did not give the shape expected, it showed a straight line parallel to the x-axis.

No further experiment for this system was carried out.

The conclusion obtained from the titration experiment is that no complexation was produced.

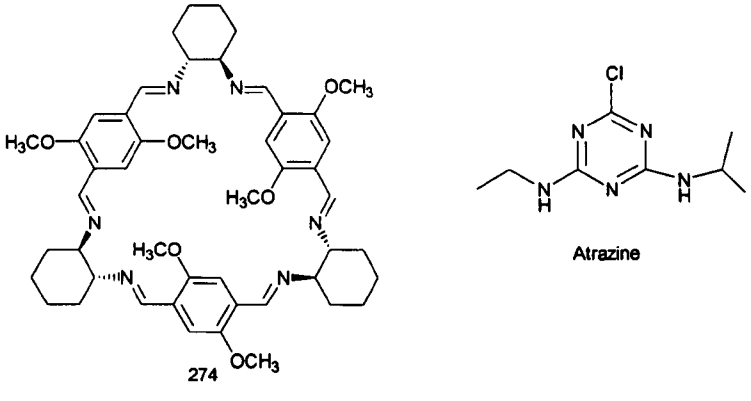

Figure 234: structures of trianglimine **289** and pesticide **atrazine**.

25.3 Trianglimine 289 and 2,4-D.

Complexation studies were also carried out with the controversial herbicide 2,4-D, whose toxicity has been extensively studied without definite conclusions. However, one of the biggest concerns about 2,4-D is related to dioxin contamination. Also, in the past, 2,4-D was frequently co-formulated with the herbicide 2,4,5-T (Figure 235).

Production of 2,4,5-T was contaminated with the carcinogenic dioxin 2,3,7,8-tetrhachlorodibenzo-*p*-dioxin (TCDD).[139]

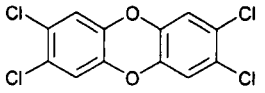

Figure 235: structure of 2,3,7,8-tetrachlorodibenzo-*p*-dioxin (TCDD)

Those who were exposed to the mixed formulations may therefore have been exposed to TCDD. The most notorious mixed formulation was Agent Orange, used first by the UK military in Malaysia and later extensively by the US military to defoliate jungle in regions in Vietnam. Furthermore, recent studies have proven that **2,4-D** lead to the disruption of cell membranes.[140]

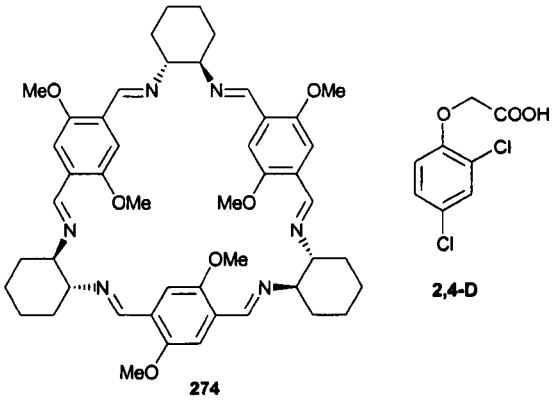

274 **2,4-D**

Figure 236: structures of trianglimine **289** and pesticide **2,4-D**

The study of the complexation between the trianglimine receptor and the pesticide was carried out in firstly by NMR shift titration. Due to the acidic nature of the 2,4-D, and the basic nature of the trianglimine, it was necessary to carry out dilution NMR experiments in order to distinguish whether or not the equilibrium between both compounds (at titration concentration) was acid-base chemistry.

Thus, a ^{1}H-NMR spectrum of 1:1 mixture was carried out. To the same sample, more $CDCl_3$ was added and again, a spectrum was recorded. In this way, four NMR spectra were recorded with the same trianglimine:pesticide proportion at several dilutions. The chemical shift of the pesticide was analysed in all spectra recorded. At the same concentrations at which the titrations were carried out, the dilution experiment did not show variation in the chemical shift in the pesticide signals. As a consequence, it can be stated that acid-base chemistry occurs in the system under study, possibly along with complexation.

The titration experiment carried out between trianglimine **289** and **2,4-D** (Figure 236, Figure 237) gave better results than these presented for the previous pesticides. The

concentration of the trianglimine was 0.29 mM. Unlike the two previous titrations, in this case, the difference in chemical shift in the $-CH_2-$ of the pesticide proton underwent an observable variation along the titration producing the curve shown in Figure 237.

[2,4-D] mM	$\Delta\delta(CH_2)$ ppm
0.106	0.042
0.213	0.276
0.319	0.290
0.341	0.288
0.383	0.284
0.511	0.268
0.553	0.269
0.639	0.263
0.851	0.249

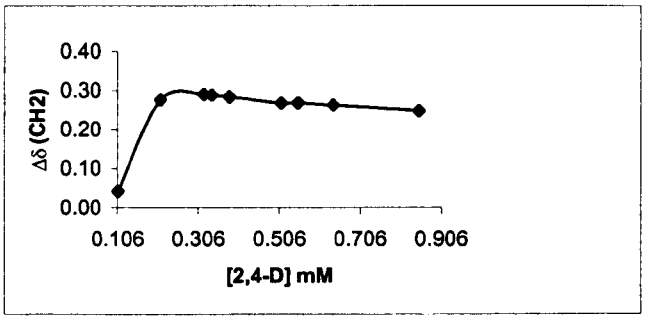

Figure 237: non-linear fitting curve for the titration of trianglimine **289** and **2,4-D**.

In order to determine the stoichiometry of the two interacting components, the method of continuous variation (often known as "job-plot") was used. In the job-plot, the molar fraction of the guest is plotted against the product of $\Delta\delta$ and the molar fraction of the guest. The binding stoichiometry is determined from the ratio of the mole fractions of the two components found at the maximum of the curve. In this particular example, the maximum of the curve shows a host:guest interaction of 1:2. There is, however, a level of uncertainty in this result. The job-plot method is only valid when the total concentration is much greater than the dissociation constant involved in the interaction. Therefore, at concentrations comparable to dissociation constants, the maximum of the curve may not permit an accurate calculation of the binding ratio.[141] In this particular case, it is not clear whether or not the concentration used in this experiment fulfils the appropriate conditions to be sure of the stoichiometric relationship obtained.

Despite the uncertainty about whether or not the host-guest stoichiometry is correct, the binding constant was calculated. The expression of the stepwise equilibrium constants K_{11} and K_{12} for a 1:2 binding model is derived as follows.[142]

$$H + G \overset{K_{11}}{\rightleftharpoons} HG \quad [HG]=K_{11}[H][G]$$

$$H + 2G \overset{K_{12}}{\rightleftharpoons} HG_2 \quad [HG_2]=K_{11}K_{12}[H][G]^2$$

$$\Delta\delta_{obs} = \frac{K_{11}\Delta\delta_{11} + 2K_{11}K_{12}[H]_{free}\Delta\delta_{12}}{1/[G]_{free} + K_{11} + 2K_{11}K_{12}[H]_{free}}$$

The binding constant was obtained from a non-linear least-square fitting using the software package SCIENTIST (Micromath, Salt Lake City, UT). The values for the K_{11} and K_{12} obtained were 60.74 and 1271 M^{-1} respectively (± 10 % error margin). The statistic analysis gave a value of R-squared of 0.92.

In order to clarify whether the pesticide is encapsulated inside the macrocycle cavity, a ^{1}H-^{1}H-NOESY experiment was carried out for a 1:1 ratio, and a strong NOE effect was found between the $-CH_2-$ of the pesticide and the methoxy of the trianglimine. This effect is attributed to the encapsulation of the pesticide in the cavity of the trianglimine.

In order to strengthen the theory of possible binding by entrapment, a DOSY experiment was carried out (Figure 238), using a solution mixture containing **289** and **2,4-D** at [289]=10.2 mM, [2,4-D]=11.5 mM in $CDCl_3$.

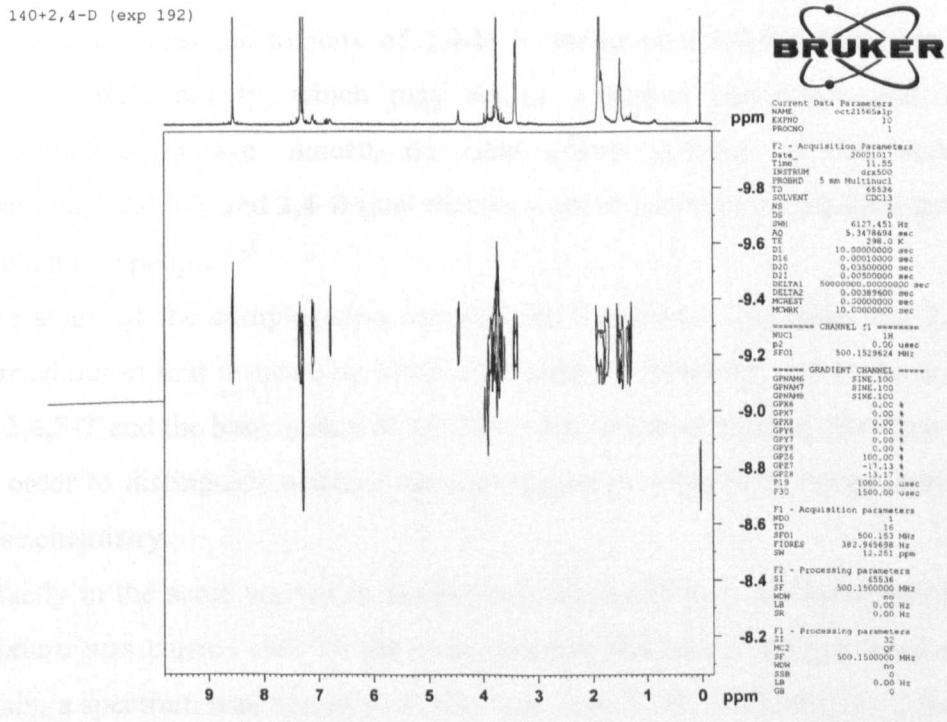

Figure 238: DOSY NMR spectrum of the 1:1 mixture of **289** and **2,4-D**.

Figure 238 shows that the binding seems to be effective, as both host and guest possess the same diffusion coefficient.

The protons of the pesticide **2,4-D** possess the same diffusion coefficient as those of trianglimine **289**, whose value is $5.6x10^{-10}$ m^2/s. In order to verify whether the diffusion coefficient values obtained are reliable, a DOSY experiment of the free pesticide (11.5 mM) was carried out. The value of the diffusion coefficient obtained for the free pesticide was $3.62x10^{-10}$ m^2/s. Therefore, there is an obvious difference between the diffusion coefficients of the free and complexed pesticide, this being the confirmation that the experiment gave dependable results.

The reason why they diffuse at the same speed can be attributed to the binding between the two molecules.

On the other hand, the molecules not bound to the trianglimine, which are the $CDCl_3$ and TMS (at 7.26 and 0.0 ppm respectively), diffuse more rapidly due to their lighter molecular weight.

The results obtained from the titration and the DOSY experiment show that the binding was effective.

25.4 Trianglimine 289 and 2,4,5-T.

As mentioned above, the herbicide **2,4,5-T** was used along with **2,4-D** to form Agent Orange. Whereas the toxicity of **2,4-D** is ambiguous, **2,4,5-T** has been proved to possess high toxicity, which may act as a human carcinogen and also cause reproductive damage. Indeed, the fatal effects (cancer, genetic mutations) of combining **2,4,5-T** and **2,4-D** (and dioxines) are still evident in the third generation of Vietnamese people.[143]

The study of the complexation between the trianglimine receptor and **2,4,5-T** was carried out in first instance by NMR shift titration. However, due to the acidic nature of **2,4,5-T** and the basic nature of the **289**, NMR dilution experiments were carried out in order to distinguish whether the equilibrium between both compounds was acid-base chemistry.

Exactly in the same way as in the previous experiment, a ^{1}H-NMR spectrum of 1:1 mixture was carried out. To the same sample, aliquots of $CDCl_3$ were added and, again, a spectrum was recorded. In this way, four NMR spectra were carried out with the same **289:2,4,5-T** equivalence at several dilutions. The chemical shift of the pesticide was analysed in all spectra recorded. The dilution experiment did not show variation in the chemical shift of the pesticide signals. As a consequence, it can be stated that acid-base chemistry occurs in the system under study and, as in the case of

the dilution experiment of **289** and **2,4-D**, it is highly probable that acid-base chemistry occurs alongside complexation.

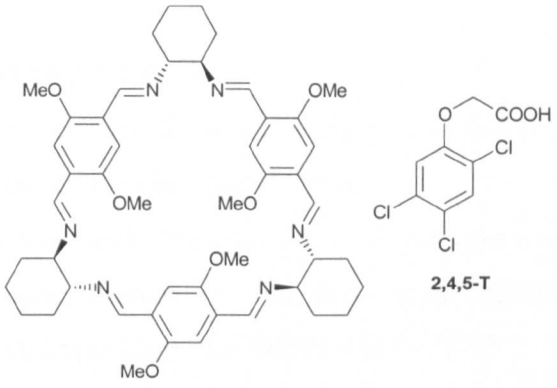

Figure 239: structures of trianglimine **289** and pesticide **2,4,5-T**.

The titration carried out for the trianglimine **289** and **2,4,5-T** (Figure 239) was carried out using a concentration of the trianglimine of 0.29 mM. The titration experiment showed the non-linear fitting curve expected for a complexation experiment.

Δδ(Ar-H) ppm	[2,4,5-T] mM
0.003	0.060
0.018	0.121
0.025	0.182
0.031	0.243
0.032	0.303
0.034	0.364
0.036	0.425
0.040	0.668
0.042	0.911
0.043	1.032
0.044	1.154
0.044	1.336
0.044	1.822

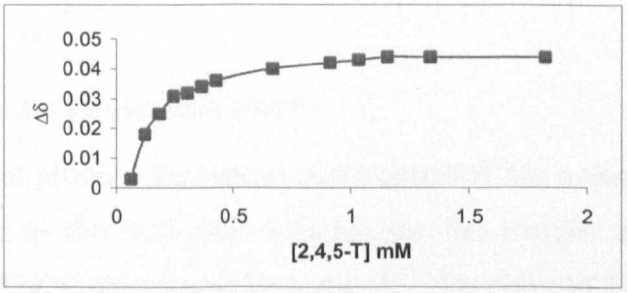

Figure 240: non-linear fitting curve for the titration of trianglimine **289** and **2,4,5-T**.

Although the non-linear fitting curve appears to be appropriate to carry out the calculations for the extraction of the binding constant, it was found (by job-plot analysis), as in the case of the titration of the same trianglimines with **2,4-D**, that the binding stoichiometry of trianglimine:pesticide was again a 1:2 relationship.

In the same way as for the titration experiment of **289** and **2,4-D**, the binding constant was obtained from a non-linear least-square fitting using the software package SCIENTIST (Micromath, Salt Lake City, UT). The values for the K_{11} and K_{12}

obtained were 82 and 1159 M^{-1} (± 10 % error margin) respectively. The statistical analysis gave a value of R-squared of 0.89.

25.5 Trianglimine 289 and 2,4-DCP.

2,4-DCP is employed in the manufacture of the herbicide **2,4-D**, and is so highly toxic that even a small amount on the skin can be lethal.[137]

The same trianglimine was used for the study of the entrapment of 2,4-dichlorophenol (Figure 241). The concentration of the host was **[289]**=0.42 mM, and the concentration of the guest was form **[2,4-DCP]**=0.21 to 1.84.

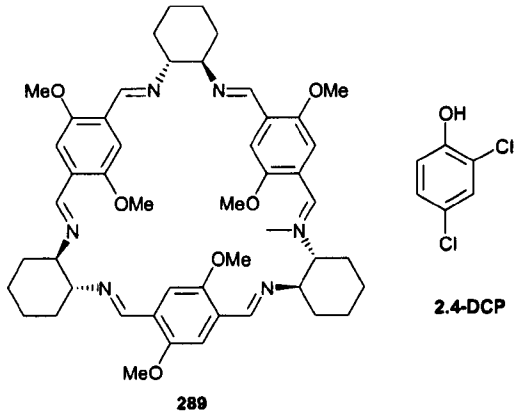

Figure 241: structures of trianglimine **289** and pesticide **2,4-DCP**.

The titration experiment did not produce the typical curve expected for a non-linear fitting curve as the difference in chemical shift between the free sample and the pesticide, in presence of trianglimine was almost imperceptible (the order of 10^{-3}-10^{-4} ppm). Since the ^{1}H-NMR shift titration seemed a non-appropriate technique for this particular system, a DOSY NMR experiment was carried out. The DOSY experiment was carried out with a 1:1 ratio and at a concentration of $1.2x10^{-3}$ mM.

The protons of the pesticide **2,4-DCP** posses the same diffusion coefficient as those of the trianglimine **289**, whose value were $7.51x10^{-10}$ m^2/s. In order to verify whether the diffusion coefficient values obtained were reliable, a DOSY experiment of the free pesticide ($1.2x10^{-3}$ mM) was carried out. The value of the diffusion coefficient obtained for the free pesticide was $9.2x10^{-10}$ m^2/s. Therefore, there is an obvious difference between the diffusion coefficients of the free and complexed pesticide. This can be interpreted as a confirmation that the experiment gave dependable results.

In addition, the diffusion coefficient of $CDCl_3$ ($1.07x10^{-09}$ m^2/s) obtained is very well distinguished, showing a diffusion rate much higher than the diffusion of the host-guest system.

As a consequence it can be assumed that complexation occur at this concentration.

25.6 Trianglimine 289 and 2,4-DP.

2,4-dichlorophenoxypropionic acid is a selective herbicide of the chlorophenoxy class that is widely used by homeowners and lawn care professionals to kill broadleaf plants. Although it is broadly used it has to be handled with care, as some studies have demonstrated that it is a possible carcinogen, as well as causing miscarriage and birth defects in laboratory rats. [137]

No ^{1}H-NMR titration experiment was carried out with this pesticide.

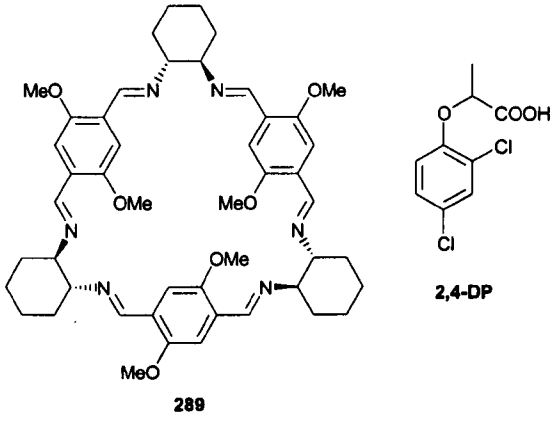

Figure 242: structures of trianglimine **289** and pesticide **2,4-DP**.

The DOSY was carried out with a ratio of trianglimine:pesticide 1:1, and in a concentration of 1.1 mM. The results obtained are shown in Table 9.

Protons of host	**HC=N**	**-OCH_3**	**$CDCl_3$**
Diffusion coefficient (m^2/s)x 10^{-10} (*)	4.02	3.91	7.82
Protons of guest	**Ar-H**	**Ar-H**	
Diffusion coefficient (m^2/s)x 10^{-10} (*)	3.93	3.87	

Table 9: values of the diffusion coefficient obtained from the mixture of **289** and pesticide **2,4-DP**. (*) ± 10 % error margin

The value of the diffusion coefficient obtained from the free pesticide was $5.27x10^{-10}$ m^2/s. This value is quite different from the value obtained form the mixture of the trianglimine and the pesticide. Although there is a slight difference between the diffusion coefficients of host and guest, comparing these values with the value obtained from the free pesticide, it can be assumed that binding is occurring. In

addition, it can be stated that $CDCl_3$ does not bind the host as the diffusion coefficient is much higher (7.82x10 m^2/s).

25.7 Trianglimine 289 and Thiofensulfon.

Thiofensulfon is a low toxicity herbicide, however the risk posed by environmental degradation products is unknown and it has moderate toxicity to fish.[144]

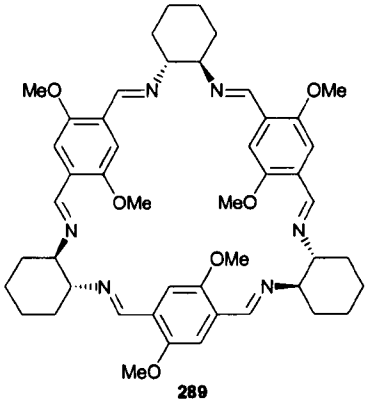

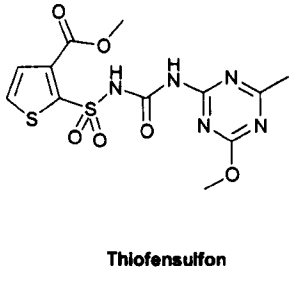

Figure 243: structures of trianglimine and pesticide **289** and **thiofensulfon**.

Thiofensulfon was titrated against trianglimine **289**. The titration did not give the results expected as no significant changes in the chemical shifts were observed. The non-linear fitting curve resulted was parallel to the x-axis, therefore the conclusions obtained from this experiment is that complexation at the concentrations used was unsuccessful.

Alternatively, a DOSY spectrum was carried out. The concentration in which the sample was analysed was 5.08 mM in a 1:1 host:guest ratio. The diffusion coefficients of the protons of the trianglimine (Table 10) were $1.00x10^{-09}$ m^2/s and coincide with the values of the selected protons of the guest. This value is well distinguished from the values of the diffusion coefficients obtained from the free pesticide, that is ($2.7x10^{-9}$ m^2/s).

Protons of host	**Ar-H**	**-OCH_3**	
Diffusion coefficient (m^2/s)x10^{-09}(*)	1.00	1.00	
Protons of guest	**Ar-H**	**Ar-H**	**-OCH_3**
Diffusion coefficient (m^2/s) x10^{-09}(*)	1.06	1.00	1.00

Table 10: values of the diffusion coefficient obtained from the mixture of **289** and pesticide **thiofensulfon**. (*) ± 10 % error margin.

Thus, the result of this experiments show that there is binding between host and guest, although this is not reflected in the titration experiment. As a consequence it can be assumed that the titration procedure is a technique unsuitable for this system.

The ESI mass spectrum of a 1:1 mixture of **thiofensulfon** and trianglimine **289** also shows that there is a peak at *m/z* 1202.9 of 15% intensity, which is the peak corresponding to the molecular ion of the host-guest complex

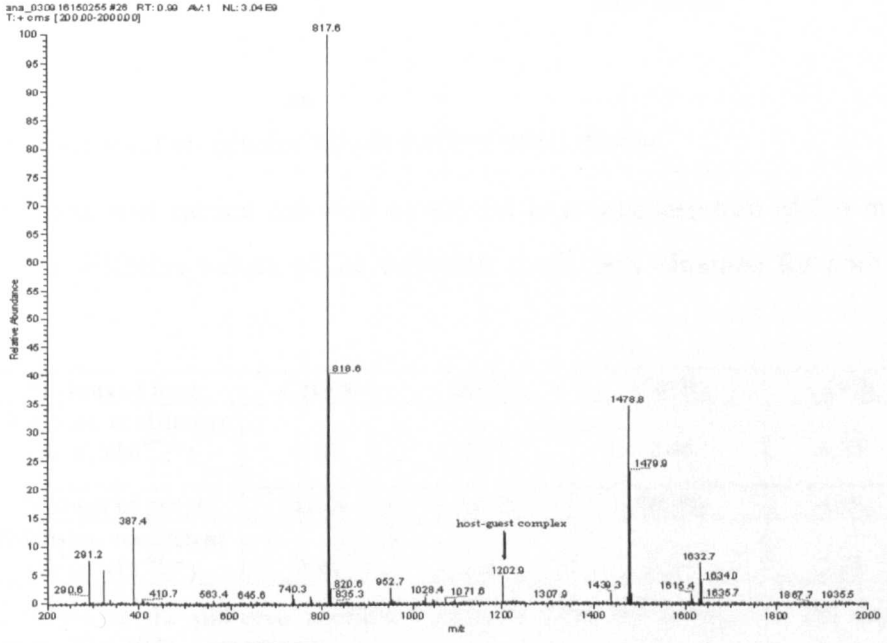

Figure 244: ESI mass spectrum of **thiofensulfon** and trianglimine **289.**

The appearance of this peak provides evidence that host-guest complexation occurs, and supports the results obtained from the DOSY experiment.

25.8 Trianglimine 289 and Chlorsulfuron.

Chlorsulfuron is used for weed control on non-crop sites such as roadsides or rights-of-way. It is classified as a toxic substance and may cause reproductive problems. [137]

As in the previous cases, NMR shift titration was carried out. Unfortunately the non-linear fitting curve did not show the curve expected as no major difference in the chemical shift was observed. However, the results obtained from the DOSY were quite different as the similar values obtained of host and guest suggest that the binding was effective.

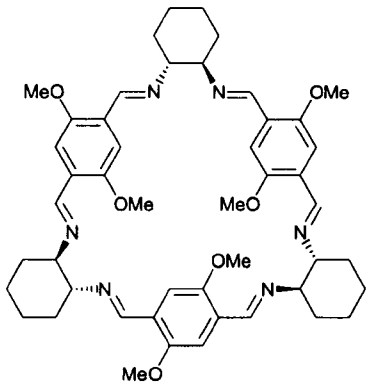

289

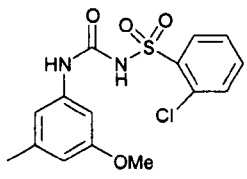

Chlorosulfuron

Figure 245: structures of trianglimine **289** and pesticide **chlorsulfuron**.

The experiment was carried out with a ratio 1:1 at a concentration of 3.6 mM. Table 11 shows the different values of the diffusion coefficient obtained for both host and guest.

Protons of host	**-CH=N-**	**Ar-H**	**$-OCH_3$**	**$CDCl_3$**
Diffusion coefficient (m^2/s) $x10^{-09}$(*)	2.55	2.43	2.46	4.55
Protons of guest	**Ar-H**	**Ar-H**	**$-OCH_3-$**	**$-CH_3$**
Diffusion coefficient (m^2/s) $x10^{-09}$(*)	2.44	2.45	2.57	2.21

Table 11: values of the diffusion coefficient obtained from the mixture of **289** and pesticide **chlorsulfuron**. (*) ± 10 % error margin.

In addition, the value for the diffusion coefficient of the free pesticide was $3.26x10^{-09}$ m^2/s. The definitive evidence showing that effective binding occurs came from the ESI mass spectrum, which shows the peak corresponding to the host-guest complex at 1171 and 1173 $(H:G)^+$ (Figure 246).

The ESI mass spectrum also shows another interesting feature. At 35 % there is a peak at *m/z* 1632, which corresponds to the molecular ion of two molecules of trianglimine **289** together. This result suggests that trianglimines associate with each other to form more complex structures.

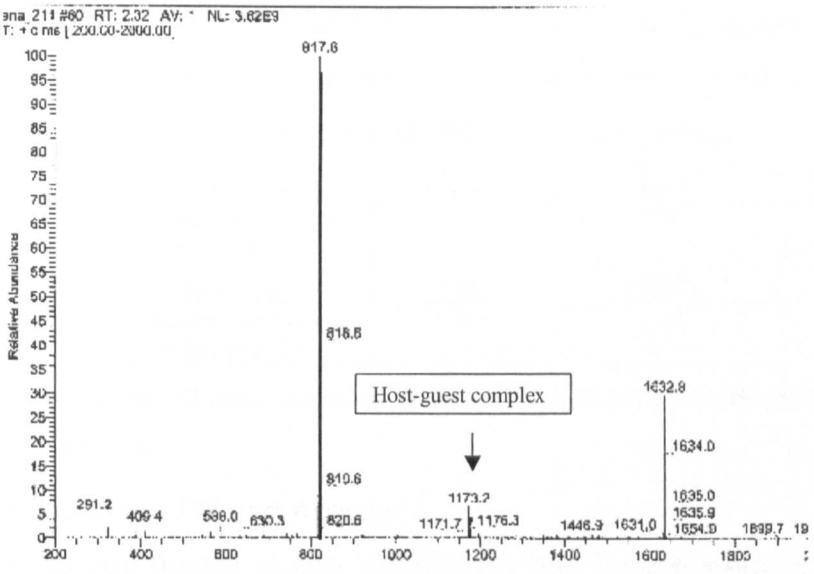

Figure 246: ESI mass spectrum of **chlorsulfuron** and trianglimine **289**.

25.9 Trianglimine 40 and Atrazine.

The titration carried out with this pesticide and trianglimine **40** did not show the results expected as no significant change in the chemical shift was observed during the titration. The results obtained from this experiment are going to be omitted from this thesis.

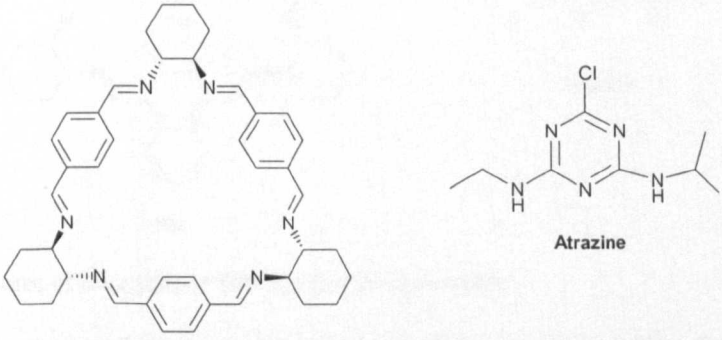

Figure 247: structures of trianglimine **40** and pesticide **atrazine**.

DOSY experiments were carried out in order to contrast the results obtained from the titration. The experiment was carried out with a 1:1 relationship (host:guest) with a concentration of 5.06 mM. The results shown in Table 12 confirm the absence of binding predicted by the ^{1}H-NMR titration. The table shows the values obtained for the diffusion coefficients of both trianglimine and pesticide. The smallest molecule, $CDCl_3$, has a diffusion coefficient of $9.67x10^{-10}m^2/s$, which is a much higher value than the trianglimine diffusion coefficient ($6.85x10^{-10}$ m^2/s). The diffusion coefficient

of the pesticide appears in between these two values. The big difference between the trianglimine and pesticide values and, in comparison with the value of the diffusion coefficient of the free pesticide, suggests that there is no binding.

Protons of host	**-CH=N-**	**Ar-H**	**-CHN=CH-**
Diffusion coefficient (m^2/s)x10^{-10}(*)	6.85	6.83	6.82
Protons of guest	**CH_3**	**$CDCl_3$**	
Diffusion coefficient (m^2/s) x10^{-10}(*)	7.85	9.67	

Table 12: values of the diffusion coefficient obtained from the mixture of **40** and pesticide **atrazine**. (*) ± 10 % error margin.

25.10 Trianglimine 300 and Atrazine.

Atrazine was also titrated against trianglimine **300**, but the results obtained were as negative as the previous one. No difference in chemical shift was observed. Further experimentation was abandoned in the case of trianglimine **289**. DOSY experiments were carried out with trianglimine **300** instead.

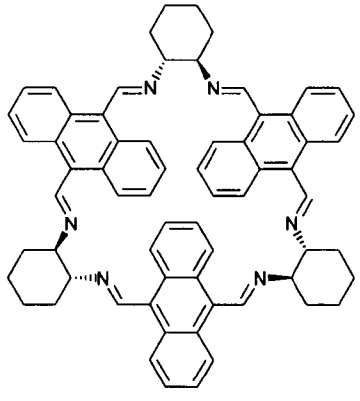

300

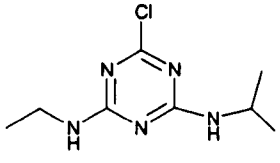

Atrazine

Figure 248: structures of trianglimine **300** and pesticide **atrazine**.

The sample was prepared with a 1:1 host-guest relation and at 2.27 mM concentration. The values obtained are shown in Table 13.

Protons of host	**-CH=N-**	**Ar-H**	**-CHN=CH-**
Diffusion coefficient (m^2/s) x10^{-10}(*)	5.34	5.24	5.89
Protons of guest	**CH_3**	**$CDCl_3$**	
Diffusion coefficient (m^2/s) x10^{-10}(*)	5.50	8.39	

Table 13: values of the diffusion coefficient obtained from the mixture of **300** and pesticide **atrazine**. (*) ± 10 % error margin.

As was already mentioned, the drawback of DOSY experiments is the lack of accuracy in the results obtained from NMR signals that are not singlets. In the case of trianglimine **300**, the values obtained from the aromatic region are not very consistent as it is an AA'XX' spin system.

The signal of the pesticide and trianglimine are overlapped at 2 ppm and also there is a water signal that hides another pesticide peak. Therefore, the only one observed is at 1.22 ppm (-CH_3-) whose value is $5.50x10^{-10}m^2/s$. The diffusion coefficient of the free pesticide at the same concentration (2.27 mM) has a value of $7.78 x10^{-10} m^2/s$.

Table 13 shows very similar diffusion coefficients between host and guest that suggests that binding probably occurs.

25.11 Trianglimine 300 and Propazine.

The same trianglimine was used to study the binding with the herbicide **propazine**. As the titration carried out with other Triazine compounds did not provide useful results, the DOSY experiment was the only test for binding carried out.

Propazine is an herbicide used for control of broadleaf weeds and is classified as a moderately toxic herbicide.[137]

The ratio of host:guest was 1:1 and the concentration was 2.23 mM.

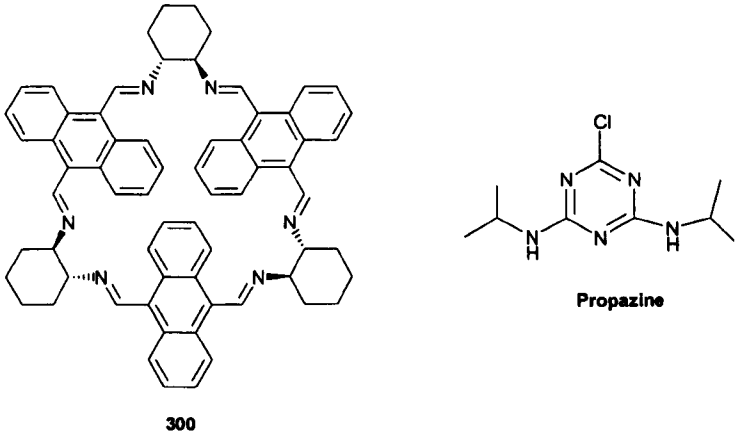

Figure 249: structures of trianglimine **300** and pesticide **propazine**.

The values obtained are shown in Table 14.

Protons of host	**-CH=N-**	**Ar-H**	**-CH_2-**	**$CDCl_3$**
Diffusion coefficient (m^2/s)x10^{-10}(*)	4.62	4.63, 4.64	4.48	7.65
Protons of guest	**CH**	**-CH_2-**		
Diffusion coefficient (m^2/s) x10^{-10} (*)	4.84	4.60		

Table 14: values of the diffusion coefficient obtained from the mixture of **300** and pesticide **propazine**. (*) ± 10 % error margin.

Table 14 shows very similar diffusion coefficients of host and guest which suggests it is quite probable binding that occurs.

The diffusion coefficient of the free pesticide at the same concentration (2.23 mM) was determined to be 6.78×10^{-10} m^2/s, a value higher than the determined in the mixture, which reinforces the theory that binding may occur.

There are many examples in the literature[142] in which binding was demonstrated by ^{1}H-NMR shift titrations experiments, whose binding constants were obtained from the experimental data. However, ^{1}H-NMR shift titrations cannot always be applied for every host-guest system. In this chapter it has been shown that NMR shift titration is not a suitable technique to apply in some systems due to the low solubility of the trianglimines.

Diffusion NMR was shown to be a valuable technique in determining qualitative binding.

CONCLUSIONS

Conclusions

The first part of this thesis dealt with novel synthetic methodology for the synthesis of aromatic dialdehydes. Indeed, this type of compound could be conveniently synthesised using different approaches. The initial method proposed was the double lithium-bromide exchange reaction, from dibrominated precursors. The yields obtained varied from good to poor depending on the method and substrates used and, in some cases, it was observed that poor yields were obtained when more that one step was involved in the synthesis. However the required materials were obtained in sufficient quantities for the use in macrocyclisation reactions.

The second method for the synthesis of aromatic dialdehydes uses the lithium-hydrogen exchange reaction using *ortho*-metalation approach. It appeared that the OMe group is an excellent stabilising group for *ortho*-metalation and allows the generation of dilithiated intermediates, and hence the successful synthesis of aromatic dialdehydes. In substrates with lithium substituents on two separated aromatic nuclei, again dilithiation proceeds smoothly and gives the dialdehydes in good yields. The use of a sequential dilithiation also allowed the preparations of the corresponding dialdehydes in good yields. All compounds synthesised were highly useful intermediates in trianglimine synthesis. Moreover, all compounds synthesised can be potentially useful intermediates in organic synthesis.

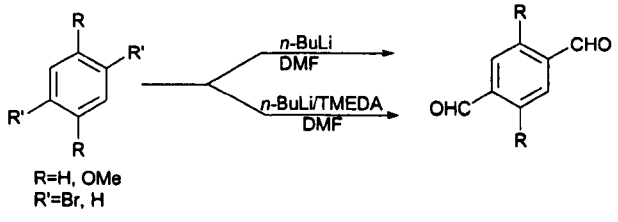

All the aromatic dialdehydes synthesised have successfully undergone macrocyclisation reactions with (1*R*, 2*R*)-diaminocyclohexane giving hexaimine and hexaamine macrocycles with ring sizes from 27 to 42.

In the majority of the reactions, trianglimine macrocycles were the only products of a [3+3]-cyclocondensation, however is some cases the [2+2]-cyclocondensation products were obtained instead.

The general feature for both [2+2]- and [3+3]-cyclocondensation products is that they adopt the conformation of highest possible symmetry in solution.

The conformation adopted by the trianglamines and [2+2]-cyclocondensation products in solution follow, in all cases, the same pattern. For the minimum energy conformation a NOE effect is observed between the imine proton and the axial proton of the diaminocyclohexane ring (shown below).

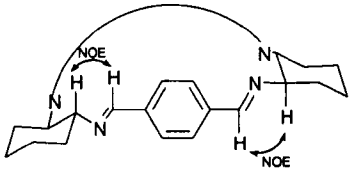

The formation of [2+2]-cyclocondensation products was shown to be, in various cases, the result of thermodynamic control of the macrocyclisation reaction. In some cases the trianglimines seem to be the kinetic product of the macrocyclisation reaction. However, a series of crossover experiments demonstrated the reversibility of the macrocyclisation reaction and lead to the conclusion that trianglimines can be the products of thermodynamic control of the reaction.

The reduction of the trianglimines to obtain a new set of trianglamine macrocycles was also successfully achieved, although in some cases the characterisation was extremely difficult.

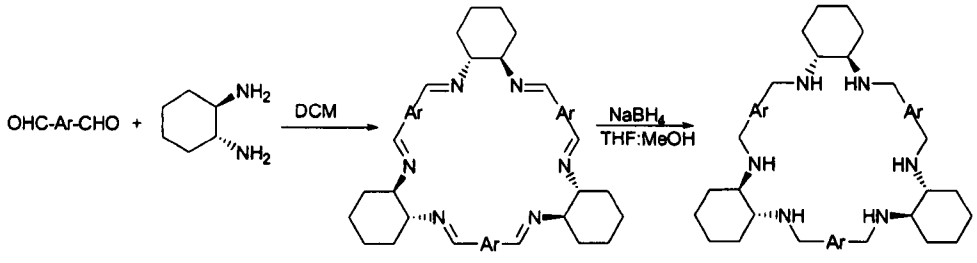

The final objective of this thesis was the study of the entrapment of commercial pesticides by some of the trianglimines synthesised. Binding of a commercial available pesticide by trianglimine **274** was supported by diffusion NMR and ESI-MS. In this respect, the goal of binding a commercial pesticide within a trianglimine receptor has been achieved.

Although there are many examples in which NMR-shift titration experiments seem to be a suitable technique to carry out binding studies, in the cases we have studied, it did not give the results expected. This was assumed to be due to the low solubility of the trianglimines, which makes this technique unsuitable for the study of complexation. Nevertheless, the use of diffusion NMR techniques showed to produce reliable results and in some of examples, showed the achievement of complexation between the synthetic host and the pesticide guest.

PART III

EXPERIMENTAL

26. General experimental.

^{1}H and ^{13}C NMR spectra were recorded on either a JEOL 270MHz, Bruker AC 300 MHz or a DRX 500 MHz spectrometer. Chemical shifts are reported as δ values in ppm relative to the solvent $CDCl_3$ as an internal standard (δ 7.26), or TMS (δ 0.00) when d_6-DMSO is used. Coupling constants (*J* and *N*) are reported in Hertz. Peak assignments in the proton NMR are abbreviated as follows: s= singlet, d=doublet, dd=doublet of doublets, t=triplet and m=multiplet.

Elemental analysis was made on a Leeman Labs CE440 Elemental Analyser. The optical rotation was measured in a Bellingham-Stanley ADP220 automatic polarimeter (L.E.D. with interference filter, 589 nm). Infrared spectra were determined on a Perkin Elmer 2000 Spectrometer. The EI, CI, LSMS and FAB data were collected on a ThermoFinnigan Mat 95 X. Additional LSIMS were recorded either by *EPSRC National Mass Spectrometry Service Centre, Swansea* or a ThermoFinnigan Mat 95 X. All The ESI-MS was recorded on a ThermoFinnigan DECA CQXP Plus. X-ray crystallography was determined by *Dr Burzlaff, Universität Konstanz.*

TLC plates were Merck Aluminium oxide or SiO_2. The typical solvent system for TLC being 1:3 petroleum ether (40-60): diethyl ether.

All chemicals/reagents were purchased from the either Aldrich Chemical Company, Acros or Lancaster, and used without further purification.

Solvents were dried and purified according to standard procedures.[145] Melting points were determined on a Kofler hot-stage apparatus and are uncorrected.

The elemental analysis is very often unreliable because of inclusion of solvent molecules and as such cannot be regarded as an appropriate criterion of purity, however, the identity of the compounds synthesised has been supported by other spectroscopic data. The same feature was observed in the elemental analysis of other macrocycles such as calixarenes, where several authors demonstrate that the inclusion of solvent molecules, as well as common solvent impurities in the macrocycle cavity perturbs the results of elemental analysis.[146,147]

The synthesis of trianglimines is a new topic in the field of supramolecular chemistry where the background is reduced to a few publications. The elemental analysis carried out by other authors, showed inclusion of solvent molecules such as ethyl acetate in trianglimine **40**, corroborated by a single crystal X-ray analysis.[42]

Some of the elemental analysis data presented in this thesis differ from the theoretical value expected. These results can be explained by the presence of solvent molecules.

Where solvents are proposed to be included, the corresponding spectroscopic data confirms their presence.

1,4-Dimethoxy-2,5-diformylbenzene-158.[91]

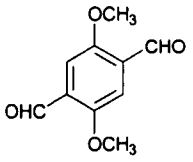

n-Butyllithium 2.5 M in hexane (4.8 ml, 10 mmol) was added to a solution of 1,4-dibromo-2,5-dimethoxybenzene **232** (1.0 g, 3.3 mmol) in dry THF (20 ml) at –78°C under nitrogen atmosphere and stirred for 2 hours at the same temperature. To the reaction mixture DMF (3.0 ml, 39 mmol) was added and the solution stirred for 60 min. The reaction mixture was allowed to warm to room temperature and 10 ml of hydrochloric acid as added. The yellow solid was filtered by suction. After drying in vacuum the title compound **158** was obtained as yellow crystals (0.4 g, 60 %); mp. 193-195°C (lit. 190 °C); IR ν_{max}(Nujol)/cm^{-1} 1682 (CHO); ^{1}H-NMR (270 MHz; $CDCl_3$) δ_H 10.52 (2H, s, C*H*O), 7.55 (2H, s, Ar-*H*), 4.03 (6H, s, -OC*H*$_3$); ^{13}C-NMR (67.8 MHz; $CDCl_3$) δ_C 189.6, 156.0, 129.4, 111.1, 56.3; MS (EI) *m/z* (194 M$^+$, 100%); CHN requires for $C_{10}H_{10}O_4$: C 61.8 %, H 5.2 %. Found: C 61.4 %, H 5.2 %.

4,4′-Diformylbiphenyl-87.[64]

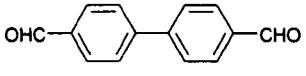

n-Butyllithium 2.5 M in hexane (6.0 ml, 15 mmol) was added to a solution of 4,4′-dibromobiphenyl **233** (1.0 g, 3.2 mmol) in dry THF (20 ml) at –78°C under nitrogen atmosphere and stirred for 2 hours at the same temperature. To the reaction mixture DMF (3.0 ml, 39 mmol) was added and the solution was stirred for 30 min. The reaction mixture was allowed to warm to room temperature, and 10 ml of 3N hydrochloric acid was added. The organic layer was separated and the aqueous layer was extracted with diethyl ether (3x15 ml). The extracts were combined, washed with 10 ml of sodium hydrogencarbonate and 10 ml of brine and dried over anhydrous $MgSO_4$. The solvent was evaporated in vacuum to give the title compound **84** as white crystals (0.34 g, 50 %); mp. 116–118°C (lit. 120°C); IR ν_{max}(Nujol)/cm^{-1} 1686 (C=O); ^{1}H-NMR (270 MHz; $CDCl_3$) δ_H 10.10 (2H, s, C*H*O), 8.01 (4H, d, *J* 8.1 Hz, Ar-*H*), 7.81 (4H, d, *J* 8.4, Ar-*H*); ^{13}C-NMR (67.8 MHz; $CDCl_3$) δ_C 192.1, 145.8, 136.2, 130.6, 128.3; MS (EI) *m/z*: 210 (M$^+$, 100%); CHN requires for $C_{14}H_{10}O_2$: C 79.9 %, H 4.7 %. Found: C 79.5 %, H 4.7 %.

9,10-Diformylanthracene-235.[119]

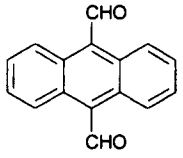

n-Butyllithium 2.5 M in hexane (6.0 ml, 15 mmol) was added to a solution of 9,10-dibromoanthracene **234** (1.2 g, 3.57 mmol) in dry THF (20 ml) at –78°C under nitrogen atmosphere and stirred for 2 hours at the same temperature. To the reaction mixture DMF (3.0 ml, 39 mmol) was added and the solution was stirred for 30 min. The reaction mixture was allowed to warm to room temperature, and 5 ml of 3N hydrochloric acid was added. The yellow solid was filtered and dried in vacuum and recrystallised from diethyl ether to give the title compound **235** as orange needles (0.37 g, 40 %); mp. 215°C (lit. 230 °C); IR ν_{max}(Nujol)/cm^{-1} 1673 (C=O); ^{1}H-NMR (270 MHz; $CDCl_3$) δ_H 11.50 (2H, s, CHO), 8.71 (4H, AA′XX′ spin system, *N* 10.0, Ar-*H*), 7.63 (4H, AA′XX′ spin system, *N* 9.7, Ar-*H*); ^{13}C-NMR (67.5 MHz; $CDCl_3$) δ_C 194.7, 130.5, 128.6, 124.5, 122.5; MS (EI) *m/z* 234 (M^+, 100%).

4,4'-Bis(formyl)phenyl-ether-237.

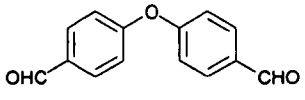

n-Butyllithium 1.6 M in hexane (6.9 ml, 11 mmol) was added to a solution of of bis-4-bromophenyl-ether (**236**) (1.45 g, 4.42 mmol) in dry THF (10 ml) at –78°C under nitrogen atmosphere and stirred for 2 hours at the same temperature. To the reaction mixture DMF (0.85 ml, 11 mmol) was added and the solution was stirred 30 min. The reaction mixture was allowed to warm to room temperature, and 7 ml of 3N hydrochloric acid was added. The organic layer was separated and the aqueous layer was washed with diethyl ether (3x15 ml). The extract was dried over Na_2SO_4, filtered, the solvents were removed in vacuum and the solids were recrystallised from petroleum ether, to give the title compound **237** as colourless crystals (0.27 g, 27 %); mp. 140 °C; IR ν_{max}(Nujol)/cm^{-1} 1676 (C=O); ^{1}H-NMR (500 MHz; $CDCl_3$) δ_H 9.98 (2H, s, C*H*O), 7.92 (4H, d, *J* 8.6, Ar-*H*), 7.18 (4H, d, *J* 8.6, Ar-*H*); ^{13}C-NMR (67.8 MHz; $CDCl_3$) δ_C 190.8, 161.2, 132.3, 132.2, 119.6; MS (CI) *m/z* 227 (M^+, 100%); CHN requires for $C_{14}H_{10}O_3$, C 74.3 %, H 4.4 %. Found: C 74.2 %, H 4.3 %.

3,6-Dibromo-9-N-methylcarbazole-239.[120]

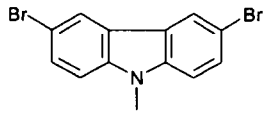

Dimethyl sulphate (0.11 ml, 1.16 mmol) was added dropwise over 15 minutes at room temperature to a stirred solution of 3,6-dibromocarbazole **238** (0.27 g, 0.83 mmol) and NaOH pellets (0.03 g, 0.8 mmol). The reaction was stirred for 8 hours and all solids were removed by filtration and the solvent was removed in vacuum to give a white solid. The residue was dissolved in ethyl acetate (5.4 ml) and washed with aqueous saturated $NaHCO_3$ (3x2 ml), brine (3x2 ml) and water (3x2 ml). The organic layer was dried over Na_2SO_4, filtered and the solvent removed to give the title compound **239** as a white powder (0.16 g, 56 %); mp. 140 °C (lit 139-141 °C); ^{1}H-NMR (270 MHz; $CDCl_3$) δ_H 8.13 (2H, s, $H_{4,5}$), 7.54 (2H, d, J 8.6, $H_{2,7}$), 7.23 (2H, d, J 8.9, $H_{1,8}$), 3.76 (3H, s, -CH_3); ^{13}C-NMR (67.8 MHz, $CDCl_3$) δ_C 129.7, 129.3, 123.4, 123.2, 121.8, 110.3, 29.5 ; MS (EI) *m/z* 336/338/340 (M^+, 100%), CHN requires for $C_{13}H_9Br_2N$: C 46.0 %, H 2.6 %, N 4.1 %. Found: C 46.0 %, H 2.6 %, N 3.5 %.

3,6- Dibromo-9-N-allylcarbazole-222.

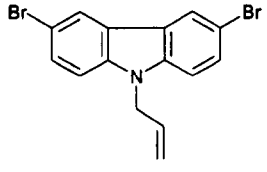

Allylbromide (0.10 ml, 1.13 mmol) was added dropwise to a stirred solution of benzyl triethylammonium chloride (4.52 mg, 0.02 mmol), aqueous 50 % sodium hydroxide solution (1 ml) and 3,6-dibromocarbazole **220** (265 mg, 0.76 mmol) in 2-butanone (1 ml). The mixture was stirred at 50 °C for 2 hours. The reaction mixture was poured into 10 ml of hot water and left to cool to room temperature. The solids were filtered and the residue was recrystallised from ethanol, to give the title compound **222** as white needles (0.17 g, 59 %); mp. 185 °C; ^{1}H-NMR (270 MHz; $CDCl_3$) δ_H 8.03 (2H, s, $H_{4,5}$); 7.54 (2H, d, J 8.6, $H_{2,7}$), 7.23 (2H, d, J 8.9, $H_{1,8}$), 5.85 (1H, m, CH_2C=CH), 5.13 (1H, d, J 10, CH=C$H_{2(cis)}$), 4.85 (2H, d, J 17, CH=C$H_{2(trans)}$), 4.84 (2H, s, CH_2); MS (EI) *m/z* 365/367/369 (M^+, 100%); CHN requires for $C_{15}H_{11}Br_2N$: C; 49.3, H; 3.0, N; 3.8 %. Found C; 49.0, H; 2.9, N; 3.6 %.

3,6- Dibromo-9-N-ethylcarbazole -241.[120]

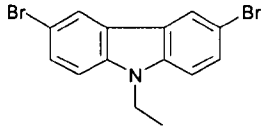

Bromoethane (0.07 ml, 0.93 mmol) was added dropwise to a stirred solution of 2,3-dibromocarbazole **238** (200 mg, 0.70 mmol), benzyl triethylammonium chloride (10 mg), and aqueous 50 % sodium hydroxide solution (1 ml) in 2-butanone (1 ml). The mixture was stirred at 60 °C for 3 hours. The reaction mixture was poured into hot water and left to cool to room temperature. The solids were filtered the residue was recrystallised from ethanol to give the title compound **241** as white needles (0.34 mg, 98 %); ^{1}H-NMR (270 MHz; $CDCl_3$) δ_H 8.15 (2H, s, $H_{4,5}$), 7.56 (2H, d, *J* 8.6, $H_{2,7}$), 7.27 (2H, d, *J* 8.9, $H_{1,8}$), 4.31 (2H, q, *J* 7.2, CH_2), 1.40 (3H, t, *J* 7.2, CH_3); ^{13}C-NMR (67.8 MHz, $CDCl_3$) δ_C 139.0, 129.1, 124.6, 123.0, 110.9, 109.9, 38.0, 14.0; MS (EI) *m/z* 353/355/357 (M^+, 100%); CHN requires for $C_{14}H_{11}Br_2N$: C 47.6 %, H 3.1 %, N 3.9 %. Found: C 46.7 %, H 3.0 %, N 3.8 %.

3,6- Diformyl- 9-N-ethylcarbazole -79.[55]

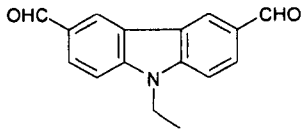

n-Butyllithium 2.5 M in hexane (1.41 ml, 3.54 mmol) was added to a solution of 3,6-dibromoethylcarbazole **241** (250 mg, 0.708 mmol) in dry THF (4 ml) at –78°C under nitrogen atmosphere and stirred for 2 hours at the same temperature. To the reaction mixture DMF (0.27 ml, 3.54 mmol) was added and the solution was stirred for 30 min. The reaction mixture was allowed to warm to room temperature, and 2 ml of 3N hydrochloric acid was added. The organic layer was separated and the aqueous layer was washed with diethyl ether (3x20 ml). The extract was dried over Na_2SO_4, filtered, the solvents were removed in vacuum and the solids were recrystallised from a mixture of (3:1) diethyl ether: petroleum ether, to give the title compound **79** as yellow crystals (0.05 g. 28 %); mp. 150 °C (lit 158 °C); ^{1}H-NMR (270 MHz; $CDCl_3$) δ_H 10.14 (2H, s, C*H*O), 8.68 (2H, s, $H_{4,5}$), 8.09 (2H, d, *J* 8.4, $H_{2,7}$), 7.56 (2H, d, *J* 8.4, $H_{1,8}$), 4.45 (2H, q, *J* 7.2, NCH_2), 1.40 (3H, t, *J* 7.2, CH_3); ^{13}C-NMR (67.8 MHz, $CDCl_3$) δ_C 191.7 (*C*HO), 144.5 (C_3), 129.9 (C_4), 128.1 (C_{ar}-*C*-N), 124.7 (C_1), 124.5 (C_2), 109.7 (C_4), 38.6 (CH_2), 11.1 (CH_3); MS (EI) *m/z* 251.2 (M^+, 100%); CHN

requires for $C_{16}H_{13}O_2$: C 76.5 %, H 5.2 %, N 5.5 %. Found: C 75.7 %, H 5.1 %, N 5.1 %.

1,5-Dihydroxy- 2,6-dibromonaphtalene -244.[121]

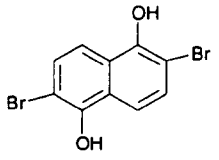

1,5-Dihydroxynaphthalene **243** (0.5 g, 3.12 mmol) was dissolved in 17.5 ml of glacial acetic acid, and the mixture heated at 80 °C. At this temperature bromine (0.32 ml, 6.24 mmol) was added dropwise. After 4 hours, the reaction mixture was allowed to warm to room temperature, and 10 ml of H_2O was added. The solid was filtered and dried in vacuum to give the title compound **243** as a black powder (0.85 g, 85 %); mp. 210 °C (lit. 215 °C); IR ν_{max}(Nujol)/cm^{-1} 3396, 650; ^{1}H-NMR (500 MHz; $CDCl_3$) δ_H 9.98 (2H, s, -O*H*), 7.54 (1H, d, *J* 9, Ar-*H*), 7.45 (2H, d, *J* 9, Ar-*H*); ^{13}C-NMR (67.8 MHz; $CDCl_3$) δ_C 149.0, 128.9, 124.4, 116.0, 105.6; MS (EI) *m/z* 316/318/320 (M^++H, 100%).

1,5-Dimethoxy- 2,6-dibromonaphthalene -245.[123]

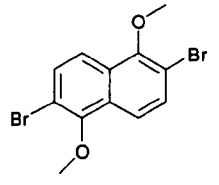

DMSO (1.8 ml) was added to powdered KOH (0.42 g, 56 mmol). After stirring for five minutes, 1,5-dihydroxy-2,6-dibromonaphtalene **244** (0.298 g, 0.93 mmol) was added followed immediately by iodomethane (0.46 ml, 7.49 mmol). The reaction mixture was stirred for 6 hours at room temperature, after which time 15 ml of H_2O was added. The precipitate was filtered and dried in vacuum to give the title compound **245** as a brown powder (0.2 g, 61 %); mp. 250 °C (220°C); IR ν_{max}(Nujol)/cm^{-1} 700; ^{1}H-NMR (500 MHz; $CDCl_3$) δ_H 7.78 (2H, d, *J* 8.8, Ar-*H*), 7.62 (2H, d, *J* 8.8, Ar-*H*), 3.99 (6H, s, -OC*H*$_3$); ^{13}C-NMR (67.8 MHz; $CDCl_3$) δ_C 153.6 (*C*$_1$ and *C*$_5$), 131.3 (*C*$_7$ and *C*$_3$), 129.8 (*C*$_9$ and *C*$_{10}$), 119.6 (*C*$_8$ and *C*$_4$), 113.7 (*C*$_2$ and *C*$_6$), 41.1 (*C*$_{1\text{-OMe}}$ and *C*$_{5\text{-OMe}}$); MS (EI) *m/z* 344/346/348 (M^+, 100%).

1,5-Dimethoxy -2, 6-diformylnaphthalene- 246.

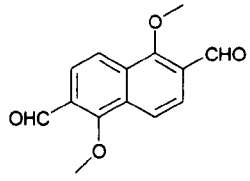

n-Butyllithium 2.5 M in hexane (1.25 ml, 2 mmol)) was added to a solution of 1,5-dimethoxy- 2,6-dibromonaphthalene **245** (0.17 g, 0.5 mmol) in dry THF (5 ml) at -78°C under nitrogen atmosphere and stirred for 2 hours at the same temperature. To the reaction mixture DMF (0.15 ml, 2 mmol) was added and the solution was stirred for 30 min. The reaction mixture was allowed to warm to room temperature, and 3 ml of 3N hydrochloric acid was added. The precipitate was filtered and dried in vacuum to give the title compound **246** as a yellow powder (16 mg, 13 %), mp. 180 °C; IR ν_{max}(Nujol)/cm^{-1} 1672 (C=O); ^{1}H-NMR (500 MHz; $CDCl_3$) δ_H 10.61 (2H, s, C*H*O), 8.08 (2H, d, *J* 8.7, Ar-*H*), 7.96 (2H, d, *J* 8.7, Ar-*H*), 4.14 (6H, s, -OCH_3); ^{13}C-NMR (67.8 MHz; $CDCl_3$) δ_C 189.6, 150.0, 124.1, 123.8, 119.8, 117.4, 66.1; MS (EI) *m/z* 245 (M^++H, 100%); CHN requires for $C_{14}H_{10}O_4$: C 68.8 %, H 4.9 %. Found C 68.5 %, H 4.7 %.

2,7-Dimethoxynaphthalene -211.[124]

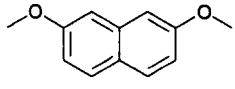

DMSO (12 ml) was added to powdered KOH (2.80 g, 50 mmol). After stirring for five minutes, 2,3-dihydroxynaphthalene **247** (1 g, 6.24 mmol) was added followed immediately by iodomethane (1.55 ml, 25 mmol). The reaction mixture was stirred for 24 hours at room temperature, after which time 15 ml of H_2O was added. The precipitate was filtered and dried in vacuum to give the title compound **211** as a yellow powder (0.8 g, 68 %); mp. 139 °C (lit. 118°C); IR ν_{max}(Nujol)/cm^{-1}1627, 1228; ^{1}H-NMR (500 MHz; $CDCl_3$) δ_H 7.65 (2H, d, *J* 9, $H_{4,5}$), 7.06 (2H, s, $H_{1,8}$), 6.99 (2H, d, *J* 8.8, $H_{3,6}$), 3.91 (6H, s, -OCH_3); ^{13}C-NMR (67.8 MHz; $CDCl_3$) δ_C 158.4 (C_2, C_7), 135.6 (C_9), 129.3 (C_4, C_5), 124.5 (C_{10}), 116.2 (C_3, C_6), 105.4 (C_1, *C8*), 55.4 (-OCH_3); MS (CI) *m/z* 189 (M^++H, 100%).

2,3-Dimethoxynaphthalene-249.[125]

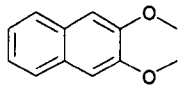

DMSO (12 ml) was added to powdered KOH (2.80 g, 50 mmol). After stirring for five minutes, 2,7-dihydroxynaphthalene **248** (1 g, 6.24 mmol) was added followed immediately by iodomethane (1.55 ml, 25 mmol). The reaction mixture was stirred for 24 hours at room temperature, after which time 15 ml of H_2O was added. The precipitate was filtered and dried in vacuum to give the title compound **249** as white crystals (0.9 g, 77 %); mp. 106 °C (lit 107.5 °C); IR ν_{max}(Nujol)/cm^{-1} 1629, 1224; ^{1}H-NMR (500 MHz; $CDCl_3$) δ_H 7.69 (2H, AA'XX' spin system, *N* 9.3, Ar-H), 7.33 (2H, AA'XX' spin system, *N* 9.3, Ar-H), 7.12 (2H, s, Ar-*H*), 4.0 (6H, s, -OC*H*$_3$); ^{13}C-NMR (67.8 MHz; $CDCl_3$) δ_C 149.6 (*C*$_2$, *C*$_3$), 129.4 (*C*$_9$, *C*$_{10}$), 126.5 (*C*$_5$, *C*$_8$), 124.4 (*C*$_6$, *C*$_7$), 106.5 (*C*$_1$, *C*$_4$), 56.0 (-O*C*H$_3$); MS (CI) *m/z* 189 (M$^+$+H, 100%).

2,3-Diethoxynaphthalene- 250.[126]

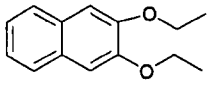

DMSO (12 ml) was added to powdered KOH (2.80 g, 50 mmol). After stirring for five minutes, 2,3-dihydroxynaphthalene **248** (1 g, 6.24 mmol) was added followed immediately by iodoethane (3.88 ml, 25 mmol). The reaction mixture was stirred for 24 hours at room temperature, after which time 15 ml of H_2O was added. The precipitate was filtered and dried in vacuum to give the title compound **250** as white crystals (0.3 g, 22 %); mp 98 °C (lit. 90 °C); IR ν_{max}(Nujol)/cm^{-1} 1259; ^{1}H-NMR (500 MHz; $CDCl_3$) δ_H 7.58 (2H, AA'XX' spin system, *N* 9.0, Ar-H), 7.65 (2H, AA'XX' spin system, *N* 9.3, Ar-H), 7.05 (2H, s, H$_{1,4}$), 4.21 (4H, q, *J* 7.1, -C*H*$_2$-), 1.54 (6H, t, *J* 7.1, -CH$_3$); MS (EI) *m/z* 217 (M$^+$+H, 100%).

1,4-Dibromo-2,3-dihydroxynaphthalene -252.[127]

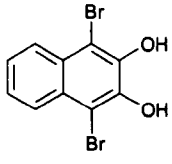

2,3-Dihydroxynaphthalene **248** (0.5 g, 3.12 mmol) was dissolved in 17.5 ml of glacial acetic acid, and the mixture heated at 80 °C. At this temperature bromine (0.32 ml, 6.24 mmol) was added dropwise. After 4 hours, the reaction mixture was mixture was allowed to warm to room temperature, and 10 ml of H_2O was added. The precipitate

was filtered and dried in vacuum to give the title compound **225** as green needles (0.75 g, 75 %); mp. 150 °C (lit 175 °C) ; IR ν_{max}(Nujol)/cm^{-1} 3459; ^{1}H-NMR (500 MHz; DMSO) δ_H 10.10 (2H, s, -O*H*), 7.87 (2H, AA'XX' spin system, *N* 10, Ar-H), 7.36 (2H, AA'XX' spin system, *N* 9.8, Ar-H); ^{13}C-NMR (67.8 MHz; $CDCl_3$) δ_C 144.9 (C_2, and C_3), 127.2 (C_9 and C_{10}), 125.5 (C_6 and C_7), 125.4 (C_5 and C_8), 105.8 (C_1 and C_4); MS (CI) *m/z* 316/318/320 (M^++H, 100%).

1,3-Diformyl-5-methylbenzene -269.

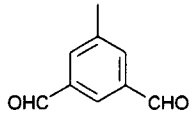

n-Butyllithium 2.5 M in hexane (1.6 ml, 4 mmol) was added to a solution of 3,5-dibromotoluene **268** (1.0 g, 4 mmol) in dry THF (20 ml) at –78°C under nitrogen atmosphere and stirred for 2 hours at the same temperature. To the reaction mixture was added 0.3 ml (4 mmol) DMF at the same temperature and the solution stirred for 30 min. Then, 4 ml (12 mmol) of *n*-butyllithium (2.5 M in hexane) was added. After 30 minutes, DMF (0.93 ml, 12 mmol) was added to the reaction mixture and stirred for 30 min. To the reaction mixture 10 ml of 3N hydrochloric acid was added and the mixture was allowed to warm to room temperature. The organic layer was separated and the aqueous layer was extracted with diethyl ether (3x15 ml). The extracts were combined and washed with 10 ml of sodium hydrogencarbonate and with 10 ml of brine and dried over anhydrous $MgSO_4$. The solvent was evaporated in vacuum. The residue was purified by silica gel column chromatography using diethyl ether: petroleum ether (3:1) as eluent to give the title compound **269** as colourless crystals (0.07 g, 11 %); mp. 58-60°C; IR ν_{max}(Nujol)/cm^{-1} 1697 (C=O); ^{1}H-NMR (270 MHz; $CDCl_3$) δ_H 10.11 (2H, s, -C*H*O), 8.22 (1H, s, H_2), 8.02 (2H, s, $H_{4,6}$) 2.55 (3H, s, -CH_3); ^{13}C-NMR (67.8 MHz; $CDCl_3$) δ_C 191.6 (*C*HO), 140.5 (C_5), 137.3 ($C_{1,3}$), 135.4 (C_2), 129.0 ($C_{4,6}$), 21.1 (CH_3); MS (EI) *m/z* 149.1 (M^+, 100%); CHN requires for $C_9H_8O_2$: C 72.9 %, H 5.5 %. Found: C 69.5 %, H 6.5 %.

1,4-diformyl-2-methylbenzene -271.

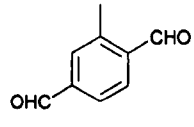

tert-Butyllithium 1.7 M in hexane (4.26 ml, 7.25 mmol) was added to a solution of 2,5-Dibromotoluene **270** (1 ml, 7.25 mmol) in dry THF (10 ml) at –78°C under

nitrogen atmosphere and stirred for 2 hours at the same temperature. To the reaction mixture DMF (0.56 ml, 7.25 mmol) was added at the same temperature and the solution stirred for 30 min. Then, 12.79 ml (21.79 mmol) of *tert*-butyllithium 1.7 M in hexane was added. After 30 minutes, DMF (1.58 ml, 21.75 mmol) was added, and the mixture was stirred for 30 minutes. The mixture was allowed to warm to room temperature, and 15 ml of 3N hydrochloric acid was added. The precipitate was filtered, recrystallised from petroleum ether and dried in vacuum to give the title compound **271** as red powder (1.07 g, 99 %); mp. 45°C; IR ν_{max}(Nujol)/cm^{-1} 1699 (C=O); ^{1}H-NMR (500 MHz; $CDCl_3$) δ_H 10.38 (1H, s, C*H*O), 10.08 (1H, s, C*H*O), 7.97 (1H, d, *J* 7.8, H_5), 7.86 (1H, d, *J* 7.8, H_4), 7.78 (1H, s, H_3), 2.76 (3H, s, -CH_3) ; ^{13}C-NMR (67.8 MHz; $CDCl_3$) δ_C 192.8 (C_4-*C*HO), 192.5 (C_1-*C*HO), 133.4 (C_4), 132.8 (C_1), 127.9 (C_2), 19.9 (-*C*H_3), (quaternary Ar-C not detected); MS (EI) *m/z* 148 (M^+, 100%). Accurate mass requires for $C_9H_8O_2$; 148.0519. Found 148.0523. (R_f 0.7).

1,2-Dimetoxy-3,6-diformylbenzene-56.[88]

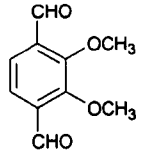

TMDEA (1.36 ml, 9 mmol) was added to a solution of 1,2-dimetoxybenzene **140** (0.23 ml, 1.8 mmol) in diethyl ether (6 ml) at 0 °C. *n*-Butyllithium 2.5 M in hexane (3.6 ml, 9 mmol) was added slowly over 1 minute. The reaction mixture was stirred under reflux for 10 hours. During this period a tannish-yellow precipitate was formed, which was assumed to be the lithium intermediate. DMF (0.70 ml, 9 mmol) was added to the mixture and the reaction stirred for 30 min. The reaction mixture was warmed to room temperature and 2 ml of water and 1 ml of 3N hydrochloric acid were added. The organic layer was separated and the aqueous layer was washed with diethyl ether (3x15 ml). The extract was dried over Na_2SO_4, filtered, the solvents were removed in vacuum and the solids were recrystallised from petroleum ether, to give the title compound **56** as a yellow powder (50.6 mg, 15 %); mp. 80 °C (lit. 85 °C); IR ν_{max}(Nujol)/cm^{-1} 1689.3 (C=O); ^{1}H-NMR (270 MHz; $CDCl_3$) δ_H 10.44 (2H, s, C*H*O), 7.63 (2H, s, $H_{3,6}$), 4.05 (6H, s, -OCH_3); ^{13}C-NMR (67.8 MHz, $CDCl_3$) δ_C 189.4 (*C*HO), 156.8 (C_1), 134.4 (C_3) 123.1 (C_4), 62.7 (-O*C*H_3); MS (EI) *m/z* 194.1 (M^+, 100%); CHN requires for $C_{10}H_{10}O_4$: C 61.8 %, H 5.2 %. Found: C 61.6 %, H 5.2 %.

1, 1'-Dimethoxy- 2, 2'-diformyl- 4, 4'–dimethylbiphenyl -273.

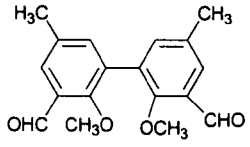

TMEDA (0.77 g, 5.15 mmol) was added to a solution of 2,2'-methoxy -5,5'-methyl-biphenyl **272** (250 mg, 1.03 mmol) in 4 ml of diethyl ether at 0 °C. *n*-Butyllithium 1.6 M in hexane (3.21 ml, 5.15 mmol) was added slowly over 1 minute. The reaction mixture was stirred under reflux for 6 hours. During this period a tannish-yellow precipitate was formed, which was assumed to be the lithium intermediate. DMF (0.4 ml, 5.15 mmol) was added to the mixture and the reaction was stirred for 30 min. The reaction mixture was warmed to room temperature and 5 ml of water and 1 ml of 3N hydrochloric acid was added. The organic layer was separated and the aqueous layer was washed with diethyl ether (3x15 ml). The combined organic extract was dried over Na_2SO_4, filtered, the solvents were removed in vacuum and the solids were recrystallised from petroleum ether to give the title compound **273** as a yellow powder (9 mg, 30 %); mp. 80 °C; IR ν_{max}(Nujol)/cm^{-1} 1694 (C=O); ^{1}H-NMR (270 MHz; $CDCl_3$) δ_H 10.41 (2H, s, C*H*O), 7.72 (2H, s, $H_{5,5'}$), 7.43 (2H, s, $H_{3,3'}$), 3.57 (6H, s, -OCH_3), 2.41 (6H, s, -CH_3); ^{13}C-NMR (67.8 MHz, $CDCl_3$) δ_C 190.3 (*C*HO), 159.1 (C_1), 138.4 (C_6), 134.3 (C_3), 131.7 (C_5), 129.3 (C_1), 128.8 (C_4), 63.5 (-O*C*H$_3$), 20.8 (*C*H$_3$); MS (EI) *m/z* 298.2 (M$^+$, 100%); CHN requires for $C_{18}H_{18}O_4$: C 72.5 %, H 6.1 %. Found: C 71.9 %, H 5.9 %.

1,3,5-Timethoxy-2,4-diformylbenzene -275.[79]

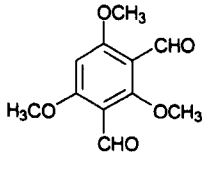

TMEDA (0.67 ml, 4.46 mmol) was added to a solution of 1,3,5-dimethoxybenzene **289** (250 mg, 1.48 mmol) in diethyl ether (4 ml) at 0 °C. *n*-Butyllithium 1.6 M in hexane (2.78 ml, 4.46 mmol) was added slowly over 1 minute. The mixture was stirred at reflux for 6 hours. During the reaction a tannish-yellow precipitate was formed, which was assumed to be the intermediate lithiosalts. DMF (0.34 ml, 4.46

mmol) was added to the mixture, and the reaction was stirred for 30 min. The reaction mixture was warmed to room temperature and hydrolysed with water and 5 ml of 3N Hydrochloric acid. The organic layer was separated and the aqueous layer was extracted with diethyl ether (3x15 ml). The combined organic extract was dried over Na_2SO_4, filtered and the solvent removed in vacuum giving the title compound **275** as a yellow powder (54 mg, 16 %); mp.70 °C (lit 98 °C); IR ν_{max}(Nujol)/cm^{-1} 1680 (C=O); ^{1}H-NMR (270 MHz; $CDCl_3$) δ_H 10.32 (2H, s, C*H*O), 6.27 (1H, s, H_6), 4.00 (9H, s, -OCH_3); ^{13}C-NMR (68.7 MHz; $CDCl_3$) δ_C 187.3 (*C*HO), 167.4 ($C_{1,3,,5}$), 112.8 ($C_{2,4}$), 91.0 (-O*C*H$_3$), 65.2 (-O*C*H$_3$), 56.6 (O-*C*H$_3$); MS (EI) *m/z* 225.2 (M$^+$+H, 100%); CHN requires for $C_{11}H_{12}O_5$: C 58.9 %, H 5.3 %. Found: C 58.6 %, H 5.2 %.

1,1'-Dformylferrocene-173.[86]

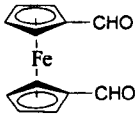

tert-Butyllithium 1.7 in hexane (1.9 ml, 3.35 mmol), was added dropwise to a stirred solution of TMDA (500 μL, 3.35 mmol), ferrocene **136** (250 mg, 1.34 mmol) and potassium *tert*-butoxide (150 mg, 1.34 mmol) in 20 ml of diethyl ether. The reaction mixture was stirred at room temperature for one hour. DMF (360 μL, 4.69 mmol) was added. After 5 minutes, 10 ml of water was added to the mixture and extracted with diethyl ether (3x10 ml). The combined organic layers were washed with brine, dried over Na_2SO_4 and the solvents removed in vacuum. The residue was purified through preparative TLC (eluent: hexane/ethyl acetate/triethylamine: 7/2/1), giving the title compound **173** as a brown powder (130 mg, 40 %); mp. 137 °C (decomposition)(lit. 136-139 °C); ^{1}H-NMR (300 MHz; $CDCl_3$) δ_H 9.93 (2H, s, *CHO*), 4.87 (4H, d, *J* 2, $H_{2,5,2',5'}$), 4.66 (4H, d, *J* 2, $H_{3,4,3',4'}$).

1, 6-Dformyl -2,7-dimethoxynaphthalene- 276.

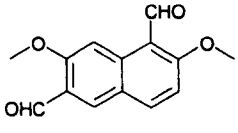

TMEDA (0.8 ml, 5.31 mmol) was added to a solution of 2,7-dimethoxynaphthalene **211** (250 mg, 1.33 mmol) in diethyl ether (10 ml) at 0 °C. *n*-Butyllithium 1.6 M in hexane (3.32 ml, 5.31 mmol) was added slowly over 1 minute. The lithiation mixture was stirred at room temperature for 6 hours. DMF (0.41 ml, 5.31 mmol) was added to

the mixture and the reaction was stirred for 30 min. The mixture reaction was warmed to room temperature and 7 ml of 3N hydrochloric acid was added. The organic layer was separated and the aqueous layer was extracted with diethyl ether (3x15 ml). The extract was dried over Na_2SO_4 and recrystallised from petroleum ether to give the title compound **276** as a white powder (8.5 mg, 44 %); mp. 140 °C; IR ν_{max}(Nujol)/cm^{-1} 1680 (C=O); ^{1}H-NMR (500 MHz; $CDCl_3$) δ_H 10.84 (1H, s, C*H*O), 10.52 (1H, s, C*H*O), 8.90 (1H, s, H_8), 8.24 (1H, s, H_5), 8.08 (1H, d, *J* 9, H_4), 7.17 (1H, d, *J* 9, H_3), 4.07 (3H, s, -OCH_3), 4.06 (3H, s, -OCH_3); ^{13}C-NMR (125.7 MHz; $CDCl_3$) δ_C 191.6, 189.7, 166.5, 161.3, 139.6, 136.6, 130.7, 124.0, 122.9, 115.3, 110.7, 104.1, 56.5, 55.8); MS (CI) *m/z* 244.1 (M^+, 100%); CHN requires for $C_{14}H_{10}O_4$: C 68.8 %, H 4.9 %. Found: C 68.5 %, H 5.4 %. Accurate mass: requires 244.0730. Found 244.075. (R_f 0.3).

1-Formyl-2,3-dimethoxynaphtalene- 277.[128]

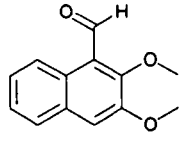

TMEDA (0.69 ml, 4.59 mmol) was added to a solution of 2,3-dimethoxynaphtalene **248** (288 mg, 1.56 mmol) in diethyl ether (15 ml) at 0 °C. *n*-Butyllithium 1.6 M in hexane (2.87 ml, 4.59 mmol) was added slowly over 1 minute. The lithiation mixture was stirred at room temperature for 7 hours. DMF (0.48 ml, 6.24 mmol) was added to the mixture, and stirred for 30 min. The reaction mixture was warmed to room temperature and 5 ml of 3N hydrochloric acid was added. The organic layer was separated and the aqueous layer was extracted with diethyl ether (3x15 ml). The extract was dried over Na_2SO_4, and recrystallised from petroleum ether to give the title compound **277** as a yellow powder (0.13, 34 %); mp. 55 °C (lit 79 °C); IR ν_{max}(Nujol)/cm^{-1} 1683; ^{1}H-NMR (300 MHz; $CDCl_3$) δ_H 10.82 (1H, s, C*H*O), 9.13 (1H, d, *J* 8.4, H_8), 7.71 (1H, d, *J* 8.4, H_5), 7.44 (2H, m, $H_{6,7}$), 7.27 (1H, s, H_4), 4.06 (3H, s, -OCH_3), 3.4 (3H, s, -OCH_3); ^{13}C-NMR (67.8 MHz; $CDCl_3$) δ_C 192.7, 157.5, 151.2, 136.1, 133.7, 131,0, 128.7, 127.1, 126.9, 114.6, 106.5, 63.1, 56.1; MS (EI) *m/z* 216 (M^+, 100%).

2,5-Diformylfurane -139.[94]

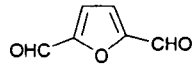

Manganese dioxide (1.82 g, 0.21 mol) was added to a solution of 5-hydroxymethylfurfural **204** (0.136 g, 1.08 mmol) in 11 ml of toluene. The reaction mixture was stirred under reflux for 24 hours. The slurry was filtered and the solid washed with chloroform (15 ml). The solution was evaporated in vacuum to give the title compound **139** as a yellow powder (0.12 g, 89 %); mp 108 °C (lit 110°C); ^{1}H-NMR (270 MHz; $CDCl_3$) δ_H 9.71 (2H, s, C*H*O), 7.32 (2H, s, Ar-*H*); ^{13}C-NMR (68.7 MHz; $CDCl_3$) δ_C 179.5, 154.0, 119.5; MS (EI) *m/z* 124.1 (M^+, 100%).

2,6-Diformylpyridine-163.[92]

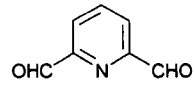

Selenium dioxide (0.46 g, 4.22 mmol) was added to a solution of 0.29 g (2.11 mmol) of 2,6-pyridinemethanol **162** in 10 ml of dioxane. The reaction mixture was stirred under reflux for 4 hours. The slurry was filtered and the solid washed with chloroform (40 ml). The solution was evaporated in vacuum to give the title compound **163**, as a light pink powder (1.25, 89 %); mp. 115 °C (lit 117 °C); ^{1}H-NMR (270 MHz; $CDCl_3$) δ_H 10.22 (2H, s, C*H*O), 7.27 (3H, m, Ar-*H*); MS (EI) *m/z* 135.1 (M^+, 100%).

1,3-Diformylazulene- 85.[61]

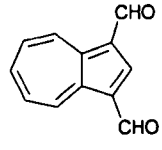

$POCl_3$ (4.5 g, 0.03 mol) was added to a solution of azulene **84** (1.28 g, 1.0 mmol) in DMF (40 ml) at 0°C and was stirred for 30 min. Then the reaction mixture was stirred for 90 min at 85°C. The reaction mixture was cooled to room temperature the red reaction mixture was poured into water (20 ml) and adjusted to pH 9 using 10 ml of NaOH. The mixture was extracted with chloroform (3x30 ml). The organic extracts were combined, washed with 20 ml sodium hydrogencarbonate solution and with 10 ml brine and dried over anhydrous Na_2SO_4. The solvent was evaporated in vacuum. The residue was recrystallised from ethanol to give the title compound **85** as red, long needles (0.73 g, 40 %); mp 175°C (lit 175 °C); IR ν_{max}(Nujol)/cm^{-1} 1656.2 (C=O), 1519-1364 (C_{ar}=C_{ar}); ^{1}H-NMR (270 MHz; $CDCl_3$) δ_H 10.45 (2H, s, C*H*O), 9.93 (2H, d, *J* 8.9, $H_{4,8}$), 8.60 (1H, s, H_2), 8.20 (2H, t, *J* 9.7, $H_{5,7}$), 8.01 (1H, t, *J* 9.7, H_6); ^{13}C-

NMR (68.7 MHz; $CDCl_3$) δ_C 187.8, 149.0, 144.8, 143.1, 141.2, 134.5, 126.3; MS (EI) *m/z* 185.19 (M^++H, 100%).CHN requires for $C_{12}H_8O_2$: C 78.3 %, H 4.4 %. Found: C 78.1 %, H 4.1 %.

(1*R*, 2*R*)-Diaminocyclohexane- 38.[129]

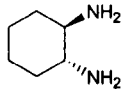

(1*RS*, 2*RS*)-Diaminocyclohexane (10 ml, 87.57 mmol) was added to a stirred solution of *L*-(+)-Tartaric acid **278** (13.14 g, 87.57 mmol) in water (100 ml). This mixture was heated on a steam bath for 0.5 hour, and then cooled in an ice-salt mixture. The *L*-(+)-tartaric acid salt precipitated as fine, white granules (10.65 g, 33 %), $[\alpha]^{25}_D$ +13° (c 0.40, H_2O, 2-dm). Decomposition of the salt with (28.17 ml, 56.0 mmol) of NaOH solution 2M gave (1*R*, 2*R*)-diaminocyclohexane, which was extracted with chloroform (3x25 ml). The solvent was evaporated in vacuum to give the title product **38** as white crystals. IR ν_{max}(Nujol)/cm^{-1} 3350 cm^{-1}; $[\alpha]^{25}_D$ –23.7 (c 4, HCl, 1-dm) (lit $[\alpha]^{25}_D$ –25.5 (c 5, HCl, 1-dm); ^{1}H-NMR (270 MHz, $CDCl_3$) δ_H 2.22 (2H, d, *J* 10, -C*H*NH_2), 1.81 (2H, d, *J* 13.5, -$CH_{2-(3)}$), 1.66 (2H, d, *J* 10, -$CH_{2-(6)}$), 1.18 (4H, m, -$CH_{2-(4,5)}$); ^{13}C-NMR (67.5 MHz, $CDCl_3$) δ_C 57.9, 35.7, 25.7, MS (EI) *m/z* 115.1 (M^++H, 100%).

(2*R*, 3*R*, 12*R*, 13*R*, 22*R*, 23*R*)-1, 4, 15, 18, 29, 32-Hexa-aza-(5, 10, 15, 20, 25, 30)-hexamethyl-(2, 3: 12, 13: 22, 23)-tributano-(6, 9: 16, 19: 26, 29)-trietheno-2H, 3H, 12H, 13H, 22H, 23H)-hexahydro-(30)-annulene-283.

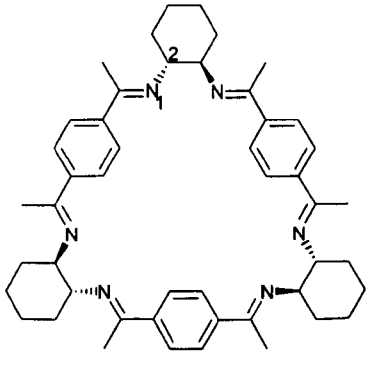

1,4-Diacetylbenzene **281** (0.7 g, 4.37 mmol) in dichloromethane (8 ml) was added to a solution of (1*R*, 2*R*)-diaminocyclohexane **38** (0.5 g, 4.37 mmol) in dichloromethane (5 ml). The mixture was stirred under reflux for 24 hours, the solvent was evaporated and repeatedly recrystallised from ethyl acetate to give the trianglimine **283** as a

golden powder (0.87 g, 28 %); mp. 90°C; IR ν_{max}(Nujol)/cm^{-1} 1631 cm^{-1}; $[\alpha]_D^{25}$ -190° (*c* 0.2, $CHCl_3$, 2-dm); ^{1}H-NMR (270 MHz, $CDCl_3$) δ_H 7.95 (12H, s, Ar-*H*), 3.70 (6H, m, C*H*-N), 2.09 (18H, s,- CH_3), 1.68 (18H, m, -CH_2-), 1.40 (6H, m, -CH_2-); ^{13}C-NMR (67.5 MHz, $CDCl_3$) δ_C 163.3, 128.5, 126.6, 65.5, 32.0, 24.8, 16.4; MS (LSIMS) *m/z* 720.3 (M^+, 100%); CHN requires for $C_{48}H_{60}N_6$: C 80.0 %, H 8.3 %, N 11.6 %. Found: C 75.8 %; H 8.2 %; N 10.2 %; (**283**+EtOAc+H_2O).

Macrocycles 285 and 286.

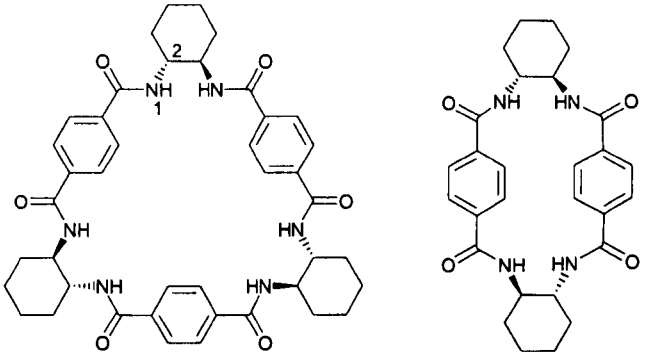

(1*R*, 2*R*)-Diaminocyclohexane **38** (140 mg, 1.23 mmol) in dichloromethane (1 ml) and potassium carbonate (340 mg, 2.46 mmol) were added at 0 °C to a solution of terephthaloyl chloride **284** (250 mg, 1.23 mmol) in dichloromethane (2 ml). The mixture was stirred under reflux for 24 hours. The solvent was evaporated and water was added. The precipitate was filtered to give the title compounds **285** and **286** as a white powder, mp. 250 °C; IR ν_{max}(Nujol)/cm^{-1} 1631 cm^{-1} ; MS FAB *m/z* 734 (M^++H, 100 %, **285**) and 490 (M^++H, 50%, **286**).

Further purification and characterisation failed be due to lack of solubility.

Macrocycle 288.

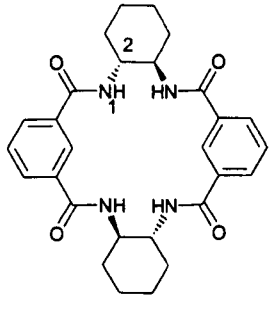

(1*R*, 2*R*)-Diaminocyclohexane **38** (140 mg, 1.23 mmol) in dichloromethane (1 ml) and potassium carbonate (340 mg, 2.46 mmol) were added at 0 °C a solution of isophthaloyl chloride **287** (250 mg, 1.23 mmol) in dichloromethane (2 ml). The mixture was stirred under reflux for 24 hours, the solvent was evaporated, and water

was added. The precipitate was filtered off to give the title compound **288** as a white powder. $T_{(decomposition)}$ 260 °C; IR ν_{max} (Nujol)/cm^{-1} 1631 cm^{-1}; *m/z* FAB 490 (M^++H, 100%)

Further purification cannot be carried out due to lack of solubility.

(2*R*, 3*R*, 12*R*, 13*R*, 22*R*, 23*R*)-1, 4, 11, 14, 21, 24-Hexa-aza-(2, 3: 12,13: 22, 23)-tributano-(6, 9: 16, 19: 26, 29)-trietheno-(2H, 3H, 12H, 13H, 22H, 23H)-hexahydro-(30)-annulene-40.[42]

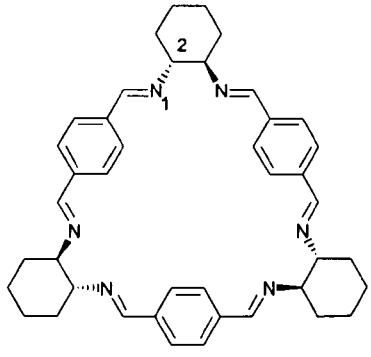

Terephthaldehyde **39** (1.34 g, 10 mmol) in dichloromethane (8.3 ml) was added to a solution of (1*R*, 2*R*)-diaminocyclohexane **38** (1.14 g, 10 mmol) in dichloromethane (5 ml). The mixture was stirred at room temperature for 3 hours, the solvent was evaporated in vacuum and the crude compound recrystallised from ethyl acetate to give the title product **40** as white needles (5.7 g, 90 %); mp. > 360 °C (lit > 360 °C); IR ν_{max} (Nujol)/ cm^{-1} 1642 C=N; $[\alpha]_D^{25}$–356 (*c* 0.5, CH_2Cl_2, 1-dm); ^{1}H-NMR (270 MHz, $CDCl_3$) δ_H 8.14 (6H, s, N=C*H*), 7.52 (12H, s, Ar-*H*), 3.37 (6H, m, C*H*-N), 1.80 (24H, m, -CH_2-), 1.48 (6H, m, -CH_2-); ^{13}C-NMR (67.5 MHz, $CDCl_3$) δ_C 160.3, 137.9, 128.1, 74.0, 32.6, 24.3; *m/z* FAB 637.8 (M^++H, 100%).

(2*R*, 3*R*, 11*R*, 12*R*, 20*R*, 21*R*)-1, 4, 10, 13, 19, 22-Hexa-aza-(2, 3: 11, 12: 20, 21)-tributano-(6, 8: 15, 17: 24, 26)-tripropeno-(2H, 3H, 11H, 12H, 20H, 21H)-hexahydro-(27)-annulene- (42).[42]

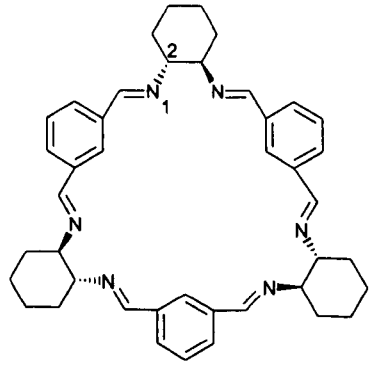

Isophthalaldehyde **41** (0.71 g, 5.3 mmol) in dichloromethane (8.3 ml) was added to a solution of (1*R*, 2*R*)-diaminocyclohexane **38** (0.61 g, 5.3 mmol) in dichloromethane (5 ml). The mixture was stirred at room temperature for 3 hours, the solvent was evaporated and the crude compound recrystallised from ethyl acetate to give the title compound **42** as a white powder (2.5 g, 74 %); mp. 280 °C (lit. 276-280 °C); IR ν_{max} (Nujol)/cm^{-1} 1647 cm^{-1}; $[\alpha]_D^{25}$ −177° (*c* 0.5, CH_2Cl_2, 1-dm); ^{1}H-NMR (270 MHz, $CDCl_3$) δ_H 8.20 (6H, s, N=C*H*), 7.95 (3H, s, Ar-*H*), 7.60 (6H, broad, Ar-*H*), 7.28 (3H, t, *J* 7.7, Ar-*H*), 3.42 (6H, m, C*H*-N), 1.85 (6H, m, -CH_2-), 1.76 (24H, m, -CH_2-), 1.50 (6H, m, -CH_2-); ^{13}C-NMR (67.5 MHz, $CDCl_3$) δ_C 163.2, 137.6, 131.9, 130.2, 128.9, 75.7, 39.9, 25.5; *m/z* FAB 636.8 (M^+, 100%).

(2*R*, 3*R*, 12*R*, 13*R*, 22*R*, 23*R*)- 1, 4, 11, 14, 21, 24- Hexa-aza-(2, 3: 12, 13: 22, 23)-tributano-(7, 8', 17, 18', 27, 28')-hexa-methoxy-(6, 9: 16, 19: 26, 29)-trietheno-(2H, 3H, 12H, 13H, 22H, 23H)-hexahydro-(30)-annulene- 289.

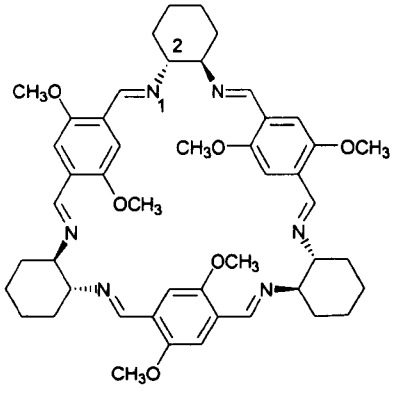

2,5-Diformyl-1,4-dimethoxybenzene (0.2 g, 1 mmol) in dichloromethane (1.5 ml) was added to a solution of (1*R*, 2*R*)-diaminocyclohexane **38** (0.11 g, 1 mmol) in dichloromethane (1 ml). The mixture was stirred for 3 hours at room temperature, the solvent was evaporated in vacuum, and the crude compound recrystallised from ethyl acetate to give the title compound **158** as white needles (0.75 g, 90 %); mp. > 200°C; $[\alpha]_D^{25}$ −442.4° (*c* 0.2, CH_2Cl_2, 1-dm); IR ν_{max}(Nujol)/cm^{-1} 1630 (C=N); ^{1}H-NMR (270 MHz; $CDCl_3$) δ_H 8.40 (6H, s, N=C*H*), 7.23 (6H, s, Ar-*H*), 3.64 (12H, s, -OCH_3), 3.35 (6H, s, C*H*-N), 1.22-1.91 (24H, m, -CH_2); ^{13}C-NMR (68.7 MHz; $CDCl_3$) δ_C 155.6 (H*C*=N), 132.1 (C_{ar}-OCH_3), 123.8 (C_{ar}-CH=N), 100.5 (C_{ar}-H), 82.3 (R_2*C*H-N=CH); 46.8 (O-*C*H$_3$), 29.1 (s, N-CH-*C*H$_2$), 13.4 (s, C-*C*H$_2$-C); MS (LSIMS) *m/z* 817.4 (M^++H, 100%); CHN requires for $C_{48}H_{60}N_6O_6$: C 70.5 %, H 7.4 %, N 10.3 %. Found: C 63.7 %, H 7.7 %, N 8.3 % (**289**+EtOAc +3H_2O).

(2*R*, 3*R*, 12*R*, 3*R*, 22*R*, 23*R*)-1, 4, 11, 14, 21, 24-Hexa-aza-(7, 8, 17, 18, 27, 28)-hexamethoxy-(2, 3: 12, 13: 22, 23)-tributano-(6, 9: 16, 19: 26, 29)-trietheno-(2H, 3H, 12H, 13H, 22H, 23H)-hexahydro-(30)-annulene-290.

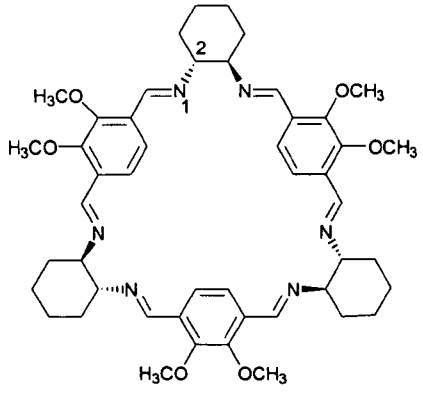

1,2-Dimethoxy-3,6,-diformylbenzene **56** (250 mg, 1.28 mmol) in dichloromethane (6ml) was added to a solution of (1*R*, 2*R*)-diaminocyclohexane **38** (140 mg, 1.28 mmol) in dichloromethane (6 ml) and stirred for 2 hours under reflux. The solvent was evaporated the residue was recrystallised from ethyl acetate to give the title compound **290** as a yellow powder (256 mg, 25 %); mp. 70 °C; IR ν_{max}(Nujol)/cm^{-1} 1634.5 (C=N); $[\alpha]_D^{25}$ –313.7° (*c* 0.10, $CHCl_3$, 1-dm); ^{1}H-NMR (500 MHz; $CDCl_3$) δ_H 8.35 (6H, s, N=C*H*), 7.42 (6H, s, Ar-*H*), 3.50 (18H, s, -OCH_3), 3.35 (6H, s, C*H*-N), 1.45-1.80 (24H, m, CH_2); ^{13}C-NMR (67.8 MHz, $CDCl_3$) δ_C 159.3 (HC=N), 156.1 (C_2), 134.8 (C_3), 124.7 (C_4), 77.2 (*C*HN=CH), 69.3 (-O*C*H$_3$), 35.3 (N-CH-*C*H$_2$), 27.0 (C-CH$_2$-C); MS *m/z* (LSIMS) 817.3 (M^++H, 100%); (FAB) *m/z* 817.25 (M^++H, 100%); CHN requires for $C_{48}H_{60}N_6O_6$: C 70.5 %, H 7.4 %, N 10.3 %. Found C 67.4 %, H 8.4 %, N 7.9 % (**290**+2EtOAc).

(2*R*, 3*R*, 11*R*, 12*R*, 20*R*, 21*R*)-1, 4, 10, 13, 19, 22-Hexa-aza- (7, 16, 25)-trimethoxy-(2, 3: 11, 12: 20, 21)-tributano-(6, 8: 15, 17: 24, 26)-tris(1,3-dimethoxy-propeno)-(2H, 3H, 11H, 12H, 20H, 21H)-hexahydro-(27)-annulene-291.

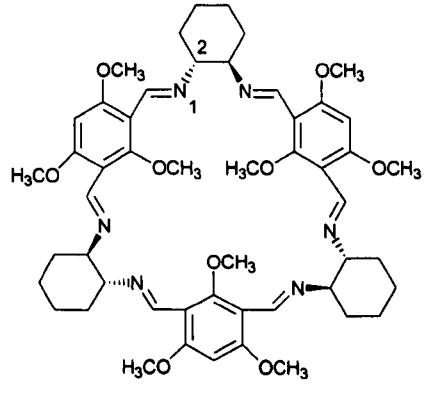

1,3,5-Trimethoxy-2,4-diformylbenzene **275** (30 mg, 0.133 mmol) in dichloromethane (1.33 ml) was added to a solution of (1*R*, 2*R*)-diaminocyclohexane **38** (15 mg, 1.33 mmol) in dichloromethane (1.33 ml) and stirred for 3 hours under reflux. The solvent was evaporated and the residue was recrystallised from ethyl acetate to give the title compound **275** as a white powder (32 mg, 26 %); mp.100 °C; IR ν_{max}(Nujol)/cm^{-1} 1642.3 (C=N); $[\alpha]_D^{25}$ - 200° (*c* 0.04, $CHCl_3$, 1-dm); ν_{max} (Nujol)/cm^{-1} 1642 (C=N); ^{1}H-NMR (300 MHz; $CDCl_3$) δ_H 8.71 (6H, s, N=C*H*), 8.39 (3H, s, Ar-*H*), 3.61 (6H, m, C*H*-N), 3.24 (12H, s, -OCH_3), 3.21 (24H, s, -OCH_3), 2.03-1.51 (24H, m, CH_2); ^{13}C-NMR (67.8 MHz, $CDCl_3$) δ_C 155.35 (CH=N), 90.7 (C_{ar}-H), 90.4 (C_{ar}-H), 56.2 (-OCH_3), 56.1 (-OCH_3), 33.6 (CH_2), 25.5 (CH_2), 25.1 (CH_2), 24.9 (CH_2); MS (LSIMS) *m/z* 907.2 (M^+, 100%); CHN requires for $C_{51}H_{66}N_6O_9$: C 67.5 %, H 7.3 %, N 9.2 %. Found C 67.5 %, H 6.9 %, N 8.7 %.

(2*R*, 3*R*, 12*R*, 13*R*, 22*R*, 23*R*)-1, 4, 11, 14, 21, 24-Hexa-aza- (8, 18, 27)-trimethyl-(2, 3: 12, 13: 22, 23)-tributano-(6, 9: 16, 19: 26, 29)-tripropano- (2H, 3H, 12H, 13H, 22H, 23H)-hexahydro-(30)-annulene-294

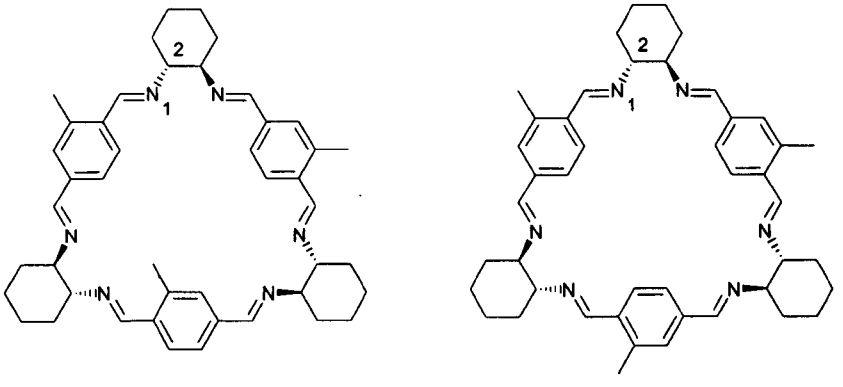

1,4-Diformyl-2-methylbenzene **251** (56 mg, 0.37 mmol) was added to a solution of (1*R*, 2*R*)-diaminocyclohexane **38** (43 mg, 0.37 mmol) in dichloromethane (3.78 ml) and stirred for 3 hours at room temperature. The solvent was evaporated and the residue was recrystallised from ethyl acetate to give the title compound **294** as a pale yellow powder (120 mg, 46 %); mp.>250 °C; $[\alpha]_D^{25}$ -361° (*c* 0.03, CH_2Cl_2, 1-dm); IR ν_{max}(Nujol)/cm^{-1} 1643 (C=N); ^{1}H-NMR (500 MHz; $CDCl_3$) δ_H 8.45 (6H, t, N=C*H*), 8.14 (6H, dd, N=C*H*), 7.66 (6H, m, Ar-*H*), 7.55 (6H, d, Ar-*H*), 7.51 (3H, s, Ar-*H*), 7.11 (3H, broad, Ar-*H*), 3.36 (12H, broad, C*H*-N), 2,43 (18H, s, -CH_3), 1.85-1.47 (48H, m, CH_2); ^{13}C-NMR (67.8 MHz, $CDCl_3$) δ_C 161.0, 160.9, 54.7, 33.0, 24.9, 19.15 (the signals of the other rotamer are overlapped); MS (CI) *m/z* 679 (M^+, 100%).

Accurate mass 679.447, requires for $C_{25}H_{55}N_6$, 679.4483 (R_f 0.4); CHN requires C 79.6 %, H 8.0 %, N 12.3 %. Found: C 78.4 %, H 8.2 %, N 12.2 %.

(2*R*, 3*R*, 11*R*, 12*R*, 20*R*, 21*R*)-1, 4, 7, 10, 13, 16, 19, 22, 25-Nona-aza-(2, 3: 11, 12: 20, 21)-tributano-(6, 8: 15, 17: 24, 26)-tripropeno-(2H, 3H, 11H, 12H, 20H, 21H)-hexahydro-(27)-annulene-296.

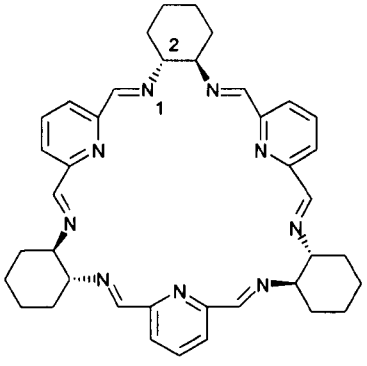

2,6-Diformylpyridine **163** (180 mg, 1.33 mmol) in dichloromethane (6.5 ml) was added to a solution of (1*R*, 2*R*)-diaminocyclohexane **38** (150 mg, 1.33 mmol) in dichloromethane (6 ml) and stirred for 3 hours at room temperature. The solvent was evaporated and the residue was recrystallised from ethyl acetate to give the title compound **296** as a yellow glassy solid (69.9 mg, 70 %), mp. 180 °C, $[\alpha]_D^{25}$ -56.8 ° (*c* 0.21, $CHCl_3$, 2-dm); IR ν_{max} (Nujol)/cm^{-1} 1642 (C=N); ^{1}H-NMR (270 MHz; $CDCl_3$) δ_H 8.22 (6H, s, N=C*H*), 7.79 (9H, m, Ar-*H*), 3.45 (6H, m, C*H*-N), 1.46-1.84 (24H, m, CH_2); ^{13}C-NMR (67.8 MHz, $CDCl_3$) δ_C 161.2, 154.3, 136.8, 123.8, 76.7, 33.1, 24.7; MS (CI) *m/z* 639.4 (M^+, 100 %); CHN requires for $C_{39}H_{45}N_9$: C, 73.2 %, H 7.1 %, N 19.7 %. Found: C 69.7 %, H 7.3 %; N 18.3 % (**296**+2H_2O)

(2*R*, 3*R*, 11*R*, 12*R*, 20*R*, 21*R*)-1, 4, 10, 13, 19, 22-Hexa-aza-(7, 16, 25)-trithia-(2, 3: 11, 12: 20, 21)-tributano-(6, 8: 15, 17: 24, 26)-trietheno-(2H, 3H, 11H, 12H, 20H, 21H)-hexahydro-(27)-annulene-298.

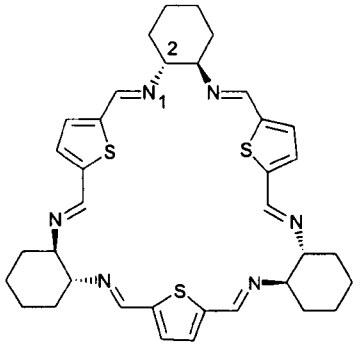

2,5-Diformylthiophene **280** (50 mg, 0.35 mmol) in dichloromethane (2 ml) was added to a solution of (1*R*, 2*R*)-diaminocyclohexane **38** (40 g, 0.35 mmol) in dichloromethane (3 ml) and stirred for 3 hours under reflux. The solvent was evaporated and the residue was recrystallised from ethyl acetate to give the title compound **298** as a brown glassy solid (82 mg, 35 %); mp 220 °C; $[\alpha]_D^{25}$ (could not be determined due to low solubility); IR ν_{max} (Nujol)/cm^{-1} 1634 (C=N); ^{1}H-NMR (300 MHz; $CDCl_3$) δ_H 9.92 (6H, s, N=C*H*), 8.06 (6H, s, Ar-*H*), 3.32 (6H, m, C*H*-N), 1.52-1.83 (24H, m, CH_2); ^{13}C-NMR (67.8 MHz, $CDCl_3$) δ_C 153.5, 128.4, 76.8, 32.9, 24.6 (quartenary Ar-C could not be detected due to low solubility); MS (CI) *m/z* 655 (M^++H, 100%). Accurate mass requires for $C_{36}H_{43}N_6S_3$ 655.2706. Found: 655.269 (R_f 0.5).

(2*R*, 3*R*, 11*R*, 12*R*, 20*R*, 21*R*)-1, 4, 10, 13, 19, 22-Hexa-aza-(7, 16, 25)-trioxo-(2,3: 11, 12: 20, 21)-tributano-(6, 8: 15, 17: 24, 26)-trietheno-(2H, 3H, 11H, 12H, 20H, 21H)-hexahydro-(27)-annulene-299.

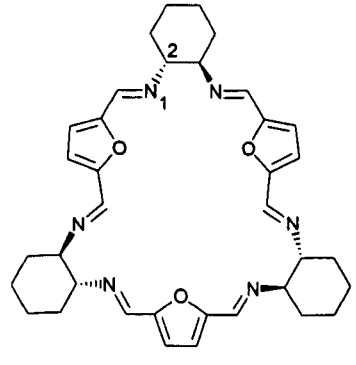

2,5-Diformylfurane **139** 20 mg (0.16 mmol) was added to a solution of (1*R*, 2*R*)-diaminocyclohexane **38** (9 mg, 0.16 mmol) in dichloromethane (3 ml) and stirred for 4 hours at room temperature. The solvent was evaporated and the title compound was

obtained after recrystallisation from ethyl acetate to give the title compound **299** as a brown oil (14 mg, 14 %); ($[\alpha]_D^{25}$ could not be determined due to the sample being opaque); ^{1}H-NMR (270 MHz; $CDCl_3$) δ_H 8.22 (6H, s, N=C*H*), 6.86 (2H, s, Ar-*H*), 3.54 (6H, m, C*H*-N), 1.5-1.8 (24H, m, CH_2); ^{13}C-NMR (67.8 MHz, $CDCl_3$) δ_C 152.8, 114.9, 33.9, 33.15, 24.5 (quartenary Ar-C could not be detected due to low solubility); MS (EI) *m/z* 607 (M^++H, 100%).

(2*R*, 3*R*, 12*R*, 13*R*, 22*R*, 23*R*)-1, 4, 15, 18, 29, 32-Hexa-aza-(2, 3: 12, 13: 22, 23)-tributano-(6, 9: 16, 19: 26, 29)-tribenzo-(6', 9': 16', 19': 26', 29')-tributadieno-(2H, 3H, 12H, 13H, 22H, 23H)-hexahydro-(30)-annulene-300.

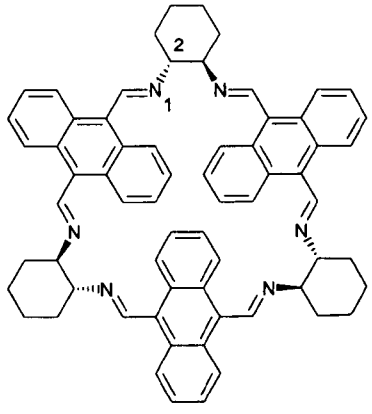

9,10-Diformylanthracene **235** (0.30 g, 1.3 mmol) in dichloromethane (5.0 ml) was added to a solution of (1*R*, 2*R*)-diaminocyclohexane **38** (0.14 g, 1.3mmol) in dichloromethane (1.5 ml) and stirred for 3 hours at room temperature. The solvent was evaporated and the residue was recrystallised from ethyl acetate to give the title compound **300** as an orange powder (0.32 g, 80 %); mp. > 200°C; $[\alpha]_D^{25}$ +250° (*c* 0.2, CH_2Cl_2, 1-dm); IR ν_{max}(Nujol)/cm^{-1} 1632 (C=N); ^{1}H-NMR (270 MHz; $CDCl_3$) δ_H 9.45 (6H, s, N=C*H*), 8.14 (12H, AA'XX' spin system, *N* 10.0, Ar-*H*), 6.56 (12H, AA'XX' spin system, *N* 10.0, Ar-*H*), 3.92 (6 H, s, C*H*-N), 2.14-1.94 (24H, m, CH_2); ^{13}C-NMR (67.5 MHz; $CDCl_3$) δ_C 160.8, 130.4, 129.4, 126.3, 126.2, 126.0, 125.1, 76.6, 33.6, 24.7; MS (LSIMS) *m/z* 938.3 (M^++H, 100%); CHN requires for $C_{66}H_{60}N_6$: C 84.6 %, H 6.5 %, N 8.9 %. Found: C 84.1 %, H 6.7 %, N 8.7 %.

(2*R*, 3*R*, 16*R*, 17*R*, 30*R*, 31*R*)-1, 4, 15, 18, 29, 32-Hexa-aza-(2,3 : 16,17 : 30,31)-tributano-(6, 9: 10, 13: 20, 23: 24, 27: 34, 37: 38, 41)-hexaetheno-(2H, 3H, 16H, 17H, 30H, 31H)-hexahydro-(42)-annulene-301.

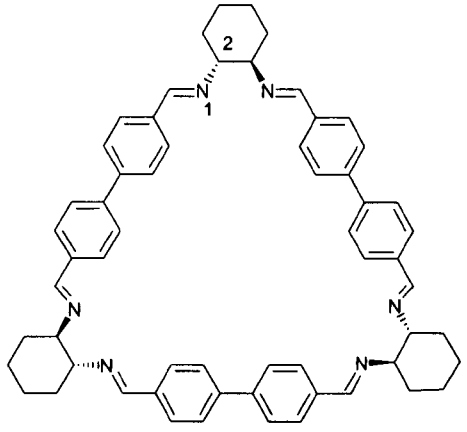

4, 4'-Diformylbiphenyl **87** (0.42 g, 2.0 mmol) in dichloromethane (2.0 ml) was added to a solution of (1*R*, 2*R*)-diaminocyclohexane (0.23 g, 2.0 mmol) in dichloromethane (3.0 ml) and stirred for 3 hours at room temperature. The solvent was evaporated and the residue was recrystallised from ethyl acetate to give the title compound **301** as a white powder (0.55 g, 32 %); mp. > 200°C; $[\alpha]_D^{25}$+ 250° (*c* 0.1, $CHCl_3$, 1-dm); IR ν_{max}(Nujol)/cm^{-1} 1636 (C=N); ^{1}H-NMR (270 MHz; $CDCl_3$) δ_H 8.14 (6H, s, N=C*H*), 7.52 (12H, d, *J* 7.8, Ar-*H*), 7.39 (12H, d, *J* 8.4, Ar-*H*), 3.34 (6H, s, C*H*-N), 1.81-1.22 (24H, m, CH_2); ^{13}C-NMR (67.5 MHz; $CDCl_3$) δ_C 160.9, 142.0, 135.6, 128.3, 127.0, 73.9, 32.6, 24.4; MS (LSIMS) *m/z* 866.3 (M^++H, 100%); CHN requires for $C_{60}H_{60}N_6$: C 77.3 %, H 7.0 %, N 8.7 %. Found: C 77.6 %, H 6.8 %, N 8.8 %.

(2*R*, 3*R*, 14*R*, 15*R*, 26*R*, 27*R*)-1, 4, 13, 16, 25, 28 –Hexa-aza-(2, 3: 14, 16: 26, 27)-tributano-(6, 8: 9, 11: 18, 20: 21, 23: 30, 32: 33, 35)-hexakis-(2-methoxy-4-methyl)-propeno-(2H, 3H, 14H, 15H, 26H, 27H)-hexahydro- (36)-annulene-302.

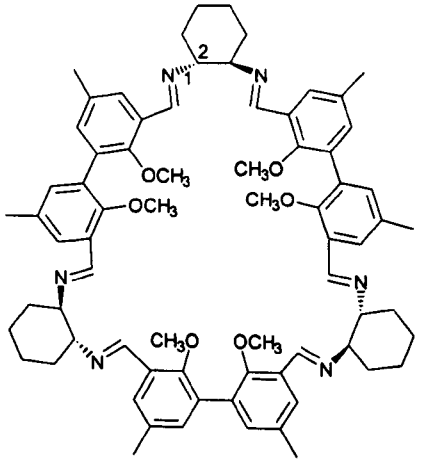

1,1'-Dimethoxy, 2,2'–diformyl-4,4'-dimethyl-biphenyl **273** (300 mg, 1 mmol) was added to a solution of (1*R*, 2*R*)-diaminocyclohexane **38** (114 mg, 1 mmol) in 10 ml of dichloromethane, and stirred for 3 hours under reflux. The solvent was evaporated and the title compound was obtained after recrystallisation from ethyl acetate as a white powder **302** (377 mg, 50 %) and as a 3:1 mixture of diastereoisomers, mp. 70 °C; $[\alpha]_D^{25}$ + 250° (*c* 0.1, $CHCl_3$, 1-dm); IR ν_{max} (Nujol)/cm^{-1} 1635 (C=N); ^{1}H-NMR (500 MHz; $CDCl_3$) δ_H 8.58 (6H, s, N=C*H*, minor isomer), 8.45 (6H, s, N=C*H*, major isomer), 7.64 (6H, s, Ar-*H*, minor isomer), 7.54 (6H, s, Ar-*H*, major isomer), 7.17 (6H, s, Ar-*H*, major isomer), 6.99 (6H, s, Ar-*H*, minor isomer), 3.47 (6H, m, C*H*-N, both isomers), 3.29 (9H, s, -OCH_3, minor isomer), 2.84 (9H, s, -OCH_3, major isomer), 2.23 (9H, s, CH_3, major isomer), 2.18 (9H, s, CH_3, minor isomer), 1.21-1.93 (24H, m, CH_2, both isomers); ^{13}C-NMR (67.8 MHz, $CDCl_3$) δ_C 158.7, 157.3, 134,3, 129.2, 127.5, 73.2, 61.4, 33.0, 24.7, 24.5, 20.8; MS (LSIMS) *m/z* 1130.5 (M^++H, 100%); CHN requires for $C_{72}H_{84}N_6O_6$: C, 76.6 %, H 7.5 %, N 7.4 %. Found: C 76.7 %, H 7.5 %; N 7.5 %.

Trianglimine 303.

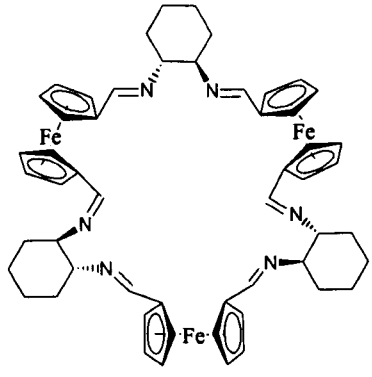

1,1'-Diformylferrocene **137** (50 mg, 0.21 mmol) was added to a solution of (1*R*, 2*R*)-diaminocyclohexane **38** (23 mg, 0.21 mmol) in dichloromethane (3 ml) and stirred for 45 hours at room temperature. The solvent was evaporated and recrystallised from ethyl acetate to give the title compound **303** as a brown powder (2.8 mg, 13 %); mp > 250 °C; $[\alpha]_D^{25}$ (could not be determined due to the sample being opaque); ^{1}H-NMR (270 MHz; $CDCl_3$) δ_H 8.12 (6H, s, N=C*H*), 4.45 (6H, s, Ar-*H*), 4.36 (6H, s, Ar-H), 4.02 (6H, s, Ar-*H*), 3.90 (6H, s, Ar-*H*), 2.86 (6H, m, C*H*-N), 1.5-1.78 (24H, m, CH_2); ^{13}C-NMR (67.8 MHz, $CDCl_3$) δ_C 160.0, 83.6, 76.8, 73.4, 70.2, 33.9, 25.5; MS (FAB) *m/z* 961(M^++H, 100%); CHN requires for $C_{54}H_{60}Fe_3N_6$: C 67.5 %, H 5.7 %, N 8.8 %. Found 65.39 % C, 4.4 % H; 8.5 %N.

(2*R*, 3*R*, 13*R*, 14*R*, 24*R*, 25*R*)-(1, 4, 12, 15, 23, 26)-Hexa-aza-(7', 18', 29')-trimethoxy-(6, 9: 17, 20: 28, 31)-trietheno-(8, 10: 19, 21: 30, 32)-tris(tri-3-methoxy)propeno-(2H, 3H, 13H, 14H, 24H, 25H)-hexahydro-(33)-annulene-304.

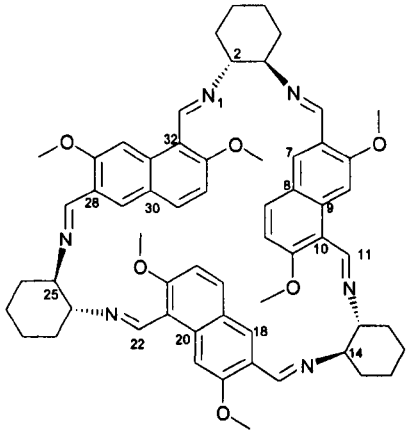

2,7-Dimethoxy-1,6-diformylnaphthalene **276** (0.55 mg, 0.02 mmol) was added to a solution of (1*R*, 2*R*)-diaminocyclohexane **38** (2.57 mg, 0.02 mmol) in dichloromethane (1 ml) and stirred for 4 hours at room temperature. The solvent was evaporated and recrystallised from ethyl acetate to give the title compound **304** as a yellow oil (4 mg, 18 %); IR ν_{max}(Nujol)/cm^{-1} 1636 (C=N); $[\alpha]_D^{25}$ 275° (*c* 0.04, CH_2Cl_2, 1 dm); ^{1}H-NMR (500 MHz; $CDCl_3$) δ_H 9.01 (3H, s, N=C*H*), 8.84 (3H, s, N=C*H*), 8.72 (3H, s, Ar-*H*), 8.14 (3H, s, Ar-*H*), 7.63 (3H, d, *J* 9, Ar-*H*), 6.90 (3H, d, *J* 9, Ar-*H*), 3.93 (9H, s, -OCH_3), 3.86 (9H, s, -OCH_3), 3.52 (6H, s, C*H*-N), 1.86 -1.51 (24H, m, CH_2); ^{13}C-NMR (67.5 MHz, $CDCl_3$) δ_C 158.3, 158.2, 155.9, 134.7, 133.4, 127.3, 124.3, 116.2, 110.8, 110.5, 104.0, 76.4, 76.1, 55.5, 55.4, 33.5, 33.4, 24.8; MS (LSIMS) *m/z* 967 (M^+, 100%).

(2*R*, 3*R*, 14*R*, 15*R*, 26*R*, 27*R*)-(1, 4, 11, 13, 16, 25, 28)-Hexa-aza-(7, 10, 19, 22, 31, 34)-hexamethoxy-(2, 3: 14, 15: 26, 27)-tributano -(6, 9: 8, 11: 18, 21: 20, 23: 30, 33: 32, 35)-hexaetheno-(2H, 3H, 14H, 15H, 26H, 27H)-hexahydro-(36)-annulene-305.

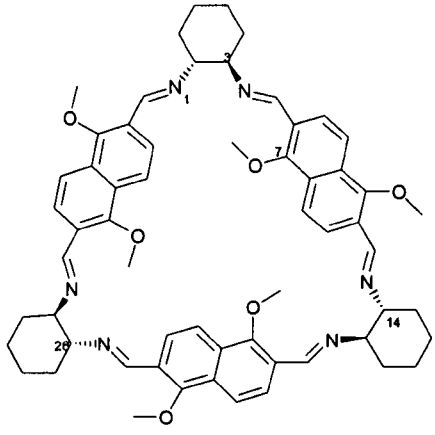

1,5-Dimethoxy-2,6-difomylnaphthalene **246** (16 mg, 0.06 mmol) was added to a solution of (1*R*, 2*R*)-diaminocyclohexane **38** (7.5 mg, 0.06 mmol) in dichloromethane (3 ml) and stirred for 4 hours at room temperature. The solvent was evaporated and recrystallised from ethyl acetate to give the title compound **305** as a brown powder (9 mg, 14 %); mp.>250; $[\alpha]_D^{25}$ (could not be determined due to the sample being opaque); IR ν_{max}(Nujol)/cm^{-1} 1636 (C=N); ^{1}H-NMR (500 MHz; $CDCl_3$) δ_H 8.64 (6H, s, N=C*H*), 7.88 (6H, d, *J* 8.8, Ar-*H*), 7.63 (6H, d, *J* 8.8, Ar-*H*), 3.71 (18H, s, -OCH_3), 3.51 (6H, broad, C*H*-N), 1.88-1.42 (24H, m, CH_2); ^{13}C-NMR (67.5 MHz, $CDCl_3$) δ_C 157.3, 153.1, 124.1, 118.6, 75.3, 64.2, 33.0, 27.7; MS (FAB) *m/z* 967 (M^+, 100%); CHN requires for $C_{60}H_{66}N_6O_6$: C 74.5 %, H 6.8 %, N 8.6 %. Found: C 72.5 %, H 6.1 %, N 7.5 %.

(2*R*, 3*R*, 11*R*, 12*R*, 20*R*, 21*R*)-1, 4, 10, 13, 19, 22-Hexa-aza- (2, 3: 11, 12: 20, 21)-tributano-(6, 8: 15, 17: 24, 26)-tri-cycloheptatrieno-(2H, 3H, 11H, 12H, 20H, 21H-)-hexahydro- (27)-annulene (306)

(2*R*, 3*R*, 11*R*, 12*R*)-1, 4, 10, 13-Tetraaza- (2, 3: 11, 12)-dibutano-(6, 8: 15, 17)-di-cycloheptatrieno-(2H, 3H, 11H, 12H)-tetrahydro- (18)-annulene (307).

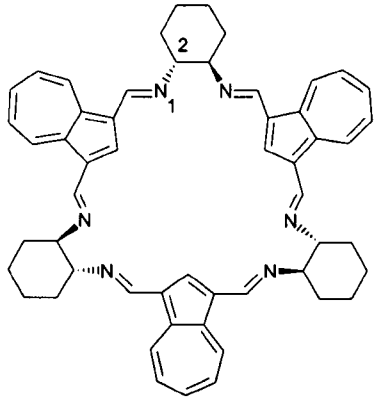

306

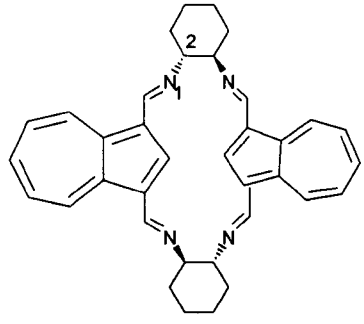

307

1,3-Diformylazulene **85** (368 mg, 2 mmol) in dichloromethane was added to a solution of (1*R*, 2*R*)-diaminocyclohexane **38** (228 mg, 2 mmol) in dichloromethane (20 ml) and stirred for 3 hours under reflux. The solvent was evaporated giving gave an unseparable 4:1 mixture of trianglimine (**306**) and macrocycle (**307**) as a black glassy powder. (0.12 g 15 %); mp. 180-183 °C; $[\alpha]_D^{25}$ (could not be determined since solution completely absorbs polarised light); IR ν_{max} (Nujol)/cm^{-1} 1644 (C=N) ; ^{1}H-NMR (500 MHz; d^6-DMSO) δ_H 9.00 (6H, d, *J* 9.7, Ar-*H*, **306**), 8.58 (6H, s, N=C*H*, **306**), 8.49 (4H, s, N=C*H*, **307**), 8.27 (2H, s, Ar-*H*, **307**), 8.19 (4H, d, *J* 9.7, Ar-*H*, **307**), 8.09 (3H, s, Ar-*H*, **306**), 7.47 (2H, t, *J* 9.7, Ar-*H*, **307**), 7.11 (6H, t, *J* 9.7, Ar-*H*, **306**), 6.56 (4H, t, *J* 9.7, Ar-*H*, **307**), 6.33 (3H, t, *J* 9.7, Ar-*H*, **306**), 3.50 (4H, m, C*H*-N, **307**), 3.44 (6H, m, C*H*-N, **306**), 1.12-2.15 (24H, m, CH_2, **307** and **306**); MS (LSIMS) *m/z* 788.0 (M$^+$+H, 80 %, **306**), 526.4 (M$^+$, 20 %, **307**).

(2*R*, 3*R*, 17*R*, 18*R*)- 1, 4, 16, 19-Hexa-aza-(2, 3: 17, 18)-dibutano-(6, 9: 11, 14: 21, 24: 26, 29)-tetraethene-10, 25-dioxo-(2H, 3H, 17H, 18H)- tetrahydro-(30)-annulene-308.

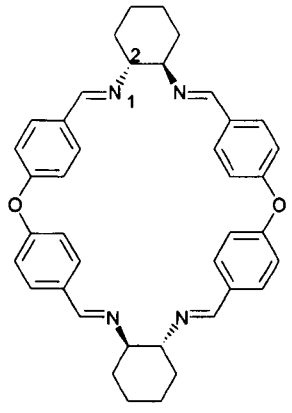

4,4'-Bis(formyl)phenyl-ether **237** (70 mg, 0.31 mmol) in dichloromethane (1.0 ml) was added to a solution of (1*R*, 2*R*)-diaminocyclohexane **38** (35 mg, 0.31 mmol) in dichloromethane (1.0 ml) and stirred for 24 hours at room temperature. The solvent was evaporated and the title compound **308** was obtained as a white powder (80 mg, 42 %); mp 120 °C (decomposition); IR ν_{max}(Nujol)/cm^{-1} 1636 (C=N); ^{1}H-NMR (500 MHz; $CDCl_3$) δ_H 8.33 (4H, s, N=C*H*), 7.73 (8H, d, *J* 8.6, Ar-*H*), 7.04 (8H, d, *J* 8.6, Ar-*H*), 2.9 (4H, m, C*H*-N), 1.91-1.65 (16H, m, CH_2); ^{13}C-NMR (67.8 MHz, $CDCl_3$) δ_C 160.0, 130.1, 129.8, 119.1, 74.0, 33.8, 25.3, 25.0; MS (FAB) *m/z* 609.7 (M^++H, 100%); CHN requires for $C_{40}H_{40}N_4O_2$: C 78.9 %, H 6.6 %, N 9.2 %. Found C 77.4 %, H 6.6 %, N 9.0 %.

(2*R*, 3*R*, 17*R*, 18*R*)-1, 4, 10, 16, 28, 28-Hexa-aza-(10, 25)-diethyl-(2, 3: 17, 18)-dibutano-(6, 9: 11, 14, 21: 24, 26: 29)-dibutadieno-(2H, 3H, 17H, 18H)-tetrahydro-(30)-annulene-309.

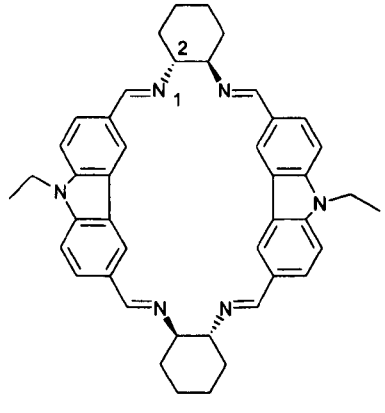

3,6-Diformyl-9-N-ethylcarbazole **79** (40 mg, 0.59 mmol) in dichloromethane (2 ml) was added to a solution of of (1*R*, 2*R*)-diaminocyclohexane **38** (18.20 mg, 0.59 mmol)

in dichloromethane (2 ml) and stirred for 3 hours under reflux. The solvent was evaporated and the residue was recrystallised from ethyl acetate, to give the title compound **309** as a yellow powder (45 mg, 30 %); mp. 250 °C; IR ν_{max}(Nujol)/cm^{-1} 1620 (C=N); $[\alpha]_D^{25}$ –295.4° (*c* 0.04, CH_2Cl_2, 1-dm); ^{1}H-NMR (500 MHz; $CDCl_3$) δ_H 8.73 (2H, s, N=C*H*), 8.48 (2H, s, N=C*H*), 8.24 (2H, s, Ar-*H*), 8.18 (2H, s, Ar-*H*), 7.09 (4H, t, *J* 8.6, Ar-*H*), 6.82 (2H, d, *J* 8.6, Ar-*H*), 3.99 (4H, q, *J* 7.1, NCH_2), 3.74 (2H, m, C*H*-N), 3.40 (2H, m, C*H*-N), 2.06 (2H, m, -CH_2), 1.20-1.92 (14H, m, -CH_2), 0.99 (6H, t, *J* 7.1, CH_3); ^{13}C-NMR (67.8MHZ, $CDCl_3$) δ_C 162.9, 161.5, 141.5, 141.0, 128.4, 128.3, 123.8, 123.6, 117.3, 109.3, 107.7, 75.9, 72.9, 37.1, 33.8, 32.7, 24.1, 24.9, 13.1; MS (LSIMS) *m/z* 658.4 (M^+, 100%); CHN requires for $C_{44}H_{46}N_6$: C 80.0 %, H 7.0 %, N 12.7 %). Found: C 71.4 %, H 8.1 %, N 9.9 % (**309**+3H_2O+EtOAc).

(2*R*, 3*R*, 12*R*, 13*R*, 22*R*, 23*R*)- 1, 4, 11, 14, 21, 24- Hexa-aza-(2, 3: 12, 13: 22, 23)-tributano-(7, 8', 17, 18', 27, 28')-hexamethoxy-(6, 9: 16, 19: 26, 29)-trietheno-(1H, 2H, 3H, 4H, 5H, 10H, 11H, 12H, 13H, 14H, 15H, 21H, 22H, 23H, 24H, 25H, 30H)-octadecahydro- (30)-annulene-319.

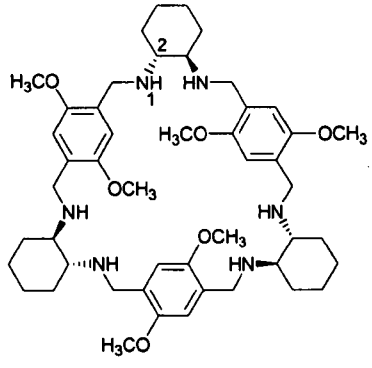

To a stirred solution of compound **289** (0.127 g, 0.15 mmol) in THF:MeOH (1:1, 3 ml) gradually was added solid $NaBH_4$ (0.05 g, 1.2 mmol), and the solution was stirred for 2 hours at room temperature. After removal of solvents under vacuum, the residue was extracted CH_2Cl_2 (3x15 ml) and 10 ml water, the organic extracts were combined, dried over $MgSO_4$, filtered and the solvent removed under vacuum. Recrystallisation from toluene gave the title compound **319** as a white powder (0.1 g, 80 %); mp. 165°C; $[\alpha]_D^{25}$ -219.8° (*c* 0.2, CH_2Cl_2, 1-dm); IR ν_{max}(Nujol)/cm^{-1}:1460, 1378; ^{1}H NMR (270 MHz; $CDCl_3$) δ_H 6.74, (6H, s, Ar-*H*), 3.81 (12H, d, *J* 12.6 Hz, CH_AH_BN), 3.59 (18H, s, OCH_3), 3.56 (12H, AB doublet, *J* 12.6, CH_AH_BN), 2.12-1.81 (36H, m, C*H*-N, CH_2 and N*H*); ^{13}C NMR (67.5 MHz; $CDCl_3$) δ_C 151.6, 128.0, 112.8, 60.8, 55.0, 45.8,

31.2, 25.1; MS (LSIMS) *m/z* 829.3 (M^+, 100%); CHN requires for $C_{48}H_{72}N_6O_6$: C 69.5 %, H 8.7 %, N 10.0 %. Found: C 69.4 %, H 8.7 %, N 9.5 %.

(2*R*, 3*R*, 12*R*, 13*R*, 22*R*, 23*R*)-1, 4, 11, 14, 21, 24-Hexa-aza- (7, 8, 17, 18, 27, 28)-hexamethoxy- (2, 3: 12, 13: 22,23)-tributano-(6, 9: 16, 19: 26, 29)-trietheno-(1H, 2H, 3H, 4H, 5H, 9H, 10H, 11H, 12H, 13H, 14H, 18H, 19H, 20H, 21H, 22H, 23H, 30H)-octadecahydro-(30)-annulene-320.

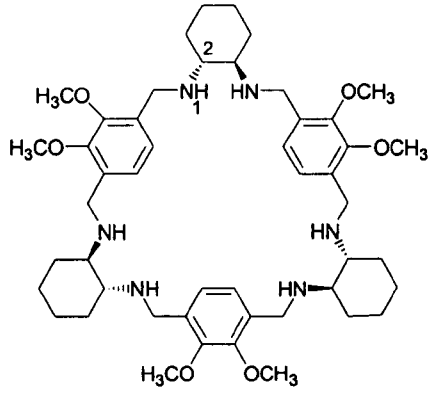

In the same way as for macrocycle **289**, macrocycle **290** (0.1 g, 0.16 mmol) and $NaBH_4$ (0.12 g, 3.21 mmol) in 2 ml of THF:MeOH (1:1) gave macrocycle **320** (20 mg, 15 %) as an oil; $[\alpha]_D^{25}$ 0 (*c* 0.1, $CHCl_3$, 1-dm); IR ν_{max} (Nujol)/cm^{-1} 3415 (N-H) ; ^{1}H-NMR (300 MHz; $CDCl_3$) δ_H 6.93 (6H, s, Ar-*H*), 3.77 (18H, s, C*H*$_3$O), 3.52 (12H, AB system, *J* 13.3, C*H*$_A$H$_B$N), 2.08-0.95 (36H, m, C*H*-N, C*H*$_2$ and N*H*); ^{13}C-NMR (67.8 MHz, $CDCl_3$) δ_C 152.3, 124.6, 61.3, 46.1, 32.1, 31.7, 25.5; MS (CI) *m/z* 831.0 (M^++H, 100%); CHN requires for $C_{48}H_{72}N_6O_6$: C 69.5 %, H 8.7 %, N 10.1 %. Found: C 68.4 %, H 8.7 %, N 9.1 %.

(2*R*, 3*R*, 11*R*, 12*R*, 20*R*, 21*R*)-1, 4, 10, 13, 19, 22-Hexa-aza- (7, 16, 25)-trimethoxy-(2, 3: 11, 12: 20, 21)-tributano-(6, 8: 15, 17: 24, 26)-tris (1', 3'-dimethoxy-propeno-(1H, 2H, 3H, 4H, 5H, 9H, 10H, 11H, 12H, 13H, 14H, 18H, 19H, 20H, 21H, 22H, 23H, 27H)-octadecahydro - (27)-annulene (321).

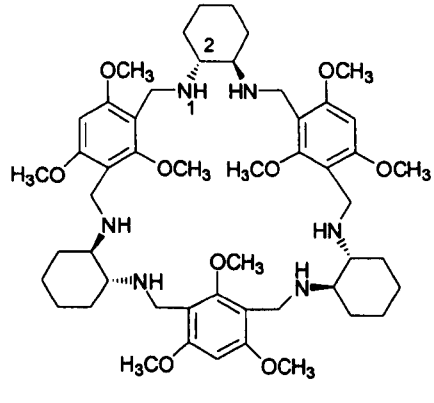

In the same way as for macrocycle **289**, macrocycle **291** (16 mg, 0.02 mmol), and $NaBH_4$ (15.54 mg, 0.411 mmol) in 0.6 ml of THF:MeOH (1:1) gave the title compound **321** as a yellow oil (2 mg 13 %); IR ν_{max}(Nujol)/cm^{-1} 3320 -broad (amine); $[\alpha]_D^{25}$ –200 ° (*c* 0.1, $CHCl_3$, 1-dm); ^{1}H-NMR (300 MHz, $CDCl_3$) δ_H 6.14 (6H, s, Ar-*H*), 3.74 and 3.72 (12H, AB system, *J* 12.7, CH_AH_BN), 3.66 (9H, s, -OCH_3), 3.62 (18H, s, -OCH_3), 1.51-2.05 (36H, m, C*H*-N, CH_2 and N*H*); ^{13}C-NMR (67.8 MHz, $CDCl_3$) δ_C 157.5, 155.3, 101.9, 98.6, 62.8, 59.5, 58.9, 36.2, 33.5; MS (CI) *m/z* 919.9 (M^+, 100%).

(2*R*, 3*R*, 11*R*, 12*R*, 22*R*, 23*R*)- 1, 4, 7, 10, 13, 16, 19, 22, 25-Nona-aza-(2, 3: 11, 12: 20, 21)-tributano-(6, 8: 15, 17: 24, 26)-tripropeno-(1H, 2H, 3H, 4H, 5H, 9H, 10H, 11H, 12H, 13H, 14H, 18H, 19H, 20H, 21H, 22H, 23H, 27H)-octadecahydro-(27)-annulene-322.

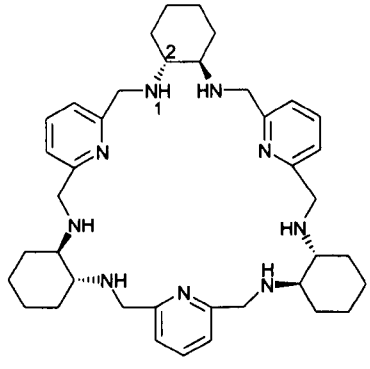

In the same way as for macrocycle **289**, macrocycle **296** (60 mg, 0.94 mmol), and $NaBH_4$ (22 mg, 5.6 mmol) in 0.6 ml of THF:MeOH (1:1) gave the title compound **322** as a yellow powder (55 mg, 90 %); mp 60°C; $[\alpha]_D^{25}$ – 240° (*c* 0.05, $CHCl_3$, 1-dm); IR ν_{max} (Nujol)/cm^{-1} 3340 (N-H, br); ^{1}H-NMR (300 MHz; $CDCl_3$) δ_H 7.55 (6H, broad, Ar-*H*), 7.04 (9H, broad, Ar-*H*), 3.80 and 3.73 (12H, AB system, *J* 12.9, CH_AH_BN), 2.42 -0.71 (36H, C*H*-N, CH_2 and N*H*); ^{13}C-NMR (67.8 MHz, $CDCl_3$) δ_C 137.0, 135.1, 120.3, 61.6, 52.7, 31.7, 25.2; MS (EI) *m/z* 651.47 (M^+, 100%); Accurate mass requires for $C_{39}H_{57}N_9$ 651.474 found 651.4731 (R_f 0.7).

(2*R*, 3*R*, 11*R*, 12*R*, 20*R*, 21*R*)-1, 4, 10, 13, 19, 22-Hexa-aza-(7, 16, 25)-trioxo-(2,3: 11, 12: 20, 21)-tributano-(6, 8: 15, 17: 24, 26)-trietheno-(1H, 2H, 3H, 4H, 5H, 9H, 10H, 11H, 12H,13H, 14H, 18H, 19H, 20H, 21H, 22H, 23H, 27H)- octadecahydro - (27)-annulene-323.

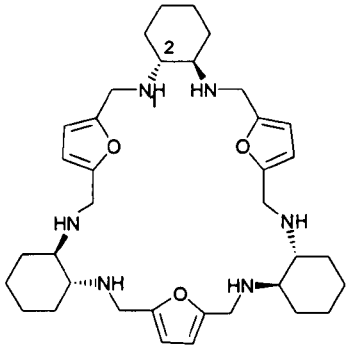

In the same way as for macrocycle **289**, macrocycle **299** (0.11 mg, 0.18 mmol), and $NaBH_4$ (21 mg, 0.56 mmol) in 10 ml of THF:MeOH (1:1) gave macrocycle **323** as a brown oil. ^{1}H-NMR (300 MHz, $CDCl_3$) δ_H 6.06 (6H, broad, Ar-*H*), 3.44-3.88 (18H, broad, C*H*$_2$N, C*H*-N), 2.17-0.97 (30H, broad, -C*H*$_2$, N*H*), ^{13}C-NMR (67.8 MHz, $CDCl_3$) δ_C 115.0, 107.4, 60.67, 43.7, 31.6, 25.1; MS (LSIMS) *m/z* 619.5 (M^++H, 100 %).

(2*R*, 3*R*, 12*R*, 13*R*, 22*R*, 23*R*)-1, 4, 15, 18, 29, 32-Hexa-aza-(2, 3: 12, 13: 22,23)-tributano-(6, 9: 16, 19: 26, 29)-tribenzo-(6', 9': 16', 19': 26', 29')-tributadieno-(1H, 2 H, 3H, 4H, 5H, 14H, 15H, 16H, 17H, 15H, 19H, 28H, 29H, 30H, 31H, 32H, 33H, 42H)-octadecahydro-(30)-annulene-324.

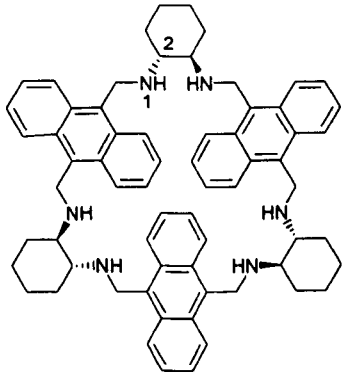

In the same way as for macrocycle **289**, macrocycle **300** (127 g, 0.15 mmol), and $NaBH_4$ (0.05 g, 3.1 mmol) in 4 ml of THF:MeOH (1:1) gave macrocycle **324** as a yellow powder. (113 mg, 88 %); mp 147°C; $[\alpha]_D^{25}$ +212.6° (*c* 0.1, CH_2Cl_2, 1-dm); IR

ν_{max}(Nujol)/cm^{-1}: 1462 - 1377 (C_{Ar}=C_{Ar}); ^{1}H NMR (270 MHz; $CDCl_3$) δ_H : 8.02-6.94 (24H, broad, Ar-*H*), 4.88 and 4.56 (12H, AB system, *J* 12.3, CH_AH_BN), 2.17-1.29 (36H, m, C*H*-N, CH_2 and N*H*); ^{13}C NMR (67.5 MHz; $CDCl_3$) δ_C 132.1, 130.0, 125.4, 124.9, 62.3, 43.5, 32.3, 25.3; MS (LSIMS) *m/z* 949.4 (M^++H, 100%); CHN requires for $C_{66}H_{72}N_6$: C 83.5 %, H 7.6 %, N 8.9 %. Found: C 83.7 %, H 7.9 %, N 8.2 %.

(2*R*, 3*R*, 16*R*, 17*R*, 30*R*, 31*R*)-1, 4, 15, 18, 29, 32-Hexa-aza-(2, 3: 16, 17: 30, 31)-tributano-(6, 9: 10, 13: 20, 23: 24, 27: 34, 37: 38, 41)-hexaetheno-(1H, 2H, 3H, 4H, 5H, 14H, 15H, 16H, 17H-18H, 19H, 28H, 29H, 30H, 31H, 32H, 33H, 42H)-duodecahydro- (42)-annulene (325).

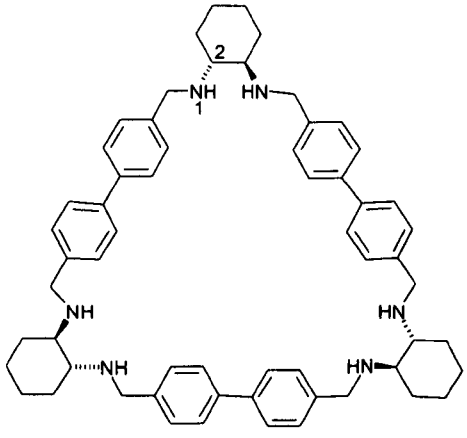

In the same way as for macrocycle **289**, macrocycle **301** (0.127 g, 0.15 mmol) and $NaBH_4$ (0.05 g, 3.1 mmol) in 3 ml of THF:MeOH (1:1) gave macrocycle **325** as a white powder (0.05 g, 40 %); mp over 200°C; $[\alpha]_D^{25}$ –227.3° (*c* 0.1, CH_2Cl_2, 1-dm); IR ν_{max}(Nujol)/cm^{-1}: 1460 - 1377 (C_{Ar}=C_{Ar}); ^{1}H NMR (270 MHz; $CDCl_3$) δ_H: 7.22- 7.61 (8H, broad, Ar-*H*) 3.99 and 3.42 (12H, AB system, *J* 12.4, CH_AH_BN), 2.11-1.15 (36H, m, C*H*-N, CH_2 and N*H*) ^{13}C NMR (67.5 MHz; $CDCl_3$) δ_C 140.1, 139.8, 128.1, 127.3, 62.3, 43.5, 32.3, 25.2; MS (LSIMS) *m/z* 877.3 (M^+, 100%); CHN requires for $C_{60}H_{72}N_6$: C 82.1 %, H 8.2 %, N 9.5 %. Found: C 79.1 %, H 8.3 %, N 9.3 % (**325**+EtOAc).

(2*R*, 3*R*, 14*R*, 15*R*)-1, 4, 13, 16 –Hexa-aza-(7, 10, 19, 22)-tetramethoxy -(2, 3: 14, 16)-dibutano-(6, 8: 9, 11: 18, 20: 21, 23: 30, 32: 33, 35)-tetrakis-(2-methoxy-4-methyl)-propeno-(2H, 3H, 4H, 5H, 12H, 13H, 14H, 15H, 16H, 24H, 25H, 26H, 27H, 28H, 29H, 36H)-duodecahydro- (24)-annulene-326.

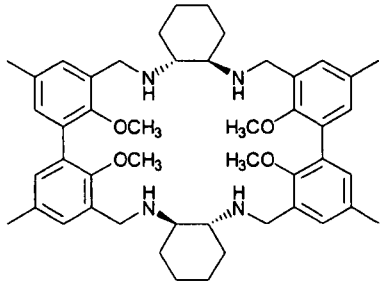

In the same way as for macrocycle **289**, macrocycle **302** (79 mg, 0.07 mmol), and $NaBH_4$ (53 mg, 1.4 mol) in 1 ml of THF:MeOH (1:1) gave macrocycle **326** as a green powder; ^{1}H-NMR (300 MHz, $CDCl_3$) δ_H 7.17 (4H, s, Ar-*H*), 6.85 (4H, s, Ar-*H*), 3.93 (8H, AB system, *J* 13.2, CH_AH_BN), 3.70 (4H, broad, C*H*-N), 3.95 (12H, s, OCH_3), 2.30 (12H, s, CH_3), 1.69-1.07 (20H, broad, CH_2, N*H*); ^{13}C-NMR (67.8 MHz, $CDCl_3$) δ_C 153.5, 134.0, 133.8, 132.1, 77.8, 61.6, 46.6, 32.0, 25.5, 21.0, 25.9 (quartenary Ar-C could not be detected due to low solubility); MS (FAB) *m/z* 783.1 (M^++Na, 100%); CHN requires for $C_{48}H_{68}N_4O_4$: C 75.5 %, H 8.4 %, N 7.2 %. Found: C 69.1%, H 8.8 %, N 6.8 % (**326**+MeOH+$NaBH_4$).

Macrocycle 308.

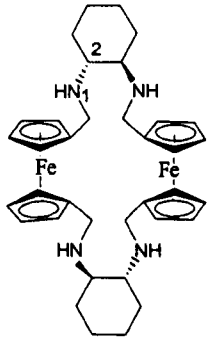

Macrocycle **303** (5 mg), was dissolved in 2 ml of THF:MeOH (1:1) at 0 °C. Gradually $NaBH_4$ (10 mg) was added slowly. After the addition the reaction was stirred for 24 hours at room temperature. Finally the solvent was removed and the solid was extracted with dichloromethane and water. The solvent was evaporated to give the title compound **327** as a brown oil; ^{1}H-NMR (500 MHz; $CDCl_3$) δ_H 3.90 (16H, broad,

Ar-*H*), 4.44-3.60 (34H, broad, C*H*$_2$N, C*H*-N), 1.95-1.20 (20H, broad, -C*H*$_2$, N*H*); MS (LSIMS) *m/z* 650.0 (M^++H, 100 %).

(2*R*, 3*R*, 13*R*, 14*R*, 24*R*, 25*R*)-(1, 4, 12, 15, 23, 26)-Hexa-aza-(7', 18', 29')-trimethoxy-(6, 9: 17, 20: 28, 31)-trietheno-(8, 10: 19, 21: 30, 32)-tris(tri-3-methoxy)propeno-(1H, 2H, 3H, 4H, 5H, 11H, 12H, 13H, 14H, 15H, 16H, 22H, 23H, 24H, 25H, 26H, 27H, 33H)-octadecahydro-(33)-annulene-328.

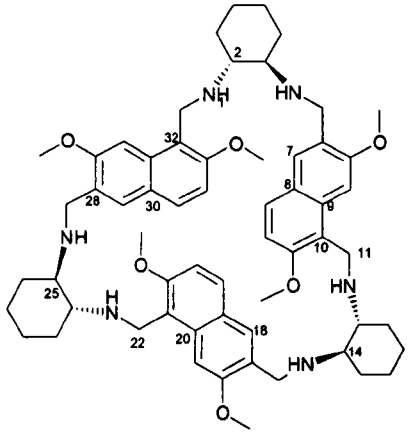

In the same way as for macrocycle **289**, macrocycle **304** (less then 3 mg), and $NaBH_4$ in 2 ml of THF:MeOH (1:1) gave macrocycle **328** as a dark yellow oil. ^{1}H-NMR (500 MHz; $CDCl_3$) δ_H 7.35 (12H, broad, Ar-*H*), 4.00-3.30 (34H, broad, C*H*$_2$N, OC*H*$_3$, C*H*-N), 1.19-1.9 (28H, broad, C*H*$_2$, N*H*); MS (ESI) *m/z* 1042 (M^++H+$NaBH_4$+Na, 100 %), 1056 (M^++H+2$NaBH_4$, 55%).

(2*R*, 3*R*, 14*R*, 15*R*, 26*R*, 27*R*)-(1, 4, 11, 13, 16, 25, 28)-Hexa-aza-(7, 10, 19, 22, 31, 34)-hexamethoxy-(2, 3: 14, 15: 26, 27)-tributano -(6, 9: 8, 11: 18, 21: 20, 23: 30, 33: 32, 35)-hexaetheno-(1H, 2H, 3H, 4H, 5H, 14H, 15H, 26H, 27H)- octadeca-hydro-(36)-annulene-329.

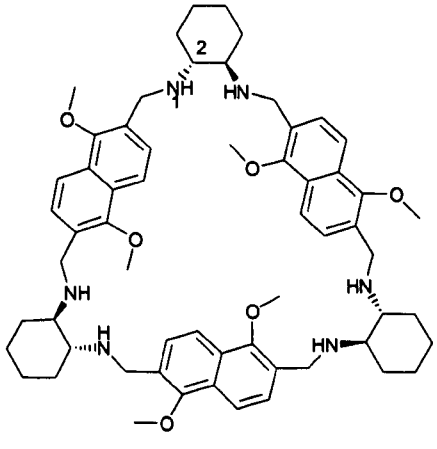

In the same way as for macrocycle **289**, macrocycle **305** (6 mg, $6.21x10^{-3}$ mmol), and $NaBH_4$ (4 mg, 0.12 mmol) in 2 ml of THF:MeOH (1:1) gave macrocycle **329** as brown oil; $[\alpha]_D^{25}$ (could not be determined due to the sample being opaque); ^{1}H-NMR (500 MHz; $CDCl_3$) δ_H 7.40 (6H, d, *J* 7.5, Ar-*H*), 6.85 (6H, d, *J* 7.5, Ar-*H*), 4.28 and 4.03 (12H, AB system, *J* 12.0, -CH_AH_BN), 3.85 (8H, s, OCH_3), 3.72 (6H, broad, C*H*-N), 1.19-1.9 (28H, m, -CH_2, N*H*); MS (LSIMS) *m/z* 1049.6 (M^++THF, 100 %), 979.7 (M^++H, 50%).

(2*R*, 3*R*, 17*R*, 18*R*)- 1, 4, 16, 19-tetra-aza-(2, 3: 17, 18)-dibutano-(6, 9: 11, 14: 21, 24: 26, 29)-tetraetheno-10, 25-dioxo-(2H, 3H, 5H, 15H, 17H, 18H, 20H, 30H)-octahydro-(30)-annulene-330.

(2*R*, 3*R*, 17*R*, 18*R*, 32*R*, 33*R*)- (1, 4, 16, 19, 31, 34)-Hexa-aza-(2, 3: 17, 18: 32, 33)-tributano-(6, 9: 11, 14: 21, 24: 26, 29: 36, 39: 41, 44)-tetraetheno-(10, 25, 40)-trioxo-(1H, 2H, 3H, 5H, 15H, 16H, 17H, 18H, 19H, 20H, 30H, 31H, 32H, 33H, 34H, 35H, 45H)- dodecahydro-(45)-annulene-331.

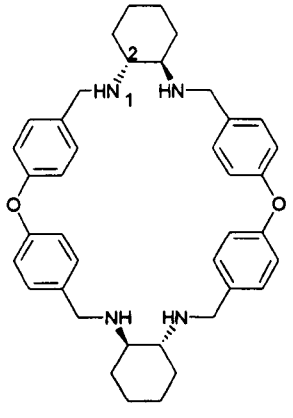

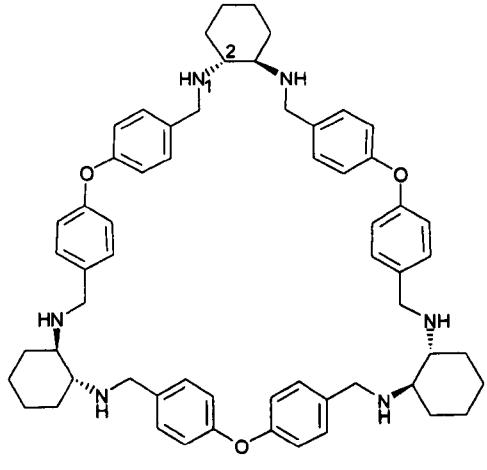

In the same way as for macrocycle **289**, macrocycle **308** (20 mg, 0.033 mmol), and $NaBH_4$ (21 mg, 0.56 mmol) in 4 ml of THF:MeOH (1:1) gave a 3:1 mixture of macrocycles **330** and **331** as a yellow powder; ^{1}H-NMR (500 MHz; $CDCl_3$) δ_H 7.16 (12H, d, *J* 8, Ar-*H*), 7.15 (12H, d, *J* 8.5, Ar-*H*), 6.84 (8H, d, *J* 8.4, Ar-*H*), 6.83 (8H, d, *J* 8.4, Ar-*H*), 3.84-3.46 (30H, broad, CH_2N, C*H*-N), 2.18-1.00 (49H, broad, CH_2, N*H*); ^{13}C-NMR (67.8 MHz, $CDCl_3$) δ_C 156.4, 129.6, 118.9, 61.3, 61.0, 50.4, 31.7, 25.2 (the signals of the two compounds are overlapped); MS (ESI) *m/z* 617.5 (M+ H, **330**, 100 %), 925.5 (M+H, 40 %, **331**).

(2*R*, 3*R*, 17*R*, 18*R*)-1, 4, 10, 16, 28, 28-Hexa-aza-(10, 25)-diethyl-(2, 3: 17, 18)-dibutano-(6, 9: 11, 14, 21: 24, 26: 29)-dibutadieno-(1H, 2H, 3H, 4H, 5H, 15H, 16H, 17H, 18H, 19H, 20H, 30H)-dodecahydro-(30)-annulene-332.

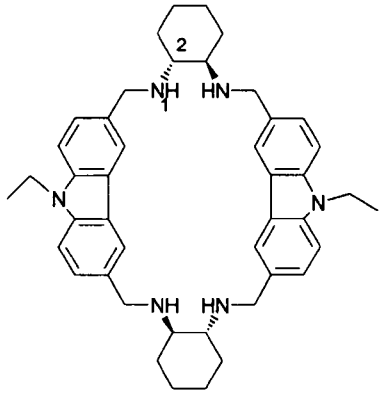

In the same way as for macrocycle **289**, macrocycle **309** (21 mg, 0.56 mmol), and $NaBH_4$ (9.75 mg, 9.75 mmol) in 1 ml of THF:MeOH (1:1) gave macrocycle **332** as a yellow oil. $[\alpha]_D^{25}$ –295 (*c* 0.04, $CHCl_3$, 1-dm); IR ν_{max}(Nujol)/cm^{-1} 3402.0 (NH); ^{1}H-NMR (300 MHz, $CDCl_3$) δ_H 8.19 (4H, s, Ar-*H*), 7.29 (8H, AB system, *J* 8.1, Ar-*H*), 4.46 (4H, q, *J* 7.0, CH_2), 4.05 and 3.78 (8H, AB system, *J* 13.5, -CH_AH_BN), 3.65 (6H, s, C*H*-N), 2.51-1.80 (20H, m, CH_2, N*H*), 1.13 (6H, t, *J* 7.0, CH_3); ^{13}C-NMR (67.8 MHz, $CDCl_3$) δ_C 130.2, 111.3, 91.5, 77.4, 55.8, 30.7, 30.2, 29.9, 28.6, 25.1 (quartenary Ar-C could not be detected due to low solubility); MS (FAB) *m/z* 666.4 (M^+, 100%); CHN requires for $C_{44}H_{49}N_6$: C 79.2 %, H 8.1 %, N 12.0 %;. Found: C 76.2 %, H 6.6 %, N 10.5 %.

(2*R*, 3*R*, 12*R*, 13*R*, 22*R*, 23*R*)-1, 4, 11, 14, 21, 24-Hexa-aza- (8, 18, 27)-trimethyl-(2, 3: 12, 13: 22, 23)-tributano-(6, 9: 16, 19: 26, 29)-tripropano-(1H, 2H, 3H, 4H, 5H, 10H, 11H, 12H, 13H, 14H, 15H, 20H, 21H, 22H, 23H, 24H, 25H, 30H)-octadecahydro-(30)-annulene-333.

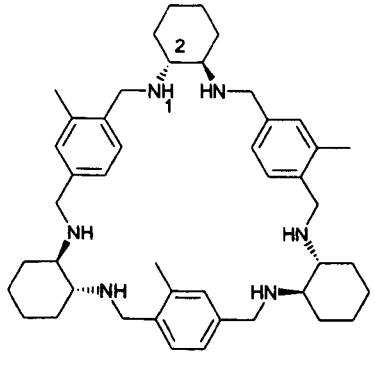

In the same way as for macrocycle **289**, macrocycles **294** (35 mg, 0.51 mmol), and $NaBH_4$ (39 mg, 1.02 mmol) in 6 ml of THF:MeOH (1:1) gave macrocycle **333** as a white powder. Mp 185°C; $[\alpha]_D^{25}$200 (*c* 0.01, $CHCl_3$, 1-dm); ^{1}H-NMR (300 MHz, $CDCl_3$) δ_H 7.27 (6H, d, *J* 8.0, Ar-*H*), 7.22 (6H, d, *J* 7.0, Ar-*H*), 7.75 (6H, d, *J* 7.0, Ar-*H*), 7.18 (3H, s, Ar-*H*), 7.15 (3H, s, Ar-*H*), 7.12 (3H, s, Ar-*H*), 3.88 and 3.56 (36H, AB system, *J* 13.5, -CH_AH_BN), 2.28 (18H, broad, C*H*-N), 2.12-1.18 (90H, m, CH_2, N*H*); ^{13}C-NMR (67.8 MHz, $CDCl_3$) δ_C 139.7, 137.4, 136.5, 130.0, 128.7, 125.5, 50.7, 48.9, 31.8, 25.8, 19.2; MS (ESI) *m/z* 691 (M^+, 100 %), 754.6 (M^++$NaBH_4$+Na, 97 %), 761.8 (M^++THF, 80%).

(2*R*, 3*R*, 12*R*, 12*R*, 22*R*, 23*R*)-1, 4, 11, 14, 21, 24-Hexa-aza-(2, 3: 12, 13: 22, 33)-tributano-(17, 18')- di-methoxy-(6, 9: 16, 19: 26, 29)- trietheno-(2H, 3H, 12H, 13H, 22H, 23H)-hexahydro-(30)-annulene-312

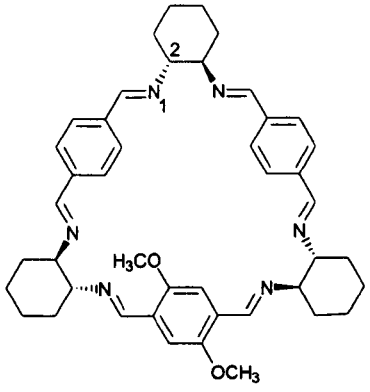

1,4-Dimethoxy-2,5-diformylbenzene (30 mg, 0.154 mmol) **158** and 41 mg (3.1 mmol) of terephthalaldehyde **39** in dichloromethane (1 ml) were added to a solution of (1*R*, 2*R*)-diaminocyclohexane (53.9 mg, 0.46 mmol) in dichloromethane (2 ml) and stirred for 3 hours at room temperature. The solvent was evaporated and the title compound was obtained after recrystallisation from ethyl acetate as a pale yellow powder (32 mg, 29 %); mp. 200; IR ν_{max}(Nujol)/cm^{-1} 1634.0 (C=N); ^{1}H-NMR (500 MHz; $CDCl_3$) δ_H 8.50 (2H, s, N=C*H*); 8.17 (2H, s, N=C*H*), 8.15 (2H,s, N=C*H*), 7.56 (8H, m, Ar-*H*), 7.11 (2H, s, Ar-*H*), 3.58 (6H, s, OCH_3), 3.37 (6H, s, C*H*-N), 1.85- 1.47 (24H, broad, -CH_2); ^{13}C-NMR (67.8 MHz, $CDCl_3$) δ_C 160.4, 157.42, 137.9, 128.4, 128.2, 128.0, 109.7, 74.6, 55.9, 32.9, 24.6; MS (CI) *m/z* 696.4 (M^+, 100%); Accurate mass requires for $C_{44}H_{52}O_2N_6$: 696.4151. Found 696.4146. (R_f 0.6).

Synthesis of trianglimines from mixtures of dialdehydes.

Synthesis of trianglimines 289 and 310.

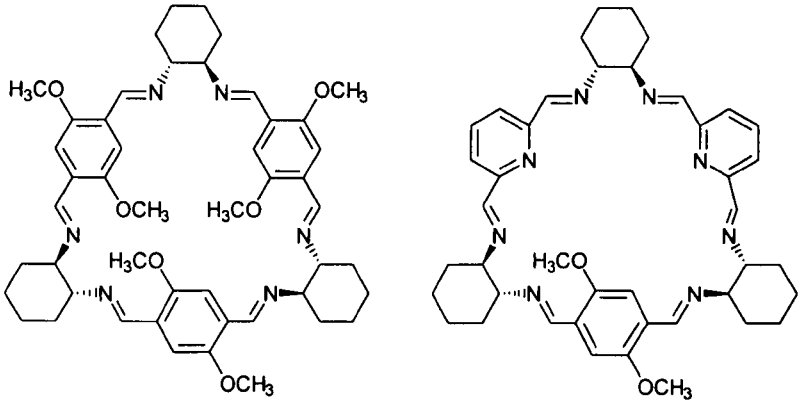

1,4-Dimethoxy-2,5-diformylbenzene (13.6 mg, 0.07 mmol) and 18.9 mg (0.14 mmol) of 2,6-diformylpyridine in dichloromethane (1 ml) were added to a solution of (1*R*, 2*R*)-diaminocyclohexane (23.9 mg, 0.21 mmol) in dichloromethane (2.3 ml) and stirred for 3 hours at room temperature. The solvent was evaporated and the mixture of trianglimines **289** and **310** were obtained after recrystallisation from ethyl acetate as a yellow powder. MS (ESI) *m/z* 817.7 (M^++H, 100 %, **289**), 697.8 (M^++H, 7 %, **310**).

Synthesis of trianglimines 289, 310 and 311.

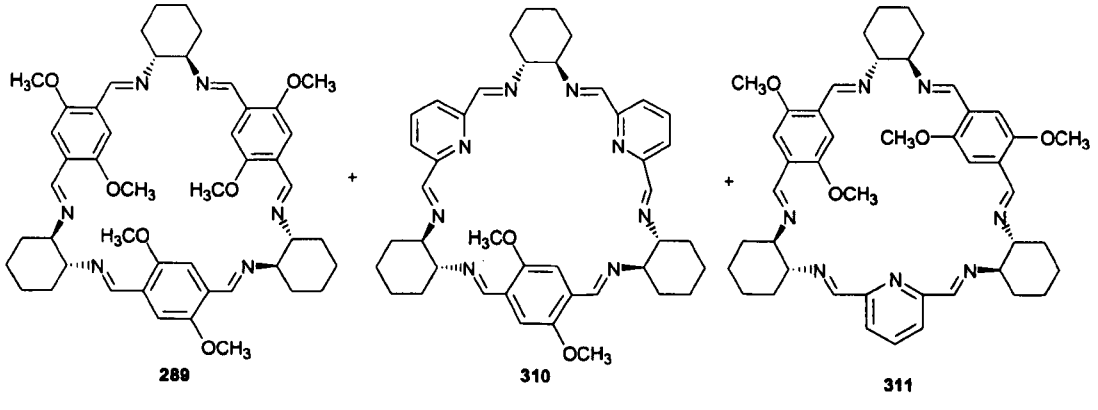

289 **310** **311**

1,4-Dimethoxy-2,5-diformylbenzene (66 mg, 0.34 mmol) **158** and 23.0 mg (0.17 mmol) of 2,6-diformylpyridine **163** in dichloromethane (0.25 ml) were added to a solution of (1*R*, 2*R*)-diaminocyclohexane (58.2 mg, 0.51 mmol) in dichloromethane (0.25 ml) and stirred for 3 hours at room temperature. The solvent was evaporated and the mixture of trianglimines **289**, **310** and **311** were obtained after recrystallisation

from ethyl acetate as a yellow powder. MS (ESI) *m/z* 817.5 (M^++H, 100 %, **289**), 757.7 (M^+, 20 %, **311**), 697.8 (M^++H, 19 %, **310**).

Synthesis of trianglimines 289, 312, 313 and 40.

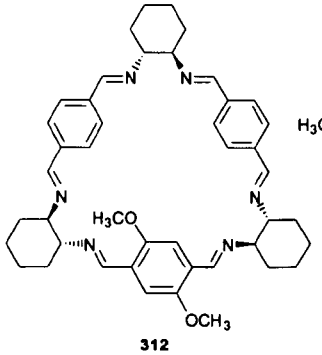
312

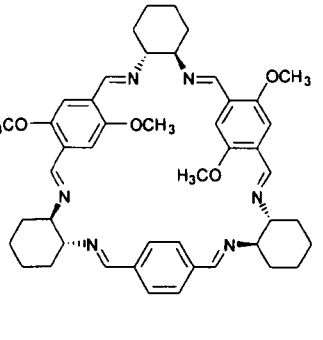
313

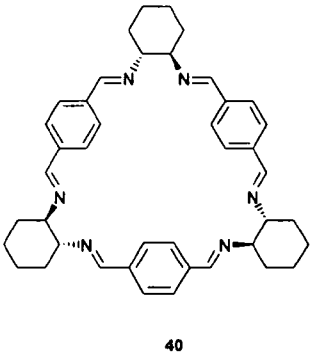
40

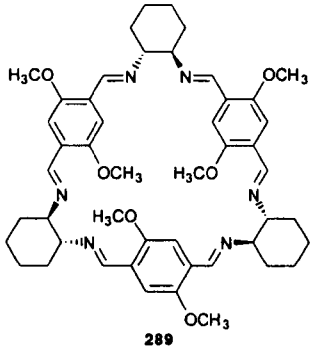
289

1,4-Dimethoxy-2,5-diformylbenzene (30 mg, 0.54 mmol) **158** and 41 mg (3.1 mmol) of terephthalaldehyde **39** in dichloromethane (0.25 ml) were added to a solution of (1*R*, 2*R*)-diaminocyclohexane (53.9 mg, 4.65 mmol) in dichloromethane (0.25 ml) and stirred for 3 hours at room temperature. The solvent was evaporated and the mixture of trianglimines **289**, **312**, **313** and **40** were obtained after recrystallisation from ethyl acetate as a yellow powder. MS (ESI) *m/z* 697.8 (M^++H, 100 %, **312**), 757.7 (M^+, 53 %, **313**), 637.9 (M^++H, 20 %, **40**), 817.6 (M^++H, 15 %, **289**).

Synthesis of trianglimines from mixtures of dialdehydes and trianglimines.

Synthesis of trianglimines 40, 312 and 313.

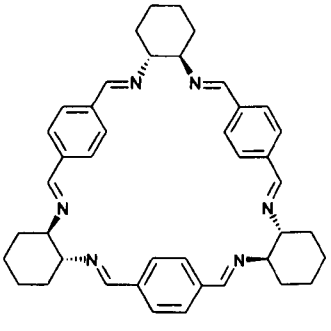
40

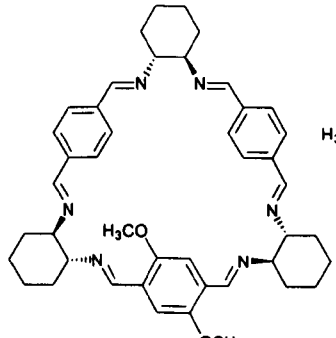
312

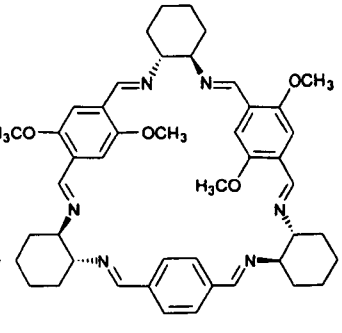
313

Trianglimine **40** (41.3 mg, 64.9×10^{-3} mmol) was mixed with 4.2 mg (21.61×10^{-3} mmol) of 1,4-dimethoxy-2,5-diformylbenzene **158** in 5 ml of $CDCl_3$ and the mixture was kept in solution for 15 days. The solvent was evaporated and the mixture of trianglimines **40, 312** and **313** were obtained after recrystallisation from ethyl acetate as a yellow powder. MS (ESI) *m/z* 638.0 (M^++H, 100 %, **40**), 697.8 (M^+, 18 %, **312**), 757.7 (M^++H, 15 %, **313**).

Synthesis of trianglimines 317, 318 and macrocycle 314.

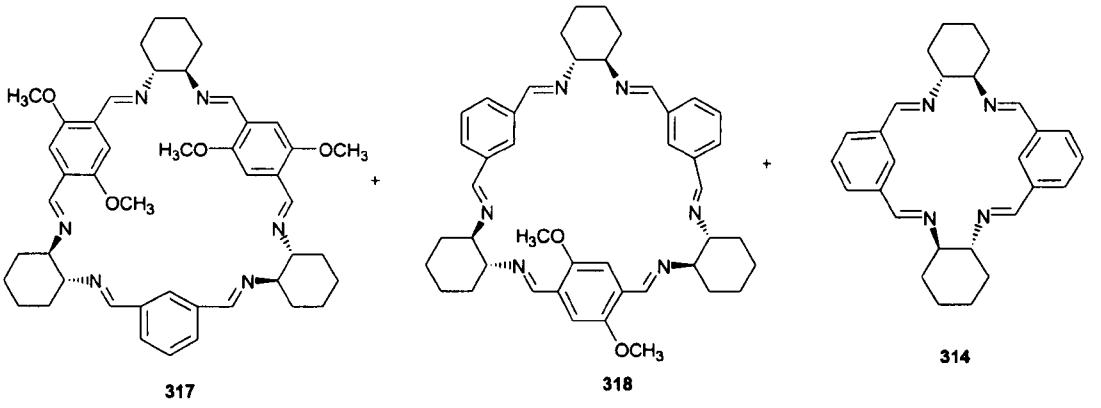

Trianglimine **42** (3.0 mg, $4.71x10^{-3}$ mmol) of was mixed with 3.4 mg ($4.71x10^{-3}$ mmol) of trianglimine **289** in 2 ml of $CDCl_3$ and the mixture was kept in solution for 15 days. The solvent was evaporated and the mixture of trianglimines **317, 318** and macrocycle **314** were obtained after recrystallisation from ethyl acetate as a yellow powder. MS (ESI) *m/z* 425.0 (M^++H, 100 %, **314**), 697.1 (M^+, 50 %, **318**), 757.0 (M^++H, 47 %, **317**).

Synthesis of trianglimines 40, 289, 312 and 313.

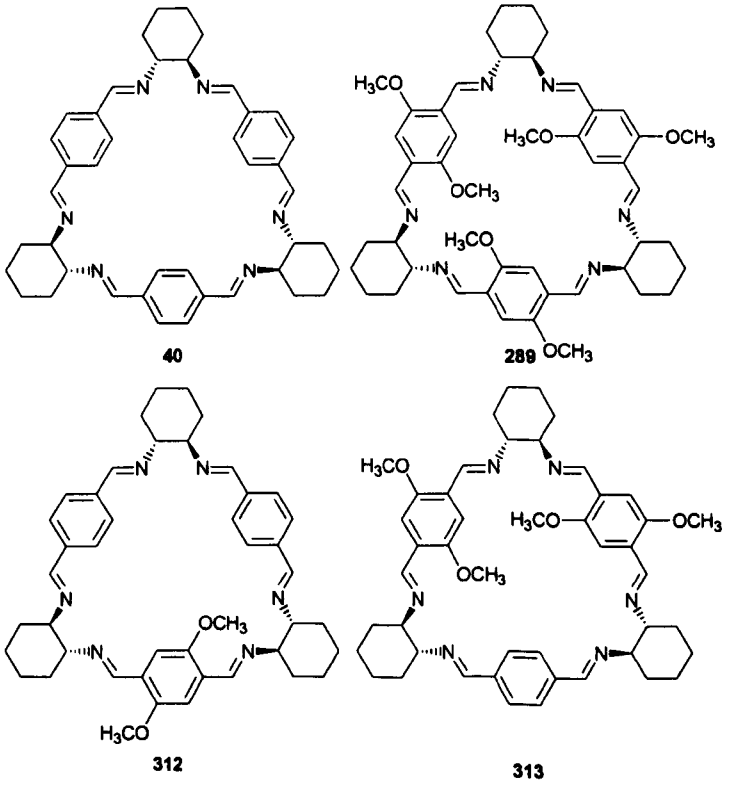

Trianglimine **40** (3.95 mg, $6.21x10^{-3}$ mmol) of was mixed with 4.5 mg ($6.21x10^{-3}$ mmol) of trianglimine **289** in 2 ml of $CDCl_3$ and the mixture was kept in solution for

15 days. The solvent was evaporated and the mixture of trianglimines **40**, **312**, **313** and **289** were obtained in a 1:3:3:1 proportion after recrystallisation from ethyl acetate as a yellow powder. MS (ESI) *m/z* 697.9 (M^++H, 100 %, **312**), 757.6 (M^++H, 99 %, **313**), 817.6 (M^++H, 24 %, **289**), 637 (M^+, 10 %, **40**).

PART IV

REFERENCES

1. Curtis, N. F.; *J. Chem. Soc.* **1960**, 4409.
2. Curtis, N. F.; *J. Chem. Soc.* **1964**, 2645.
3. Inoue, I.; Gokel, G. W.; "*Cation Binding by Macrocycles-Complexation of Cationic Species by Crown Ethers*" **1990**, Marcel Dekker Publisher, Basel, New York.
4. Pedersen, C. J.; *J. Am. Chem. Soc.* **1967**, *89*, 7017.
5. For cyclodextrins see special edition of *Chem. Rev.* **1998**, *5*.
6. Gutsche, C. D; "*Calixarenes Revisited*" in "*Monographs in Supramolecular Chemistry*"; Stoddart, J. F.; ED.; Royal Society of Chemistry: Cambridge **1998.**
7. Böhmer, V.; *Angew. Chem. Int. Ed. Engl.* 1995, *34*, 713.
8. Danil de Namor, A. F.; Cleverley, R. M.; Zapata-Ormachea, M. L.; *Chem. Rev.* **1998**, *98*, 2495.
9. Kim, J.; Jung, I. S.; Kim, S. Y.; Lee, E.; Kang, J. K.; Sakamoto, S.; Yamaguchi, K.; Kim, K.; *J. Am.Chem. Soc.* **2000**, *122*, 540.
10. Kim, S. Y.; Jung, I. S.; Lee, E.; Kim, J.; Sakamoto. S.; Yamaguchi, K.; Kim, K. *Angew. Chem. Int. Ed. Engl.* **2001**, *40*, 2119.
11. Pedersen, C. J., Frensdorff, H. K.; *Angew. Chem.* **1972**, *84*,16.
12. Dietrich, B.; Viout, P; Lehn, J.M.; "*Macrocyclic Chemistry*" **1993**, VCH, Weinheim.
13. Nelson, S. M.; Knox, C. V.; MacCann, M.; Drew, M. G. B.; *J. Chem. Soc., Dalton Trans.* **1981**, 1669.
14. Cox, B. G.; "*Modern liquid phase kinetics*" **1996**, Oxford Chemistry Primers, Oxford.
15. Lindoy, F.; "*The Chemistry of Supramolecular complexes*" **1990**, Cambridge University Press, Cambridge.
16. Lehn, J-M. ; "*Supramolecular Chemistry*" **1995**, VCH, Weinheim.
17. Fischer, E.; *Ber. Deutch. Chem. Ges.* **1894**, *27*, 2985.
18. Schneider, H-J.; Yatsimirsky, A. K.; "*Principles and methods in Supramolecular Chemistry*" **2000**, John Wiley & sons, Chichester.
19. Steed, J. W.; Atwood, J. L.; "*Supramolecular Chemistry*" **2000**, John Wiley & sons, Chichester.
20. Daintith, J. (Ed); "*Dictionary of Chemistry*" **1998**, Oxford University Press, Oxford.

21. Robinson, R. A.; Stokes, R. H., *"Electrolyte Solutions"* **1968**, Butterworths, London.
22. Hunter, C. A.; Sanders, J. K. M.; *J. Am. Chem. Soc.* **1990**, *112*, 5525.
23. Pons, M.; Millet, O.; *Prog. Nucl. Magn. Reson. Spectrosc.* **2001**, *8*, 267.
24. Chen, Z.; Mercier, L.; Tunney, J. J.; Detellier, C. L.; Echegoyen, A.; Kaifer, E., *"Physical Supramolecular Chemistry"* **1996**, Kluwer, Dordrecht.
25. Günther, H.; *"NMR spectroscopy"*. **1980**, John Wiley and Sons, Chichester.
26. Friebolin, H.; *"Basic one and two-dimensional NMR spectroscopy"*, **1998**, Wiley-VCH, Chichester. 3rd edition.
27. Sanders, J. K. M.; Hunter, C. H.; *"Modern MNR spectroscopy: a guide for chemists"*, **1993**, Oxford University Press, Oxford. 2nd edition.
28. Cram, D. J.; Tanner, M.E.; Knobler, C.B., *J. Am. Chem.* **1991**, *113*, 7717.
29. Behr, J. P.; Lehn, J.-M., *J. Am. Chem. Soc.* **1976**, 98, 1743.
30. Christensen, J. J.; Ruckman, J.; Eatough, D. J.; Izatt, R. M.; *Thermochimica Acta*. **1972**, *3*, 203.
31. Eatough, D. J.; Christensen, J. J.; Izatt, R. M.; *Thermochimica Acta*. **1972**, *3*, 219.
32. Vicenti, M.; *J. Mass. Spectrom.* **1995**, *30*, 925.
33. Blair, M. S.; Kempen, E. C.; Brodbelt, J. S.; *J. Am. Soc. Mass Spectrom.* **1998**, *10*, 1049.
34. Julian, R. R.; Akin, M.; May, J. A.; Stoltz, B. M.; Beauchamp, J. L.; *Int. J. Mass Spectrom.* **2002**, *220*, 87.
35. Heynes, M. J.; *J. Chem. Soc. Dalton Trans.* **1993**, 311.
36. Horman, I.; Dreux B.; *Anal. Chem.* **1983**, *55*, 1219.
37. Creswell. C. J.; Allred, A. L.; *J. Phys. Chem.* **1962**, *66*, 1469.
38. Danil De Namor, A.; Jafou, O.; *J. Phys. Chem.* **2001**, *105*, 8018.
39. Tyrrell, H. J. V., Harris, K. R., *Diffusion in Liquids*, **1984**, Butterworths, Borough Green, Kent.
40. Wimmer, R.; Aachmenn, F. L.; Larsen, K. L.; Petersen, S. B. *Carbohydrate Chem.* **2002**, *337*, 841.
41. Williams D. H.; Fleming I.; *"Spectroscopic Methods in Organic Chemistry"*. **1996**, McGraw-Hill, London, 5th Edition.
42. Gawronski, J., Kolbon, H.; Kwit, M.; Katrusiak, A.; *J. Org. Chem.* **2000**, *65*, 5768.

43. Lam, F.; Feng, M.; Chan, R. S.; *Tetrahedron*, **1999**, *55*, 8377.
44. Fitzsimons, P. M.; Jackels, S. C.; *Inorg. Chim. Acta* **1996**, *246*, 301.
45. Chadim, M.; Budesínský, M.; Hodacová, J.; Závada, J.; Junk, P. C.; *Tetrahedron Asym.* **2001**, *12*, 127.
46. Kwit, M.; Gawronski, J.; *Tetrahedron Asym.* **2003**, *14*, 1303.
47. Gao, J.; Martell, A. E.; *Org. Biomol. Chem.* **2003**, *1*, 2795.
48. Akine, A.; Taniguchi, T.; Nabeshima, T.; *Tetrahedron Lett.* **2001**, *42*, 8861.
49. Vilsmeier, A.; Haack; A. *Chem. Ber.*; **1927**, *60*, 119.
50. Shevchuk, S. V.; Davis, J. M.; Sessler, J. L. *Tetrahedron Lett.* **2001**, *42*, 2447.
51. Megati, S.; Rao, K.G. S; *Tetrahedron Lett.* **1995**, *32*, 5819.
52. Josemin; Nirmala, K. N.; Asokan, C. V.; *Tetrahedron Lett.* **1997**, *38*, 8391.
53. Das, G. K.; Choudhury, B.; Das, K.; Das, B. P.; *J. Chem. Res. (S).* **1999**, 244.
54. Garuti, L.; Roberti, M.; Leoni, A.; Brigidi, P.; *Pharmazie.* **1990**, *45*, 863.
55. Evans, S. L.; Lloyd, H. A.; Lebeau, D.; Sokoloski, E. B.; *Org. Prep. Proced. Int.* **1990**, *22*, 764.
56. Smith, K. M.; Bisset, G. M. F.; Case, J. J.; Tabba, H. D.; *Tetrahedron Lett.* **1980**, *21*, 3747.
57. Marson, C. M.; Giles, P. C.; "*Synthesis using Vilsmeier Reagents*", **1994**, CRC, Florida.
58. Gattermann, L.; Koch J. A.; *Chem. Ber.*, **1897**, *30*, 1622.
59. Norman, R. O. C.; Coxon, J. M.; "*Principles of Organic Synthesis*", 3rd Ed. **1993**, John Wiley & Sons, Oxford.
60. Tanaka, M.; Souma, Y.; *J. Chem. Soc. Chem. Commun.* **1991**, *21*, 1551.
61. Reimer, K.; Tiemann, F.; *Chem. Ber.* **1876**, *9*, 1268.
62. Wynberg, H.; Meijer, E. W.; *Org. React.* **1982**, *28*, 1.
63. Thoer, A.; Denis, G.; Delmas, M.; Gaset, A.; *Synthetic Comm.* **1988**, *18*, 2095.
64. Hocker, J.; Giesecke, H.; Merten, R.; *Angew. Chem. Int. Ed. Engl.* **1976**, *15*, 169.
65. Wanzlick, H. W.; *Org. Synth.* **1973**, *5*, 115.
66. Duff, J. C.; *J. Chem. Soc.* **1941**, 547.
67. Lindoy, L. F.; Meehan, G, V.; Svenstrup, N.; *Synthesis.* **1998**, *7*, 1029.
68. Stille, J. R.; Ward, J. A.; Leffelman, C.; Sullivan, K. A.; *Tetrahedron Lett.* **1996**, *37*, 9267.
69. Ackerman, J. H.; Surrey, A. R.; *Org. Synth.* **1967**, *47*, 76.

70. Okada, Y.; Kaneko, M.; Nishimura, J.; *Tetrahedron Lett.* **2001**, *42*, 1919.

71. Sereda, G.; Lapteva, V.; Skvarchenko, V.; *Patent of Russian Federation*, **1993**, Reg #21100344.

72. Wittig, G.; Fuhrmann, G.; *Chem. Ber.* **1940**, *73*, 1197.

73. Gilman, H.; Bebb, R. L.; *J. Am. Chem. Soc.* **1939**, *61*, 109.

74. Worden, L. R.; Kaufman, K. D.; Smith, P. J.; Widiger, G. N.; *J. Chem. Soc.* **1970**, 227.

75. Syper, L.; Młochowsky, J.; Kloc, K.; *Tetrahedron.* **1983**, *29*, 781.

76. Sylvester-Hvid. K.; Soerensen, J.; Schaumburg, K.; Bechgaard, K.; Christensen, J. B.; *Synth Commun.* **1993**, *23*, 1905.

77. Wittig, G.; Pockels, U.; Droge, H.; *Chem. Ber.* **1938**, *71*, 108.

78. Gilman, H.; Jacoby, A. L.; *J. Org. Chem.* **1938**, *3*, 108.

79. Snieckus, V.; *Chem. Rev.* **1990**, *90*, 879.

80. Sundberg, R. J.; Sarpeshkar, R. M.; *J. Org. Chem.* **1984**, *49*, 4657.

81. Fröhlich, G.; Zabelinskaja-Mackova, A. A.; Fechter, M. H.; Griengl, H.; *Tetrahedron Asym.* **2003**, *14*, 355.

82. Carroll, M. A.; White, A. J.; Widdowson, D. A.; Williams, D. J.; *J. Chem. Soc. Perkin Trans. 1.* **2000**, *1*, 1551.

83. Feringa, B. L.; Hulst, R.; Rikers, R.; Brandma, L.; *Synthesis.* **1988**, 316.

84. Akine, A.; Taniguchi, T.; Nabeshima, T.; *Tetrahedron Lett.* **2001**, *42*, 8861.

85. Märkl, G.; Amrheim, J.; Stoiber, T.; Striebl, U.; Kreitmeier, P.; *Tetrahedron*, **2002**, *58*, 2551.

86. Sommelet, M.; *Compt. Rend.* **1913**, *157*, 852.

87. Wood, J. H.; Tung, C. C.; Perry, M. A.; Gibson, R. E.; *J. Am. Chem. Soc.* **1949**, *72*, 2992.

88. Gelling, O. J.; Feringa, B. L.; *J. Am. Chem. Soc.* **1990**, *122*, 7599.

89. Jin, M.-J.; Ahn, S-J.; *Bull. Kor. Chem. Soc.* **1994**, *37*, 537.

90. Ogawa, H.; Shimojo, N.; Kato, H.; *Tetrahedron.* **1972**, *29*, 533.

91. Hirano, M.; Yakabe, S.; Chikamori, H.; Clark, J. H.; Morimoto, T.; *J. Chem. Res. (Synop).* **1998**, *12*, 770.

92. Sahade, D. A.; Tsukamoto, K.; Thiemann, T.; Sawada, T.; Makata, S.; *Tetrahedron.* **1999**, *55*, 2573.

93. Mataka, S.; Liu, G.-B.; Sawada, T.; Tori-I, A.; Tashiro, M.; *J. Chem. Res. (Synop).* **1995**, *10*, 410.

94. Kornblum, N.; Jones, W. J.; Anderson G. J.; *J. Am. Chem. Soc.* **1959**, *81*, 4113.

95. Farrell, J. R.; Stiles, D.; Bu, W.; Lippard, S. J.; *Tetrahedron.* **2003**, *59*, 2463.

96. Gagne, R.R.; Spiro, C.L.; Smith, T. J.; Hamann, C. A.; Thies, W. R.; Shiemke, A. K.; *J. Am. Chem. Soc.* **1981**, *103*, 4073.

97. Chang, H.-R.; Larsen, S. K.; Boyd, P. D. W.; Pierpont, C. G.; Hendrickson. D. N.; *J. Am. Chem. Soc.* **1988**, *110*, 4565.

98. Hu, Y.; Hu, H.; *Synthesis*, **1991**, *4*, 325.

99. Takada, T.; Arisawa, M.; Gyoten, M.; Hamada, R.; Tohma, H.; Kita, Y.; *J. Org. Chem.* **1998**, *22*, 63.

100. Green, G. W.; Griffith, P.; Hollingshead, D. M.; Ley, S.V.; Schoder, M.; *J. Chem. Soc. Perkin Trans.* **1984**, *1*, 681.

101. Einhorn, J.; Einhorn, C.; Ratajczak, F.; Pierre, J.-L.; *J. Org. Chem.* **1996**, *61*, 7452.

102. Kochergin, P. M.; Blinova, L. S.; Karpov, G. A.; *Khim-Farm.* **1994**, *28*, 63.

103. Eliel, E.; Rivard, D. E.; *J. Org. Chem.* **1952**, *17*, 1252.

104. Dupau, P.; Renouard, T.; Le bozec, H.; *Tetrahedron Lett.* **1996**, *47*, 7503.

105. Skowrónski, R.; Cottier, L.; Descotes, G.; Lewkowski, J.; *Synthesis.* **1996**, 1291.

106. De Las Heras, M. A.; Vaquero, J. J.; Garcia-Navio, J. L; Alvarez-Builla, J.; *Tetrahedron Lett.* **1995**, 36, 455.

107. Nagayama, K.; Shimuzu, I.; Yamamoto, A.; *Chem. Lett.* **1998**, *11*, 1143

108. Watanabe, Y.; *Bull. Chem. Soc. Jpn.* **1971**, *44*, 2569.

109. Zaluski, M.-C.; Robba, M.; Bonhomme, M.; *Bull. Soc., Chim., Fr.* **1970**, 1445.

110. Zagotto, G.; Palumbo, M.; Uriarte, E.; Bonsignore, L.; Delogu, G.; Podda, G.; *Farmaco.* **1998**, *53*, 675.

111. Hagiya, K.; Mitsui, S.; Taguchi, H.; *Synthesis.* **2003**, *6*, 823.

112. Colon, I.; Kelsey D. R.; *J. Org. Chem.* **1986**, *51*, 2627.

113. Kumagai, T.; Itsuno, S.; *Tetrahedron Asym.* **2001**, *12*, 2509.

114. Simion, C.; Simion, A.; Mitoma, Y.; Nagashima, S.; Kawaji, T.; Hashimoto, I.; Tashiro, M.; *Heterocycles.* **2000**, *53*, 2459.

115. Krebs, R.; Spanggaard, H.; *J. Org. Chem.* **2002**, *67*, 7185.

116. Hyllested, J. L.; Veje, K.; Ostergaard, K.; *Osteoarthr. Cartilage.* **2002**, *10*, 333.

117. Jiang, J.; Compere, E. L.; *Synthetic Commun.* **1998**, *28*, 1041.

118. Kim, D. H.; Cho, H. I.; Zyung, T.; Do, L.-M.; Bark, K.-M.; Shin, G. C.; Shin, S. C.; *Eur. Polym. J.* **2002**, *38*, 133.

119. Yang, E. N.; *J. Org. Chem.* **1978**, *43*, 3425.

120. Hort, D. J.; *Organic Synthesis.* **1999**, *77*, 153.

121. Wheeler, A. S.; Ergle, D. R.; *J. Am. Chem. Soc.* **1930**, *52*, 4872.

122. Johnstone, R. A. W.; Rose, M. E.; *Tetrahedron.* **1979**, *35*, 2169.

123. Bergmann, J.; *J. Chem. Soc.* **1948**, 1283.

124. Waykole, L.; Paquette, L. A.; *J. Am. Chem. Soc.* **1987**, *109*, 3174.

125. Govindachari T. R.; Arumugam, N.; *J. Chem. Soc.* **1955**, 2534.

126. Wilf J.; Ben-Waim, A.; *J. Phys. Chem.* **1979**, *70*, 3209.

127. Sparfel D.; Gobert, F.; Rigaudy, J.; *Tetrahedron (F).* **1980**, *36*, 2225.

128. Dean, F. M.; Elkass, G.; Prakash, L.; *J. Chem. Soc. Chem Commun.* **1985**, *8*, 502.

129. Smith, H. E.; Neegaard, J. R.; Burrows, E. P., Chen, F-M.; *J. Am. Chem. Soc.* **1974**, *96*, 2908.

130. Rossignolo, G.; "*Synthesis and Supramolecular chemistry of novel macrocycle receptors for the remendiation of pesticides*". PhD Thesis, University of Surrey. UK. **2004.**

131. Mislow, K., Siegel, J.; *J. Am. Chem. Soc.* **1984**, *106*, 3319

132. Rowan, S. J.; Cantrill, S. J.; Cousins, G. R. L.; Sanders, J. K. M.; Stoddart, J., F.; *Angew. Chem. Int. Ed.* **2002**, *41*, 898.

133. Gutsche, C. D., Johnston, D. E., Steward, D. R.; *J. Org. Chem.* **1999**, *64*, 3747

134. Rowan, S. J.; Brady, J. K.; Sanders J. K. M.; *Tetrahedron Lett.* **1996**, *37*, 6013.

135. Arenas, J.C.; Arenas, J. C.; Berjón A.; Fernández, M. P., *Anal. Sis. Navarra.* **1998**, *21*, 98.

136. Miller, L. T.; *http://extoxnet.orst.edu/pips/atrazine.htm. **2004**.* © Cornell University ***2004***. USA.

137. U.S. EPA Office of Pesticide Programs Health Effects division, March **2002**.

138. Kerssebaum, R.; "*DOSY and diffusion by NMR. Users guide for XWinNMR 3.1/3.5. Version 1.03*". **2000**, Bruker Biospin GmbH, Rheinstetten.

139. Verger P.; Cordier S.; Thuy L. T. B.; Bard D.; Dai L. C.; Phiet P. H.; Gonnord M. F.; Abenhaim L.; *Environmental Research.* **1994**, *65*, 226.

140. Suwalski, M.; Benites, M.; Villena, F.; Aguilar, F.; Sotomayor, C. P.; *Biochim. Biophys. Acta.* **1996**, 267.

141. Huang C. Y.; Zhou, R.; Yang, D. C. H.; Chock P. B.; *Biophys. Chem.* **2003**, *100*, 143.

142. Eliadou, K.; Yannakopoulou, K.; Rontoyianni, A.; Mavridis, I. M. *J. Org. Chem.* **1999**, *64*, 6217

143. Oakes, D. J.; Pollak, J. K.; *Toxicology.* **2000**, *151*, 1.

144. McDonald, A. S. *"Pesticide Information Division of the Plant Industry Directorate"*, **1990**, Pest Management Regulatory Agency, Ontario, Canada. http://www.hc-sc.gc.ca.

145. Riddick, J. A.; Burger, W. B.; Sakano, T. K., *Organic Solvents.* **1986**, John Wiley & Sons, New York.

146. Gutsche, C.D.; See, K. A., *J. Org. Chem.* **1992**, *57*, 4527.

147. Weber, P. R. A.; Chen, G. Z.; Drew, M. G. B.; Beer, P. D., *Angew. Chem. Int. Ed. Engl.* **2001**, *40*, 2264.

APPENDIX

X-Ray crystallographic data.

The stucture was solved by Dr. N. Burzlaff (University of Konstanz) and it is gratefully acknowledged.

4,4'-bis(formyl)phenyl-ether-237.

Crystal data: monoclinic, crystal size 0.5 x 0.4 x 0.3 mm, P2(1)/n, a=12.546(2) Å, α= 90°, b = 7.122(3) Å, β= 102.4°(3), c = 12.956(6) Å, γ= 90°, Z=4, D=1.329 Mg/m^3, F(000)=472, μ=0.094 mm^{-1}, 2834 reflections collected, 2450 unique, R_{int} 0.0456, R1 0.0495, wR2 0.1211 for I>aσI, 163 parameters, largest diff. Peak and hole 0.254 and –0.287 e. $Å^{-3}$.

Measurements were taken at 188(2)K using radiation of λ=0.71073 Å. Accurate cell dimensions and crystal orientation matrix were determined using full matrix least square refinement methods with θ in the range of 2.05 to 27.00°.

Table 2: Atomic coordinates (x 10^4) and equivalent isotropic displacement parameters (A^2 x 10^3) U(eq) is defined as one third of the trace of the orthogonalised Uij tensor.

	X	Y	Z	U(eq)
O(1)	-986(2)	3285(2)	-1681(1)	58(1)
C(1)	-91(2)	3105(3)	-1118(2)	41(1)
O(2)	783(1)	776(2)	3147(1)	43(1)
C(2)	125(2)	2537(2)	4(2)	31(1)
O(3)	1968(1)	7508(2)	6504(1)	45(1)
C(3)	1206(2)	2381(3)	575(2)	37(1)
C(4)	1441(2)	1820(3)	1621(2)	40(1)
C(5)	579(2)	1432(3)	2105(1)	33(1)
C(6)	-500(2)	1590(3)	1558(2)	34(1)
C(7)	-724(2)	2139(3)	510(2)	34(1)
C(8)	1019(2)	2088(3)	3952(1)	30(1)
C(9)	1194(2)	1382(3)	4981(1)	32(1)
C(10)	1424(1)	2620(3)	5826(1)	32(1)
C(11)	1496(1)	4560(3)	5658(1)	28(1)
C(12)	1306(1)	5228(3)	4619(1)	27(1)
C(13)	1066(1)	4016(3)	3762(1)	29(1)
C(14)	1775(2)	5838(3)	6565(2)	35(1)

Table 3: Bond length Å

Bonds	Bond length
CO(1)-C(1)	1.207(3)
C(1)-C(2)	1.478(3)
C(1)-H(1)	1.039(14)

O(2)-C(8)	1.384(2)
O(2)-C(5)	1.399(2)
C(2)-C(7)	1.395(3)
C(2)-C(3)	1.402(3)
O(3)-C(14)	1.220(3)
C(3)-C(4)	1.382(3)
C(3)-H(3)	0.9500
C(4)-C(5)	1.389(3)
C(4)-H(4)	0.9500
C(5)-C(6)	1.391(3)
C(6)-C(7)	1.383(3)
C(6)-H(6)	0.9500
C(7)-H(7)	0.9500
C(8)-C(9)	1.397(3)
C(8)-C(13)	1.399(3)
C(9)-C(10)	1.387(3)
C(9)-H(9)	0.9500
C(10)-C(11)	1.405(3)
C(10)-H(10)	0.9500
C(11)-C(12)	1.399(2)
C(11)-C(14)	1.467(3)
C(12)-C(13)	1.388(3)
C(12)-H(12)	0.9500
C(13)-H(13)	0.9500
C(14)-H(14)	1.03(2)

Table 4: Bond angles.

Bonds	**Bond angle**
O(1)-C(1)-C(2)	125.0(2)
O(1)-C(1)-H(1)	107.3(8)
C(2)-C(1)-H(1)	127.7(8)
C(8)-O(2)-C(5)	117.86(15)
C(7)-C(2)-C(3)	119.08(18)
C(7)-C(2)-C(1)	121.40(18)
C(3)-C(2)-C(1)	119.53(19)
C(4)-C(3)-C(2)	121.21(19)
C(4)-C(3)-H(3)	119.4
C(2)-C(3)-H(3)	119.4
C(3)-C(4)-C(5)	118.52(18)
C(3)-C(4)-H(4)	120.7
C(5)-C(4)-H(4)	120.7
C(4)-C(5)-C(6)	121.36(18)
C(4)-C(5)-O(2)	120.21(18)
C(6)-C(5)-O(2)	118.35(18)
C(7)-C(6)-C(5)	119.58(18)
C(7)-C(6)-H(6)	120.2
C(5)-C(6)-H(6)	120.2

C(6)-C(7)-C(2)	120.25(17)
C(6)-C(7)-H(7)	119.9
C(2)-C(7)-H(7)	119.9
O(2)-C(8)-C(9)	116.16(17)
O(2)-C(8)-C(13)	122.72(17)
C(9)-C(8)-C(13)	121.12(17)
C(10)-C(9)-C(8)	119.20(18)
C(10)-C(9)-H(9)	120.4
C(8)-C(9)-H(9)	120.4
C(9)-C(10)-C(11)	120.87(17)
C(9)-C(10)-H(10)	119.6
C(11)-C(10)-H(10)	119.6
C(12)-C(11)-C(10)	118.66(17)
C(12)-C(11)-C(14)	121.43(17)
C(10)-C(11)-C(14)	119.90(17)
C(13)-C(12)-C(11)	121.40(17)
C(13)-C(12)-H(12)	119.3
C(11)-C(12)-H(12)	119.3
C(12)-C(13)-C(8)	118.74(17)
C(12)-C(13)-H(13)	120.6
C(8)-C(13)-H(13)	120.6
O(3)-C(14)-C(11)	124.70(18)
O(3)-C(14)-H(14)	118.4(13)
C(11)-C(14)-H(14)	116.9(13)

Table 5: Anisotropic displacement parameters ($Å^2$ x 10^3).The anisotropic displacement factor exponent takes the form:$-2\pi^2 [h^2 a^{*2} U11 + . + 2 h k a^* b^* U12]$

	U11	U22	U33	U23	U13	U12
O(1)	71(1)	49(1)	45(1)	7(1)	-11(1)	-1(1)
C(1)	55(1)	28(1)	38(1)	-2(1)	5(1)	3(1)
O(2)	65(1)	28(1)	29(1)	-2(1)	-3(1)	-4(1)
C(2)	35(1)	25(1)	31(1)	-5(1)	3(1)	4(1)
O(3)	59(1)	35(1)	38(1)	-6(1)	2(1)	-4(1)
C(3)	31(1)	40(1)	39(1)	-2(1)	7(1)	6(1)
C(4)	29(1)	42(1)	43(1)	-4(1)	-3(1)	5(1)
C(5)	44(1)	25(1)	28(1)	-6(1)	1(1)	0(1)
C(6)	36(1)	33(1)	34(1)	-5(1)	7(1)	-3(1)
C(7)	30(1)	30(1)	39(1)	-5(1)	-1(1)	1(1)
C(8)	30(1)	30(1)	28(1)	-4(1)	-1(1)	-2(1)
C(9)	34(1)	26(1)	35(1)	5(1)	3(1)	-1(1)
C(10)	30(1)	36(1)	27(1)	6(1)	3(1)	1(1)
C(11)	21(1)	32(1)	28(1)	-2(1)	4(1)	0(1)
C(12)	23(1)	25(1)	32(1)	1(1)	3(1)	-1(1)
C(13)	31(1)	31(1)	25(1)	3(1)	2(1)	-1(1)
C(14)	38(1)	38(1)	28(1)	-1(1)	4(1)	1(1)

Table 6: Hydrogen coordinates (x 10^4) and isotropic displacement parameters (A^2 x 10^3).

	X	Y	Z	U(eq)
H(3)	1787	2665	236	44
H(4)	2175	1702	2000	48
H(6)	-1079	1322	1903	41
H(7)	-1460	2245	133	41
H(9)	1157	70	5100	39
H(10)	1533	2150	6527	38
H(12)	1343	6540	4498	33
H(13)	936	4486	3060	35
H(1)	477(11)	3430(20)	-1569(11)	0(3)
H(14)	1803(16)	5270(30)	7303(16)	42(6)

Table 7: Torsion angles.

Bonds	Torsion angle.
O(1)-C(1)-C(2)-C(7)	0.6(3)
O(1)-C(1)-C(2)-C(3)	-179.9(2)
C(7)-C(2)-C(3)-C(4)	0.8(3)
C(1)-C(2)-C(3)-C(4)	-178.79(19)
C(2)-C(3)-C(4)-C(5)	-0.8(3)
C(3)-C(4)-C(5)-C(6)	0.3(3)
C(3)-C(4)-C(5)-O(2)	177.00(18)
C(8)-O(2)-C(5)-C(4)	83.3(2)
C(8)-O(2)-C(5)-C(6)	-99.9(2)
C(4)-C(5)-C(6)-C(7)	0.2(3)
O(2)-C(5)-C(6)-C(7)	-176.59(16)
C(5)-C(6)-C(7)-C(2)	-0.2(3)
C(3)-C(2)-C(7)-C(6)	-0.3(3)
C(1)-C(2)-C(7)-C(6)	179.26(18)
C(5)-O(2)-C(8)-C(9)	178.65(16)
C(5)-O(2)-C(8)-C(13)	-0.5(3)
O(2)-C(8)-C(9)-C(10)	-179.40(16)
C(13)-C(8)-C(9)-C(10)	-0.3(3)
C(8)-C(9)-C(10)-C(11)	-0.9(3)
C(9)-C(10)-C(11)-C(12)	1.5(3)
C(9)-C(10)-C(11)-C(14)	-178.02(17)
C(10)-C(11)-C(12)-C(13)	-0.9(2)
C(14)-C(11)-C(12)-C(13)	178.60(16)
C(11)-C(12)-C(13)-C(8)	-0.2(3)
O(2)-C(8)-C(13)-C(12)	179.92(16)
C(9)-C(8)-C(13)-C(12)	0.8(3)
C(12)-C(11)-C(14)-O(3)	-7.5(3)
C(10)-C(11)-C(14)-O(3)	172.05(19)